Electronic Supplementary Material (ESI) for Chemical Science.

Folding-controlled assembly of *ortho*-phenylene-based macrocycles

Supporting Information

*Viraj C. Kirinda and C. Scott Hartley**

Department of Chemistry & Biochemistry, Miami University, Oxford, OH 45056, United States

Table of Contents

List of Figures

List of Schemes

List of Tables

Experimental NMR assignments of key compounds

The aromatic protons of *o*-phenylenes are in slow conformational exchange at room temperature. Sharper aromatic proton peaks were observed at low temperature;[1] therefore, characterization was done at 0 °C in $CDCl_3$. Typically, a predominant set of signals is observed corresponding to the major conformer, along with smaller signals corresponding to minor conformers (as confirmed by EXSY). Chemical shift assignments are based on analysis of the 2D NMR spectra (COSY, TOCSY, HSQC, and HMBC).

ortho-Phenylene octamers

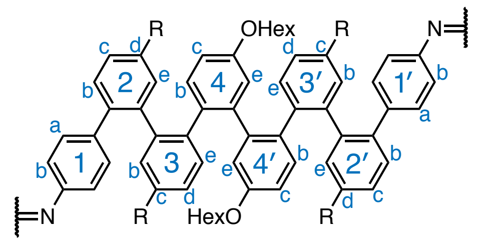

Figure S1. Labeling scheme for *o*-phenylene octamers.

oP^{8}F(NH$_2$)

Proton	^{1}H (ppm)	^{13}C (ppm)
1a	6.12	129.6
1b	6.33	116.1
1c		142.7
1d		132.7
2a		135.6
2b	6.79	131.0
2c	6.73	114.3
2d		161.7
2e	5.83	117.5
2f		140.6
3a		140.6
3b	6.73	117.4
3c		161.2
3d	6.63	115.2
3e	6.10	133.1
3f		137.7
4a		140.8
4b	5.71	132.8
4c	6.34	112.4
4d		158.5
4e	5.52	117.4
4f		140.7

Table S1. Experimental ^{1}H and ^{13}C chemical shifts of **oP^{8}F(NH$_2$)**, major conformer.

$oP^8F(M)$

Proton	^{1}H (ppm)	^{13}C (ppm)
1a	6.31	129.6
1b	6.77	120.4
1c		149.8
1d		138.2
2a		134.9
2b	6.91	131.1
2c	6.79	114.1
2d		161.2
2e	5.84	117.2
2f		138.2
3a		139.6
3b	6.77	117.1
3c		160.3
3d	6.66	115.1
3e	6.10	132.8
3f		137.4
4a		130.3
4b	5.71	132.5
4c	6.29	129.3
4d		157.8
4e	5.57	117.2
4f		140.4

Table S2. Experimental ^{1}H and ^{13}C chemical shifts of **$oP^8F(M)$**, major conformer.

$oP^8F(DPB)_{2+2}$

Proton	^{1}H (ppm)	^{13}C (ppm)	Proton	^{1}H (ppm)	^{13}C (ppm)
1a	6.49	129.8	4f'		n.d.
1b	6.91	120.7	4e'	5.44	118.1
1c		149.2	4d'		157.8
1d		139.1	4c'	6.91	112.0
2a		135.3	4b'	6.97	133.3
2b	7.03	131.1	4a'		131.1
2c	6.92	114.6	3f'		138.6
2d		161.1	3e'	6.15	115.4
2e	6.12	117.9	3d'	6.56	114.0
2f		140.6	3c'		159.9
3a		141.4	3b'	6.15	118.2
3b	7.01	117.1	3a'		139.2
3c		161.2	2f'		139.3
3d	6.85	115.0	2e'	6.07	118.2
3e	6.23	135.1	2d'		160.7
3f		137.0	2c'	6.87	115.1
4a		131.7	2b'	7.07	131.9
4b	5.66	132.3	2a'		138.2
4c	6.13	117.6	1d'		n.d.
4d		157.9	1c'		149.2
4e	5.44	116.1	1b'	6.89	120.5
4f		141.0	1a'	5.97	130.9

Table S3. Experimental ^{1}H and ^{13}C chemical shifts of **$oP^8F(DPB)_{2+2}$**, major conformer.

$oP^8F(Phen)_{2+2}$

Proton	^{1}H (ppm)	^{13}C (ppm)	Proton	^{1}H (ppm)	^{13}C (ppm)
1a	6.50	130.3	4f'		141.2
1b	6.93	120.7	4e'	5.61	118.7
1c		148.6	4d'		158.7
1d		138.7	4c'	6.93	111.7
2a		138.4	4b'	6.98	132.9
2b	7.06	132.0	4a'		131.0
2c	6.95	114.2	3f'		136.8
2d		160.2	3e'	6.19	118.5
2e	6.13	118.3	3d'	6.59	114.1
2f		140.6	3c'		159.8
3a		131.7	3b'	6.17	118.2
3b	7.02	117.4	3a'		141.4
3c		161.1	2f'		139.3
3d	6.86	114.5	2e'	6.09	118.4
3e	6.23	115.7	2d'		160.2
3f		137.1	2c'	6.85	114.8
4a		131.7	2b'	7.09	131.9
4b	5.63	132.3	2a'		136.3
4c	6.14	115.4	1d'		149.2
4d		157.8	1c'		138.0
4e	5.43	115.7	1b'	6.92	120.3
4f		141.0	1a'	5.98	130.7

Table S4. Experimental ^{1}H and ^{13}C chemical shifts of **$oP^8F(Phen)_{2+2}$**, major conformer.

$oP^8H(NH_2)$

Proton	^{1}H (pp)	^{13}C (ppm)
1a	6.15	129.8
1b	6.27	115.3
1c		143.2
1d		132.9
2a		129.8
2b	6.86	126.2
2c	7.00	126.3
2d	6.74	127.1
2e	6.17	131.7
2f		140.0
3a		139.7
3b	6.99	131.9
3c	7.10	125.9
3d	6.80	128.3
3e	5.99	131.5
3f'		141.3
4a		132.5
4b	5.72	132.7
4c	6.27	112.9
4d		157.8
4e	5.41	116.6
4f		140.9

Table S5. Experimental ^{1}H and ^{13}C chemical shifts of **$oP^8H(NH_2)$**, major conformer.

oP⁸H(M)

Proton	^{1}H (ppm)	^{13}C (ppm)
1a	6.35	129.4
1b	6.77	120.4
1c		149.3
1d		140.1
2a		138.5
2b	6.91	129.1
2c	7.02	126.2
2d	6.81	128.0
2e	6.19	131.6
2f		141.2
3a		139.1
3b	7.04	131.0
3c	7.12	125.8
3d	6.81	128.3
3e	5.99	131.1
3f'		141.2
4a		132.1
4b	5.68	132.3
4c	6.23	112.7
4d		157.4
4e	5.43	116.1
4f		141.3

Table S6. Experimental ^{1}H and ^{13}C chemical shifts of **oP^{8}H(M)**, major conformer.

oP^{8}H(DPB)$_{2+2}$

Proton	^{1}H (ppm)	^{13}C (ppm)	Proton	^{1}H (ppm)	^{13}C (ppm)
1a	6.53	130.4	4f'		141.4
1b	6.92	120.6	4e'	5.42	117.3
1c		149.3	4d'		158.0
1d		148.8	4c'	6.84	113.0
2a		139.2	4b'	6.94	133.2
2b	7.04	129.3	4a'		132.9
2c	7.18	126.7	3f'		140.9
2d	7.06	128.1	3e'	6.09	114.7
2e	6.44	132.0	3d'	6.78	126.6
2f		140.2	3c'	6.73	125.5
3a		140.8	3b'	6.44	132.0
3b	7.24	131.3	3a'		138.4
3c	7.37	127.1	2f'		138.8
3d	7.06	127.2	2e'	6.36	131.9
3e	6.20	133.7	2d'	6.84	126.2
3f'		140.8	2c'	7.10	126.4
4a		133.3	2b'	7.12	126.5
4b	5.63	133.0	2a'		140.1
4c	6.14	132.4	1d'		140.0
4d		157.5	1c'		153.3
4e	5.26	116.1	1b'	6.89	120.3
4f		141.5	1a'	6.06	131.5

Table S7. Experimental ^{1}H and ^{13}C chemical shifts of**oP^{8}H(DPB)$_{2+2}$**, major conformer.

$oP^8H(Phen)_{2+2}$

Proton	^1H (ppm)	^{13}C (ppm)	Proton	^1H (ppm)	^{13}C (ppm)
1a	6.55	130.6	4f'		141.2
1b	6.95	120.2	4e'	5.43	117.7
1c		148.5	4d'		158.0
1d		140.2	4c'	6.86	113.1
2a		139.1	4b'	6.96	133.4
2b	7.08	129.2	4a'		133.0
2c	7.20	126.4	3f'		140.7
2d	7.05	127.5	3e'	6.12	115.0
2e	6.43	131.8	3d'	6.80	126.5
2f		140.4	3c'	6.76	125.8
3a		140.7	3b'	6.47	132.0
3b	7.25	131.4	3a'		138.5
3c	7.37	127.2	2f'		138.8
3d	7.07	127.5	2e'	6.37	132.0
3e	6.20	133.7	2d'	6.86	126.2
3f'		140.4	2c'	7.13	126.5
4a		133.1	2b'	7.16	126.3
4b	5.60	132.4	2a'		140.1
4c	6.08	131.0	1d'		140.2
4d		157.6	1c'		157.3
4e	5.25	116.0	1b'	6.93	120.5
4f		141.4	1a'	6.07	131.0

Table S8. Experimental ^1H and ^{13}C chemical shifts of $oP^8H(Phen)_{2+2}$, major conformer.

ortho-Phenylene decamers

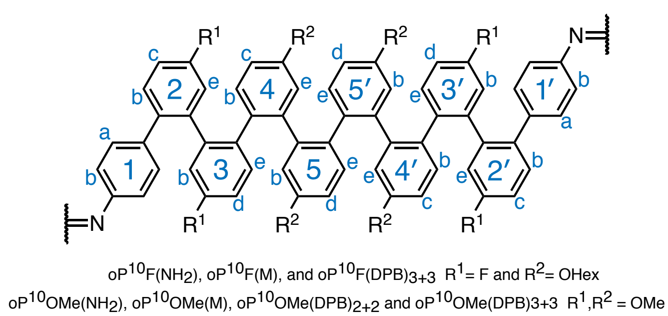

Figure S2. Labeling scheme for *o*-phenylene decamers.

oP^{10}F(NH$_2$)

Proton	^{1}H (ppm)	^{13}C (ppm)
1a	6.05	129.1
1b	6.34	112.2
1c		140.3
1f		129.2
2a		134.9
2b	6.74	130.1
2c	6.74	113.7
2d		160.7
2e	5.80	116.9
2f		140.2
3a		139.4
3b	6.66	116.2
3c		160.5
3d	6.44	114.3
3e	5.87	132.5
3f		137.4
4a		130.3
4b	5.49	131.3
4c	6.10	117.1
4d		157.2
4e	5.33	115.3
4f		140.4
5a		140.2
5b	5.42	117.2
5c		157.0
5d	6.33	114.0
5e	5.97	130.9
5f		130.1

Table S9. Experimental ^{1}H and ^{13}C chemical shifts of **oP^{10}F(NH$_2$)**, major conformer.

oP^{10}F(M)

Proton	^{1}H (ppm)	^{13}C(ppm)
1a	6.24	130.1
1b	6.71	121.4
1c		149.0
1f		132.3
2a		134.9
2b	6.82	131.6
2c	6.76	114.8
2d		161.3
2e	5.85	118.2
2f		140.8
3a		139.5
3b	6.70	117.2
3c		160.1
3d	6.46	115.3
3e	5.89	133.8
3f		137.6
4a		130.1
4b	5.49	138.2
4c	6.01	114.1
4d		157.6
4e	5.45	118.3
4f		140.6
5a		140.2
5b	5.34	116.3
5c		157.4
5d	6.34	112.9
5e	5.99	133.1
5f		132.4

Table S10. Experimental ^{1}H and ^{13}C chemical shifts of **oP^{10}F(M)**, major conformer.

oP^{10}F(DPB)$_{3+3}$

Proton	^{1}H (ppm)	^{13}C (ppm)
1a	6.25	128.9
1b	6.72	120.9
1c		148.8
1f		139.0
2a		134.6
2b	6.84	130.9
2c	6.77	113.7
2d		161.2
2e	5.85	117.4
2f		140.8
3a		139.4
3b	6.70	116.7
3c		160.3
3d	6.46	114.3
3e	5.88	132.7
3f		137.6
4a		130.2
4b	5.48	131.5
4c	6.00	112.8
4d		157.6
4e	5.35	115.0
4f		140.8
5a		140.2
5b	5.46	117.3
5c		157.4
5d	6.34	111.6
5e	6.00	131.8
5f		132.7

Table S11. Experimental ^{1}H and ^{13}C chemical shifts of **oP^{10}F(DPB)$_{3+3}$**, major conformer.

oP^10OMe(NH_2)

Proton	^1H (ppm)	^{13}C (ppm)
1a	6.05	129.3
1b	6.20	114.4
1c		143.7
1f		132.1
2a		132.3
2b	6.76	130.1
2c	6.62	112.5
2d		157.8
2e	5.71	115.0
2f		140.6
3a		140.1
3b	6.55	115.6
3c		157.5
3d	6.36	112.9
3e	5.81	132.2
3f		134.2
4a		131.5
4b	5.57	132.1
4c	6.16	112.3
4d		157.2
4e	5.35	114.7
4f		140.9
5a		139.9
5b	5.70	115.6
5c		157.2
5d	6.28	112.6
5e	5.96	131.5
5f		132.9

Table S12. Experimental ^1H and ^{13}C chemical shifts of **oP^10OMe(NH_2)**.

oP^{10}OMe(M)

Proton	^{1}H (ppm)	^{13}C (ppm)
1a	6.29	129.6
1b	6.73	120.5
1c		149.2
1f		139.6
2a		131.9
2b	6.83	130.8
2c	6.68	112.7
2d		158.4
2e	5.76	115.8
2f		141.3
3a		139.7
3b	6.60	116.2
3c		157.8
3d	6.37	113.2
3e	5.83	132.5
3f		134.3
4a		131.5
4b	5.54	132.4
4c	6.10	112.7
4d		157.3
4e	5.37	115.2
4f		140.9
5a		140.5
5b	5.47	116.1
5c		157.4
5d	6.31	113.1
5e	5.99	132.0
5f		133.0

Table S13. Experimental ^{1}H and ^{13}C chemical shifts of **oP^{10}OMe(M)**, major conformer.

oP^{10}OMe(DPB)$_{3+3}$

Proton	^{1}H (ppm)	^{13}C (ppm)
1a	6.27	129.3
1b	6.73	120.5
1c		148.9
1f		140.2
2a		131.7
2b	6.82	130.2
2c	6.64	112.6
2d		158.5
2e	5.75	115.6
2f		141.3
3a		139.7
3b	6.58	115.8
3c		157.7
3d	6.34	112.9
3e	5.82	132.4
3f		134.2
4a		131.5
4b	5.52	131.9
4c	6.05	112.5
4d		157.3
4e	5.34	115.0
4f		140.8
5a		140.4
5b	5.45	115.9
5c		157.5
5d	6.27	112.4
5e	5.97	131.7
5f		132.9

Table S14. Experimental ^{1}H and ^{13}C chemical shifts of **oP^{10}OMe(DPB)$_{3+3}$**, major conformer.

oP^{10}OMe(DPB)$_{2+2}$ (major conformer)

Proton	^{1}H (ppm)	^{13}C (ppm)
1a	6.98	126.6
1b	7.00	129.1
1c		149.5
1f		141.0
2a		
2b	7.15	131.3
2c	6.79	114.8
2d		157.6
2e	5.96	114.7
2f		139.7
3a		138.8
3b	5.98	115.7
3c		157.0
3d	6.35	114.0
3e	6.03	133.0
3f		133.1
4a		132.5
4b	6.97	132.7
4c	6.83	112.4
4d		158.4
4e	5.73	116.8
4f		142.2
5a		141.5
5b	5.53	114.5
5c		158.1
5d	6.52	115.7
5e	6.29	134.3
5f		133.7

Table S15. Experimental ^{1}H and ^{13}C chemical shifts of **oP^{10}OMe(DPB)$_{2+2}$**, major conformer.

oP^{10}OMe(DPB)$_{2+2}$ (minor conformer AAAABBB)

Proton	^{1}H (ppm)	^{13}C (ppm)	Proton	^{1}H (ppm)	^{13}C (ppm)
1a	6.52	120.8	5f'		
1b	6.87	129.2	5e'	5.99	115.5
1c			5d'	6.39	114.3
1f			5c'		
2a			5b'	6.12	113.8
2b			5a'		
2c			4f'		
2d			4e'	5.89	114.4
2e			4d'		
2f			4c'	6.38	114.4
3a			4b'	6.71	132.6
3b	6.87		4a'		
3c			3f'		
3d	6.75	120.2	3e'	4.57	135.1
3e	6.25		3d'	6.15	114.9
3f			3c'		
4a			3b'	6.17	134.9
4b	5.75	131.9	3a'		
4c	6.19	115.3	2f'		
4d			2e'		
4e	5.34	115.3	2d'		
4f			2c'		
5a			2b'		
5b	5.57	116.6	2a'		
5c			1f'		
5d	6.87	116.4	1c'		
5e	6.97	130.4	1b'	7.06	120.8
5f			1a'	7.16	131.5

Table S16. Experimental ^{1}H and ^{13}C chemical shifts of **oP^{10}OMe(DPB)$_{2+2}$**, minor conformer (AAAABBB). The chemical shifts were assigned using only the COSY, TOCSY, and NOESY/EXSY spectra because the HMBC cross-peaks were very weak. The aromatic rings were arranged to minimize the RMSD between the experimental and predicted chemical shifts for various conformers. While this makes the ultimate geometry assignment (AAAABBB) less certain, we note that this same geometry was observed as the major conformer for **oP^{10}H(DPB)$_{2+2}$**, where the chemical shift assignments were conclusive.[2]

Computational

Cartesian coordinates for all optimized geometries are given in a separate plain text file.

Model compounds

Geometry assignments

Having determined the experimental chemical shifts (δ_{exp}) of the major conformers of the model compounds **oP^{10}F(M)**, **oP^{10}OMe(M)**, **oP^{8}F(M)**, and **oP^{8}H(M)** (given above), geometries were assigned as previously described.[1] Briefly, the geometries of candidate conformers (chosen on the basis of our previous experience with *o*-phenylenes) were optimized at the PCM(chloroform)/B97-D/cc-pVDZ level, which we have previously shown does a good job for *o*-phenylene geometries.[2] ^{1}H NMR properties were then calculated at the PCM(chloroform)/WP04/6-31G(d) level,[3] a method that is known to provide good accuracy at low computational cost,[4] and which we have used extensively with *o*-phenylenes.[5] The predicted isotropic shieldings were then converted to chemical shifts (δ_{calc}) by scaling using linear regression,[4] and then RMSDs were calculated for each folding state.

The best match was always the perfectly folded (AA…A) conformer. As shown below, RMSDs were on the order of 0.1 ppm, which is typical for successful matches using this method. We then used a non-parametric statistical test to confirm that the match was better than the next-best possibility at an acceptable confidence level, as previously described.[1,6] The basis for the comparison is the F statistic

$$F = \frac{s^2_{\text{match}}}{s^2_{\text{alt}}} \tag{1}$$

where s^2_{match} is the standard error of the regression of a plot of δ_{calc} against δ_{exp} for the proposed match, and s^2_{alt} is the analogous standard error for a permutation of the data where chemical shifts have been swapped. The confidence level (p) is determined by generating a large list of permutations (all possibilities or 2^{20}, whichever is smaller) and determining the rank of the proposed match in the list. This was done using a program written in Python, which is given on p S41.

Decamer models

Conformer	Energy (E_h)	IF
AAAAAAA	−3874.535572	0
AAAAAAB	−3874.530525	0
AAAABBB	−3874.526531	0
BAAAAAB	−3874.526688	0
BAAABBB	−3874.517140	0
AAABBBA	−3874.525825	0

Table S17. Energies for optimized **oP^{10}OMe(M)**. IF = number of imaginary frequencies.

Position	AAAAAAA	AAAAAAB	AAAABBB	AAABBBA	BAAAAAB	BAAABBB
1a	26.09	26.97	25.35	25.41	26.58	25.21
1a	26.21	25.34	24.97	26.24	25.24	24.96
1b	25.84	25.48	25.37	24.93	25.25	25.31
1b	25.88	25.63	24.90	25.16	25.22	25.21
2b	25.66	25.37	25.01	25.43	25.27	24.99
2c	25.83	25.85	25.63	25.54	25.77	25.60
2e	26.81	26.92	26.15	25.74	26.76	26.10
3b	26.16	26.83	26.48	25.62	26.69	26.41
3d	26.09	26.24	26.40	26.25	26.22	26.18
3e	26.55	26.44	27.41	26.08	26.30	27.43
4b	26.84	25.73	25.48	26.08	25.57	25.39
4c	26.24	25.73	26.18	26.28	25.59	26.09
4e	27.26	27.05	27.02	27.57	26.67	26.63
5b	27.05	27.24	26.34	28.24	26.93	26.20
5d	26.13	26.24	26.02	26.52	26.04	25.71
5e	26.48	26.17	26.28	26.53	25.75	25.58
5e'	26.48	26.08	25.59	26.19	25.75	25.26
5d'	26.13	25.87	25.60	26.35	26.04	25.77
5b'	27.05	26.75	26.83	26.82	26.93	27.13
4e'	27.26	26.87	27.25	26.27	26.67	27.20
4c'	26.24	26.12	26.24	26.17	25.59	25.70
4b'	26.84	26.69	26.54	26.83	25.57	25.32
3e'	26.55	26.43	25.93	26.86	26.30	25.61
3d'	26.09	26.10	25.66	26.12	26.22	25.75
3b'	26.16	26.03	25.81	25.67	26.69	26.56
2e'	26.81	26.61	26.47	25.88	26.76	26.50
2c'	25.83	25.75	25.68	25.65	25.77	25.68
2b'	25.66	25.58	25.50	25.44	25.27	25.17
1b'	25.88	25.80	25.73	25.85	25.22	25.57
1b'	25.84	25.73	25.76	25.61	25.25	25.40
1a'	26.21	26.06	26.07	25.99	25.24	25.18
1a'	26.09	25.98	25.91	25.92	26.58	27.05

Table S18. Calculated (GIAO/PCM(chloroform)/WP04/6-31G(d)//PCM(chloroform)/B97-D/cc-pVDZ) ^{1}H isotropic shieldings for **oP^{10}OMe(M)**.

Hexyloxy groups in **oP^{10}F(M)** were replaced with methoxy groups for the purpose of optimization, giving **oP^{10}-F(M)$'$**.

Conformer	Energy (E_h)	IF
AAAAAAA	−3813.472864	0
AAAAAAB	−3813.464855	0
AAAABBB	−3813.463178	0
BAAAAAB	−3813.458550	0
BAAABBB	−3813.450718	0
AAABBBA	−3813.458539	0

Table S19. Energies for optimized **oP^{10}F(M)$'$**. IF = number of imaginary frequencies.

Position	AAAAAAA	AAAAAAB	AAAABBB	AAABBBA	BAAAAAB	BAAABBB
1a	26.08	27.23	25.40	25.39	26.72	25.23
1a	26.19	25.29	24.93	26.16	25.18	24.92
1b	25.79	25.45	25.31	25.28	25.21	25.29
1b	25.83	25.61	24.85	25.16	25.23	25.10
2b	25.53	25.24	24.87	25.31	25.13	24.85
2c	25.65	25.67	25.42	25.34	25.57	25.39
2e	26.53	26.62	25.82	25.40	26.43	25.75
3b	25.86	26.44	26.17	25.31	26.38	26.07
3d	25.92	26.03	26.24	26.07	26.03	25.99
3e	26.43	26.32	27.32	26.00	26.15	27.31
4b	26.81	25.73	25.51	26.02	25.60	25.39
4c	26.20	25.66	26.13	26.14	25.53	26.04
4e	27.24	27.07	27.00	27.73	26.68	26.51
5b	27.09	27.23	26.41	27.98	26.86	26.26
5d	25.98	26.16	25.97	26.46	26.00	25.69
5e	26.35	26.10	26.22	26.42	25.67	25.59
5e'	26.35	25.98	25.51	26.33	25.67	25.18
5d'	25.98	25.75	25.50	26.34	26.00	25.73
5b'	27.09	26.78	26.89	26.80	26.86	27.11
4e'	27.24	26.84	27.19	26.20	26.68	27.17
4c'	26.20	26.07	26.19	26.12	25.53	25.63
4b'	26.81	26.69	26.54	26.79	25.60	25.33
3e'	26.43	26.29	25.85	26.68	26.15	25.52
3d'	25.92	25.92	25.48	25.84	26.03	25.54
3b'	25.86	25.72	25.51	25.40	26.38	26.17
2e'	26.53	26.33	26.20	25.37	26.43	26.09
2c'	25.65	25.55	25.49	25.42	25.57	25.49
2b'	25.53	25.43	25.36	25.27	25.13	25.03
1b'	25.83	25.75	25.69	25.81	25.23	25.56
1b'	25.79	25.67	25.71	25.56	25.21	25.39
1a'	26.19	26.05	26.04	25.91	25.18	25.12
1a'	26.08	25.98	25.90	25.86	26.72	27.18

Table S20. Calculated (GIAO/PCM(chloroform)/WP04/6-31G(d)//PCM(chloroform)/B97-D/cc-pVDZ) ^{1}H isotropic shieldings for **oP^{10}F(M)′**.

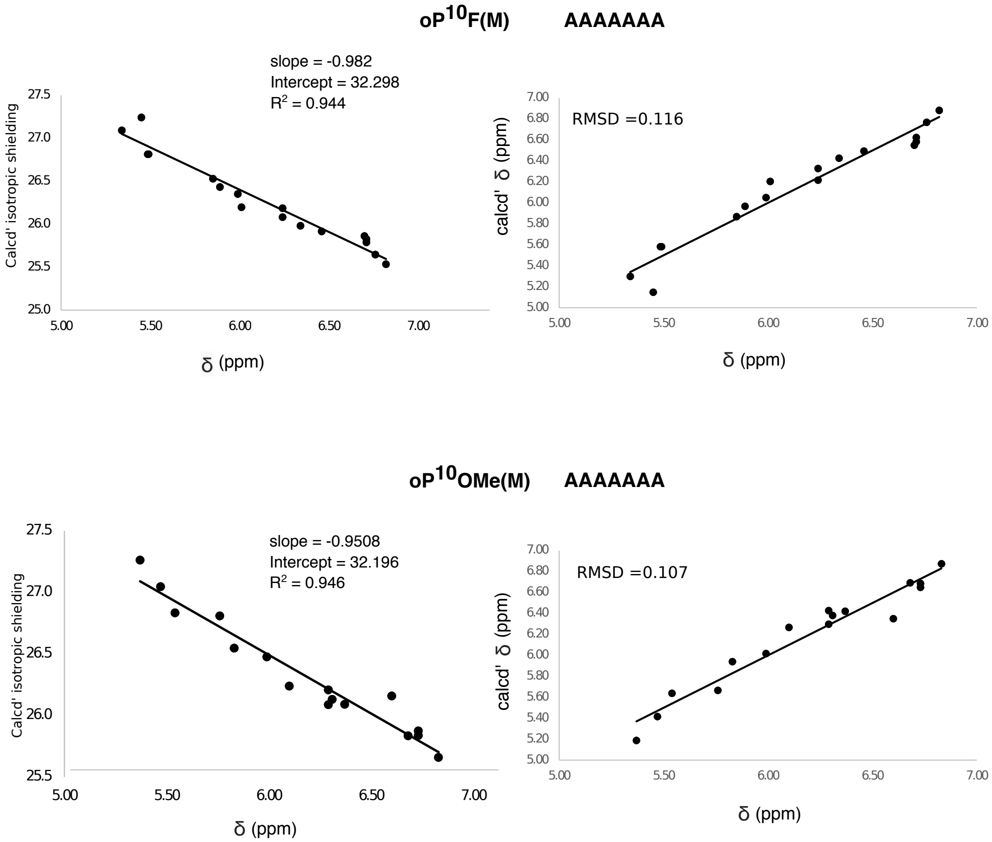

Figure S3. Comparisons of the calculated (GIAO/PCM(chloroform)/WP04/6-31G(d)//PCM(chloroform)/B97-D/ccpVDZ) isotropic shieldings (left) and corresponding scaled chemical shifts (right) against experimental chemical shifts for **oP^{10}F(M)′**/**oP^{10}F(M)** (top) and **oP^{10}OMe(M)′**/**oP^{10}-OMe(M)** (bottom).

Compound	Assigned geometry	p
oP^{10}F(M)	AAAAAAA	>99.99%
oP^{10}OMe(M)	AAAAAAA	>99.99%

Table S21. Geometry assignments to the major conformers of **oP^{10}F(M)** and **oP^{10}OMe(M)**.

Octamer models

Hexyloxy groups in **oP^{8}F(M)** were replaced with methoxy groups for the purpose of optimization, giving **oP^{8}F-(M)′**.

Conformer	Energy (E_h)	IF
AAAAA	−3122.730697	0
AAAAB	−3122.722679	0
AABBA	−3122.724903	0
BAAAB	−3122.715500	0
AAABB	−3122.718420	0
BAABB	−3122.714908	0

Table S22. Energies for optimized **oP^{8}F(M)′**. IF = number of imaginary frequencies.

Position	AAAAA	AAAAB	AAABB	AABBA	BAAAB	BAABB
1a	26.02	27.43	25.60	25.92	27.17	25.41
1a	26.10	25.25	24.95	25.83	25.11	25.00
1b	25.74	25.48	25.32	25.62	25.37	25.34
1b	25.76	25.77	25.59	25.56	25.55	25.56
2b	25.47	25.20	24.98	25.16	25.03	25.01
2c	25.58	25.59	25.42	25.66	25.49	25.78
2e	26.57	26.54	27.84	26.91	26.06	28.27
3b	25.80	26.37	26.18	25.68	26.15	26.17
3d	25.78	25.92	26.17	25.29	25.61	25.96
3e	26.17	26.12	26.20	25.16	25.60	25.77
4b	26.60	25.52	25.68	26.55	25.20	25.15
4c	25.99	25.45	25.97	26.71	25.66	25.73
4e	26.96	26.80	26.68	28.42	27.03	26.50
4e'	26.96	27.12	26.06	26.67	27.03	25.77
4c'	25.99	26.15	26.05	26.10	25.66	25.39
4b'	26.60	26.32	26.60	26.02	25.20	25.32
3e'	26.17	25.81	26.52	27.50	25.60	26.16
3d'	25.78	25.56	25.85	25.92	25.61	25.90
3b'	25.80	25.50	25.30	25.30	26.15	25.85
2e'	26.57	26.19	25.65	25.36	26.06	26.15
2c'	25.58	25.46	25.31	25.42	25.49	25.51
2b'	25.47	25.35	25.17	25.41	25.03	25.10
1b'	25.76	25.59	25.63	25.38	25.55	26.27
1b'	25.74	25.72	25.46	26.11	25.37	25.43
1a'	26.10	25.95	25.82	26.49	25.11	25.10
1a'	26.02	25.83	25.66	25.53	27.17	27.84

Table S23. Calculated (GIAO/PCM(chloroform)/WP04/6-31G(d)//PCM(chloroform)/B97-D/cc-pVDZ) ^{1}H isotropic shieldings for **oP^{8}F(M)**.

Conformer	Energy (E_h)	IF
AAAAA	−2725.936446	0
AAAAB	−2725.930261	0
AABBA	−2725.934333	0
BAAAB	−2725.924762	0
AAABB	−2725.924425	0
BAABB	−2725.921736	0

Table S24. Energies for optimized **oP^{8}H(M)′**. IF = number of imaginary frequencies.

Position	AAAAA	AAAAB	AAABB	AABBA	BAAAB	BAABB
1a	26.04	27.38	25.62	25.94	27.09	25.43
1a	26.06	25.23	24.97	25.76	25.08	24.95
1b	25.71	25.50	25.37	25.63	25.38	25.35
1b	25.81	25.81	25.69	25.62	25.59	25.61
2b	25.52	25.21	25.03	25.20	25.05	25.04
2c	25.27	25.29	25.12	25.28	25.18	25.36
2d	25.48	25.26	25.13	25.23	25.55	25.49
2e	26.13	26.22	27.45	26.33	25.68	27.63
3b	25.48	26.02	25.85	25.33	25.79	25.75
3c	25.29	25.69	25.36	24.99	25.50	25.60
3d	25.54	25.66	25.81	24.96	25.32	25.66
3e	26.29	26.26	26.15	25.17	25.65	25.84
4b	26.66	26.33	26.59	26.17	25.21	25.33
4c	26.17	25.65	26.15	26.74	25.74	25.85
4e	27.02	26.89	26.69	28.38	27.17	26.60
4e'	27.02	27.25	26.05	26.63	27.17	25.82
4c'	26.17	26.20	26.06	26.24	25.74	25.44
4b'	26.66	25.58	25.70	26.54	25.21	25.22
3e'	26.29	25.86	26.47	27.58	25.65	26.23
3d'	25.54	25.24	25.52	25.60	25.32	25.61
3c'	25.29	25.00	25.20	25.59	25.50	25.44
3b'	25.48	25.17	25.07	24.98	25.79	25.56
2e'	26.13	25.76	25.63	25.08	25.68	25.80
2d'	25.48	25.76	25.70	24.99	25.55	26.00
2c'	25.27	25.15	24.99	25.09	25.18	25.20
2b'	25.52	25.39	25.20	25.46	25.05	25.10
1b'	25.81	25.64	25.69	25.43	25.59	26.04
1b'	25.71	25.72	25.48	26.12	25.38	25.33
1a'	26.06	25.94	25.76	26.51	25.08	25.05
1a'	26.04	25.86	25.68	25.54	27.09	27.46

Table S25. Calculated (GIAO/PCM(chloroform)/WP04/6-31G(d)//PCM(chloroform)/B97-D/cc-pVDZ) ^{1}H isotropic shieldings for **oP^{8}H(M)**.

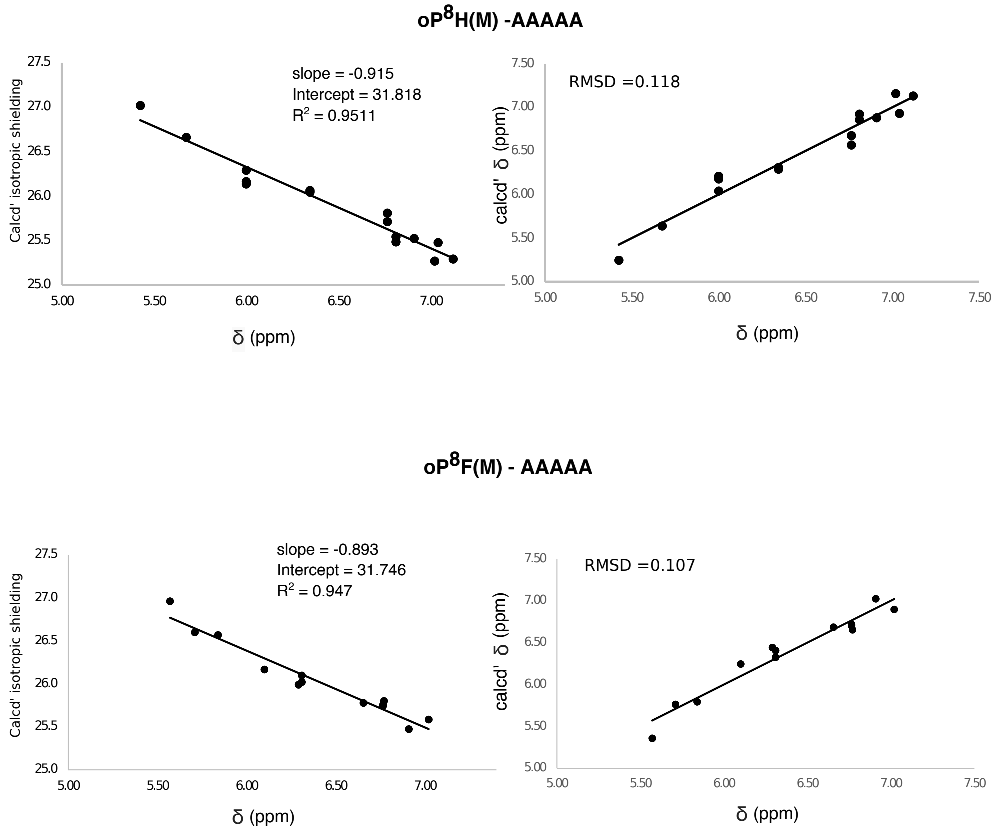

Figure S4. Comparisons of the calculated (GIAO/PCM(chloroform)/WP04/6-31G(d)//PCM(chloroform)/B97-D/ccpVDZ) isotropic shieldings (left) and corresponding scaled chemical shifts (right) against experimental chemical shifts for **oP^{8}H(M)′/oP^{8}H(M)** (top) and **oP^{8}F(M)′/oP*F(M)** (bottom).

Compound	Assigned geometry	p
oP^{8}H(M)	AAAAA	>99.99%
oP^{8}F(M)	AAAAA	>99.99%

Table S26. Geometry assignments to the major conformers of **oP^{8}H(M)** and **oP^{8}F(M)**.

Parent conformer libraries

Parent oligomer geometries were optimized at the (gas-phase) B97-D/cc-pVDZ level.

Geometry assignments

Assignments of *o*-phenylene geometries within the macrocycles were made by comparison of the experimental $\Delta\delta^{\text{exp}}$ values to the $\Delta\delta^{\text{calc}}$ values obtained for computational libraries of the parent oligomers, as described in the manuscript and in previous work.[2] The best matches all had RMSD values below 0.2 ppm, and most were around 0.1 ppm, as expected.

To establish the statistical significance of the match, comparisons are made using the F statistic

$$F = \frac{\sum\left(\Delta\delta_{\text{match}}^{\text{exp}} - \Delta\delta_{\text{match}}^{\text{calc}}\right)^2}{\sum\left(\Delta\delta_{\text{alt}}^{\text{exp}} - \Delta\delta_{\text{alt}}^{\text{calc}}\right)^2} \tag{2}$$

where $\Delta\delta_{\text{match}}^{\text{exp}}$ and $\Delta\delta_{\text{match}}^{\text{calc}}$ refer to the identified match and $\Delta\delta_{\text{alt}}^{\text{exp}}$ and $\Delta\delta_{\text{alt}}^{\text{calc}}$ refer to a random permutation of the data with analogous $\Delta\delta$ values swapped. The total number of permutations was capped at 2^{20}. The p value is then determined by the ranking of the true data in the list of permutations.[2] This algorithm was applied using the Python program on p S41.

Deca(*o*-phenylene library)

Energies, bite angles, and NMR predictions for the 37 conformers of deca(*o*-phenylene) were previously reported.[2]

Octa(*o*-phenylene) library

Conformer	Energy (E_h)	IF	Bite angle (°)
AAAAA	-1848.397825	0	179.17
AAAAB	-1848.393153	0	35.99
AAABB	-1848.389950	0	93.39
AABBA	-1848.390830	0	25.86
AABBB	-1848.386352	0	116.19
ABBAB	-1848.387994	0	128.89
ABBBA	-1848.385605	0	109.87
ABBBB	-1848.380482	0	99.13
BAAAB	-1848.390128	0	107.52
BAABB	-1848.388118	0	85.6
BABBB	-1848.383527	0	85.56
BBABB	-1848.383668	0	170.74
BBBBB	-1848.375774	0	57.14

Table S27. Conformer energies and bite angles for octa(*o*-phenylene). IF = number of imaginary frequencies.

Position	AAAAA	AAAAB	AAABB	AABBA	AABBB	ABBAB
1a	26.22	25.99	25.74	26.03	25.92	25.50
1a	26.15	26.03	25.82	25.57	25.43	26.46
1b	25.51	25.50	25.32	25.16	25.10	25.61
1c	25.48	25.41	25.35	25.21	25.15	25.38
1b	25.74	25.58	25.58	25.50	25.42	25.26
2e	26.22	25.89	25.64	26.61	26.41	25.17
2d	25.63	25.40	25.23	25.73	25.44	25.04
2c	25.41	25.26	25.01	25.41	25.19	25.11
2b	25.67	25.54	25.27	25.31	25.15	25.56
3e	26.24	25.89	26.60	25.40	25.33	27.73
3d	25.50	25.21	25.57	25.01	24.94	25.90
3c	25.26	24.96	25.18	25.03	24.95	25.34
3b	25.45	25.14	25.03	25.42	25.31	25.04
4e	26.43	26.68	25.48	28.27	25.68	25.32
4d	25.70	25.87	25.20	26.09	25.68	25.39
4c	25.79	25.90	25.61	25.81	25.63	25.65
4b	26.65	26.49	26.61	26.72	26.55	26.18
4b'	26.65	25.48	25.66	26.05	25.39	25.03
4c'	25.79	25.17	25.66	25.73	25.55	25.28
4d'	25.70	25.47	25.56	25.75	25.68	25.84
4e'	26.43	26.37	26.18	26.07	25.92	28.12
3b'	25.44	26.09	25.84	24.99	25.73	25.92
3c'	25.26	25.76	25.66	25.26	25.61	25.53
3d'	25.50	25.63	25.81	25.72	25.68	25.19
3e'	26.24	26.21	26.21	27.75	27.66	24.91
2b'	25.66	25.36	25.08	25.56	24.99	25.31
2c'	25.40	25.32	25.17	25.09	25.17	25.14
2d'	25.64	25.75	25.44	24.96	25.46	25.31
2e'	26.21	26.34	27.55	25.02	25.50	25.33
1b'	25.74	25.67	25.58	25.33	25.34	25.94
1c'	25.48	25.36	25.32	25.49	25.18	25.44
1b'	25.51	25.20	25.06	25.71	24.97	25.25
1a'	26.15	25.30	24.98	26.48	24.90	25.28
1a'	26.21	27.37	25.62	25.53	25.35	27.83

Table S28. Calculated (GIAO/PCM(chloroform)/WP04/6-31G(d)//B97-D/cc-pVDZ) ^{1}H isotropic shieldings for parent octa(*o*-phenylene) conformers.

Position	ABBBA	ABBBB	BAAAB	BAABB	BABBB	BBABB
1a	25.37	25.36	27.38	27.65	27.59	25.58
1a	26.02	26.31	25.16	25.13	25.14	25.02
1b	25.11	25.39	25.11	25.09	25.15	25.06
1c	25.11	25.24	25.27	25.33	25.38	25.28
1b	25.17	25.16	25.56	25.99	25.83	25.51
2e	25.01	24.96	25.75	25.97	25.16	27.67
2d	24.94	24.90	25.60	25.57	25.21	25.76
2c	25.02	25.02	25.19	25.19	25.02	25.28
2b	25.43	25.45	25.17	25.19	25.10	25.13
3e	25.86	25.54	25.63	26.16	24.81	25.14
3d	25.68	25.51	25.28	25.58	25.13	25.32
3c	25.26	25.17	25.52	25.42	25.46	25.42
3b	24.89	24.81	25.84	25.57	25.79	25.72
4e	28.41	25.45	26.81	25.24	25.47	24.80
4d	25.97	25.56	25.67	24.92	25.39	25.11
4c	25.82	25.67	25.38	24.93	25.10	25.40
4b	26.04	25.89	25.27	25.26	24.82	25.40
4b'	26.04	25.39	25.26	25.20	25.48	25.39
4c'	25.81	25.65	25.37	25.47	25.47	25.41
4d'	25.97	25.92	25.68	25.66	25.33	25.10
4e'	28.42	28.06	26.82	26.10	25.13	24.80
3b'	24.90	25.63	25.84	25.75	25.75	25.72
3c'	25.27	25.60	25.51	25.60	25.67	25.42
3d'	25.68	25.62	25.29	25.71	25.86	25.32
3e'	25.85	25.51	25.63	25.95	27.54	25.13
2b'	25.42	24.97	25.16	25.00	25.05	25.13
2c'	25.03	25.10	25.20	25.19	25.18	25.28
2d'	24.95	25.31	25.60	25.87	25.46	25.76
2e'	25.00	25.31	25.76	27.64	25.51	27.67
1b'	25.17	25.41	25.57	25.54	25.61	25.51
1c'	25.10	25.23	25.28	25.30	25.31	25.28
1b'	25.11	25.00	25.11	25.04	25.06	25.06
1a'	26.00	24.89	25.15	24.91	24.97	25.02
1a'	25.36	25.35	27.38	25.50	25.62	25.58

Table S29. Calculated (GIAO/PCM(chloroform)/WP04/6-31G(d)//B97-D/cc-pVDZ) ^{1}H isotropic shieldings for parent octa(*o*-phenylene) conformers (cont.).

Position	BBBBB
1a	25.28
1a	24.87
1b	24.97
1c	25.18
1b	25.36
2e	25.21
2d	25.32
2c	25.10
2b	24.93
3e	25.19
3d	25.46
3c	25.51
3b	25.55
4e	25.23
4d	25.49
4c	25.49
4b	25.19
4b'	25.19
4c'	25.49
4d'	25.49
4e'	25.23
3b'	25.55
3c'	25.51
3d'	25.46
3e'	25.19
2b'	24.93
2c'	25.10
2d'	25.31
2e'	25.21
1b'	25.36
1c'	25.19
1b'	24.96
1a'	24.87
1a'	25.29

Table S30. Calculated (GIAO/PCM(chloroform)/WP04/6-31G(d)//B97-D/cc-pVDZ) ^{1}H isotropic shieldings for parent octa(*o*-phenylene) conformers (cont.).

Decamer macrocycles

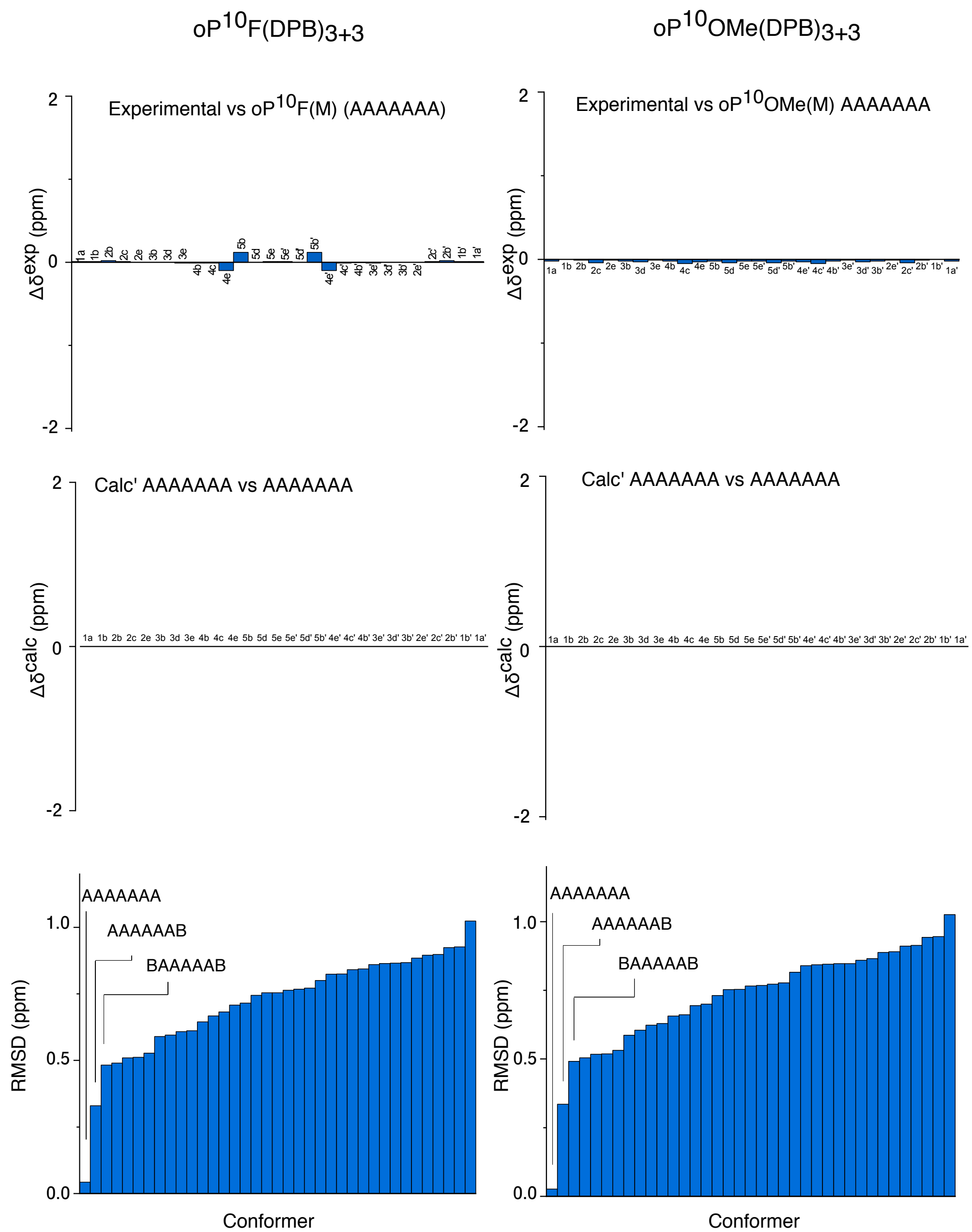

Figure S5. For **oP^{10}F(DPB)$_{3+3}$** (left) and **oP^{10}OMe(DPB)$_{3+3}$** (right), experimental $\Delta\delta^{exp}$ (top), calculated $\Delta\delta^{calc}$ values for the AAAAAAA conformer of deca(*o*-phenylene) (middle), and RMSD values of $\Delta\delta_{calc}$ vs $\Delta\delta_{exp}$ for all possible deca(*o*-phenylene) conformers (bottom).

Conformer	RMSD
AAAAAAA	0.043
AAAAAAB	0.330
BAAAAAB	0.483
AAAAABB	0.490
AAABBAA	0.510
AAAABBB	0.511
AAAABBA	0.528
AAABBBA	0.590
AABBBAA	0.595
AAABBBB	0.608
AABBAAB	0.611
BAAAABB	0.645
ABBAAAB	0.667
AAABBAB	0.682
AABBBBA	0.708
BAAABBB	0.715
BAABBBB	0.745
AABBBBB	0.754
ABBBAAB	0.754
BAABBAB	0.763
ABBAABB	0.768
ABBBBBA	0.772
BBAAABB	0.800
AABBABB	0.824
BBAABBB	0.825
ABBBBBB	0.841
AABBBAB	0.843
ABBABBB	0.860
ABBABBA	0.864
BBABBBB	0.865
ABBBBAB	0.868
ABBBABB	0.884
BABBBBB	0.895
BBBABBB	0.898
BABBABB	0.924
BBBBBBB	0.927
BABBBAB	1.024

Table S31. RMSDs of $\Delta\delta_{exp}$ for **oP^{10}F(DPB)$_{3+3}$** (vs **oP^{10}F(M)**) compared to $\Delta\delta_{calc}$ for deca(*o*-phenylene) (XXXXXXX vs AAAAAAA).

Conformer	RMSD
AAAAAAA	0.026
AAAAAAB	0.335
BAAAAAB	0.491
AAAAABB	0.504
AAABBAA	0.517
AAAABBA	0.519
AAAABBB	0.532
AAABBBA	0.586
AABBBAA	0.605
AABBAAB	0.623
AAABBBB	0.630
BAAAABB	0.656
ABBAAAB	0.661
AAABBAB	0.694
AABBBBA	0.700
BAAABBB	0.731
ABBBBBA	0.753
ABBBAAB	0.754
BAABBBB	0.766
AABBBBB	0.768
ABBAABB	0.773
BAABBAB	0.777
BBAAABB	0.816
AABBABB	0.840
ABBBBBB	0.843
ABBABBA	0.845
AABBBAB	0.847
BBAABBB	0.847
ABBABBB	0.859
ABBBBAB	0.865
BBABBBB	0.888
ABBBABB	0.890
BABBBBB	0.911
BBBABBB	0.913
BABBABB	0.943
BBBBBBB	0.945
BABBBAB	1.026

Table S32. RMSDs of $\Delta\delta_{exp}$ for **oP^{10}OMe(DPB)$_{3+3}$** (vs **oP^{10}OMe(M)**) compared to $\Delta\delta_{calc}$ for deca(*o*-phenylene) (XXXXXXX vs AAAAAAA).

Conformer	RMSD
BAAAAAB	0.198
AAAAAAB	0.405
BAAAABB	0.468
AAAABBB	0.474
BAAABBB	0.482
AAAAABB	0.514
BAABBBB	0.532
AAAAAAA	0.533
AAABBBB	0.545
AABBAAB	0.613
ABBAAAB	0.620
BBAABBB	0.620
BBBBBBB	0.626
AABBBBB	0.641
BAABBAB	0.647
BBAAABB	0.657
ABBBBBB	0.658
BABBBBB	0.665
AAABBBA	0.666
BBABBBB	0.671
BBBABBB	0.672
AAAABBA	0.675
ABBBAAB	0.678
AAABBAA	0.682
AAABBAB	0.698
ABBAABB	0.699
AABBBAA	0.709
ABBBBBA	0.715
AABBBBA	0.731
ABBABBB	0.757
ABBBBAB	0.763
BABBABB	0.793
AABBABB	0.829
AABBBAB	0.836
ABBBABB	0.840
ABBABBA	0.883
BABBBAB	0.954

Table S33. RMSDs of $\Delta\delta_{exp}$ for **oP[10]OMe(DPB)$_{2+2}$** major conformer (vs **oP[10]OMe(M)**) compared to $\Delta\delta_{calc}$ for deca(*o*-phenylene) (XXXXXXX vs AAAAAAA).

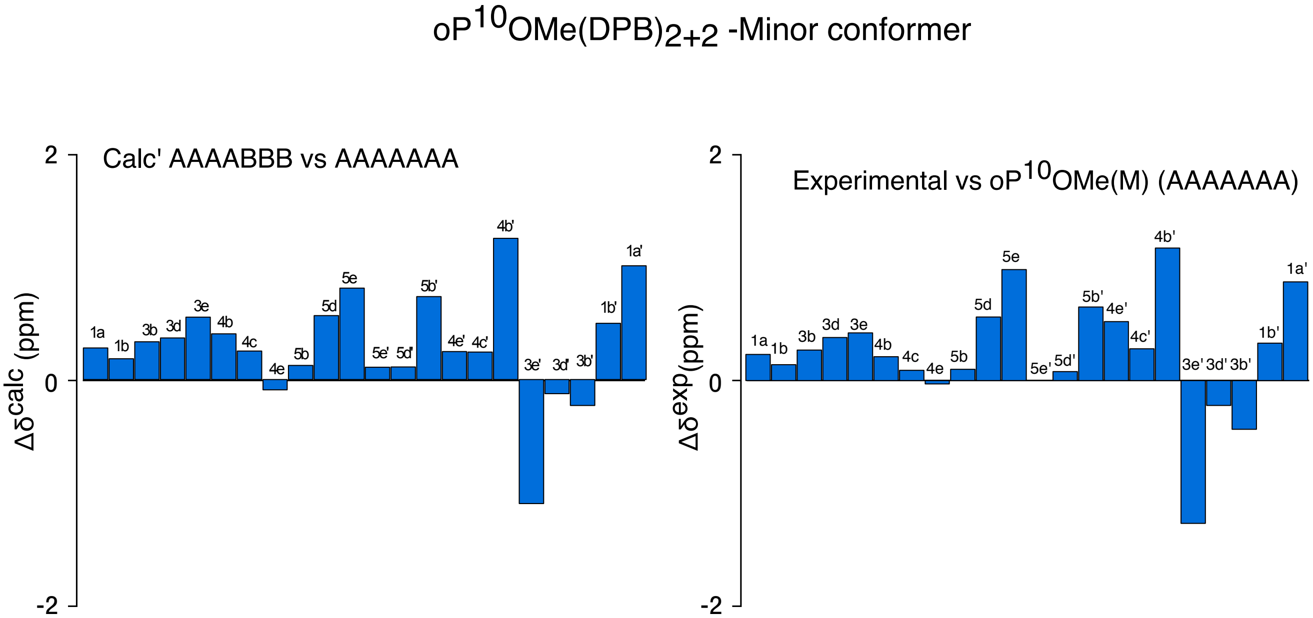

Figure S6. Calculated $\Delta\delta_{calc}$ for the parent deca(*o*-phenylene) AAAABBB vs AAAAAAA (left) and experimental $\Delta\delta_{exp}$ for the minor conformation of **oP^{10}OMe(DPB)$_{2+2}$** *o*-phenylene (vs **oP^{10}OMe(M)**). Note: ring 2 could not assigned clearly due to lack of clear cross-peaks in the 2D NMR spectra.

Conformer	RMSD	Conformer	RMSD
AAAABBB	0.111	ABBAAAA	0.713
BAAABBB	0.398	BBBBABB	0.716
AAAAAAB	0.407	AAABBBA	0.719
AAAAABB	0.424	ABBAAAB	0.727
BBAABBB	0.460	ABBBABB	0.737
BAAAAAB	0.481	BBBAAAB	0.740
AAAAAAA	0.487	BABBBBB	0.744
BBAAAAA	0.540	AABBBBA	0.754
AAAABBA	0.541	BABBABB	0.757
BAAAAAA	0.542	AABBBAA	0.757
AABBAAA	0.547	BBBBBBB	0.758
AABBAAB	0.559	BBBABBA	0.779
AAABBBB	0.563	ABBBBBA	0.783
BBAAAAB	0.563	AAABBAA	0.795
BAAAABB	0.564	BBABBBB	0.798
BBAABBA	0.592	ABBABBA	0.814
BBBBAAA	0.598	BBBBBBA	0.823
BAAABBA	0.599	ABBBBAA	0.833
AABBBBB	0.615	BAABBAA	0.842
ABBBAAA	0.621	BAABBBA	0.844
ABBABBB	0.638	AABBBAB	0.845
BBBABBB	0.654	BBBBBAA	0.849
ABBAABB	0.657	AAABBAB	0.855
AABBABB	0.663	BABBBBA	0.876
BBAAABB	0.663	BAABBAB	0.905
BBBBAAB	0.667	BBBBBAB	0.905
BBBAAAA	0.675	ABBBBAB	0.906
ABBBBBB	0.681	BABBBAA	0.913
BAABBBB	0.683	BBABBBA	0.925
ABBBAAB	0.699	BBABBAA	0.951
BABBAAB	0.707	BBABBAB	0.957
BABBAAA	0.708	BABBBAB	0.996
BBBAABB	0.711		

Table S34. RMSDs of $\Delta\delta_{exp}$ for **oP^{10}OMe(DPB)$_{2+2}$** minor conformer (vs **oP^{10}OMe(M)**) compared to $\Delta\delta_{calc}$ for deca(*o*-phenylene) (XXXXXXX vs AAAAAAA).

Compound	Assigned geometry	p
oP^{10}F(DPB)$_{3+3}$	AAAAAAA	>99.99%
oP^{10}OMe(DPB)$_{3+3}$	AAAAAAA	>99.99%
oP^{10}OMe(DPB)$_{2+2}$, major conf.	BAAAAAB	>99.99%
oP^{10}OMe(DPB)$_{2+2}$, minor conf.	AAAABBB	>99.99%

Table S35. Geometry assignments for *o*-phenylenes in decamer macrocycles.

Octamer macrocycles

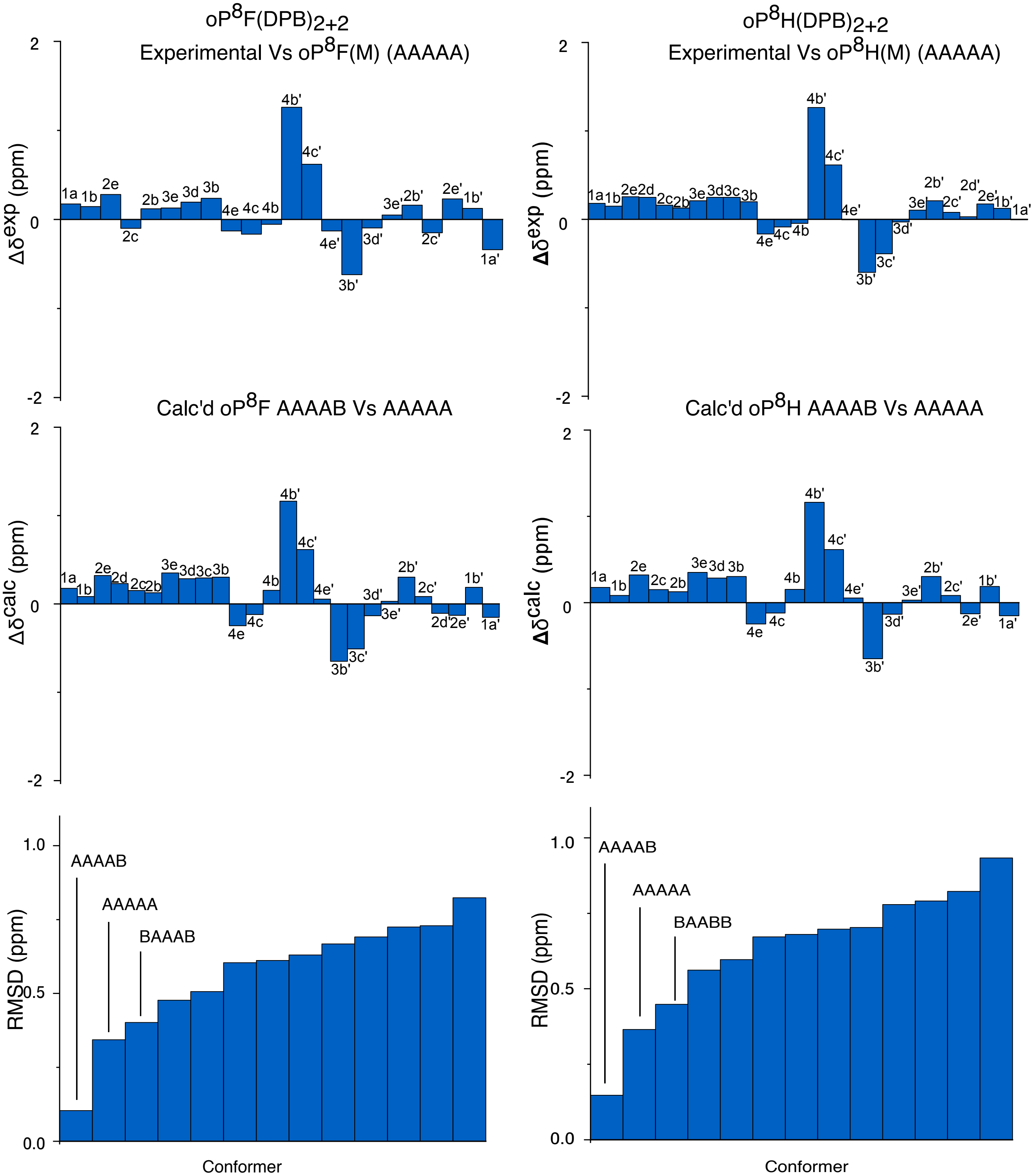

Figure S7. For **oP**[8]**F(DPB)**$_{2+2}$ (left) and **oP**[8]**H(DPB)**$_{2+2}$ (right), experimental $\Delta\delta^{exp}$ (top), calculated $\Delta\delta^{calc}$ values for the AAAAB conformer of octa(*o*-phenylene) (middle), and RMSD values of $\Delta\delta_{calc}$ vs $\Delta\delta_{exp}$ for all possible octa(*o*-phenylene) conformers (bottom).

Conformer	RMSD
AAAAB	0.147
AAAAA	0.365
BAAAB	0.448
BAAAA	0.549
AAABB	0.562
AABBB	0.597
BBAAB	0.656
ABBBB	0.672
AABBA	0.680
BBAAA	0.694
ABBAB	0.698
BAABB	0.703
BBBAA	0.736
BBBBA	0.741
ABBAA	0.742
BBBAB	0.748
ABBBA	0.779
BBBBB	0.791
BABBB	0.822
BABBA	0.842
BBABB	0.933

Table S36. RMSDs of $\Delta\delta_{exp}$ for **oP^{8}F(DPB)$_{2+2}$** (vs **oP^{8}F(M)**) compared to $\Delta\delta_{calc}$ for octa(*o*-phenylene) (XXXXX vs AAAAA).

Conformer	RMSD
AAAAB	0.145
AAAAA	0.369
BAAAB	0.451
BAAAA	0.553
AAABB	0.559
AABBB	0.591
BBAAB	0.642
AABBA	0.677
BBAAA	0.684
ABBBB	0.685
BAABB	0.701
ABBAB	0.712
BBBAA	0.724
BBBBA	0.725
BBBAB	0.732
ABBAA	0.758
BBBBB	0.773
ABBBA	0.794
BABBB	0.813
BABBA	0.835
BBABB	0.919

Table S37. RMSDs of $\Delta\delta_{exp}$ for **oP^{8}F(Phen)$_{2+2}$** (vs **oP^{8}F(M)**) compared to $\Delta\delta_{calc}$ for octa(*o*-phenylene) (XXXXX vs AAAAA).

Conformer	RMSD
AAAAB	0.104
AAAAA	0.344
BAAAB	0.402
AAABB	0.477
AABBB	0.507
BAAAA	0.529
BBAAB	0.601
ABBBB	0.604
BAABB	0.612
AABBA	0.630
BBAAA	0.632
ABBAB	0.668
BBBAA	0.675
BBBBA	0.679
BBBBB	0.691
BBBAB	0.694
ABBAA	0.701
BABBB	0.725
ABBBA	0.729
BABBA	0.767
BBABB	0.824

Table S38. RMSDs of $\Delta\delta_{exp}$ for **oP^{8}H(DPB)$_{2+2}$** (vs **oP^{8}H(M)**) compared to $\Delta\delta_{calc}$ for octa(*o*-phenylene) (XXXXX vs AAAAA).

Conformer	RMSD
AAAAB	0.111
AAAAA	0.355
BAAAB	0.406
AAABB	0.501
AABBB	0.530
BAAAA	0.541
BBAAB	0.598
ABBBB	0.624
AABBA	0.634
BAABB	0.637
BBAAA	0.639
ABBAB	0.665
BBBBA	0.681
BBBAA	0.683
BBBAB	0.690
BBBBB	0.706
ABBAA	0.712
ABBBA	0.735
BABBB	0.746
BABBA	0.777
BBABB	0.835

Table S39. RMSDs of $\Delta\delta_{exp}$ for **oP^{8}H(Phen)$_{2+2}$** (vs **oP^{8}H(M)**) compared to $\Delta\delta_{calc}$ for octa(*o*-phenylene) (XXXXX vs AAAAA).

Compound	Assigned geometry	p
oP⁸F(DPB)$_{2+2}$	AAAAB	96.7%
oP⁸H(DPB)$_{2+2}$	AAAAB	99.9%

Table S40. Geometry assignments for *o*-phenylenes in octamer macrocycles.

Macrocycle geometries

Full macrocycles were optimized at the PCM(chloroform)/B97-D/cc-pVDZ level. Beyond the folding state of the *o*-phenylene, the primary consideration is the orientation of the imine groups. Here, these are based on PES scans at the ends of acyclic oligomers (at the PCM(chloroform)/B97-D/cc-pVDZ level). The two lowest-energy orientations were optimized separately, then the lowest-energy overall used to construct starting macrocycle geometries. The full macrocycles were then optimized first at the PM7 level and then at the PCM(chloroform)/B97-D/cc-pVDZ level to obtain the final geometries. This does not, of course, guarantee that we obtain the global conformational energy minimum, but it should provide a reasonable geometry for the purposes of gauging the fit of the *o*-phenylene within the macrocycle.

Decamer macrocycles

Note that geometries of the [2+2] macrocycles were previously reported.[2]

Conformer	Energy (E_h)	IF
Homochiral	−9329.452639	0
Heterochiral	−9329.452422	0

Table S41. Energies for optimized (AAAAAAA)$_3$ *o*-phenylene decamer [3+3] macrocycles. IF = number of imaginary frequencies.

Octamer macrocycles

Conformer	Energy (E_h)	IF
Homochiral-parallel	−5296.015304	0
Homochiral-antiparallel	−5296.019483	0
Heterochiral-parallel	−5296.020113	0
Heterochiral-antiparallel	−5296.019483	0

Table S42. Energies for optimized (AAAAB)$_3$ *o*-phenylene octamer [2+2] macrocycles. IF = number of imaginary frequencies.

Program for statistical analysis

The following program was used previously[2] but is included here for reference.

```
"""NMR comparison module.

Allows an experimental NMR spectrum to be compared to two calculated
spectra, one presumed to be a good match, the other not. Provides a
one-tailed, non-parametric statistical comparison by ranking the quality
of the good match vs a large sample of permutations, as described in
2010 JOC 8627. If it is possible to consider all possible permutations,
it will do so. Otherwise, a number of random permutations is considered
up to the constant max_swaps.

Requires 3 arguments:
    1. A text file with the experimental data. This is a simple list of
```

```
        numbers (1 per line).
    2. A text file with the proposed "good" match to the data. The order
        of the numbers must match.
    3. A text file of the proposed "bad" match.

Optional arguments:
    output_file: Filename for output.
    max_swaps (int): Maximum number of permutations that will be
        considered.
    direct: switches to the test_func_direct error function if no
        regression is needed.
"""

import sys
import scipy.stats
import numpy as np
import argparse


def test_func_reg(exp, calc1, calc2):
    """Quantify quality of match given an experimental spectrum and two
    calculated spectra. This function uses the standard error of a
    linear regression as its basis, and is appropriate for direct
    comparisons of spectra.

    Args:
        exp (list): The experimental spectrum as a list of chemical
            shifts.
        calc1 (list): The proposed "good" spectrum.
        calc2 (list): The proposed "bad" spectrum.

    Returns:
        The F-statistic comparing the variances on linear fits between
        the two calculated spectra and the experimental spectrum.
    """

    s1_regress = scipy.stats.linregress(exp, calc1)
    s2_regress = scipy.stats.linregress(exp, calc2)

    # The std error of the fit is stored as the 5th element of each
    # tuple.
    return s2_regress[4]**2/s1_regress[4]**2


def test_func_direct(exp, calc1, calc2):
    """Quantify quality of match given two sets of experimental data.
    This function uses the sum squared error and is appropriate for
    comparisons where the data will not be scaled by refitting after
    swaps have been made (e.g., changes in chemical shifts).
```

```
    """

    sq_err1 = [(exp[n] - calc1[n])**2 for n in range(len(exp))]
    sq_err2 = [(exp[n] - calc2[n])**2 for n in range(len(exp))]

    return sum(sq_err2)/sum(sq_err1)


def permute_spec(seed, s1, s2):
    """Permute two sets of data.

    Args:
        seed (int): Number used to seed the permutation. Will be
            converted into binary and then used as follows: 0=no swap,
            1=swap on an element by element basis.
        s1, s2 (lists): The sets to be permuted. Must be the same
            length.

    Returns:
        The new sets, as a tuple.
    """

    s1_new = []
    s2_new = []

    # Converts seed to a binary string with leading zeros, of matching
    # length to the lists.
    swap_key = "{seed:0{length}b}".format(seed=seed, length=len(s1))

    for n in range(len(s1)):
        if swap_key[n] == "0":
            s1_new.append(s1[n])
            s2_new.append(s2[n])
        elif swap_key[n] == "1":
            s1_new.append(s2[n])
            s2_new.append(s1[n])

    return s1_new, s2_new


def main():
    parser = argparse.ArgumentParser()
    parser.add_argument(
        "exp_data",
        help="Datafile for experimental NMR spectrum")
    parser.add_argument(
        "good_match",
        help="Datafile for proposed good computational match")
    parser.add_argument(
        "bad_match",
```

```
    help="Datafile for proposed bad computational match")
parser.add_argument(
    "-o", "--output_file",
    help="Output filename")
parser.add_argument(
    "-m", "--max_swaps",
    help="Maximum number of permutations",
    type=int, default=2**20)
parser.add_argument(
    "-d", "--direct",
    help="Use direct errors (no regression)",
    action="store_true")
args = parser.parse_args()

max_swaps = args.max_swaps

if args.direct:
    test_func = test_func_direct
else:
    test_func = test_func_reg

exp = []   # The experimental data
set1 = []  # The first (better) comparison data
set2 = []  # The second comparison data

with open(args.exp_data) as exp_data_file:
    for line in exp_data_file:
        exp.append(float(line))

with open(args.good_match) as set1_data_file:
    for line in set1_data_file:
        set1.append(float(line))

with open(args.bad_match) as set2_data_file:
    for line in set2_data_file:
        set2.append(float(line))

# The error value for the original spectra.
comp_err = test_func(exp, set1, set2)

tests = [comp_err]  # Stores the results of the permutations

# Checks to see if it is possible to consider all possible
# permutations of the two spectra.
if 2**len(exp) <= max_swaps:
    all_possible = True
    num_considered = 2**len(exp)
    print("Able to consider all {:,} possibilities.".format(
            num_considered))
else:
```

```
        all_possible = False
        num_considered = max_swaps
        print("Number of permutations considered capped at {:,}.".format(
                num_considered))

    # Used in a progress indicator.
    increment = num_considered // 100

    for n in range(1, num_considered):
        # Simple progress indicator.
        if n % increment == 0:
            sys.stdout.write('\r')
            sys.stdout.write("Progress: {:4.0%}".format(n/num_considered))
            sys.stdout.flush()

        # If considering all possible spectra, the seed for permute_spec
        # is simply n. Otherwise, a random integer is generated between
        # 00...0 and 11...1.
        if all_possible:
            s1_perm, s2_perm = permute_spec(n, set1, set2)
        else:
            ranseed = np.random.randint(2**len(exp))
            s1_perm, s2_perm = permute_spec(ranseed, set1, set2)

        tests.append(test_func(exp, s1_perm, s2_perm))

    # Finishes progress indicator.
    sys.stdout.write("\n")
    sys.stdout.flush()

    tests.sort(reverse=True)  # Sort tests list for ranking

    rank = tests.index(comp_err) + 1  # Rank of original F stat in total list

    output_text = "Test function for true comparison: {}\n".format(comp_err)
    output_text += "Rank: {:,} out of {:,}\n".format(rank, len(tests))
    output_text += "p = {} ({:.4%})\n".format(
            rank/len(tests), 1 - rank/len(tests))

    if args.output_file:
        with open(args.output_file, 'w') as output_file:
            output_file.write(output_text)
    else:
        print(output_text)
```

GPC characterization

All GPC data was collected using a refractive index detector. While UV–vis absorbance could also be used, it is possible that the changing folding state of the *o*-phenylenes could significantly affect the absorptivities of different species, complicating analysis. This is not expected to be a significant issue with RI detection.

GPC traces of crude model compounds

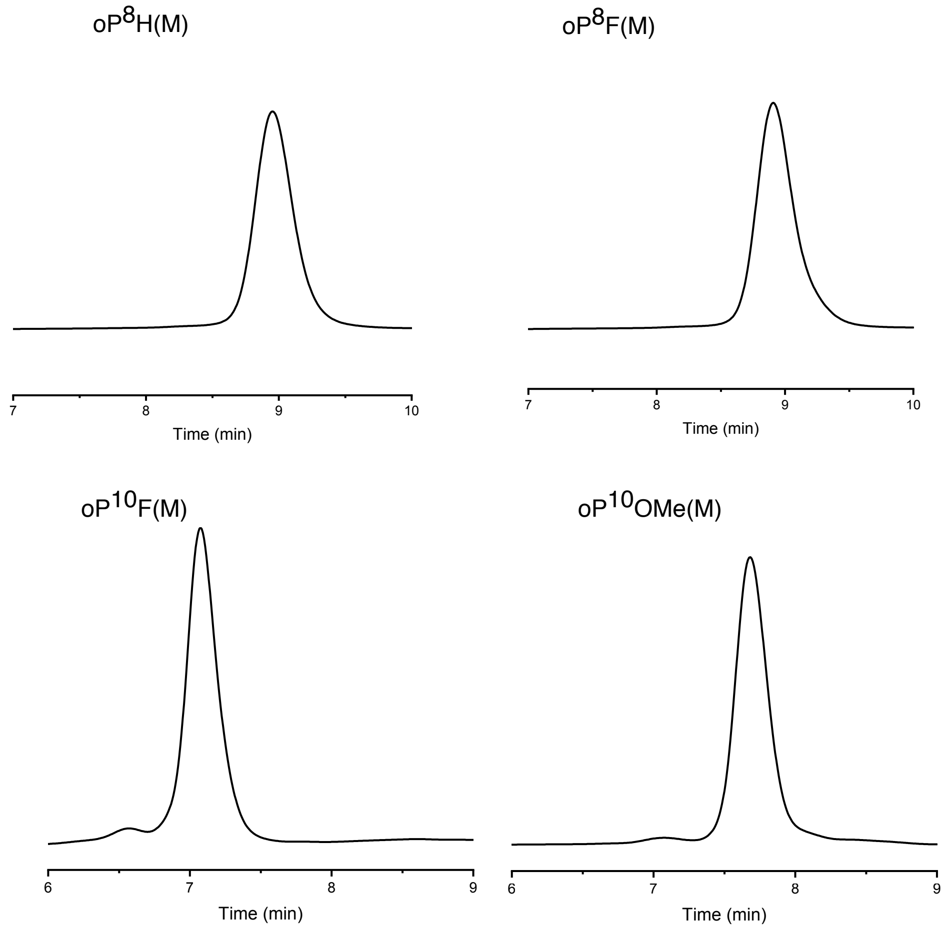

Figure S8. GPC traces of crude **oP⁸H(M)**, **oP⁸F(M)**, **oP¹⁰F(M)**, and **oP¹⁰OMe(M)**.

GPC traces of purified macrocycles

Octa(*o*-phenylene) macrocycles

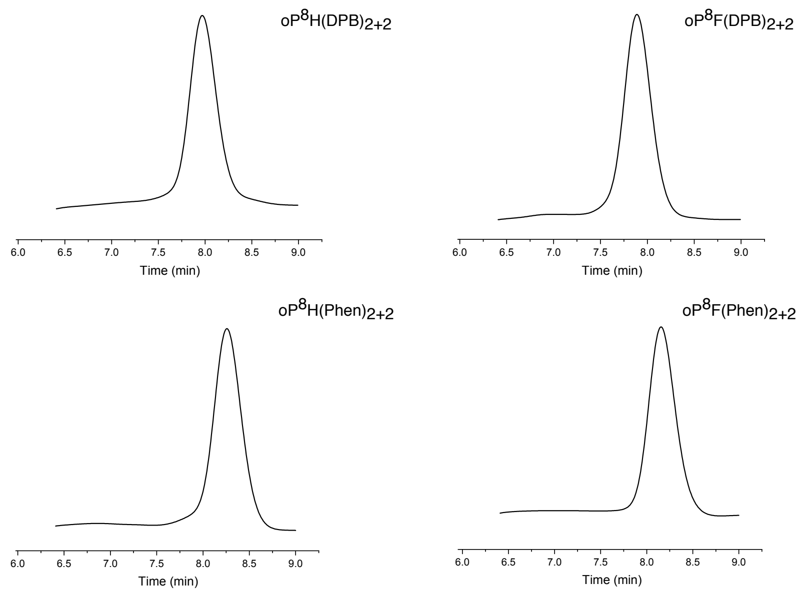

Figure S9. GPC traces of purified **oP^{8}H(DPB)$_{2+2}$**, **oP^{8}F(DPB)$_{2+2}$**, **oP^{8}H(Phen)$_{2+2}$**, and **oP^{8}F(Phen)$_{2+2}$**.

Deca(*o*-phenylene) macrocycles

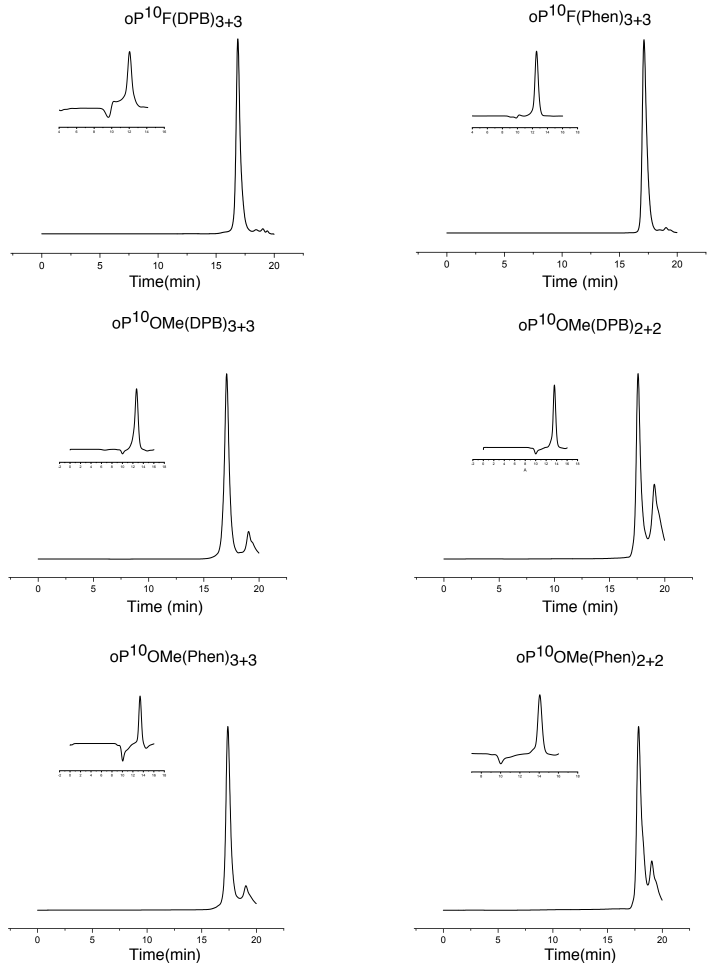

Figure S10. GPC traces of purified **oP^{10}F(DPB)$_{3+3}$**, **oP^{10}F(Phen)$_{3+3}$**, **oP^{10}OMe(DPB)$_{3+3}$**, **oP^{10}OMe(DPB)$_{2+2}$**, **oP^{10}OMe(Phen)$_{3+3}$**, and **oP^{10}OMe(Phen)$_{2+2}$**. Note: The peak at 19 min in the analytical GPC traces was seen for all compounds and was determined to be an artifact as it was not observed in the original semi-preparative traces (shown as insets).

Experimental

General

Unless otherwise noted, all starting materials, reagents, and solvents were purchased from commercial sources and used without further purification. Melting points were determined using a Thermal Analysis Q20 differential scanning calorimeter at a heating rate of 10 ℃/min. NMR spectra were measured for $CDCl_3$ solutions using Bruker Avance 200, 500, and 600 MHz NMR spectrometers. Semi-preparative gel permeation chromatography (GPC) was performed using a Waters Breeze 2 HPLC equipped with a 19×300 mm Ultrastyragel 500 Å GPC column with toluene (flow rate = 3 mL/min) as the eluent. Peaks were detected from Breeze 2 refractive index detector. Analytical GPC was performed using an Agilent (SEC) system equipped with an autosampler, an Agilent 1260 isocratic pump, 1× Agilent MixedB-guard and 2× Agilent MixedB analytical columns, and an Agilent 1260 refractive index detector. The eluent was THF at 30 ℃ at 1 mL/min.

Synthesis

Terephthalaldehyde (Phen) is commercially available. The dialdehyde linkers 4,4′-(buta-1,3-diyne-1,4-diyl)dibenzaldehyde (DPB),[7] **B1**[8], **B2**,[9] and **B3**[10] were synthesized according to literature procedures. *o*-Phenylene decamers **oP^{10}F(NH$_2$)** and **oP^{10}OMe(NH$_2$)** were synthesized as shown in Scheme S1. The syntheses of *o*-phenylene octamers **oP⁸H(NH₂)** and **oP⁸F(NH₂)** are shown in Scheme S2.

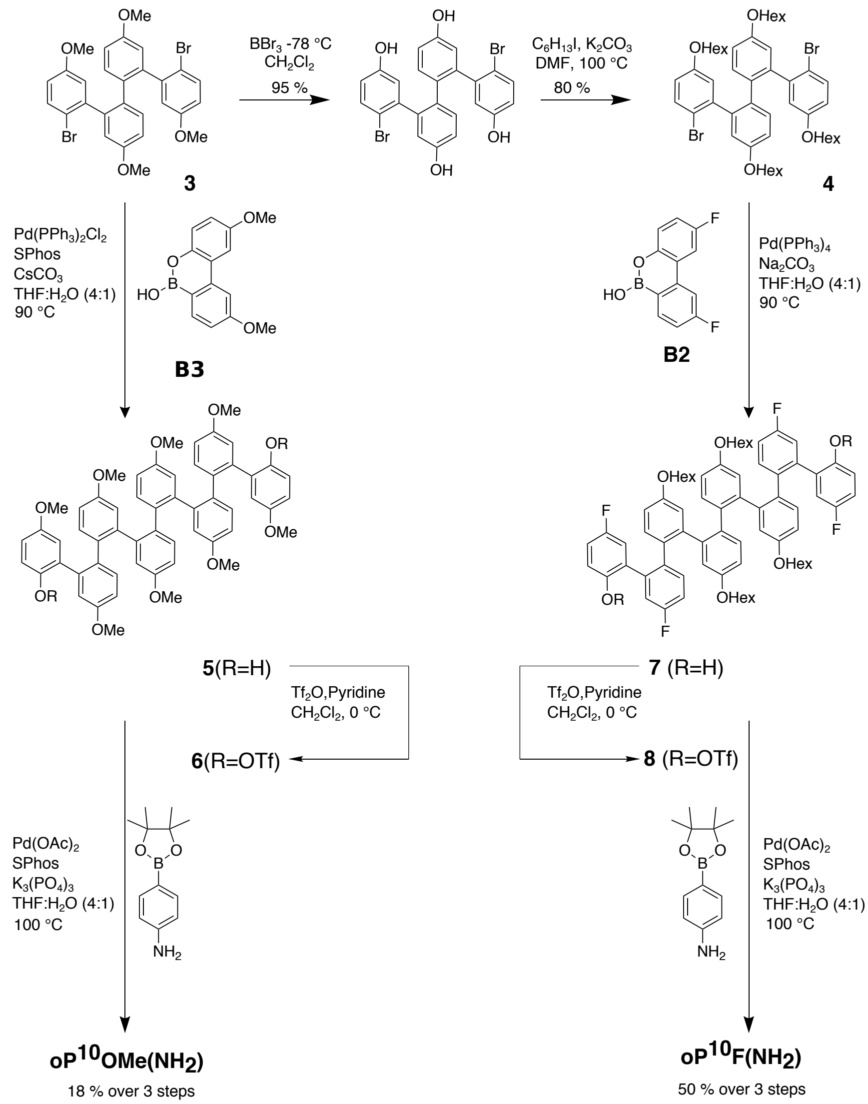

Scheme S1. Synthesis of *o*-phenylene decamers.

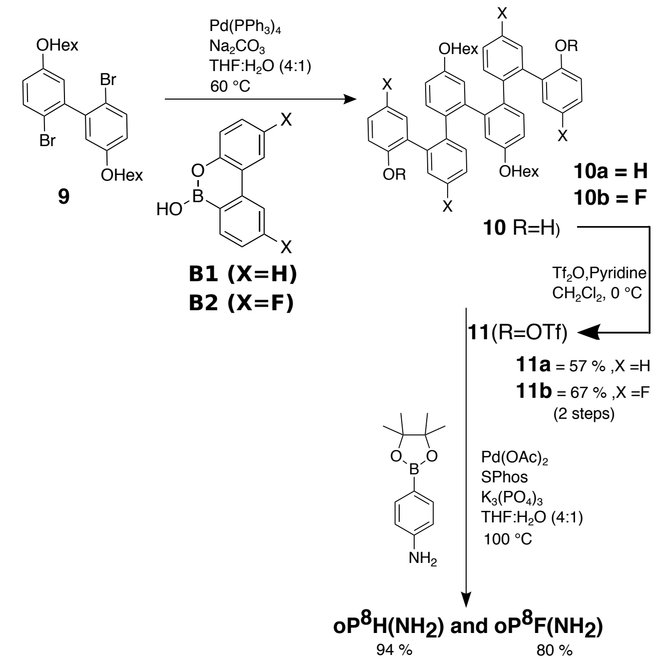

Scheme S2. Synthesis of *o*-phenylene octamers.

oP^{10}OMe(NH$_2$)

A round-bottom flask was charged with compound **3**[11] (1.0 g, 1.71 mmol), **B3**[10] (1.10 g , 4.29 mmol), Pd(PPh_3)$_2$$Cl_2$ (240 mg , 0.343 mmol, SPhos (168.4mg, 0.410 mmol), Cs_2CO_3 (2.77 g, 8.55 mmol), THF (40 mL), and H_2O (10 mL). The reaction mixture was sparged with argon for 10 min, then refluxed under argon overnight, cooled to rt, and diluted with EtOAc (20 mL) and 1 M HCl(aq) (20 mL). The aqueous layer was extracted with EtOAc (3 × 30 mL). The combined organic layers were washed with water and brine, dried over anhydrous $MgSO_4$, filtered, and concentrated. Purification was done by flash chromatography (hexanes:EtOAc, 8:2), and gave **5** as a light brown solid. Without further purification, **5** was dissolved in CH_2Cl_2 (100 mL). Pyridine (0.28 mL, 3.46 mmol) was added to the reaction mixture and allowed to stir for 30 min at rt. Then, reaction mixture was cooled to 0 ℃ for 10 min. and trifluoromethanesulfonic anhydride (0.43 mL, 2.55 mmol) was dropwise added to the reaction mixture and allowed to stir while warming up to rt overnight. The reaction was quenched with 1 M HCl(aq) (40 mL), extracted with EtOAc (4 × 100 mL), and organic layers were combined. The combined organic layers were washed with water and brine, dried over anhydrous $MgSO_4$, filtered, and concentrated. Purification by flash chromatography (hexanes:EtOAc, 9:1) gave **6** as a white solid (719 mg) (see Figure S72 and S73 (^{1}H and ^{19}F NMR spectra)).

Compound **6** was added to a round bottom flask with 4-aminophenylboronic acid pinacol ester (1.5 g, 6.84 mmol), Pd(OAc)$_2$ (19.1 mg, 0.062 mmol), SPhos (44.3 mg, 0.073 mmol), K_3PO_4 (625 mg, 2.94 mmol), THF (20 mL), and H_2O (5 mL). The reaction mixture was sparged with argon for 10 min, then heated to reflux at 100 ℃ overnight. The reaction mixture was cooled to rt and diluted with EtOAc (20 mL) and water (30 mL). The aqueous layer was extracted with EtOAc (5 × 50 mL). The combined organic layers were washed with water and brine, dried over anhydrous $MgSO_4$, filtered, and concentrated. Purification by flash chromatography (hexanes:EtOAc, 7:3) gave **oP^{10}OMe(NH$_2$)** as a light brown solid (312 mg, 18% over three steps): mp 137.46 ℃ (dec.); NMR spectra broadened due to slow conformational exchange, see Table S12 for ^{1}H and ^{13}C assignments, and Figures S80 (^{1}H), S81 (COSY), S82 (HSQC), S83 (HMBC), and S84 (NOESY/EXSY); HRMS (LDI) calcd for $C_{68}H_{60}N_2O_8$ (M^+) 1032.434968, found 1032.434418.

oP^{10}F(NH$_2$)

A round-bottom flask was charged with compound **4**[2] (500 mg, 0.578 mmol), **B2**[9] (591.8 g, 2.551 mmol) Pd(PPh_3)$_4$ (137 mg, 0.118 mmol), 2 M Na_2CO_3(aq) (10 mL, 0.02 mmol), and THF (16 mL) and H_2O (4 mL). The flask was purged with argon for 10 min then, refluxed under argon overnight. The reaction mixture was cooled and diluted with EtOAc (20 mL) and 1 M HCl(aq) (10 mL). The aqueous layer was extracted with EtOAc (3 × 25 mL). The combined organic layers were washed with water and brine, dried over anhydrous $MgSO_4$, filtered, and concentrated. Purification by flash chromatography (hexanes:EtOAc, 9:1) gave **7** as a brown solid. Without further purification, **7** was dissolved in CH_2Cl_2(100 mL). Pyridine (0.23 mL, 2.85 mmol) was added to the reaction mixture which was stirred for 30 min at rt, then cooled to 0 ℃. After 10 min, trifluoromethanesulfonic anhydride (0.35 mL, 2.08 mmol) was added to the reaction mixture which was stirred while warming up to rt overnight. The reaction was quenched with 1 M HCl(aq) (20 mL) and extracted with EtOAc (3 × 40 mL). The combined organic layers were washed with water and brine, dried over $MgSO_4$, filtered, and concentrated. Purification by flash chromatography (hexanes:EtOAc, 9:1) gave **8** as a light brown solid (555 mg) (see Figure S74, S75 S76, S77,S78,and S79 (^{1}H, ^{19}F, COSY, HSQC, HMBC, and NOESY/EXSY NMR spectra respectively)).

Compound **8** was added to a round bottom flask with 4-aminophenylboronic acid pinacol ester (317.5 mg, 1.44 mmol), $Pd(OAc)_2$ (16.3 mg, 0.072 mmol), SPhos (39.5 mg, 0.096 mmol), K_3PO_4 (339.9 mg, 1.60 mmol), THF (16 mL), and H_2O (4 mL). The reaction mixture was purged with argon for 10 min then heated to reflux at 100 ℃ overnight. The reaction mixture was cooled to rt and diluted with EtOAc (10 mL) and water (10 mL). The aqueous layer was extracted with EtOAc (3 × 20 mL). The combined organic layers were washed with brine, dried over anhydrous $MgSO_4$, filtered, and concentrated. Purification by flash chromatography (hexanes:EtOAc, 8:2) gave **oP^{10}F(NH$_2$)** as a brown solid (367 mg, 50% over three steps): mp 73.40 ℃ (dec.); NMR spectra broadened due to slow conformational exchange, see Table S9 for ^{1}H and ^{13}C assignments, and Figures S85 (^{1}H), S86 (^{19}F), S87 (COSY), S88 (HSQC), S89 (HMBC), and S90 (NOESY/EXSY); HRMS (LDI) calcd for $C_{84}H_{88}F_4N_2O_4$ (M^+) 1264.66802, found 1264.66597.

o-Phenylene hexamer 11a

A round-bottom flask was charged with compound **9**[12] (1.00 g, 1.95 mmol), **B1**[8] (1.5 g, 7.65 mmol), $Pd(PPh_3)_4$ (90.1 mg, 0.078 mmol), 2 M Na_2CO_3(aq) (10 mL, 0.02 mmol), THF (16 mL), and H_2O (4 mL). The reaction mixture was purged with argon for 10 min then heated to 60 ℃ under argon for 20 h. The reaction mixture was cooled to rt and diluted with EtOAc (20 mL) and 1 M HCl(aq) (20 mL). The aqueous layer was extracted with EtOAc (3 × 30 mL). The combined organic layers were washed with water and brine, dried over anhydrous $MgSO_4$, filtered, and concentrated. Purification by flash chromatography (hexanes:EtOAc, 6:4) gave **10a** as a light brown solid (0.98 g) (mp 188.34 ℃ (dec.), see Figure S11 and S12 (^{1}H and ^{13}C NMR spectra)).

Compound **10a** was dissolved in CH_2Cl_2 (100 mL). Pyridine (0.46 mL, 5.70 mmol) was added to the reaction mixture which was stirred for 30 min at rt. Then the reaction mixture was bought to 0 ℃ using an ice water bath. After 10 min, trifluoromethanesulfonic anhydride (0.71 mL, 4.22 mmol) was added and the reaction mixture stirred while warming up to rt overnight. The reaction was quenched with 1 M HCl(aq) (20 mL) and the organic layer extracted with EtOAc (3 × 40 mL). The combined organic layers were washed with water and brine, dried over anhydrous $MgSO_4$, filtered, and concentrated. Purification by flash chromatography (hexanes:EtOAc, 8:2) gave **11a** as a white solid (1.08 g, 57% yield over two steps): mp 177.54 ℃ (dec.); ^{1}H NMR (500 MHz, $CDCl_3$) δ 7.17 (dq, J = 11.4, 6.0, 3.8 Hz, 2H), 7.11–7.08 (m, 2H), 7.06–7.03 (m, 4H), 6.98–6.94 (m, 4H), 6.91 (d, J = 7.8 Hz, 2H), 6.86 (dd, J = 8.1, 4.9 Hz, 2H), 6.77 (dd, 2H), 6.42–6.38 (m, 2H), 6.29 (d, J = 8.0 Hz, 2H), 3.72 (td, J = 6.5, 4.6 Hz, 4H), 1.78 (qd, J = 10.0, 9.2, 4.5 Hz, 4H), 1.55–1.46 (m, 4H), 1.40 (dp, J = 7.3, 3.7 Hz, 8H), 0.99–0.90 (m, 6H); ^{13}C NMR (126 MHz, $CDCl_3$) δ 158.6, 158.1, 147.8, 146.3, 141.7, 141.1, 140.8, 140.2, 135.9, 135.8, 134.4, 134.2, 134.0, 133.8, 133.7, 133.6, 133.1, 132.7, 132.4, 131.9, 131.6, 131.6, 131.2, 131.0, 130.3, 130.2, 129.7, 129.2, 128.7, 128.5, 128.0, 127.9, 127.8, 126.8, 126.3, 126.1, 126.0, 125.9, 120.9, 120.6, 120.5, 119.6, 116.6, 116.4, 113.4, 113.1, 112.5, 67.6, 32.1, 29.8, 26.4, 23.1, 14.5. see Figures S15 (^{1}H), S16 (^{13}C), S17 (COSY), S18 (HSQC), S19 (HMBC), and S20 (NOESY/EXSY); HRMS (ESI) calcd for $C_{50}H_{48}F_6O_8S_2Na$ ([M + Na$^+$]) 977.25870, found 977.25749.

o-Phenylene hexamer 11b

A round-bottom flask was charged with compound **9**[12] (1.00 g, 1.95 mmol), **B2**[9] (1.80 g , 7.76 mmol), $Pd(PPh_3)_4$ (450 mg , 0.39 mmol), 2 M Na_2CO_3(aq) (10 mL, 0.02 mmol), THF (16 mL), H_2O (4 mL). The reaction mixture was purged with argon for 10 min, then heated to 60 ℃ under argon for 20 h. The reaction mixture was cooled to rt and diluted with EtOAc (20 mL) and 1 M HCl(aq) (20 mL). The aqueous layer was extracted with EtOAc (3 × 30 mL). The combined organic layers were washed with water and brine, dried over $MgSO_4$, filtered, and concentrated. Purification by flash chromatography (hexanes:EtOAc, 6:4) gave **10b** as a light brown solid (1.2 g) (see Figure S13 and S14 (^{1}H and ^{13}C NMR spectra)).

Compound **10b** was dissolved in CH_2Cl_2 (100 mL). Pyridine (0.46 mL, 5.70 mmol) was added to the reaction mixture, which was stirred for 30 min at rt. The reaction mixture was then cooled to 0 ℃. After 10 min at 0 ℃, trifluoromethanesulfonic anhydride (0.71 mL, 4.22 mmol) was added to the reaction mixture, which was stirred while warming up to rt overnight. The reaction was quenched with 1 M HCl(aq) (20 mL), extracted with EtOAc (3 × 40 mL), and organic layers were combined. The combined organic layers were washed with water and brine, dried over anhydrous $MgSO_4$, filtered, and concentrated. Purification by flash chromatography (hexanes:EtOAc, 8:2) gave **10b** as a white solid (1.34 g , 67% yield over two steps): mp 110.94℃ (dec.); ^{1}H NMR (500 MHz, $CDCl_3$) δ 7.05 (d, J = 8.6 Hz, 2H), 6.86–6.80 (m, 8H), 6.68 (dd, J = 9.1, 2.7 Hz, 2H), 6.41 (dd, J = 8.6, 5.7 Hz, 2H), 6.07–6.01 (m, 2H), 5.56 (d, J= 2.7 Hz, 2H), 3.82 (qt, J = 5.3, 2.5 Hz, 4H), 1.79 (ddd, J = 10.8, 8.1, 4.6 Hz, 4H), 1.55−1.45 (m, 4H), 1.44−1.32 (m, J = 5.9, 5.0 Hz, 8H), 0.95 (h, J = 3.0 Hz, 6H); ^{13}C NMR (126 MHz, $CDCl_3$) δ 162.4, 162.1, 160.4, 160.1, 158.8, 158.2, 141.5, 141.5, 141.0, 140.1, 139.6, 137.6 137.6, 136.1, 136.1, 134.4, 134.3, 133.8, 132.6, 132.6, 130.3, 122.5, 122.5, 121.8, 119.3,118.2, 118.1, 118.0, 117.4, 117.3, 117.2, 116.6, 116.5, 115.6, 115.4, 112.0, 67.5, 31.8, 29.5, 26.0, 22.8, 14.2. ^{19}F NMR (188 MHz, $CDCl_3$) δ -73.74, -74.22, -112.39, -113.75, -116.36, -116.65. see Figures S21 (^{1}H),S22 ^{13}C, S23 (^{19}F), S24 (COSY), S25 (HSQC), S26 (HMBC), and S27 (NOESY/EXSY); HRMS (LDI) calcd for $C_{50}H_{44}F_{10}O_8S_2$ (M^+) 1026.23179, found 1026.23035.

oP^{8}H(NH$_2$)

A round-bottom flask was charged with **11a** (50 mg, 0.052 mmol), 4-amino-phenylboronic acid pinacol ester (45.8 mg, 0.209 mmol), $Pd(OAc)_2$ (2.3 mg, 0.010 mmol), SPhos (5.12 mg, 0.013 mmol), and K_3PO_4 (33.1 mg, 0.156 mmol), THF (4 mL), and H_2O (1 mL). The solution was purged with argon for 10 min, then the reaction mixture was heated to reflux at 100 ℃ overnight. It was cooled to rt and diluted with EtOAc (10 mL) and water (10 mL). The aqueous layer was extracted with EtOAc (3 × 20 mL). The combined organic layers were washed with brine, dried over anhydrous $MgSO_4$, filtered, and concentrated. Purification by flash chromatography (hexanes:EtOAc, 6:4) gave **oP^{8}H(NH$_2$)** as a light brown solid (41 mg, 94%): mp 54.72 ℃ (dec.); NMR spectra broadened due to slow conformational exchange, see Table S5 for ^{1}H and ^{13}C assignments, and Figures S28 (^{1}H), S29 (COSY), S30 (HSQC), S31 (HMBC), and S32 (NOESY/EXSY); HRMS (LDI) calcd for $C_{60}H_{60}N_2O_2$ (M^+) 840.46548, found 840.46462.

oP^{8}F(NH$_2$)

A round-bottom flask was charged with **11b** (50 mg, 0.048 mmol), 4-aminophenylboronic acid pinacol ester (44.0 mg, 0.201 mmol), $Pd(OAc)_2$ (2.2 mg, 0.010 mmol), SPhos (4.92 mg, 0.012 mmol), and K_3PO_4 (31.8 mg, 0.150 mmol), THF (4 mL), and H_2O (1 mL). The reaction mixture was purged with argon for 10 min, then heated at reflux overnight. It was cooled to rt, then diluted with EtOAc (10 mL) and water (10 mL). The aqueous layer was extracted with EtOAc (3 × 20 mL). The combined organic layers were washed with brine, dried over anhydrous $MgSO_4$, filtered, and concentrated. Purification by flash chromatography (hexanes:EtOAc, 6:4) gave **oP^{8}F(NH$_2$)** as a light brown solid (35 mg, 80%): mp 72.76℃ (dec.); NMR spectra broadened due to slow conformational exchange, see Table S1 for ^{1}H and ^{13}C assignments, also see Figures S33 (^{1}H), S34 (^{19}F), S35 (COSY), S36 (HSQC), S37 (HMBC), and S38 (NOESY/EXSY); HRMS (LDI) calcd for $C_{60}H_{56}F_4N_2O_2$ (M^+) 912.42779, found 912.42687.

oP^{8}H(M)

An oven-dried round-bottom flask was charged with **oP^{8}H(NH$_2$)** (35 mg, 0.042 mmol), benzaldehyde (8.46 μL, 0.083 mmol), and $CHCl_3$ (27 mL). To the reaction mixture, 3 Å molecular sieves were added, followed by TFA (0.47 mg, 0.004 mmol). The reaction mixture was allowed to stand at room temperature overnight with occasional stirring, then quenched with NEt_3 (3 mL) and concentrated under vacuum. Purification was by semi-preparative GPC, and gave **oP^{8}H(M)** as a yellow solid (12.1 mg, 28%): NMR spectra broadened due to slow conformational exchange, see Table S6 for ^{1}H and ^{13}C assignments, and Figures S39 (^{1}H), S40 (COSY), S41 (HSQC), S42 (HMBC), and S43 (NOESY/EXSY); HRMS (LDI) calcd for $C_{74}H_{69}N_2O_2$ ($[M + H]^+$) 1017.53536, found 1017.53503.

oP^{8}F(M)

An oven-dried round bottom flask was charged with **oP^{8}F(NH$_2$)** (20 mg, 0.021 mmol), benzaldehyde (4.45 μL, 0.054 mmol), and $CHCl_3$ (14.4 mL). To the reaction mixture, 3 Å molecular sieves were added, followed by TFA (0.26 mg, 0.003 mmol). The reaction mixture was allowed to stand at room temperature overnight with occasional stirring, then quenched with NEt_3 (3 mL) and concentrated. Purification by semi-preparative GPC gave **oP^{8}F(M)** as a yellow solid (8.2 mg, 36%): NMR spectra broadened due to slow conformational exchange, see Table S2 for ^{1}H and ^{13}C assignments, and Figures S44 (^{1}H), S45 (^{19}F), S46 (COSY), S47 (HSQC), S48 (HMBC), and S49 (NOESY/EXSY); HRMS (LDI) calcd for $C_{74}H_{65}F_4N_2O_2$ ([M + H]$^+$) 1089.49767, found 1089.49748.

oP^{10}OMe(M)

An oven-dried round bottom flask was charged with **oP^{10}OMe(NH$_2$)** (31 mg, 0.030 mmol), benzaldehyde (6.05 μL, 0.038 mmol), and $CHCl_3$ (12.6 mL). To the reaction mixture, 3 Å molecular sieves were added, followed by addition of TFA (0.32 mg, 0.002 mmol). The reaction mixture was allowed to stand at room temperature for overnight with occasional stirring, then quenched with NEt_3 (3 mL) and concentrated. Purification by GPC gave **oP^{10}OMe(M)** as a yellow solid (18.6 mg, 51%): mp 233.85 ℃; NMR spectra broadened due to slow conformational exchange, see Table S13 for ^{1}H and ^{13}C assignments, also see Figures S91 (^{1}H), S92 (COSY), S93 (HSQC), S94 (HMBC), S95 (NOESY/EXSY) and S96 (TOCSY); HRMS (LDI) calcd for $C_{82}H_{67}N_2O_8$ ([M − H]$^+$) 1207.48919, found 1207.48817

oP^{10}F(M)

An oven-dried round-bottom flask was charged with **oP^{10}F(NH$_2$)** (20 mg, 0.015 mmol), benzaldehyde (3.21 μL, 0.031 mmol), and $CHCl_3$ (10 mL). To this, 3 Å molecular sieves were added, followed by TFA (0.17 mg, 0.0015 mmol). The reaction mixture was allowed to stand at room temperature overnight with occasional stirring, then quenched with NEt_3 (3 mL) and concentrated. Purification by GPC gave **oP^{10}F(M)** as a yellow solid (15.6 mg, 72%): mp 183.55 ℃; NMR spectra broadened due to slow conformational exchange, see Table S10 for ^{1}H and ^{13}C assignments, and Figures S97 (^{1}H), S98 (19F), S99 (COSY), S100 (HSQC), S101 (HMBC), S102 (NOESY/EXSY) and S103 (TOCSY); HRMS (LDI) calcd for $C_{98}H_{95}F_4N_2O_4$ ([M − H]$^+$) 1439.722250, found 1439.722249.

General procedure for macrocyclization

An oven-dried round-bottom flask was charged with *o*-phenylene diamine (1.1 equiv), dialdehyde linker (1.0 equiv), and $CHCl_3$ (giving a dialdehyde concentration of 1.5 mM). To the reaction mixture, 3 Å molecular sieves were added, followed by TFA (0.10 equiv). The reaction mixture was allowed to stand at room temperature with occasional stirring for 5 d (*o*-phenylene octamers) or 11 d (*o*-phenylene decamers). The reaction mixtures were then quenched with NEt_3 (3 mL) and concentrated. The crude products were purified via GPC.

oP^{8}H(DPB)$_{2+2}$

From **oP^{8}H(NH$_2$)** (10.0 mg, 0.012 mmol) and **DPB** (2.79 mg, 0.010 mmol) were obtained compound **oP^{8}H(DPB)$_{2+2}$** (2.8 mg, 26%) as a yellow solid: NMR spectra broadened due to slow conformational exchange, see Table S7 for ^{1}H and ^{13}C assignments, and Figures S50 (^{1}H), S51 (COSY), S52 (HSQC), S53 (HMBC), and S54 (NOESY/EXSY); HRMS (LDI) calcd for $C_{156}H_{132}N_4O_4$ (M$^+$) 2125.01981, found 2125.01891.

oP^{8}H(Phen)$_{2+2}$

From **oP^{8}H(NH$_2$)** (21.4 mg, 0.025 mmol) and **Phen** (3.1 mg, 0.023 mmol) were obtained compound **oP^{8}H(Phen)$_{2+2}$** (11.2 mg, 52%) as a yellow solid: NMR spectra broadened due to slow conformational exchange, see Table S8 for ^{1}H and ^{13}C assignments, and Figures S55 (^{1}H), S56 (COSY), S57 (HSQC), S58 (HMBC), and S59 (NOESY/EXSY); HRMS (LDI) calcd for $C_{136}H_{124}N_4O_4$ (M$^+$) 1876.95720, found 1876.95586.

oP^{8}F(DPB)$_{2+2}$

From **oP^{8}F(NH$_2$)** (20.0 mg, 0.022 mmol) and **DPB** (5.14 mg, 0.019 mmol) were obtained compound **oP^{8}F(DPB)$_{2+2}$** (8 mg, 37%) as a yellow solid: NMR spectra broadened due to slow conformational exchange, see Table S3 for ^{1}H and ^{13}C assignments, and Figures S60 (^{1}H), S61 (^{19}F), S62 (COSY), S63 (HSQC), S64 (HMBC), and S65 (NOESY/EXSY); HRMS (LDI) calcd for $C_{156}H_{124}F_8N_4O_4$ (M$^+$) 2268.94444, found 2268.94338.

oP^{8}F(Phen)$_{2+2}$

From **oP^{8}F(NH$_2$)** (18.6 mg, 0.020 mmol) and **Phen** (2.5 mg, 0.018 mmol) were obtained compound **oP^{8}F(Phen)$_{2+2}$** (5.8 mg, 32%) as a yellow solid: NMR spectra broadened due to slow conformational exchange, see Table S4 for ^{1}H and ^{13}C assignments, and Figures S66 (^{1}H), S67 (^{19}F), S68 (COSY), S69 (HSQC), S70 (HMBC), and S71 NOESY/EXSY); HRMS (LDI) calcd for $C_{136}H_{116}F_8N_4O_4$ (M$^+$) 2020.88183, found 2020.88058.

oP^{10}F(DPB)$_{3+3}$

From **oP^{10}F(NH$_2$)** (38.8 mg, 0.030 mmol) and **DPB** (7.20 mg, 0.027 mmol) were obtained compound **oP^{10}F(DPB)$_{3+3}$** (36.9 mg, 92%) as a yellow solid: NMR spectra broadened due to slow conformational exchange, see Table S11 for ^{1}H and ^{13}C assignments, and Figures S104 (^{1}H), S105 (^{19}F), S106 (COSY), S107 (HSQC), S108 (HMBC), S109 (NOESY/EXSY) and S110 (TOCSY); HRMS (LDI) calcd for $C_{306}H_{282}F_{12}N_6O_{12}$ (M^+) 4460.14437, found 4460.12822.

oP^{10}F(Phen)$_{3+3}$

From **oP^{10}F(NH$_2$)** (35.2 mg, 0.027 mmol) and **Phen** (3.29 mg, 0.024 mmol) were obtained compound **oP^{10}F-(Phen)$_{3+3}$** (32 mg, 98%) as a yellow solid: NMR spectra broadened due to slow conformational exchange, see Figures S111 (^{1}H), S112 (^{19}F), S113 (COSY), S114 (HSQC), S115 (HMBC), S116 (NOESY/EXSY) and S117 (TOCSY); HRMS (LDI) calcd for$C_{276}H_{270}F_{12}N_6O_{12}$ (M^+) 4088.04598, found 4088.04544.

oP^{10}OMe(DPB)$_{3+3}$ and oP^{10}OMe(DPB)$_{2+2}$

From **oP^{10}OMe(NH$_2$))** (38.3 mg, 0.037 mmol) and **DPB** (8.7 mg, 0.033 mmol) were obtained compounds **oP^{10}-OMe(DPB)$_{3+3}$** (7.5 mg, 18 %) and **oP^{10}OMe(DPB)$_{2+2}$** (10.1 mg, 24 %).

oP^{10}OMe(DPB)$_{3+3}$: Yellow solid: NMR spectra broadened due to slow conformational exchange, see Table S14 for ^{1}H and ^{13}C assignments, and Figures S118 (^{1}H), S119 (COSY), S120 (HSQC), S121 (HMBC), S122 (NOESY/EXSY) and S123 (TOCSY); HRMS (LDI) calcd for $C_{258}H_{198}N_6O_{24}$ (M^+) 3763.44071, found 3762.45228.

oP^{10}OMe(DPB)$_{2+2}$: Yellow solid: NMR spectra broadened due to slow conformational exchange, see Table S15 and S16 for ^{1}H and ^{13}C assignments, and Figures S124 (^{1}H), S125 (COSY), S126 (HSQC), S127 (HMBC), S128 (NOESY/EXSY) and S129 (TOCSY); HRMS (LDI) calcd for $C_{172}H_{132}N_4O_{16}$ (M^+) 2508.95879, found 2508.95598.

oP^{10}OMe(Phen)$_{3+3}$ and oP^{10}OMe(Phen)$_{2+2}$

From **oP^{10}OMe(NH$_2$)** (37.2 mg, 0.036 mmol) and **Phen** (4.3 mg, 0.032 mmol) were obtained compounds **oP^{10}-OMe(Phen)$_{3+3}$** (13.2 mg, 36%) and **oP^{10}OMe(Phen)$_{2+2}$** (6.7 mg, 19%).

oP^{10}OMe(Phen)$_{3+3}$: Yellow solid: NMR spectra broadened due to slow conformational exchange, see Figures S130 (^{1}H), S131 (COSY), S132 (HSQC), S133 (HMBC), S134 (NOESY/EXSY) and S135 (TOCSY); HRMS (LDI) calcd for $C_{228}H_{186}N_6O_{24}$ (M^+) 3391.34680, found 3391.36681.

oP^{10}OMe(Phen)$_{2+2}$: Yellow solid: NMR spectra broadened due to slow conformational exchange, see Figures S136 (^{1}H), S137 (COSY), S138 (HSQC), S139 (HMBC), S140 (NOESY/EXSY) and S141 (TOCSY); HRMS (LDI) calcd for $C_{152}H_{124}N_4O_{16}$ (M^+)) 2260.89619, found 2260.89410.

NMR spectra

Hexamer 10a

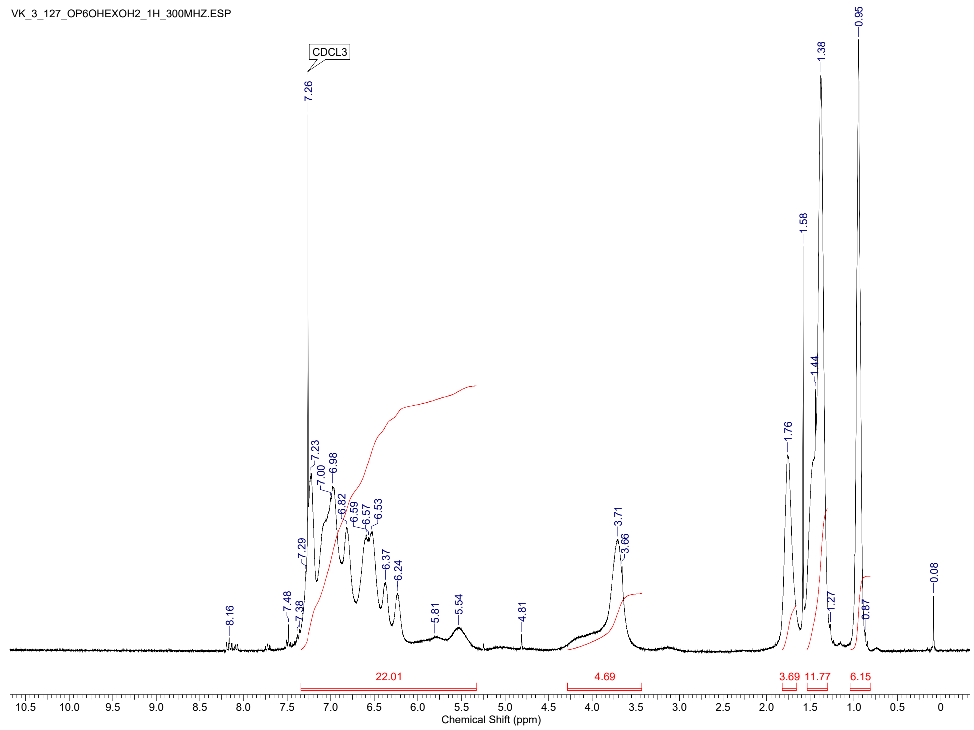

Figure S11. [1]H NMR spectrum (500 MHz, $CDCl_3$, 0 °C) of **10a**.

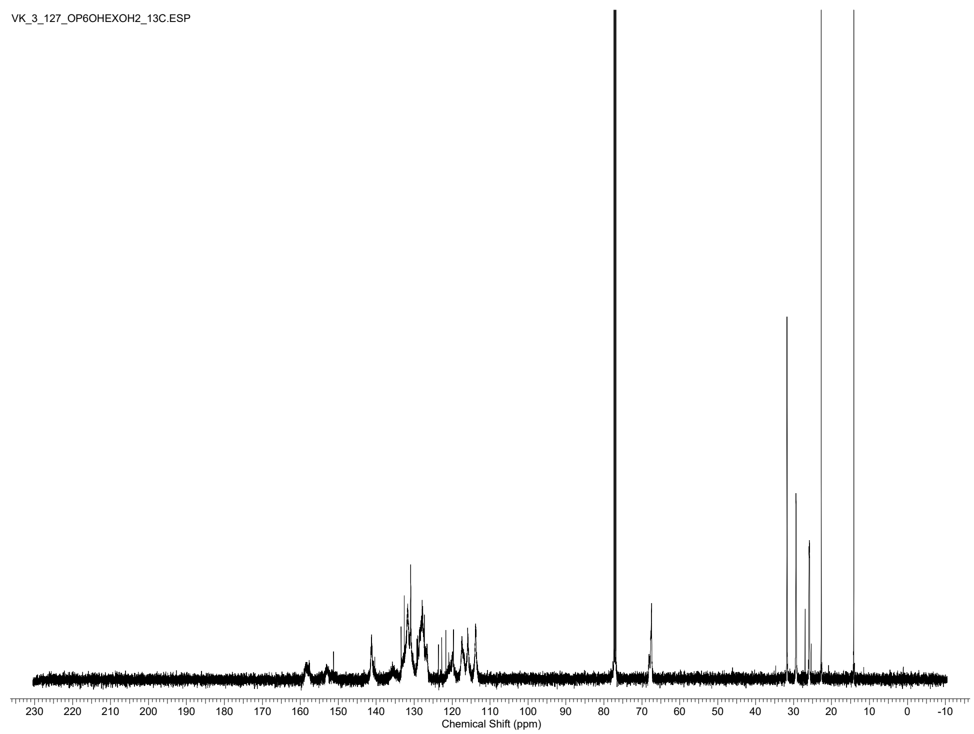

Figure S12. ^{13}C NMR spectrum (125 MHz, $CDCl_3$, 0 ℃) of **10a**.

Hexamer 10b

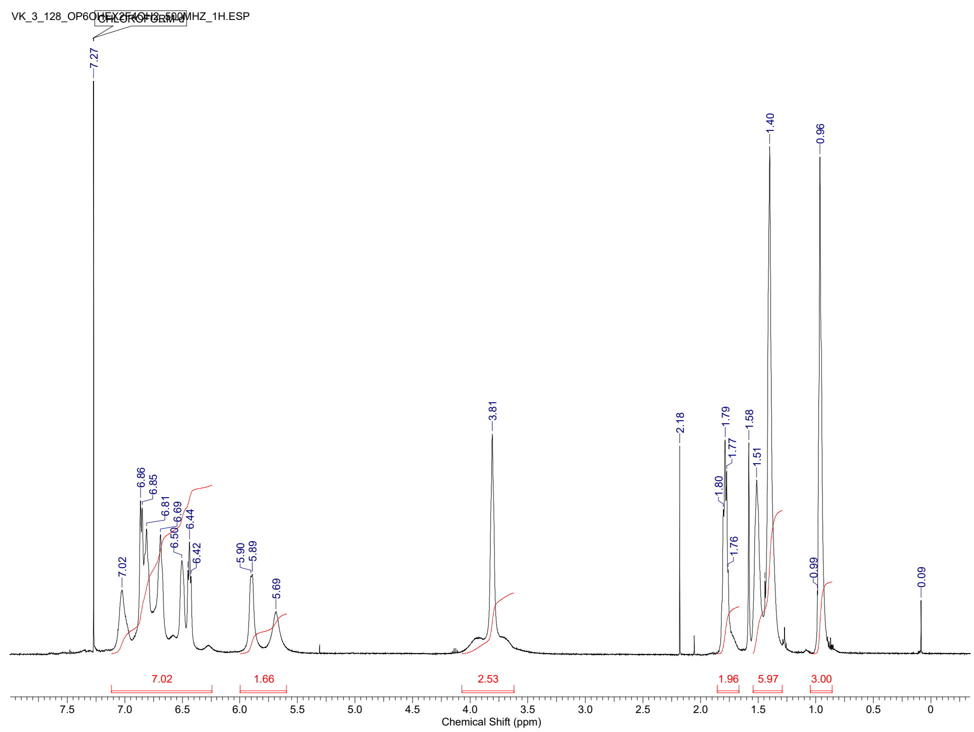

Figure S13. [1]H NMR spectrum (500 MHz, $CDCl_3$, 0 ℃) of **10b**.

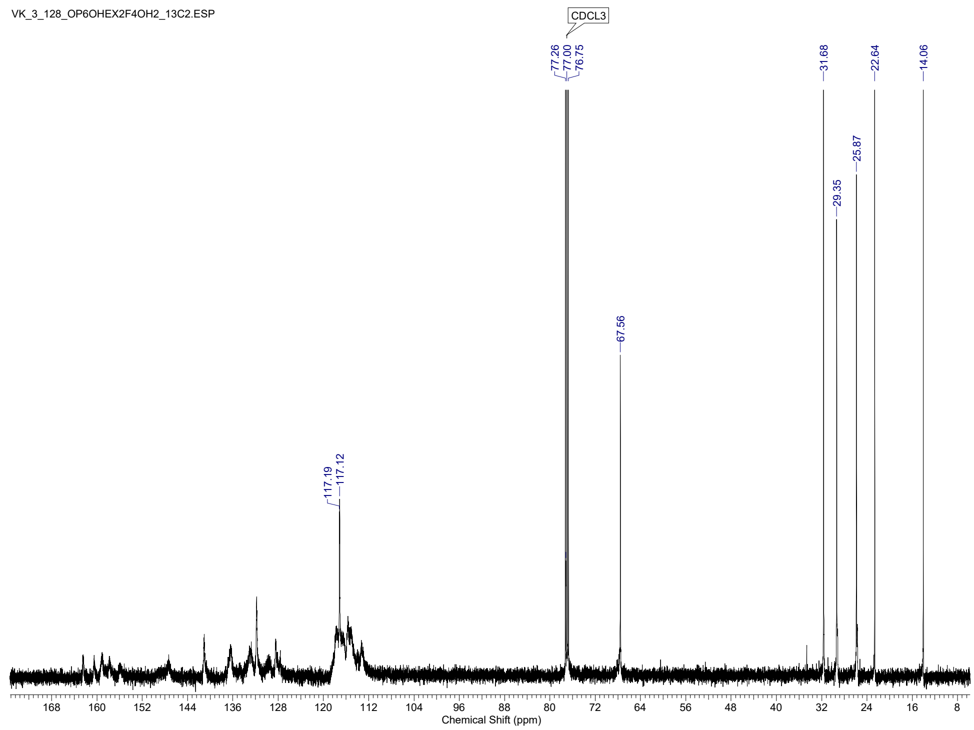

Figure S14. ^{13}C NMR spectrum (125 MHz, $CDCl_3$, 0 ℃) of **10b**.

Hexamer 11a

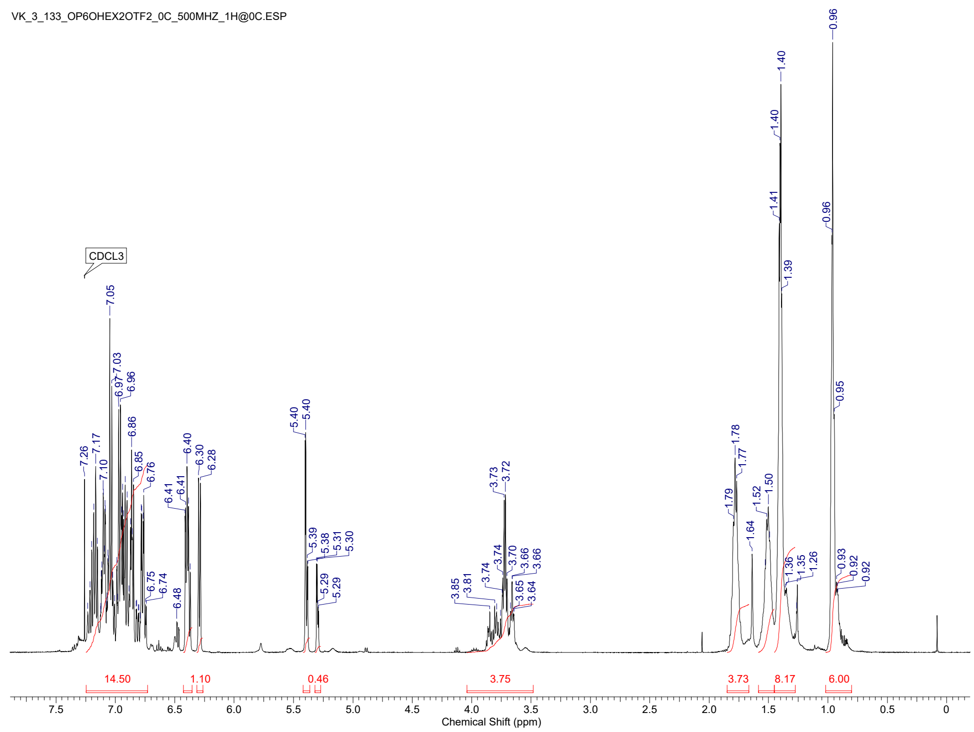

Figure S15. ^{1}H NMR spectrum (500 MHz, $CDCl_3$, 0 ℃) of **11a**.

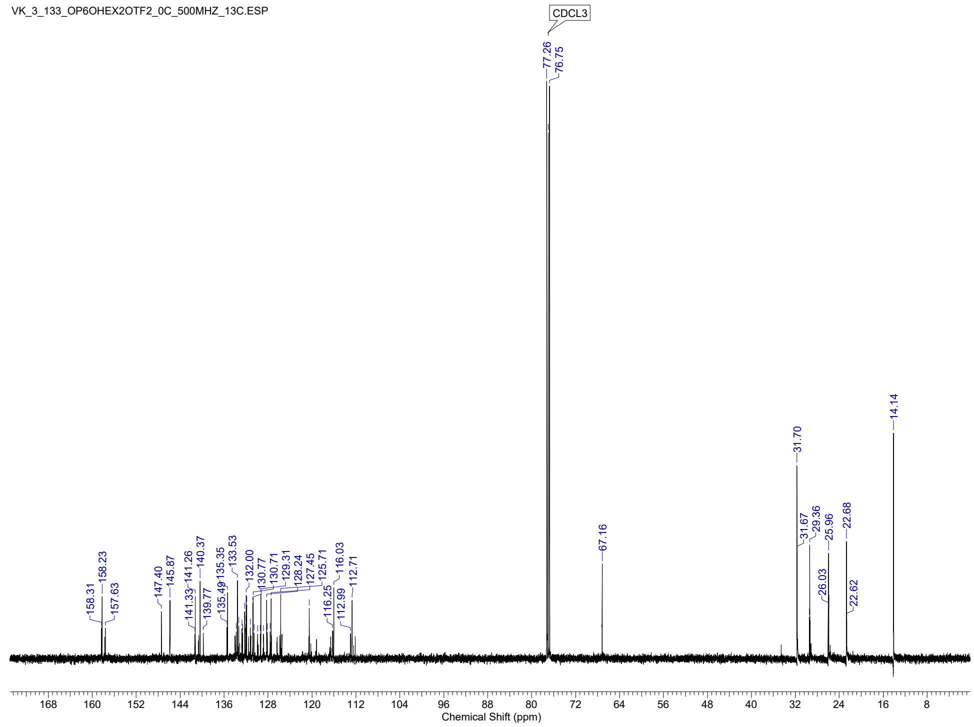

Figure S16. ^{13}C NMR spectrum (125 MHz, $CDCl_3$, 0 ℃) of **11a**.

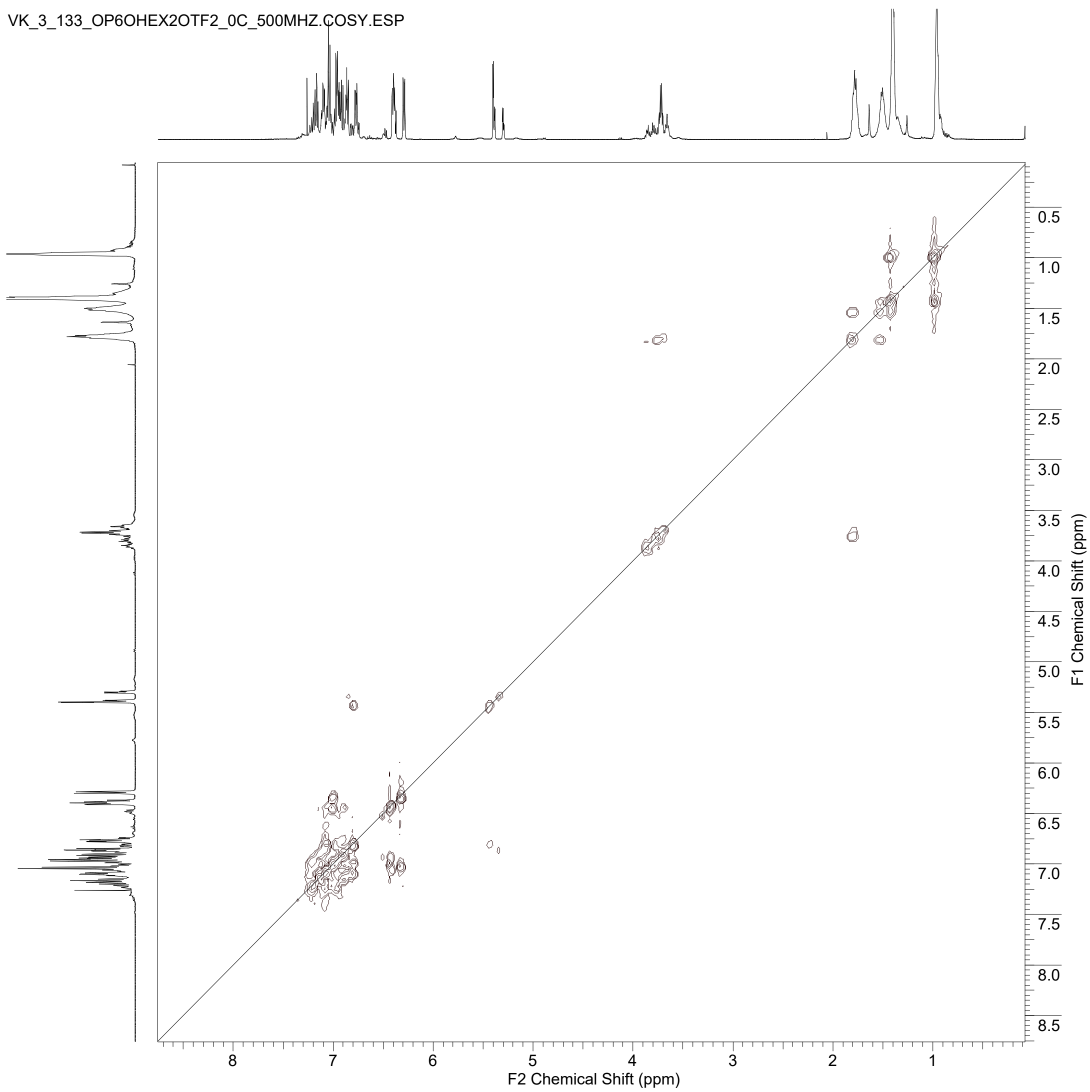

Figure S17. COSY NMR spectrum (500 MHz, $CDCl_3$, 0 ℃) of **11a**.

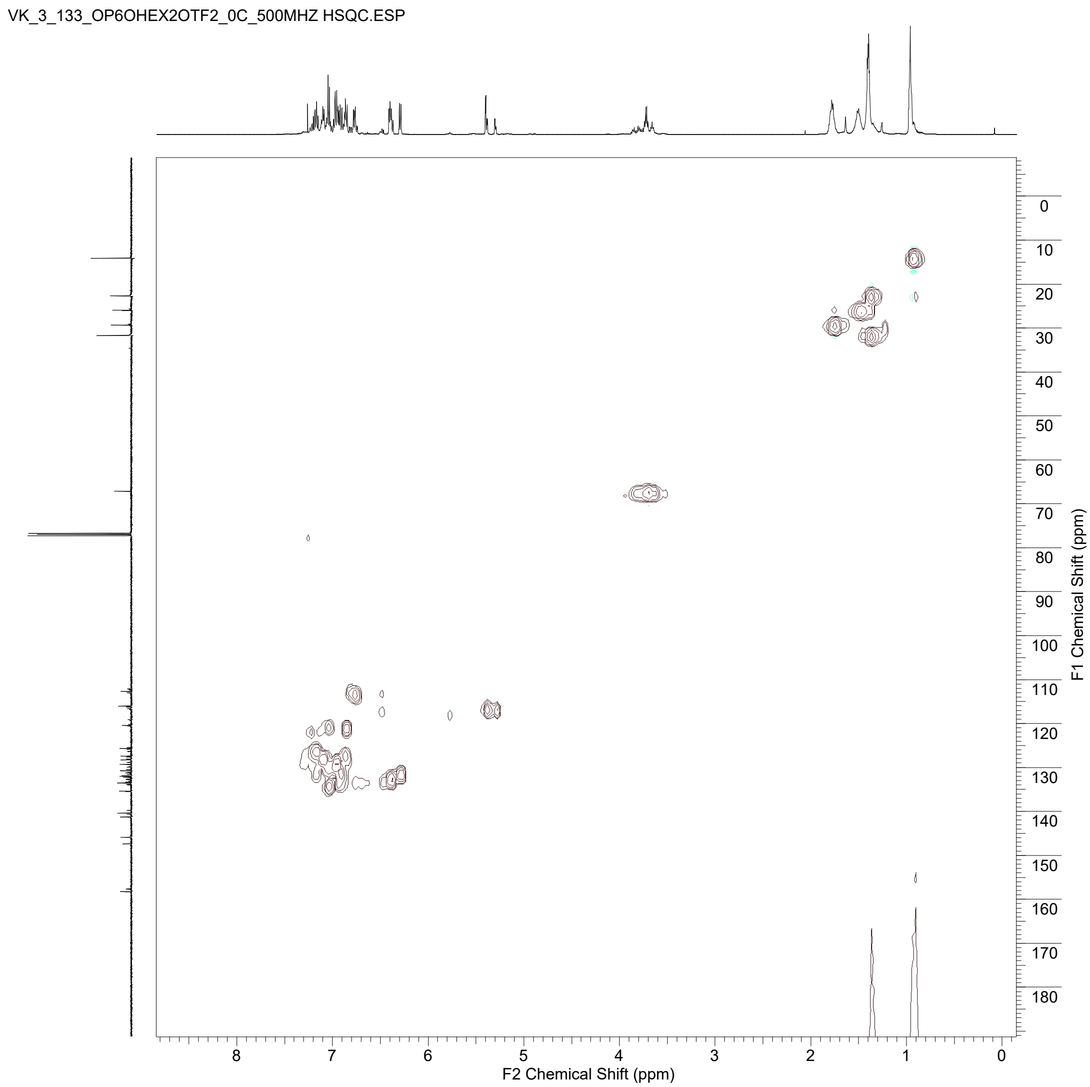

Figure S18. HSQC NMR spectrum (500 MHz, $CDCl_3$, 0 ℃) of **11a**.

VK_3_133_OP6OHEX2OTF2_0C_500MHZ.HMBC.ESP

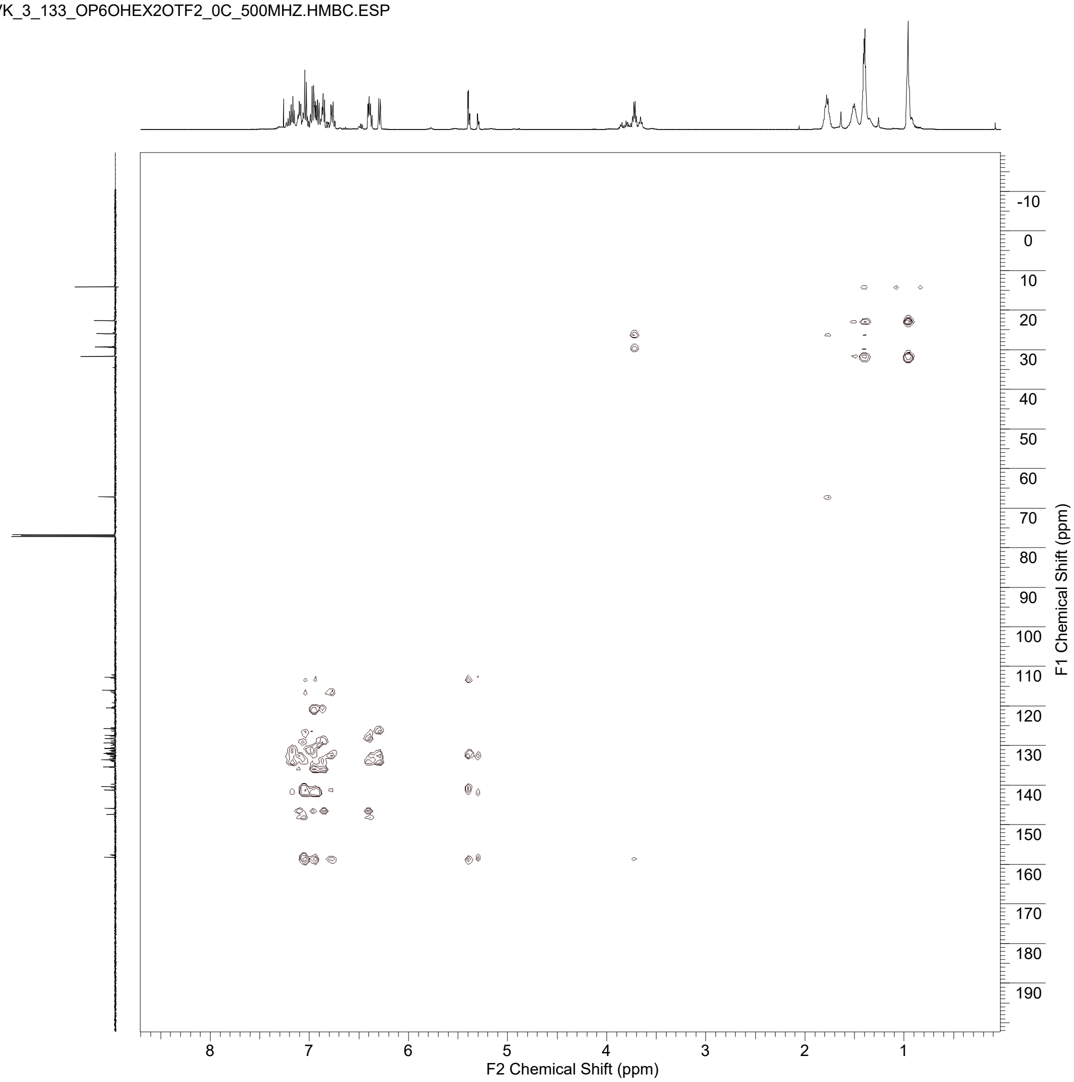

Figure S19. HMBC NMR spectrum (500 MHz, $CDCl_3$, 0 ℃) of **11a**.

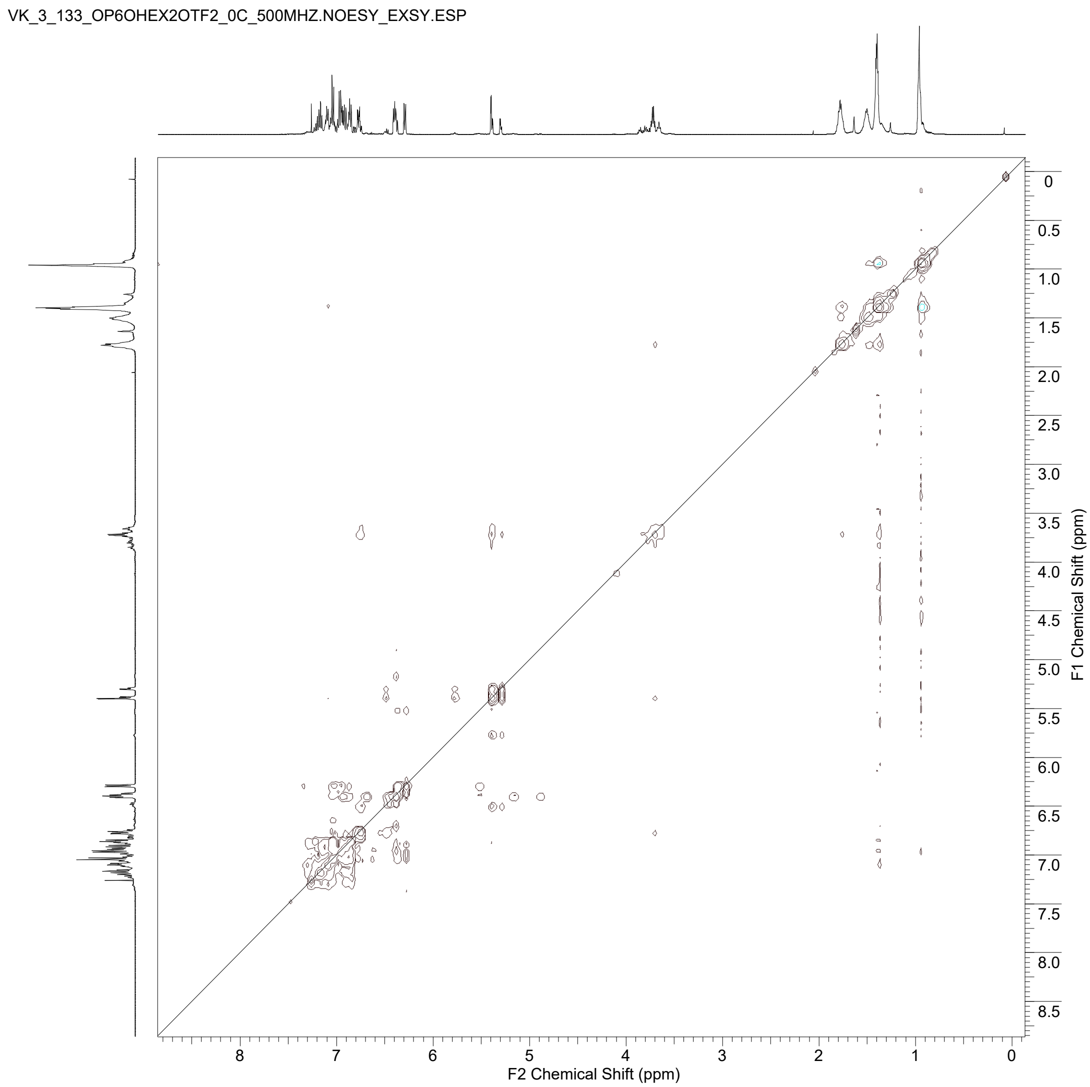

Figure S20. NOESY/EXSY NMR spectrum (500 MHz, $CDCl_3$, 0 ℃) of **11a**.

Hexamer 11b

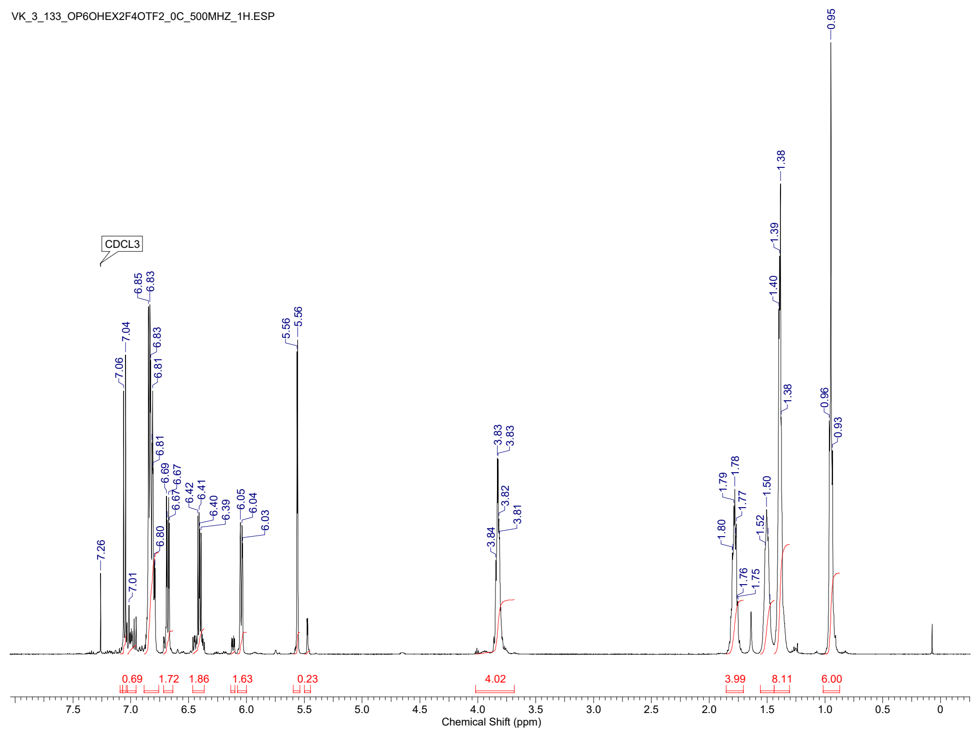

Figure S21. ^{1}H NMR spectrum (500 MHz, $CDCl_3$, 0 ℃) of **11b**.

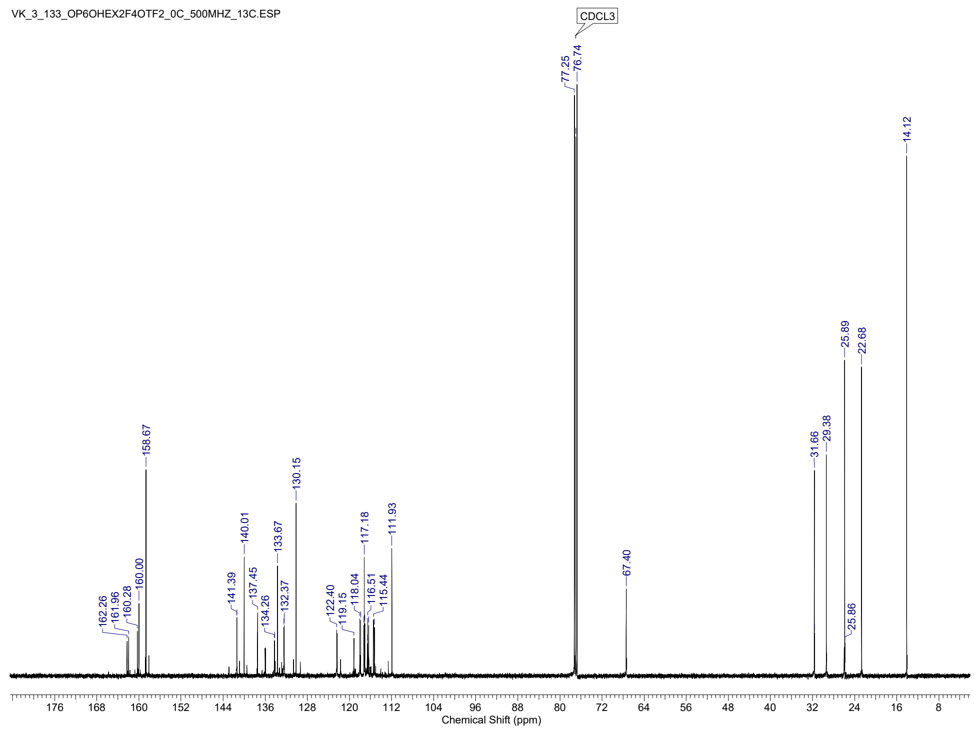

Figure S22. ^{13}C NMR spectrum (125 MHz, $CDCl_3$, 0 ℃) of **11b**.

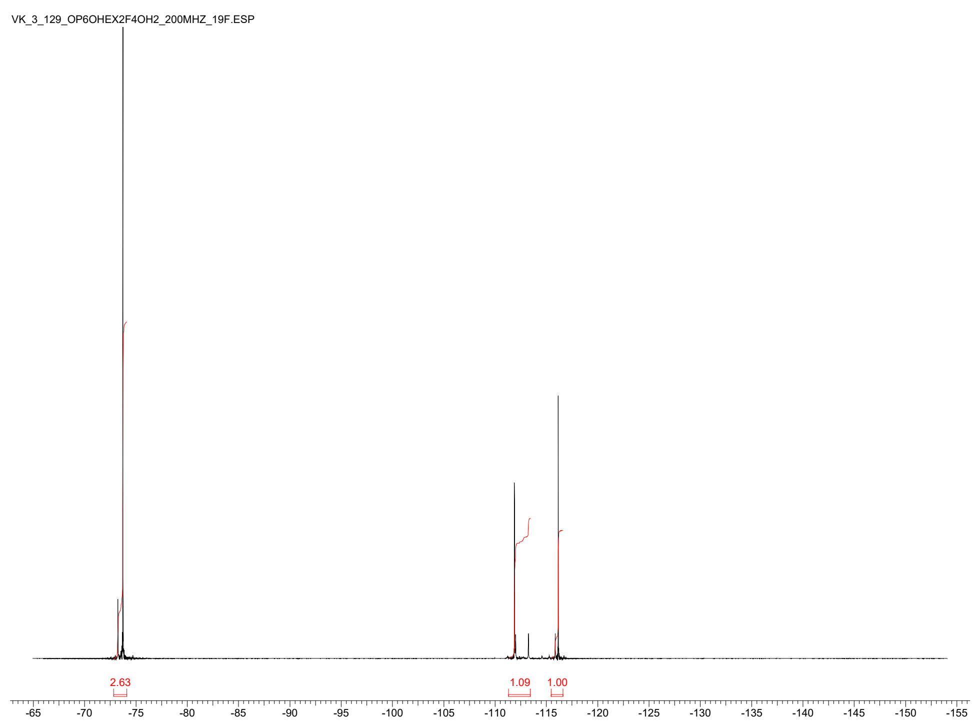

Figure S23. ^{19}F NMR spectrum (188 MHz, $CDCl_3$, 0 ℃) of **11b**.

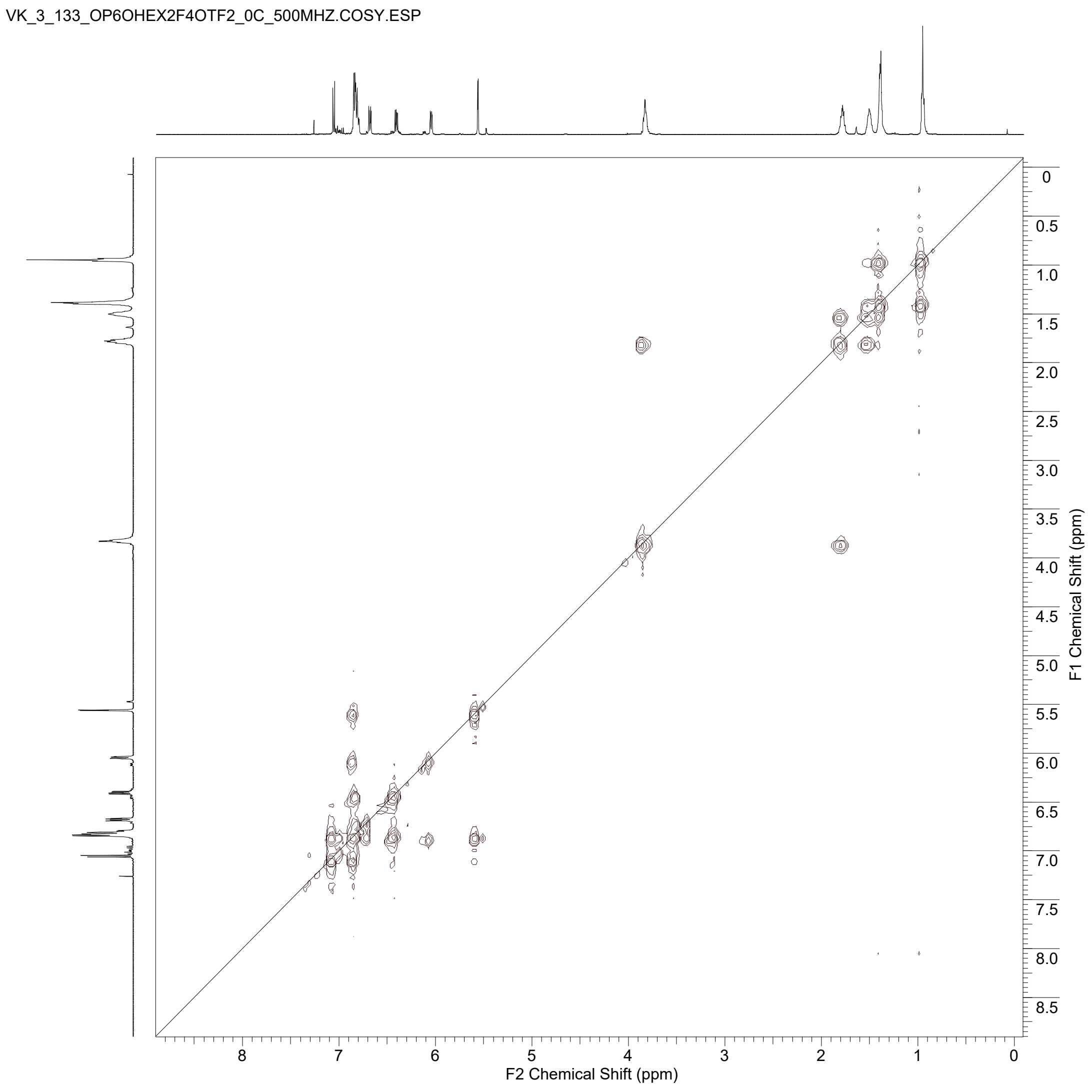

Figure S24. COSY NMR spectrum (500 MHz, $CDCl_3$, 0 ℃) of **11b**.

VK_3_133_OP6OHEX2F4OTF2_0C_500MHZ.HSQC.ESP

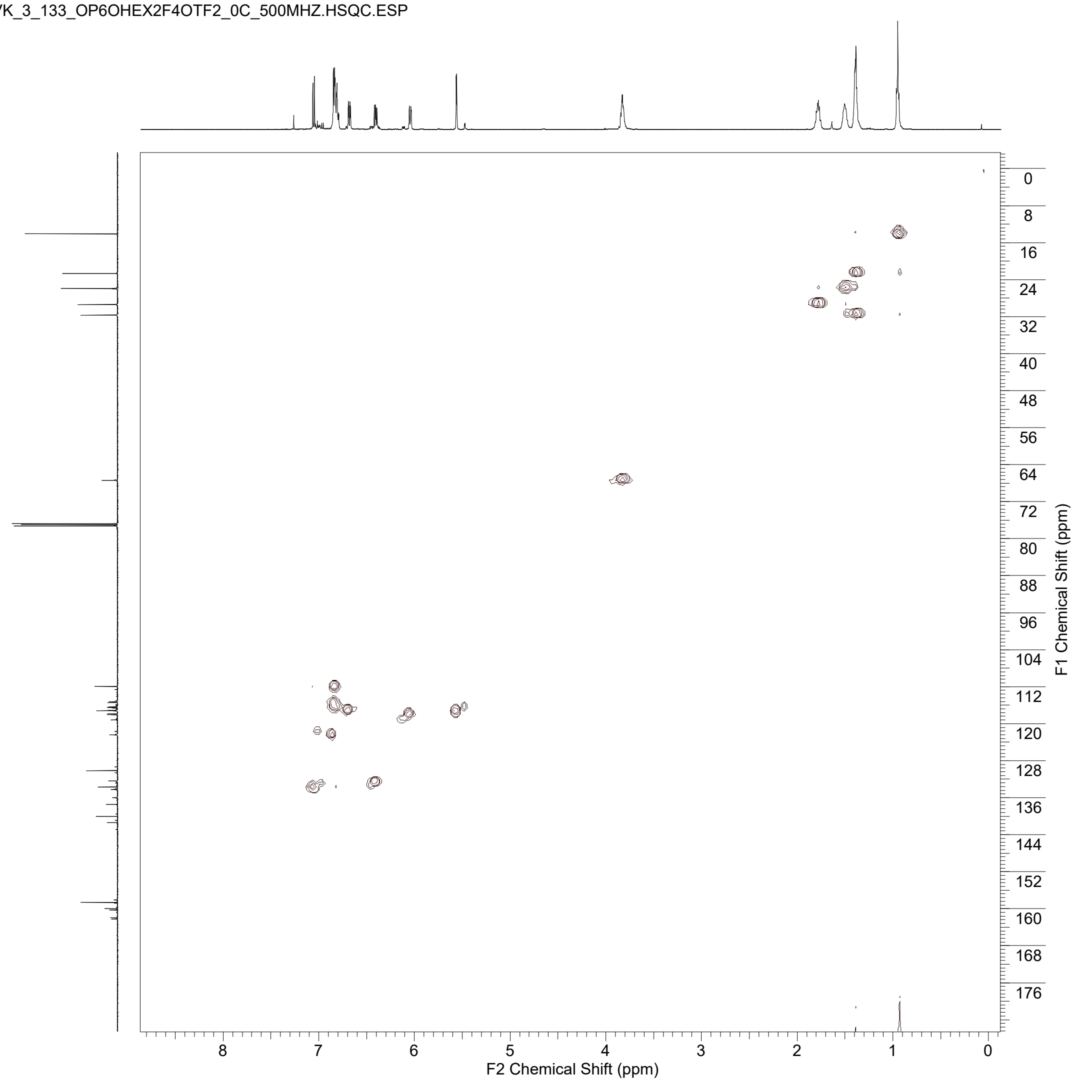

Figure S25. HSQC NMR spectrum (500 MHz, $CDCl_3$, 0 ℃) of **11b**.

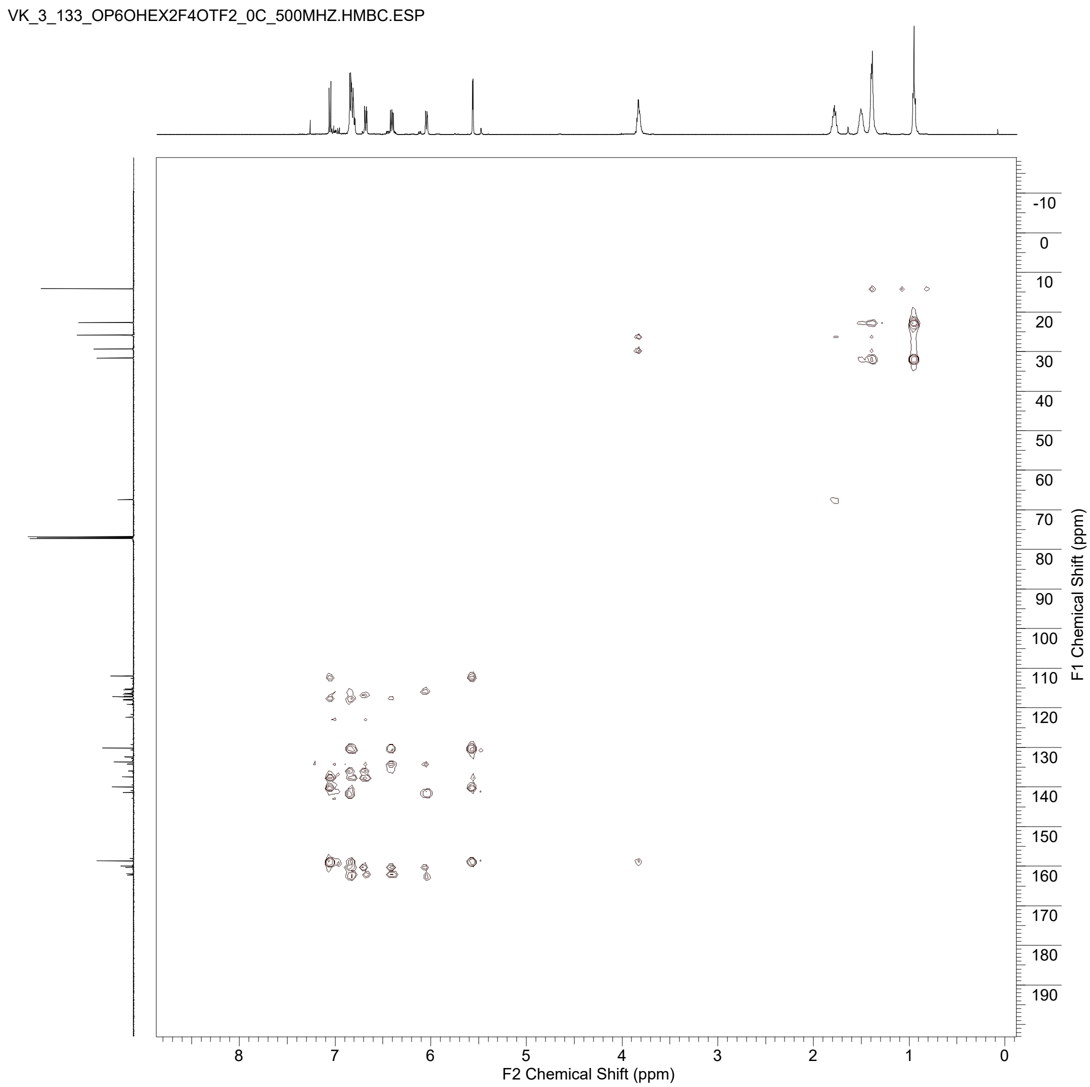

Figure S26. HMBC NMR spectrum (500 MHz, $CDCl_3$, 0 ℃) of **11b**.

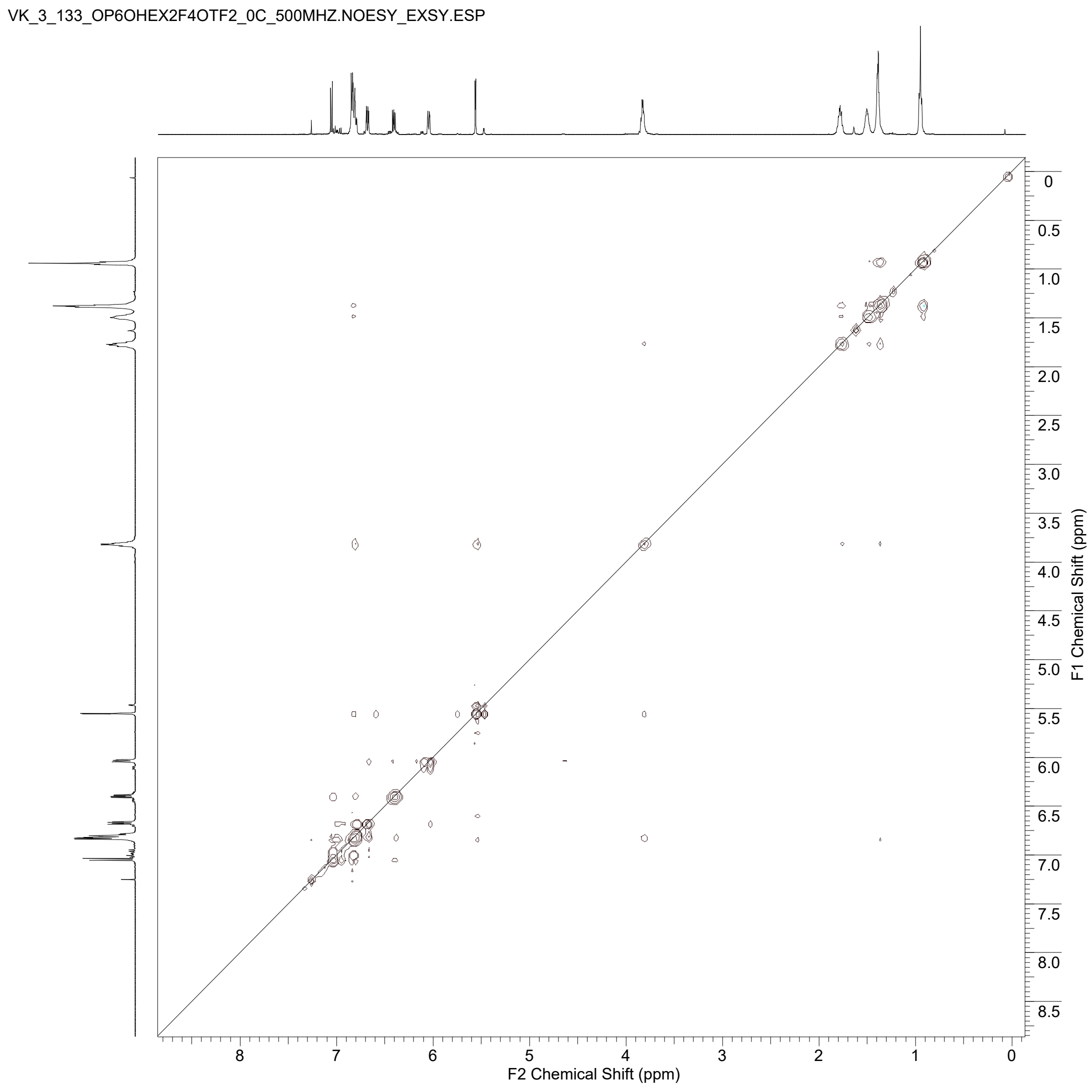

Figure S27. NOESY/EXSY NMR spectrum (500 MHz, $CDCl_3$, 0 ℃) of **11b**.

oP^{8}H(NH$_2$)

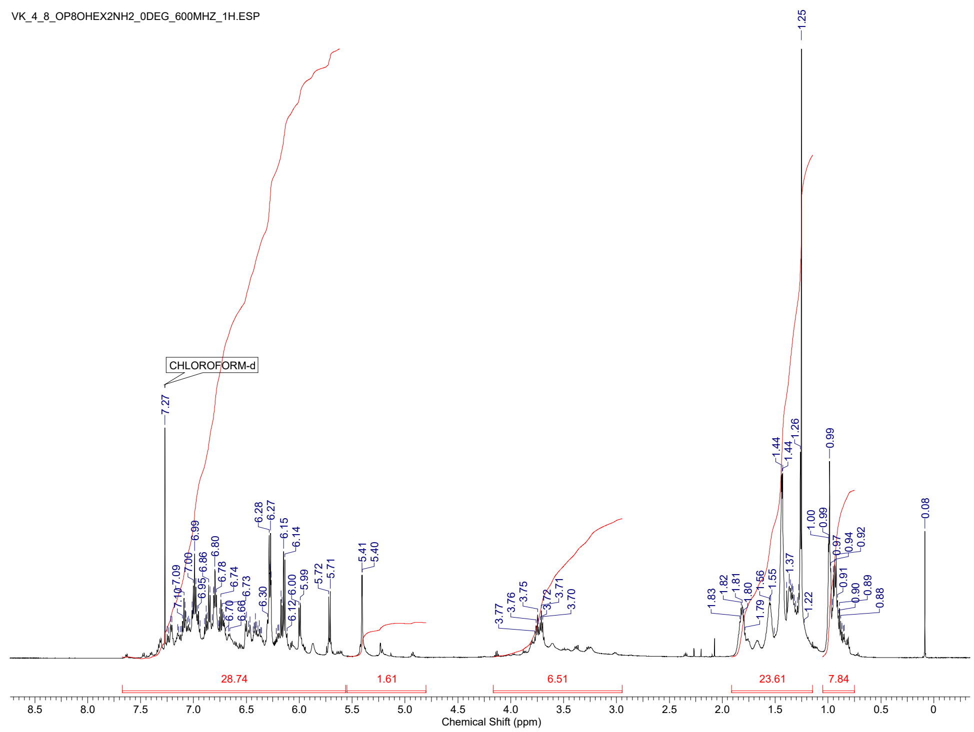

Figure S28. ^{1}H NMR spectrum (600 MHz, $CDCl_3$, 0 ℃) of **oP^{8}H(NH$_2$)**.

VK_4_8_OP8OHEX2NH2_0DEG_600MHZ.COSY.ESP

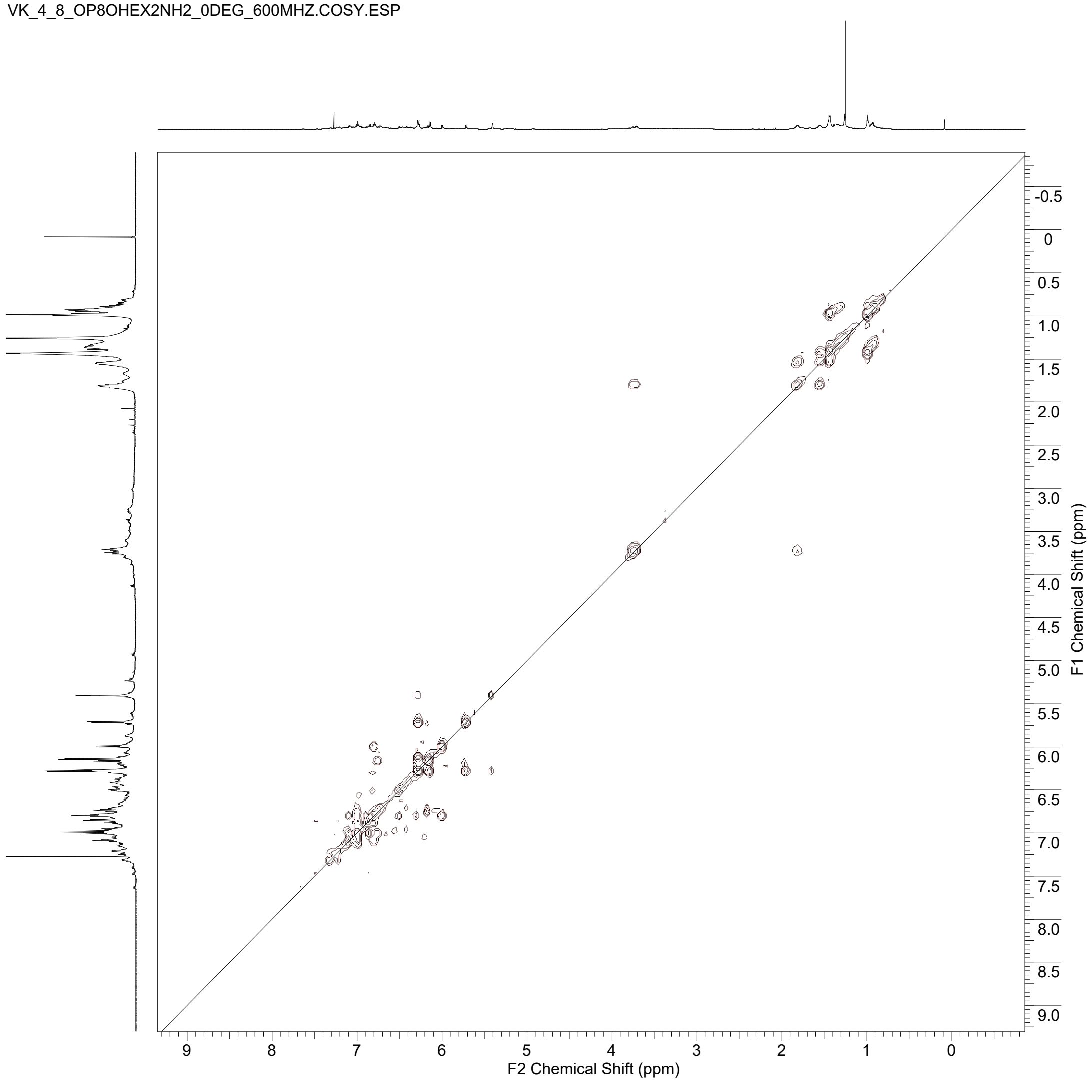

Figure S29. COSY NMR spectrum (600 MHz, $CDCl_3$, 0 ℃) of **oP^{8}H(NH_2)**.

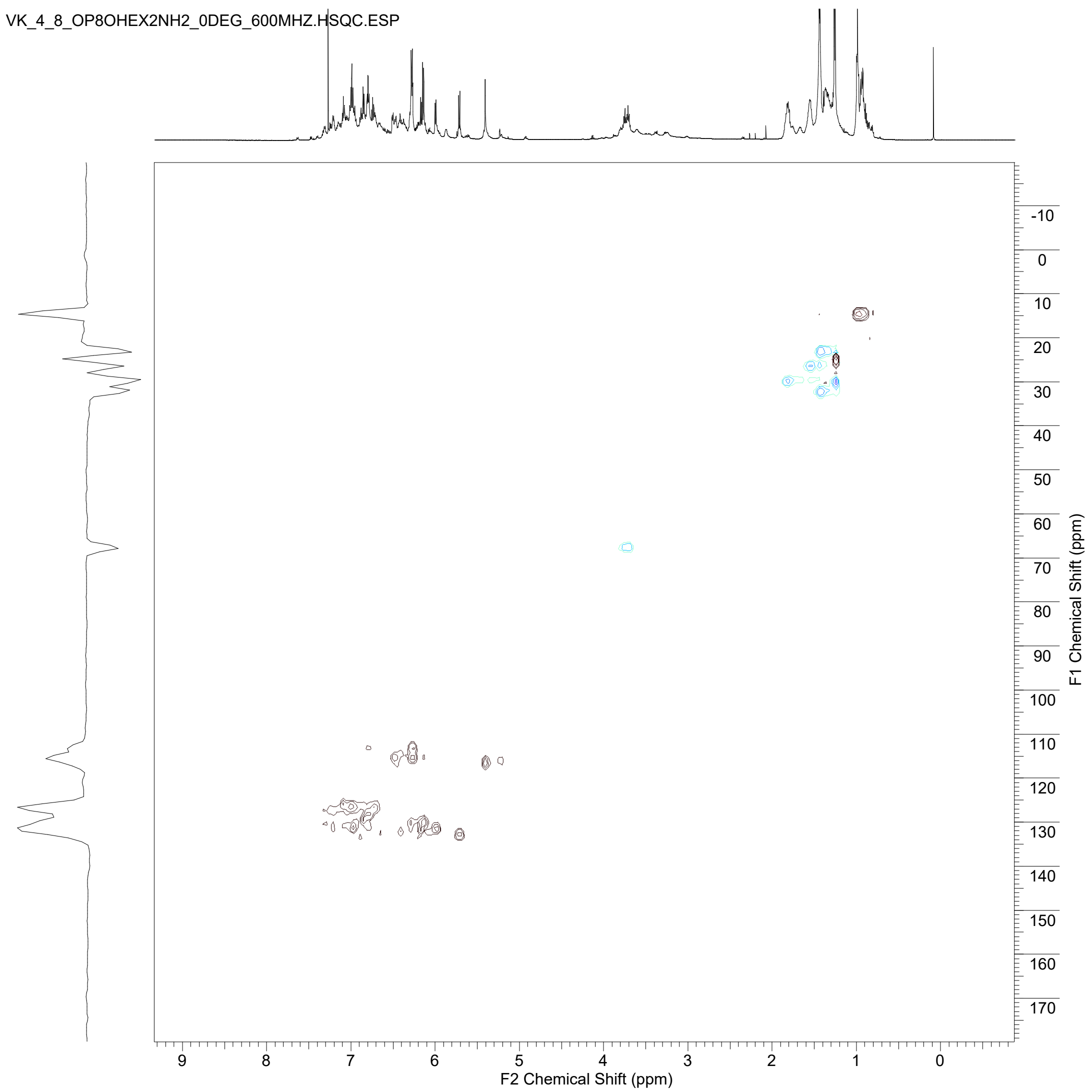

Figure S30. HSQC NMR spectrum (600 MHz, $CDCl_3$, 0 ℃) of **oP^{8}H(NH$_2$)**.

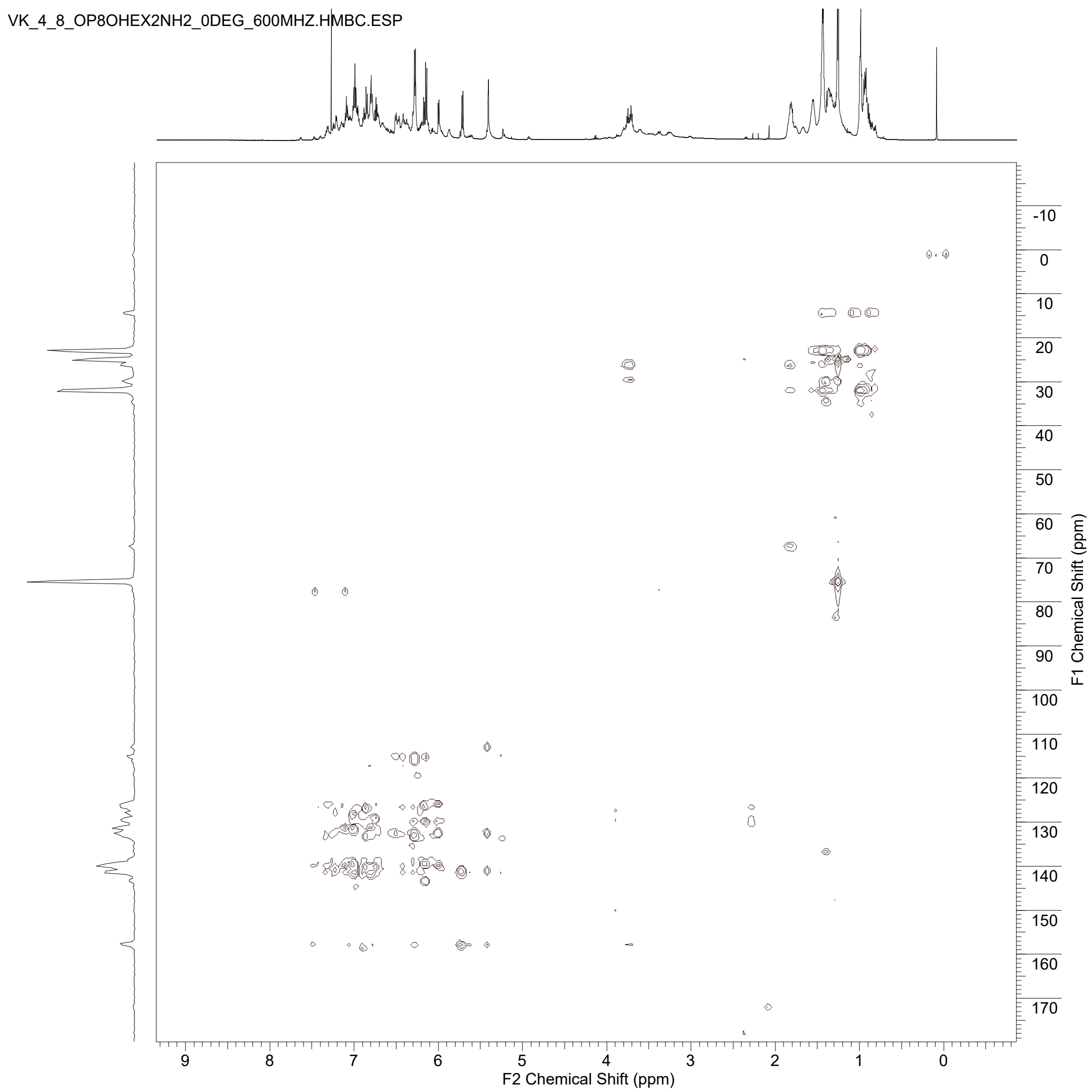

Figure S31. HMBC NMR spectrum (600 MHz, $CDCl_3$, 0 ℃) of **oP[8]H(NH$_2$)**.

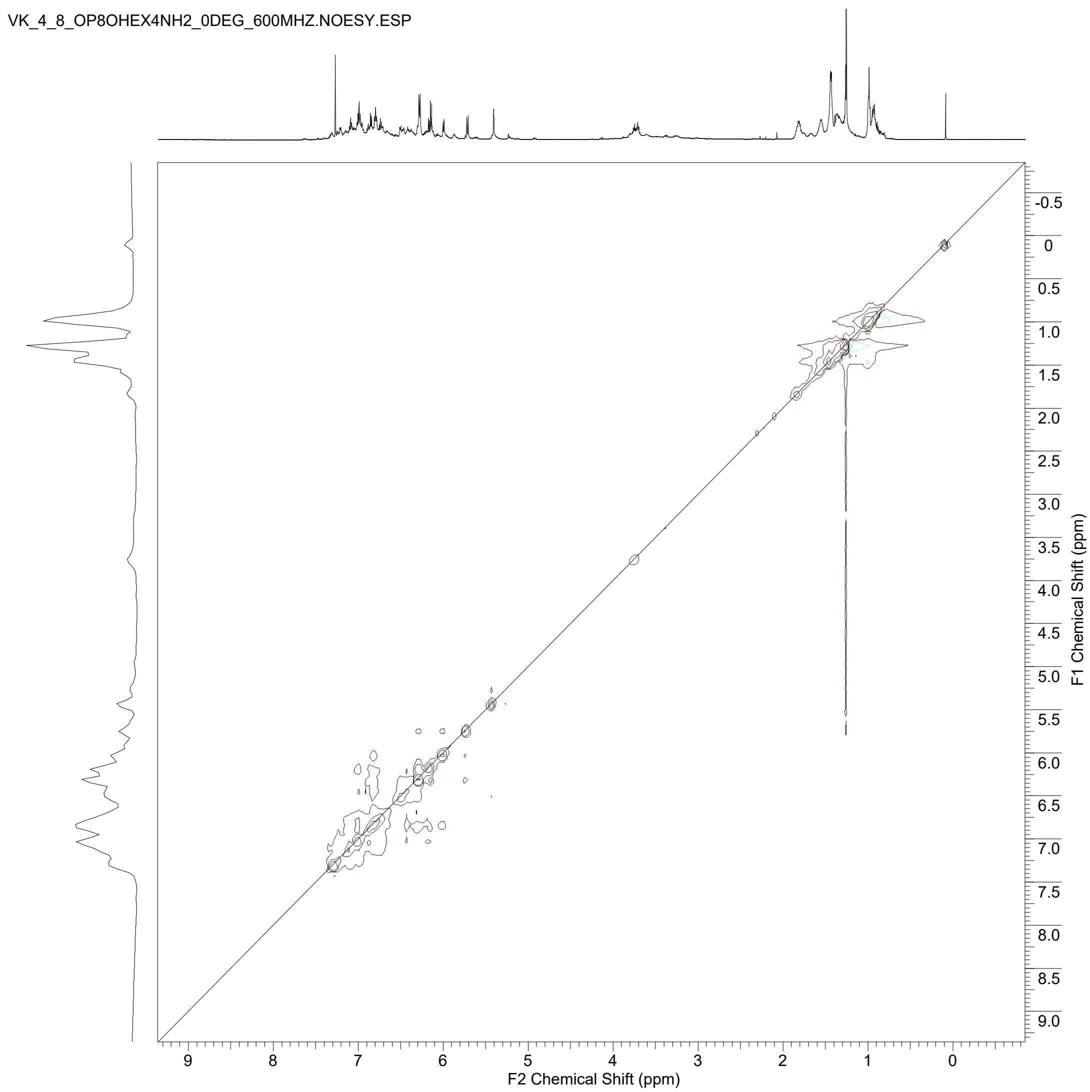

Figure S32. NOESY/EXSY NMR spectrum (600 MHz, $CDCl_3$, 0 ℃) of **oP^{8}H(NH$_2$)**.

oP⁸F(NH₂)

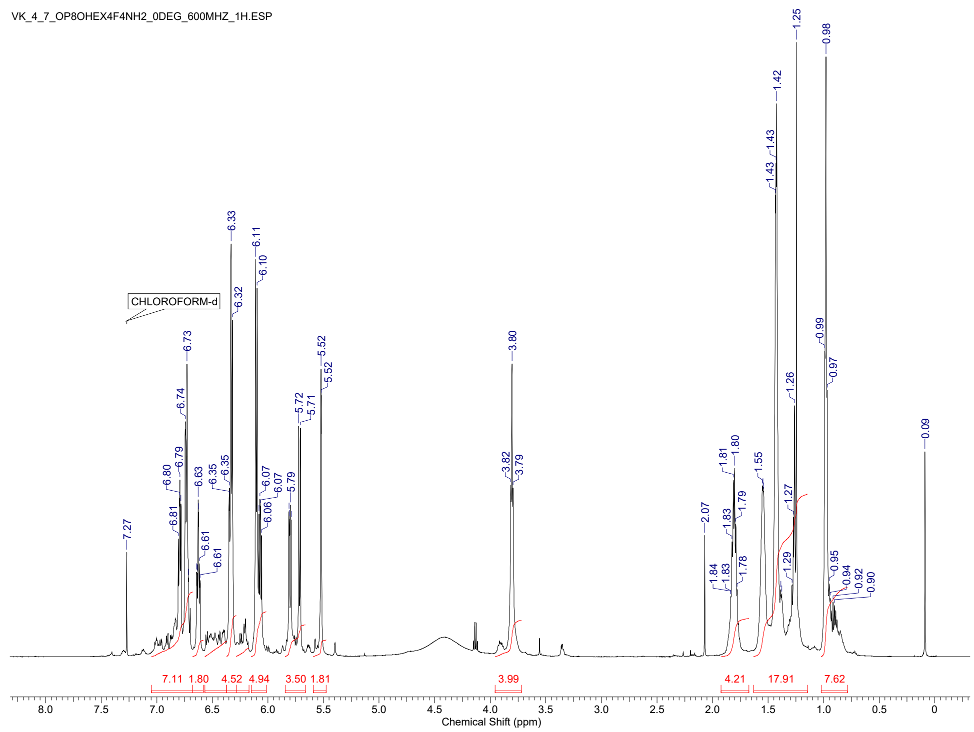

Figure S33. ^{1}H NMR spectrum (600 MHz, $CDCl_3$, 0 ℃) of **oP⁸F(NH₂)**.

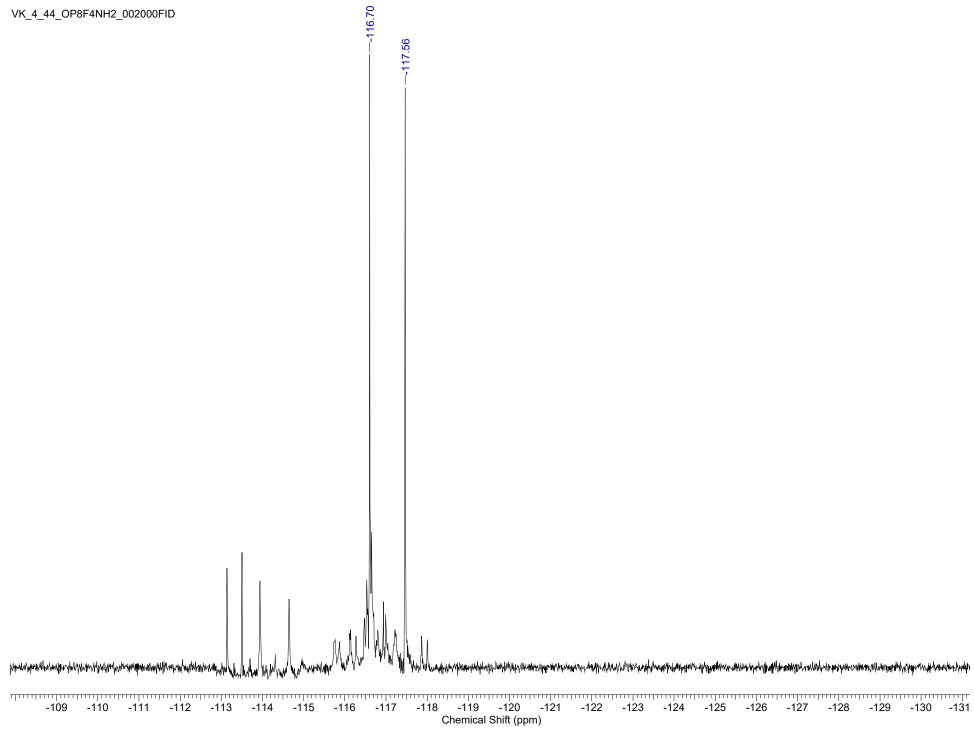

Figure S34. ^{19}F NMR spectrum (188 MHz, $CDCl_3$, 0 ℃) of **oP^{8}F(NH$_2$)**.

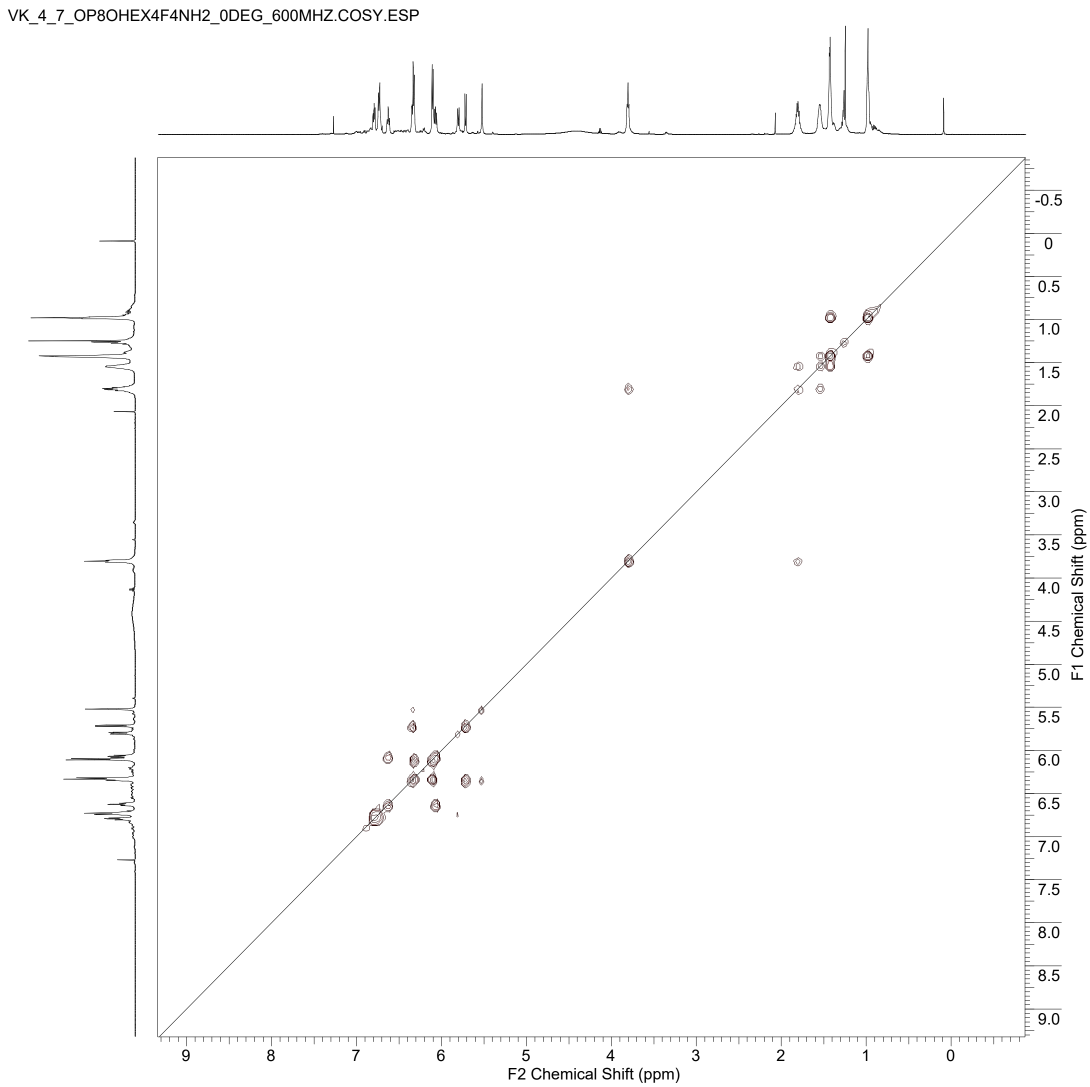

Figure S35. COSY NMR spectrum (600 MHz, $CDCl_3$, 0 ℃) of $\mathbf{oP^8F(NH_2)}$.

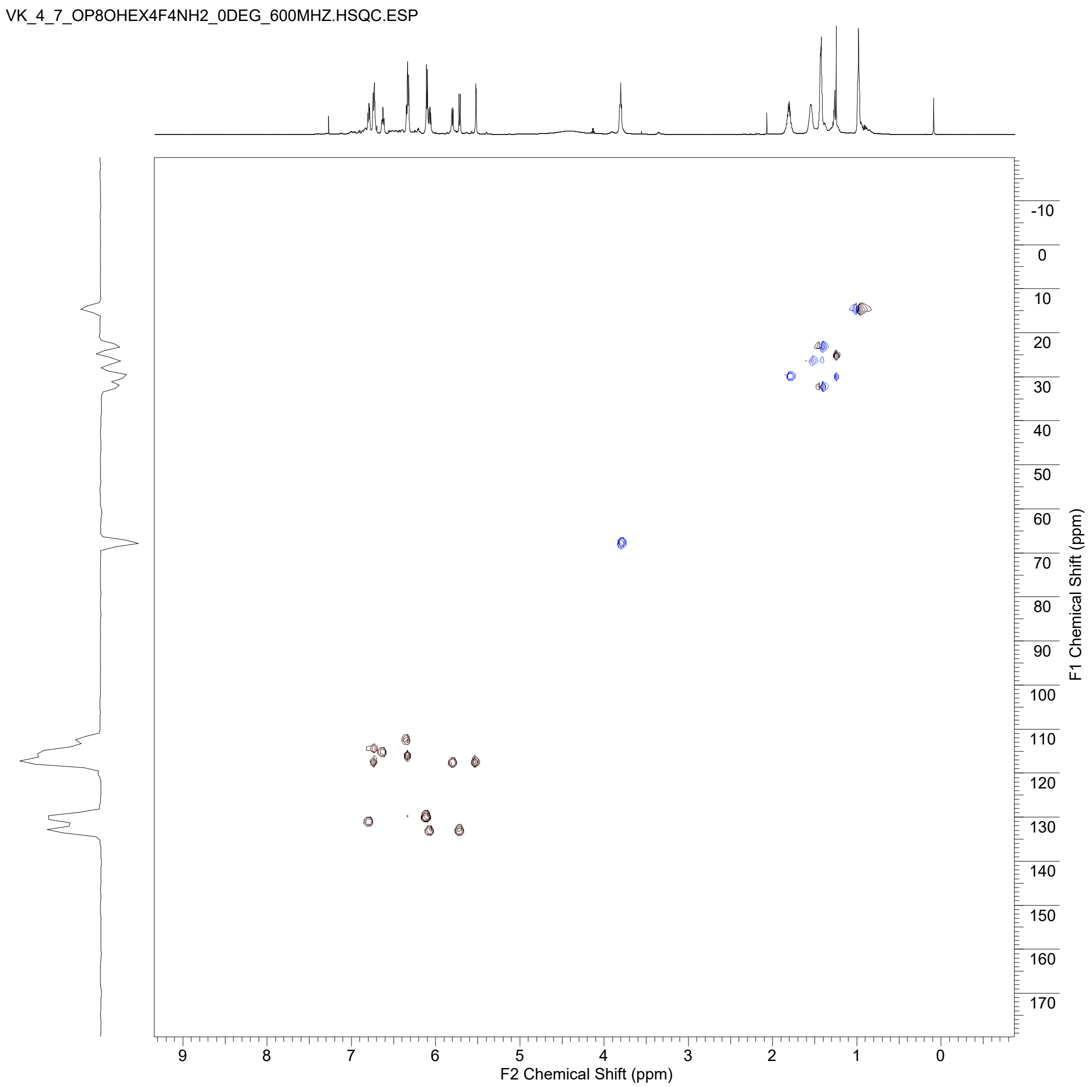

Figure S36. HSQC NMR spectrum (600 MHz, $CDCl_3$, 0 ℃) of **oP^{8}F(NH$_2$)**.

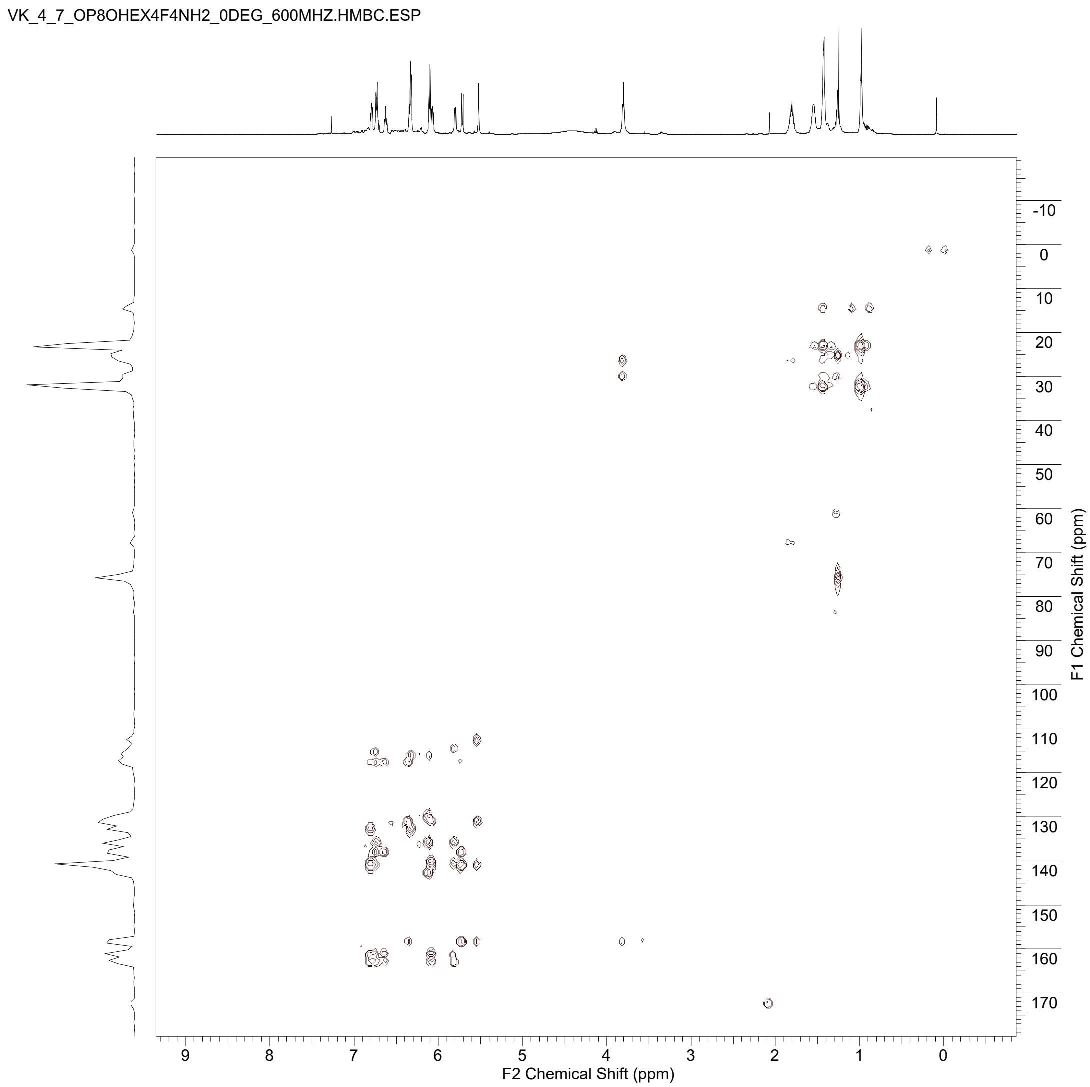

Figure S37. HMBC NMR spectrum (600 MHz, $CDCl_3$, 0 ℃) of **oP^{8}F(NH_2)**.

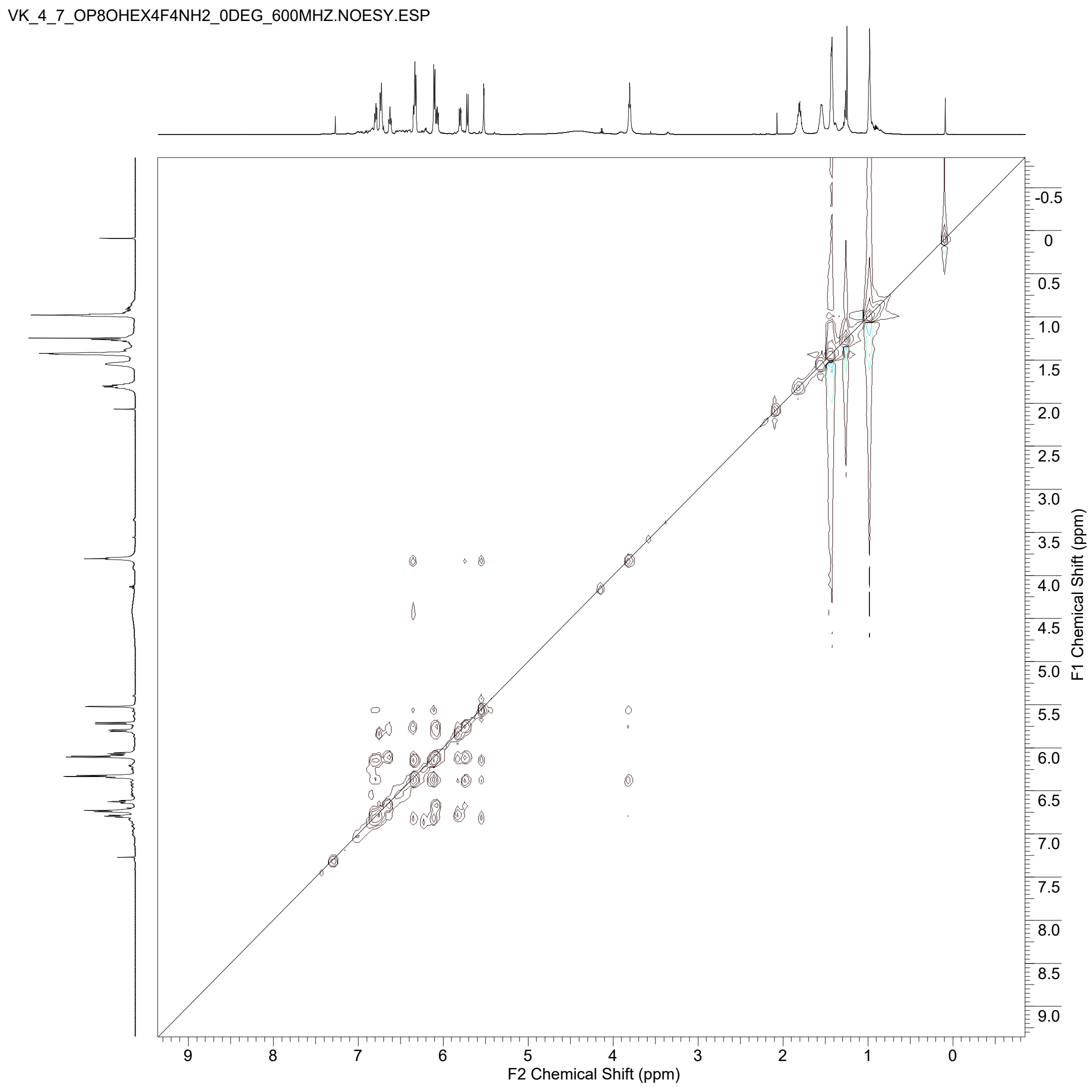

Figure S38. NOESY/EXSY NMR spectrum (600 MHz, $CDCl_3$, 0 ℃) of **oP⁸F(NH₂)**.

oP⁸H(M)

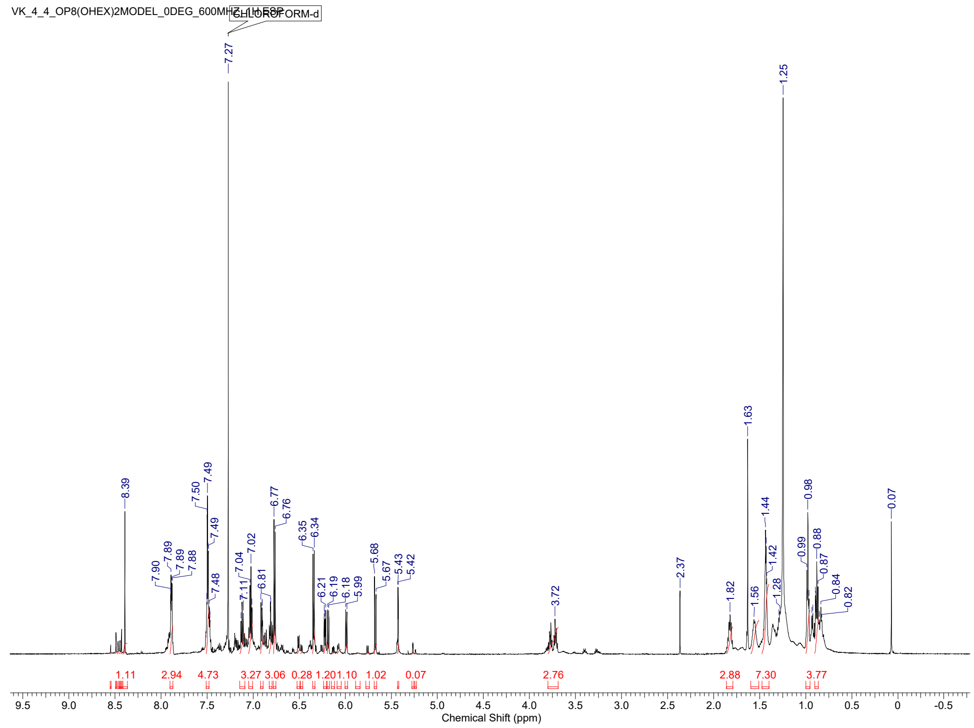

Figure S39. ¹H NMR spectrum (600 MHz, $CDCl_3$, 0 ℃) of **oP⁸H(M)**.

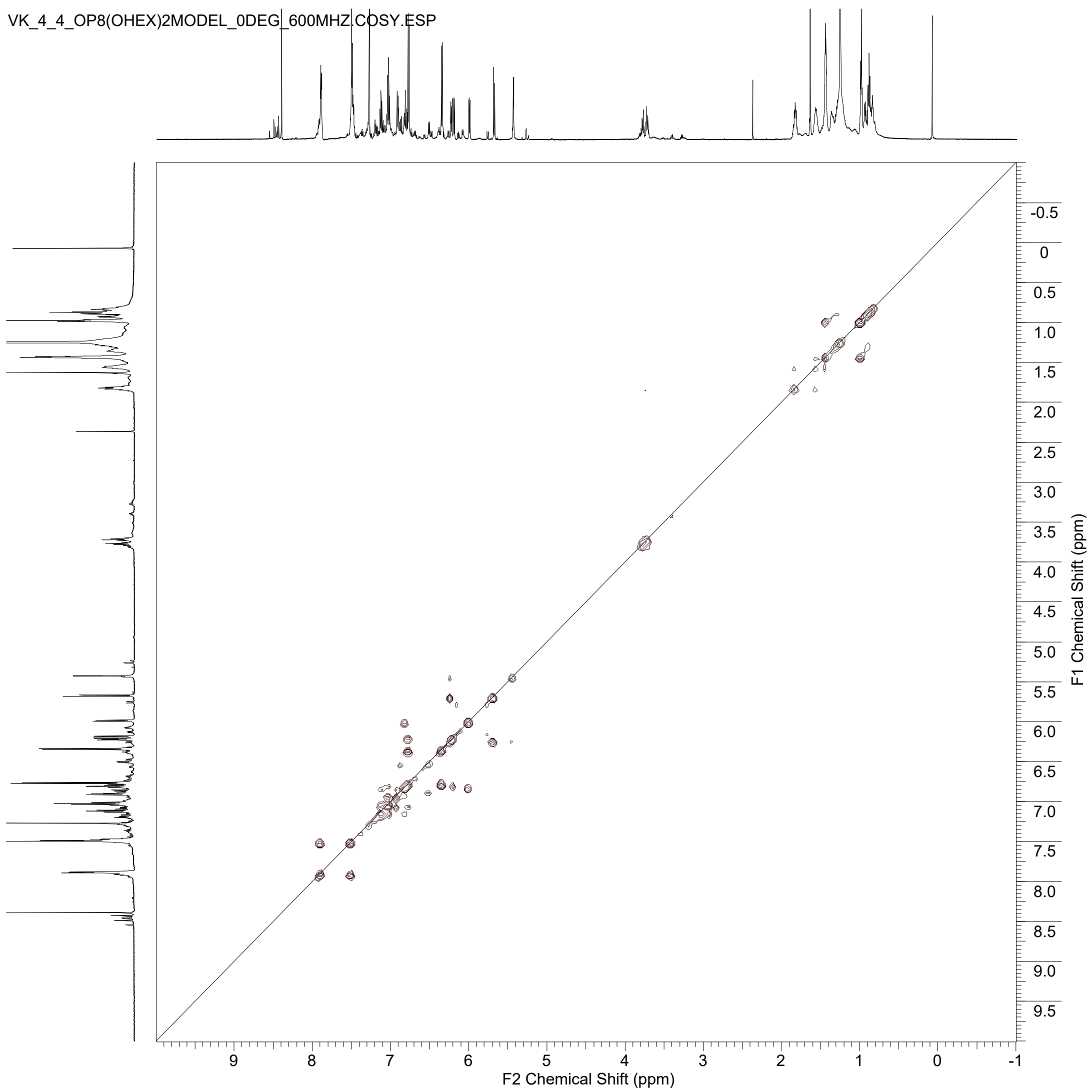

Figure S40. COSY NMR spectrum (600 MHz, $CDCl_3$, 0 ℃) of **$oP^8H(M)$**.

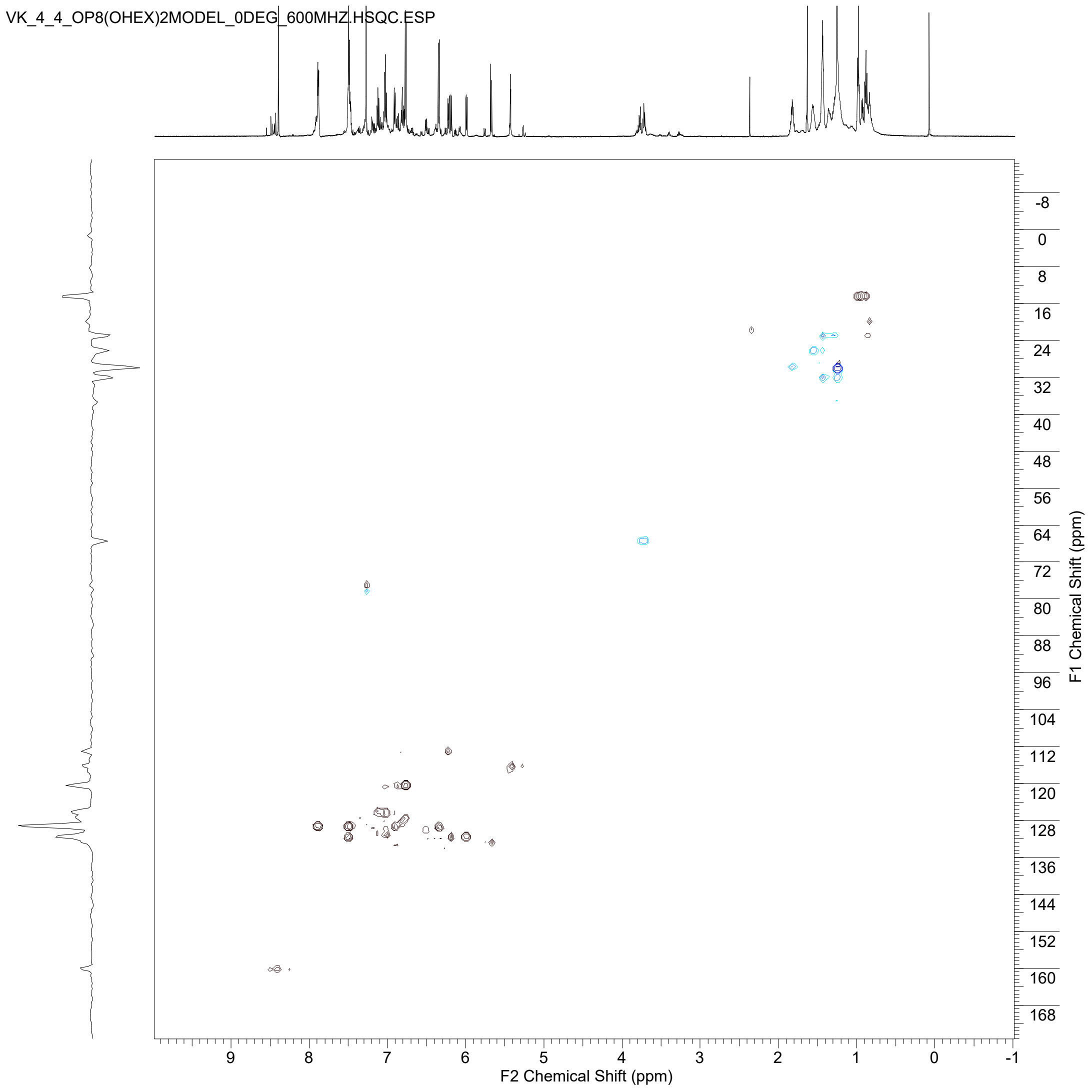

Figure S41. HSQC NMR spectrum (600 MHz, $CDCl_3$, 0 ℃) of **oP⁸H(M)**.

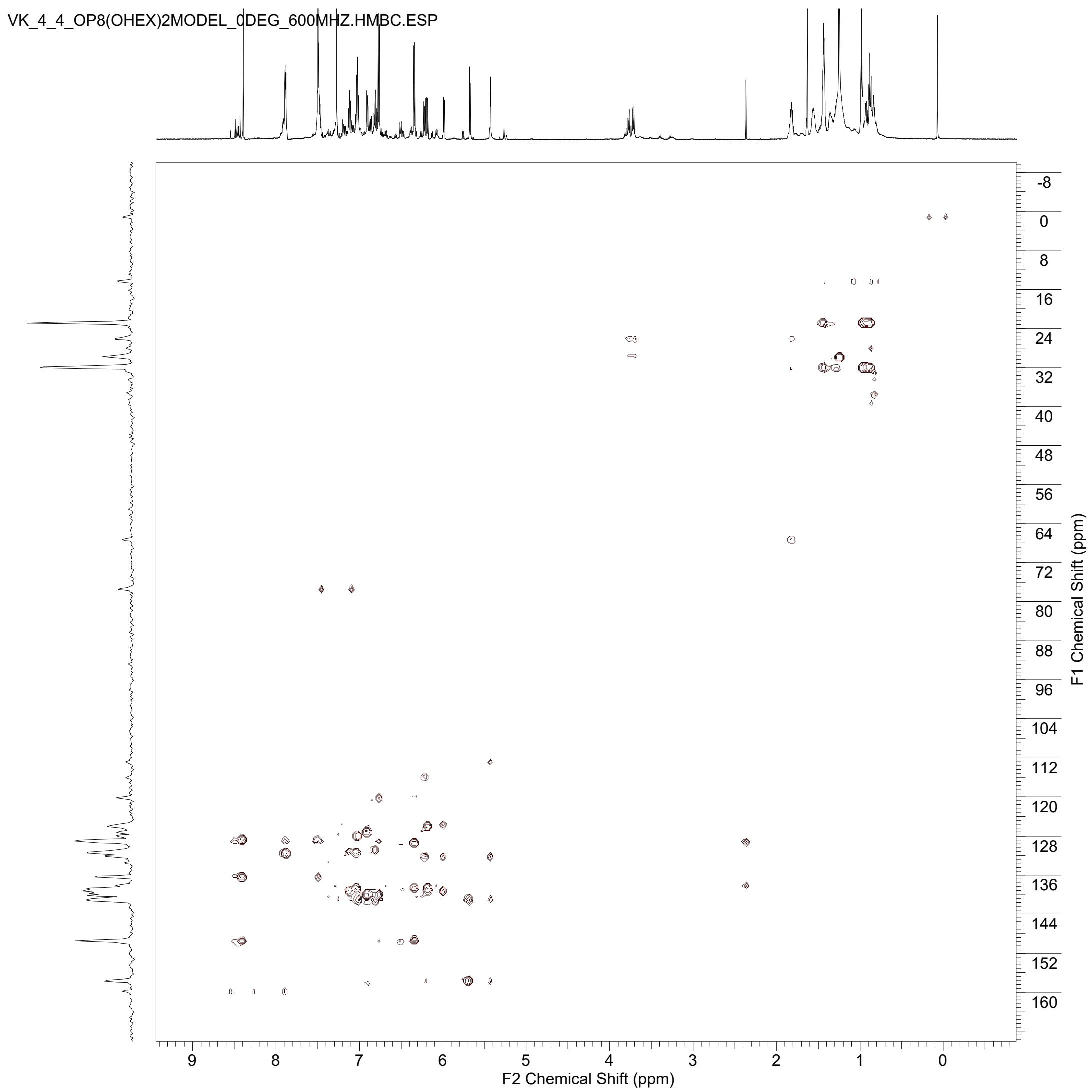

Figure S42. HMBC NMR spectrum (600 MHz, $CDCl_3$, 0 ℃) of **oP^{8}H(M)**.

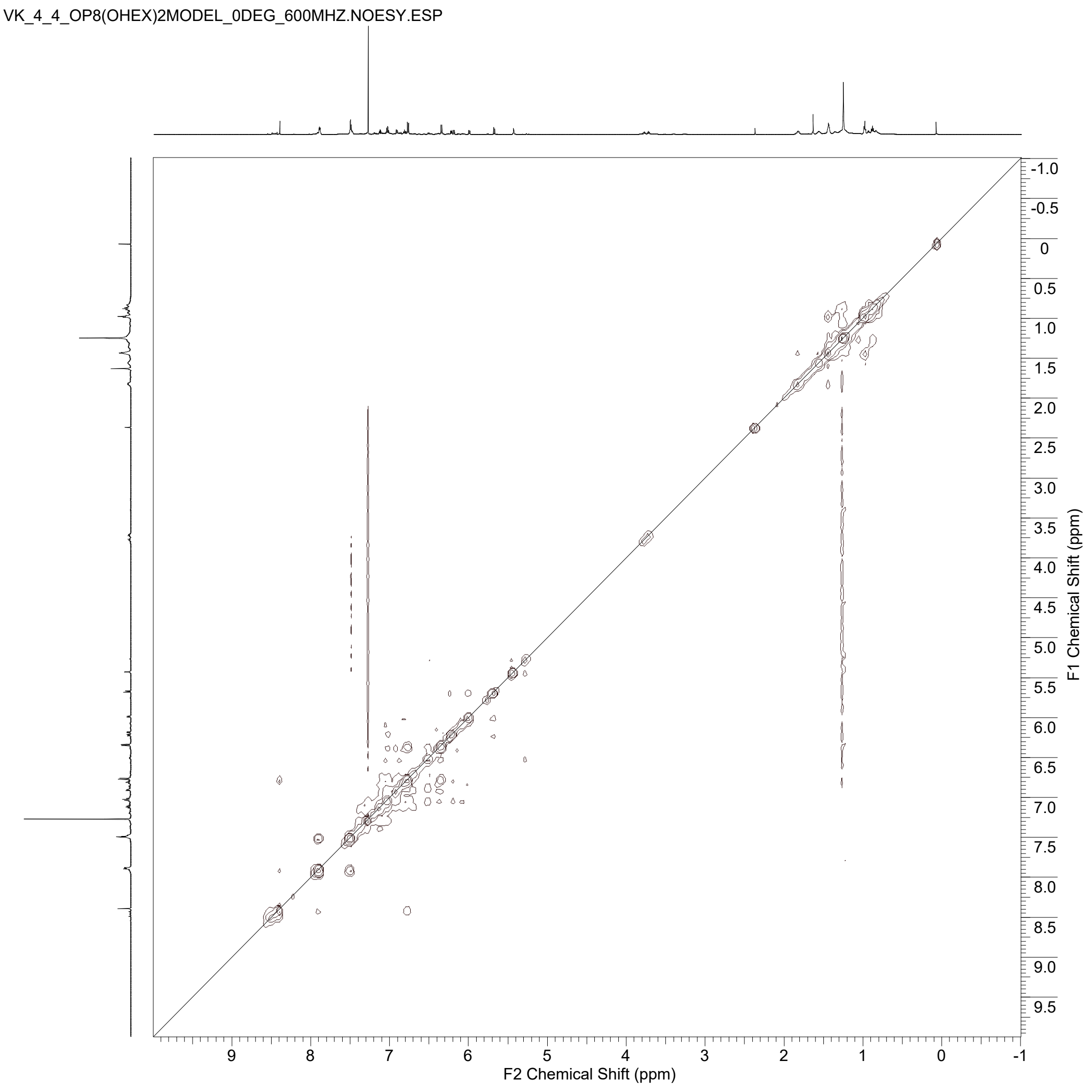

Figure S43. NOESY/EXSY NMR spectrum (600 MHz, $CDCl_3$, 0 ℃) of **oP^{8}H(M)**.

oP^{8}F(M)

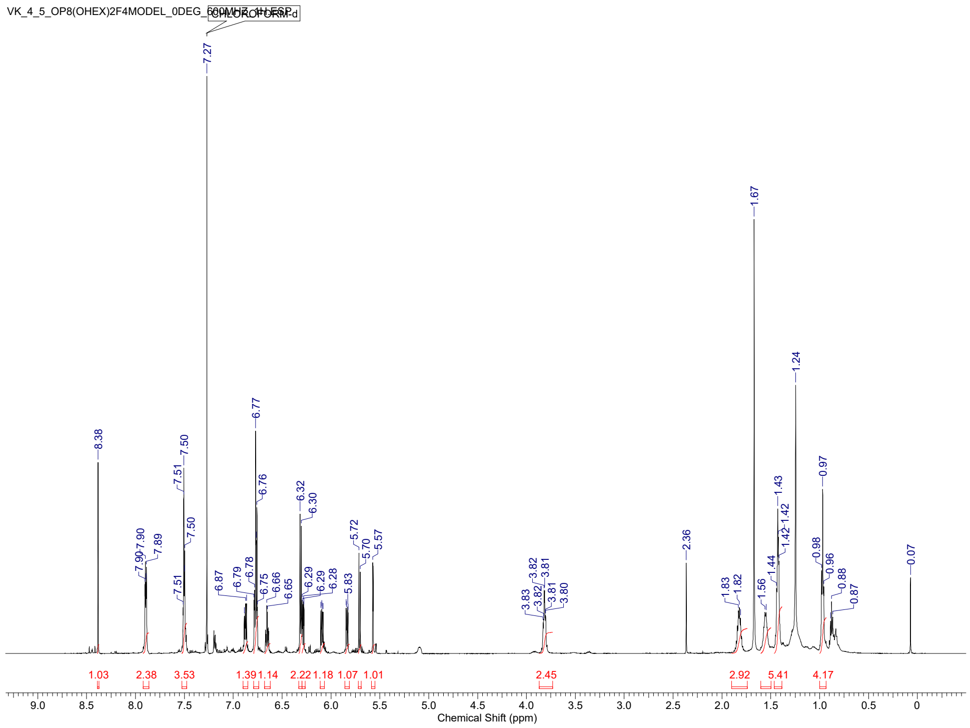

Figure S44. ^{1}H NMR spectrum (600 MHz, $CDCl_3$, 0 ℃) of **oP^{8}F(M)**.

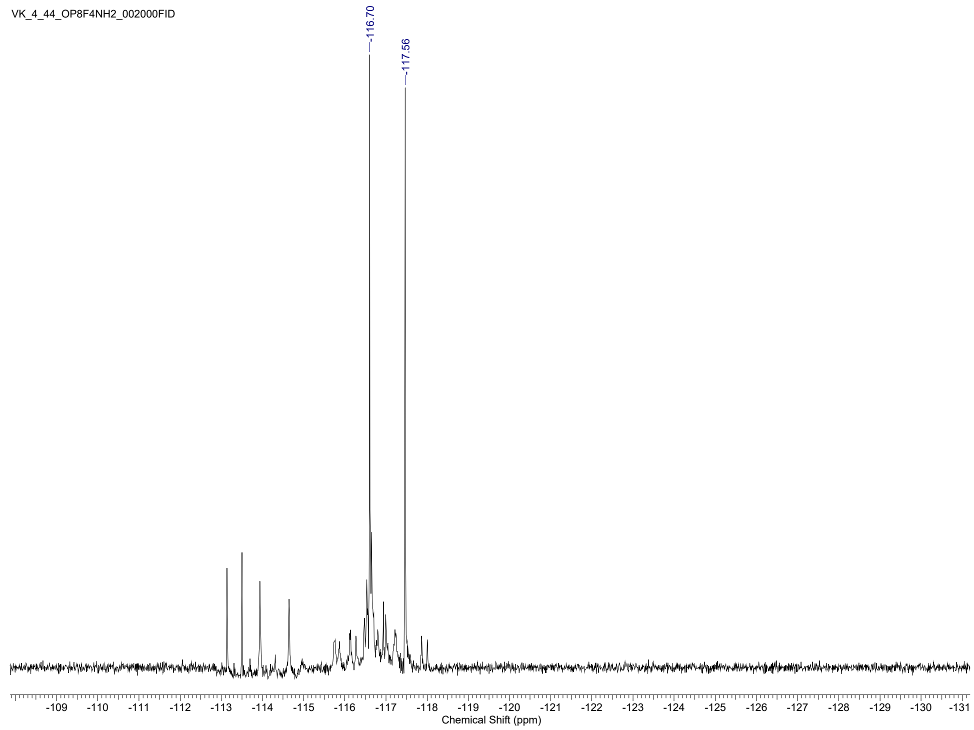

Figure S45. ^{19}F NMR spectrum (188 MHz, $CDCl_3$, 0 ℃) of **oP^{8}F(M)**.

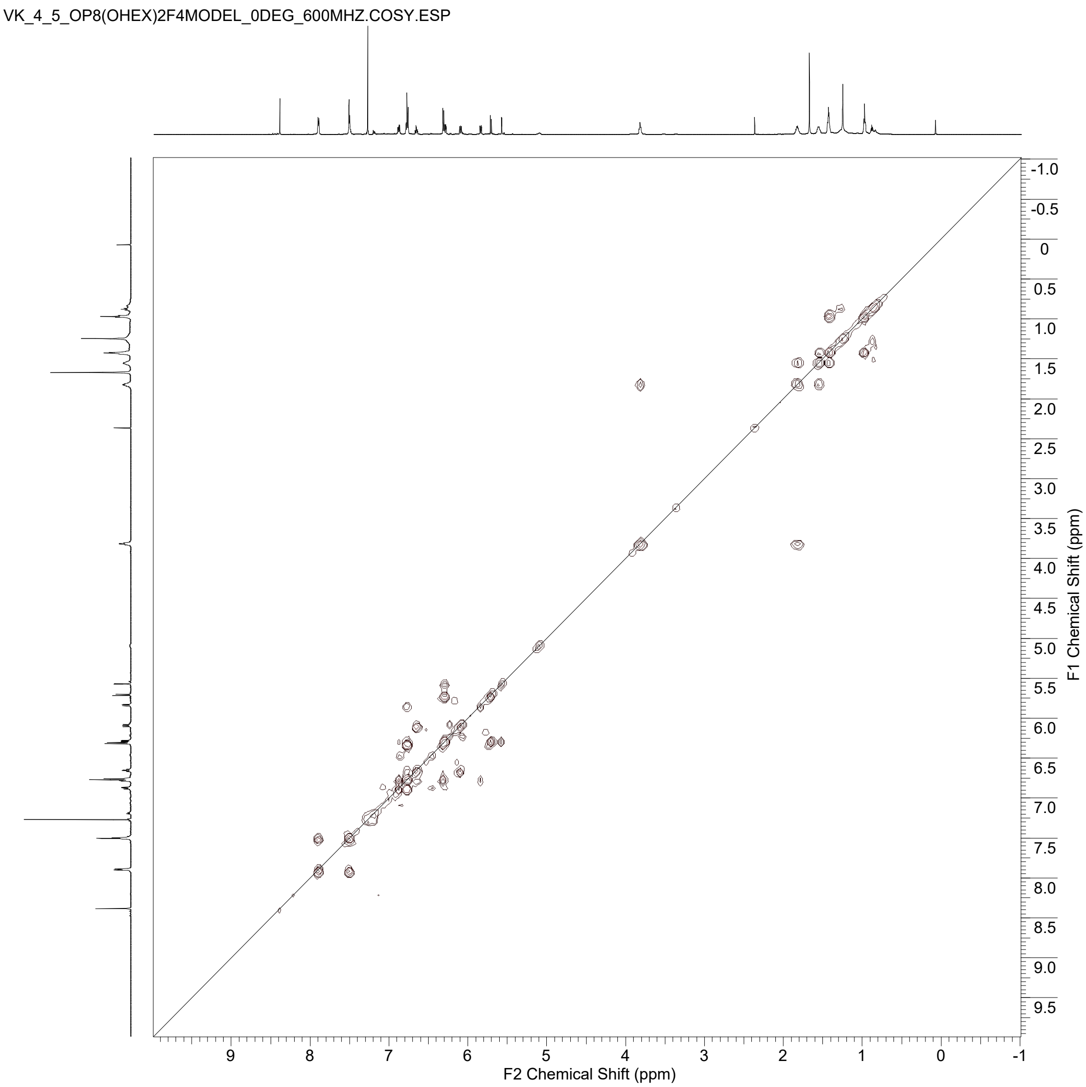

Figure S46. COSY NMR spectrum (600 MHz, $CDCl_3$, 0 ℃) of $\mathbf{oP^8F(M)}$.

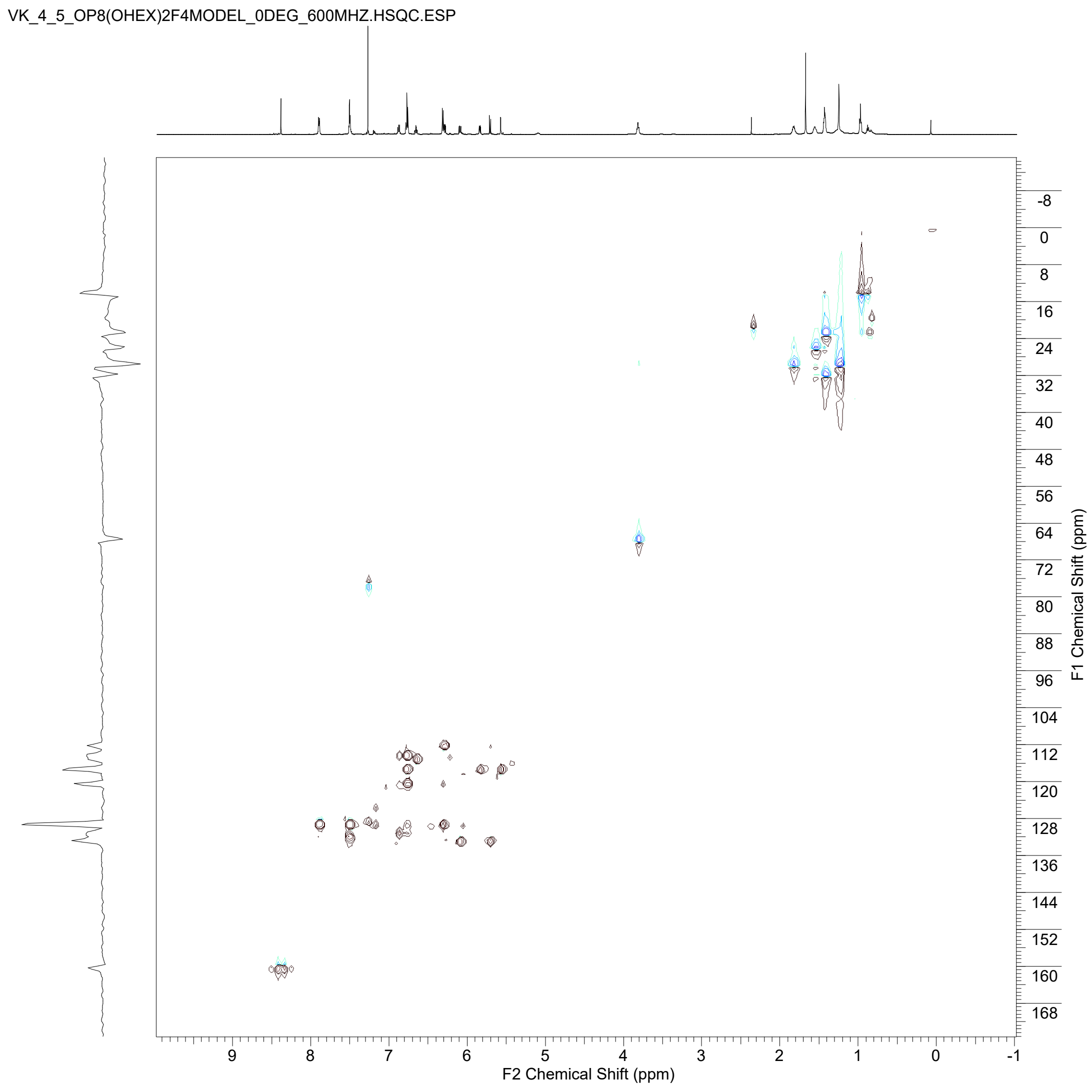

Figure S47. HSQC NMR spectrum (600 MHz, $CDCl_3$, 0 ℃) of **oP^{8}F(M)**.

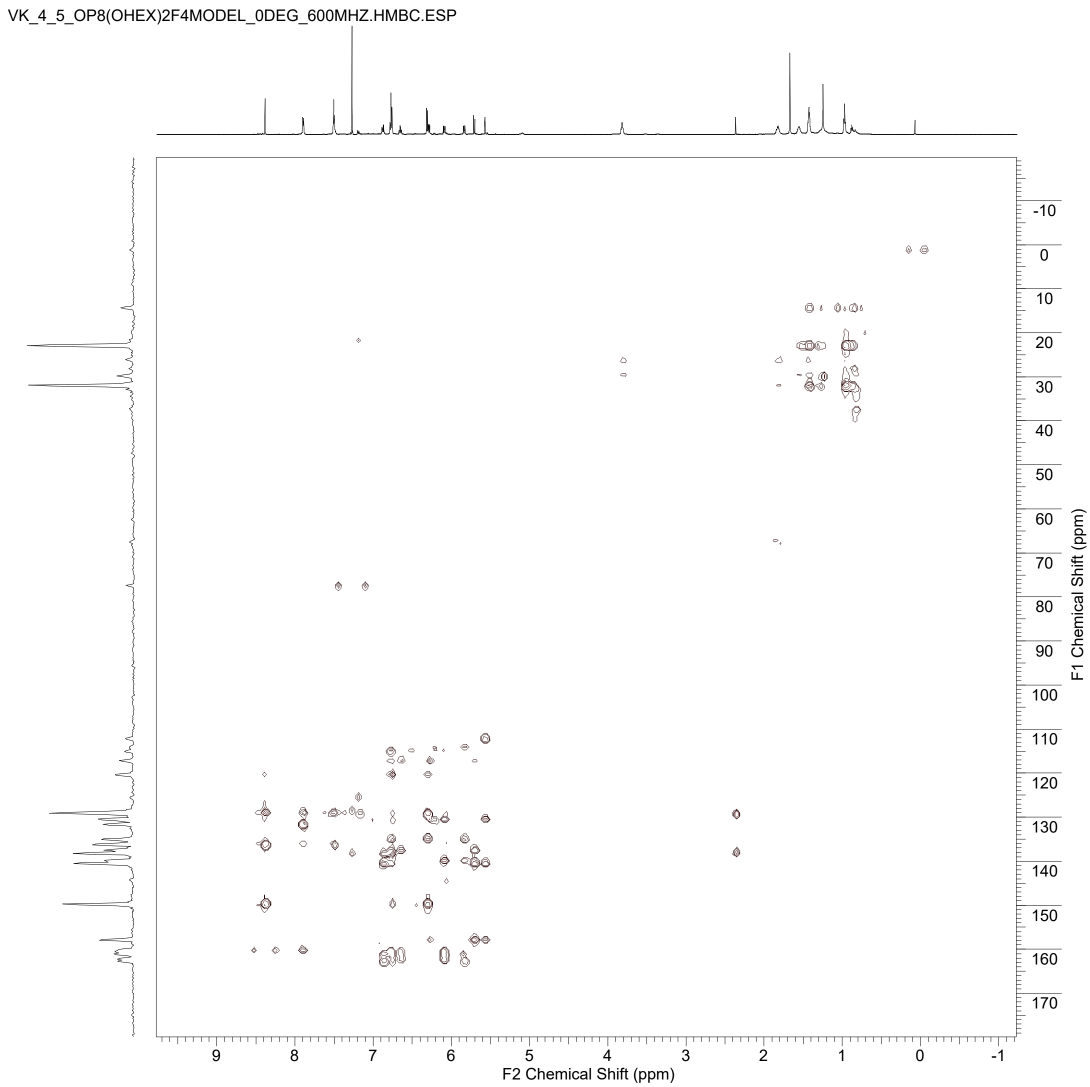

Figure S48. HMBC NMR spectrum (600 MHz, $CDCl_3$, 0 ℃) of **oP^{8}F(M)**.

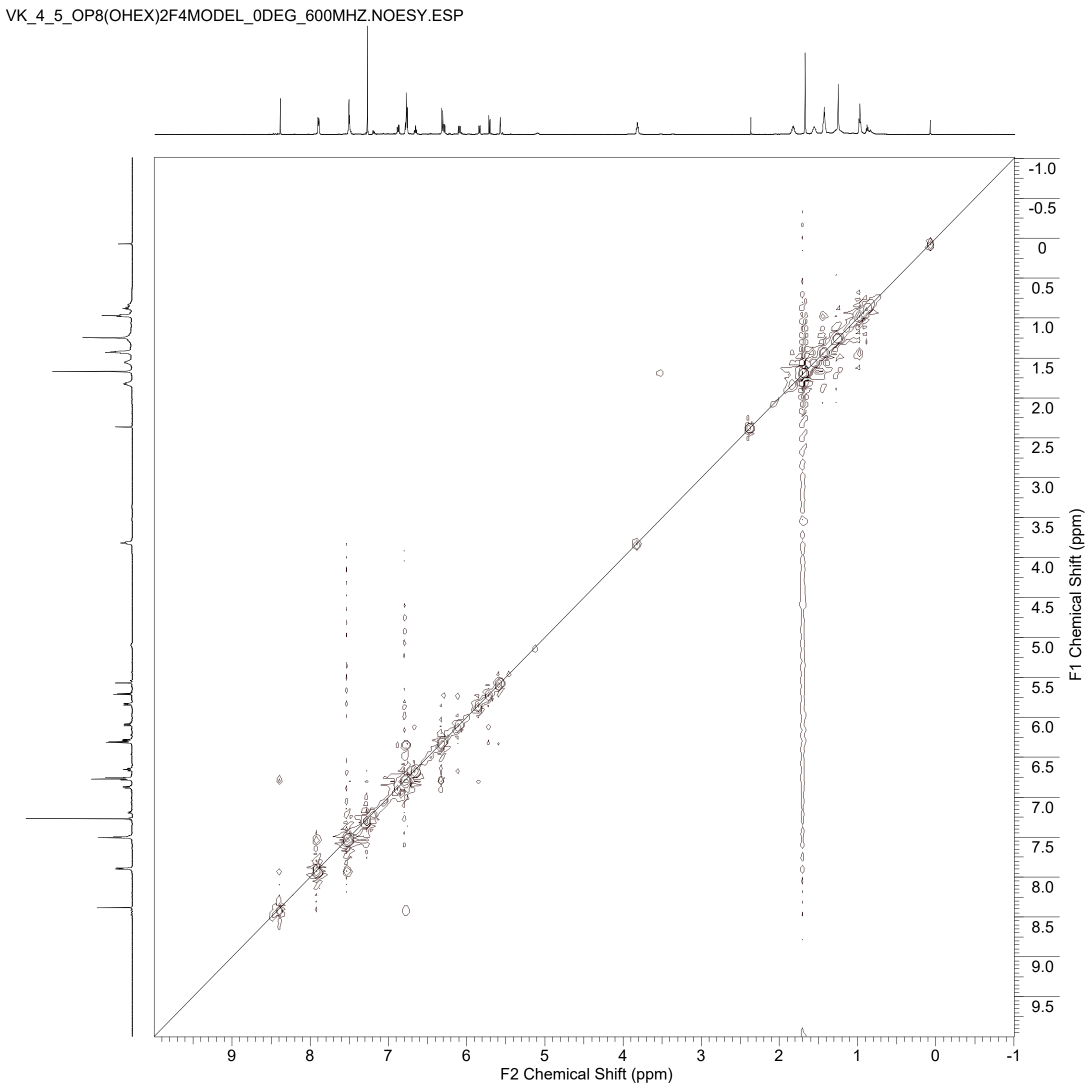

Figure S49. NOESY/EXSY NMR spectrum (600 MHz, $CDCl_3$, 0 ℃) of **oP^{8}F(M)**.

oP^{8}H(DPB)$_{2+2}$

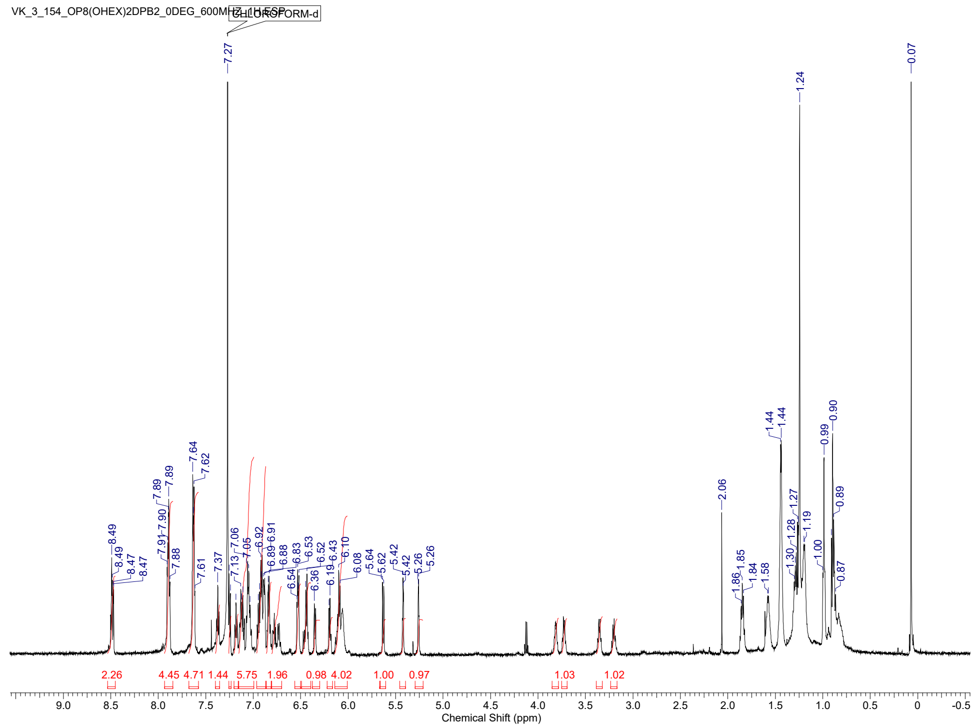

Figure S50. ^{1}H NMR spectrum (600 MHz, $CDCl_3$, 0 ℃) of **oP^{8}H(DPB)$_{2+2}$**.

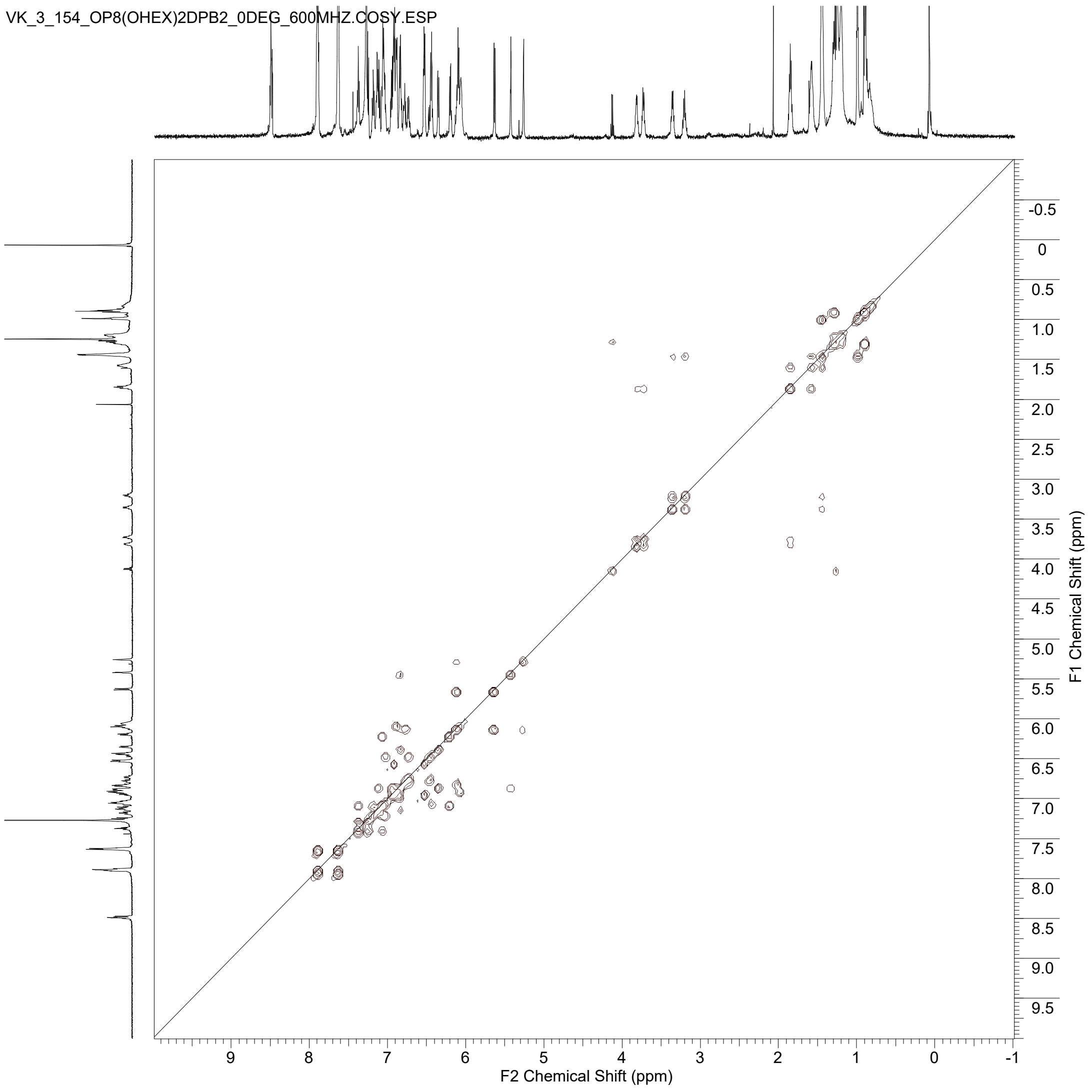

Figure S51. COSY NMR spectrum (600 MHz, $CDCl_3$, 0 ℃) of $\mathbf{oP^8H(DPB)_{2+2}}$.

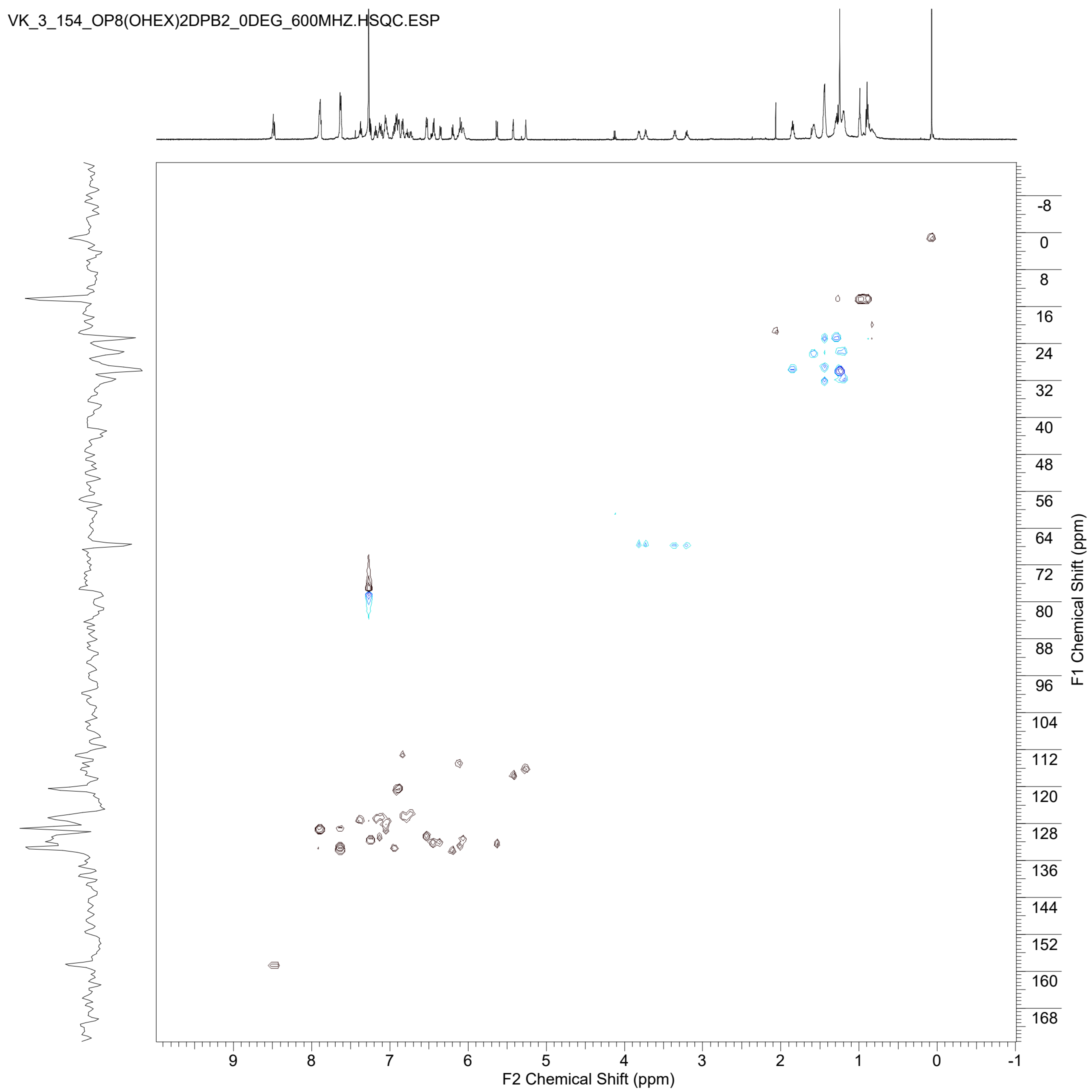

Figure S52. HSQC NMR spectrum (600 MHz, $CDCl_3$, 0 ℃) of **oP^{8}H(DPB)$_{2+2}$**.

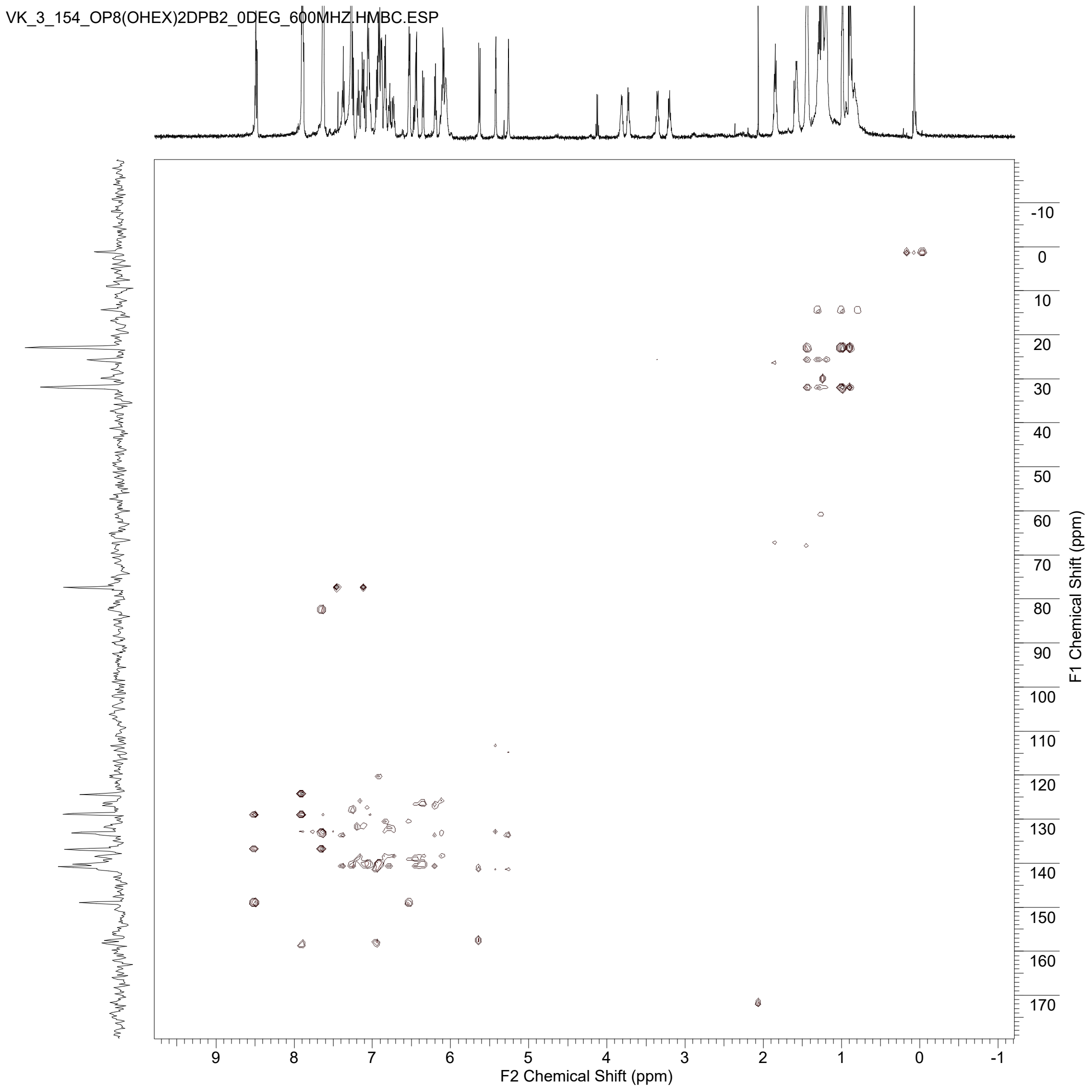

Figure S53. HMBC NMR spectrum (600 MHz, $CDCl_3$, 0 ℃) of $\mathbf{oP^8H(DPB)_{2+2}}$.

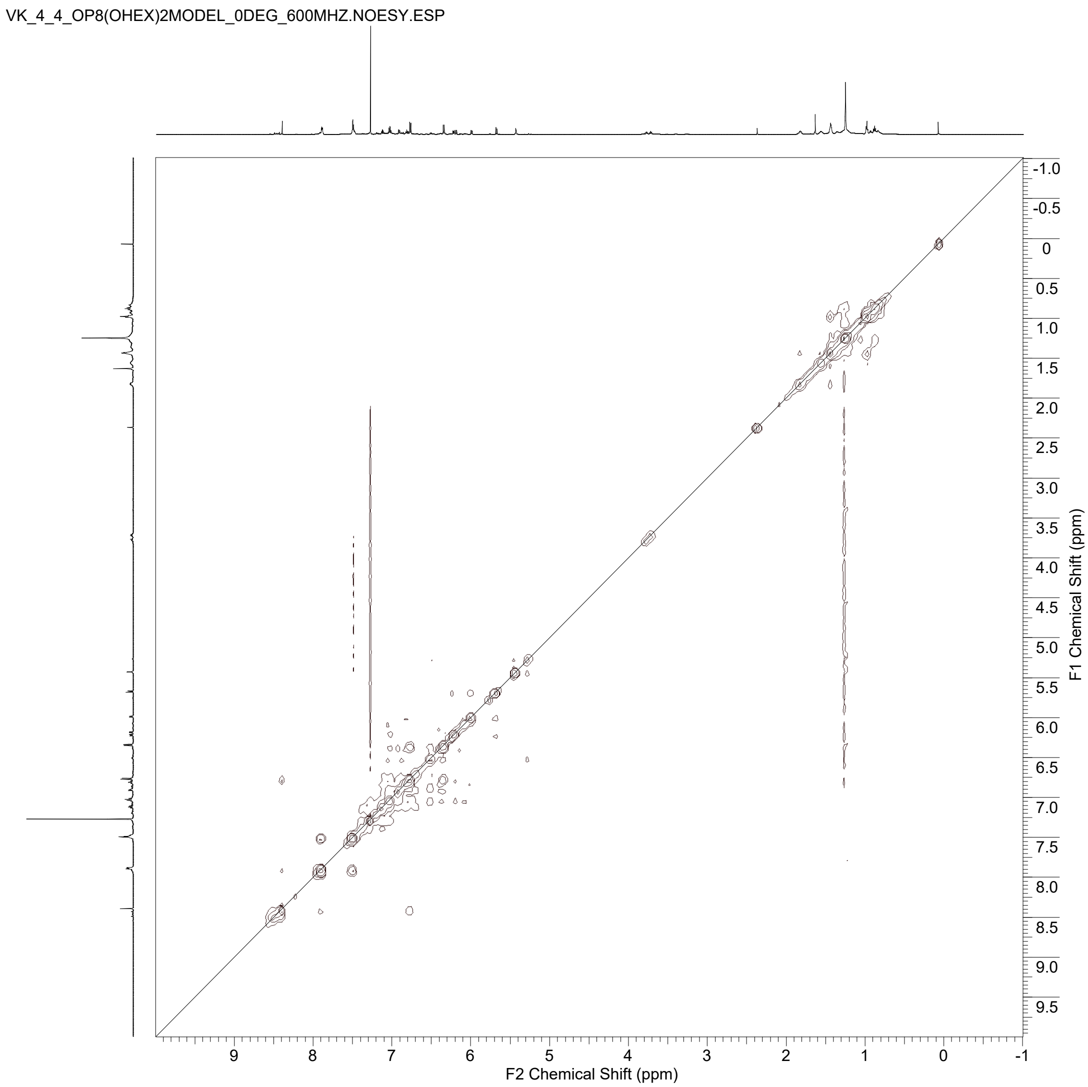

Figure S54. NOESY/EXSY NMR spectrum (600 MHz, $CDCl_3$, 0 ℃) of **oP^{8}H(DPB)$_{2+2}$**.

oP⁸H(Phen)$_{2+2}$

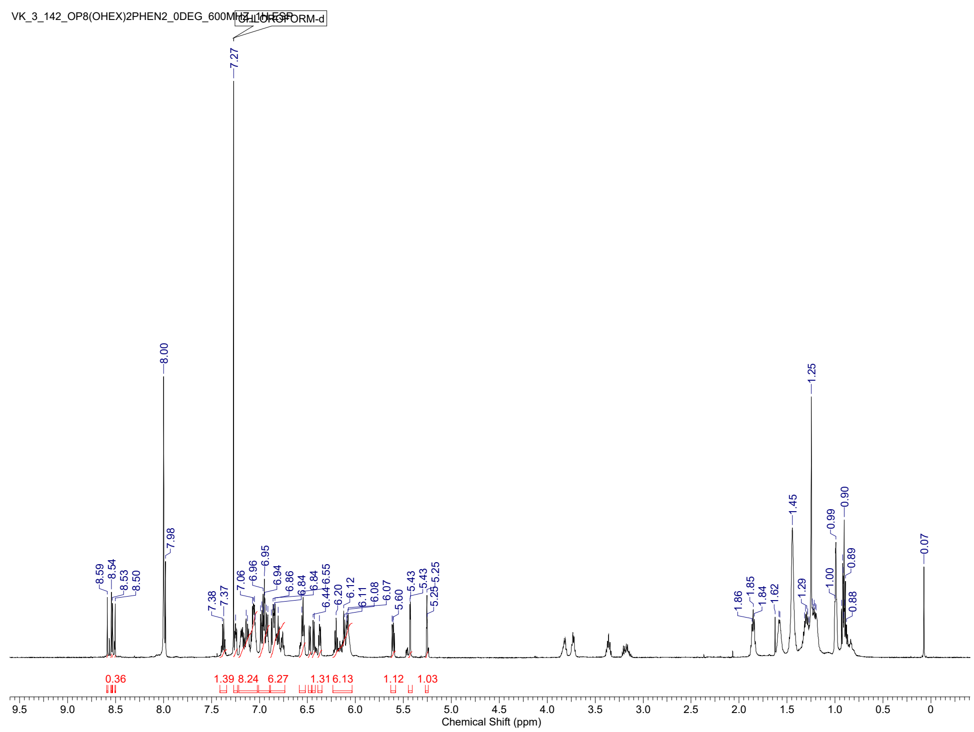

Figure S55. [1]H NMR spectrum (600 MHz, $CDCl_3$, 0 ℃) of **oP^{8}H(Phen)$_{2+2}$**.

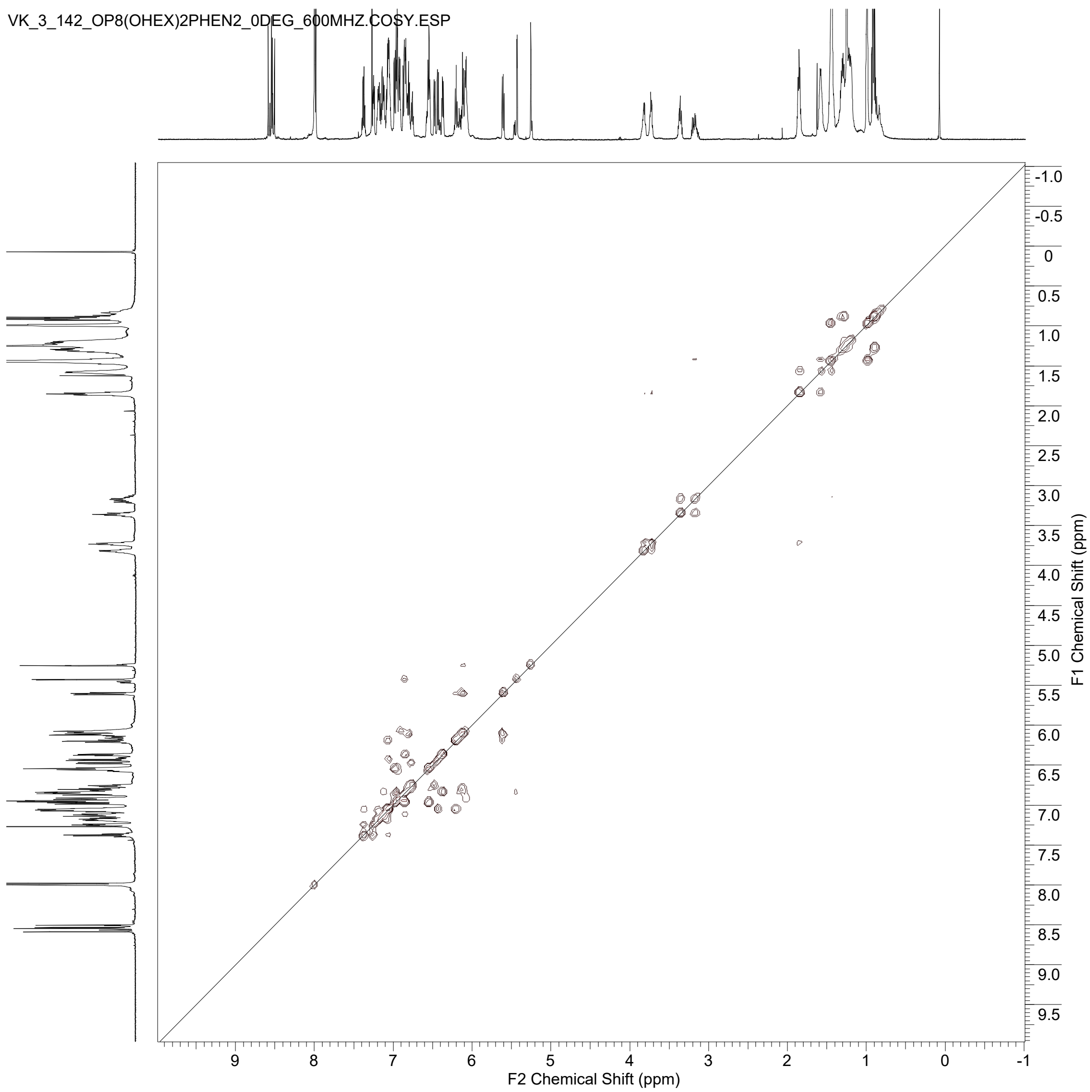

Figure S56. COSY NMR spectrum (600 MHz, $CDCl_3$, 0 ℃) of **oP[8]H(Phen)$_{2+2}$**.

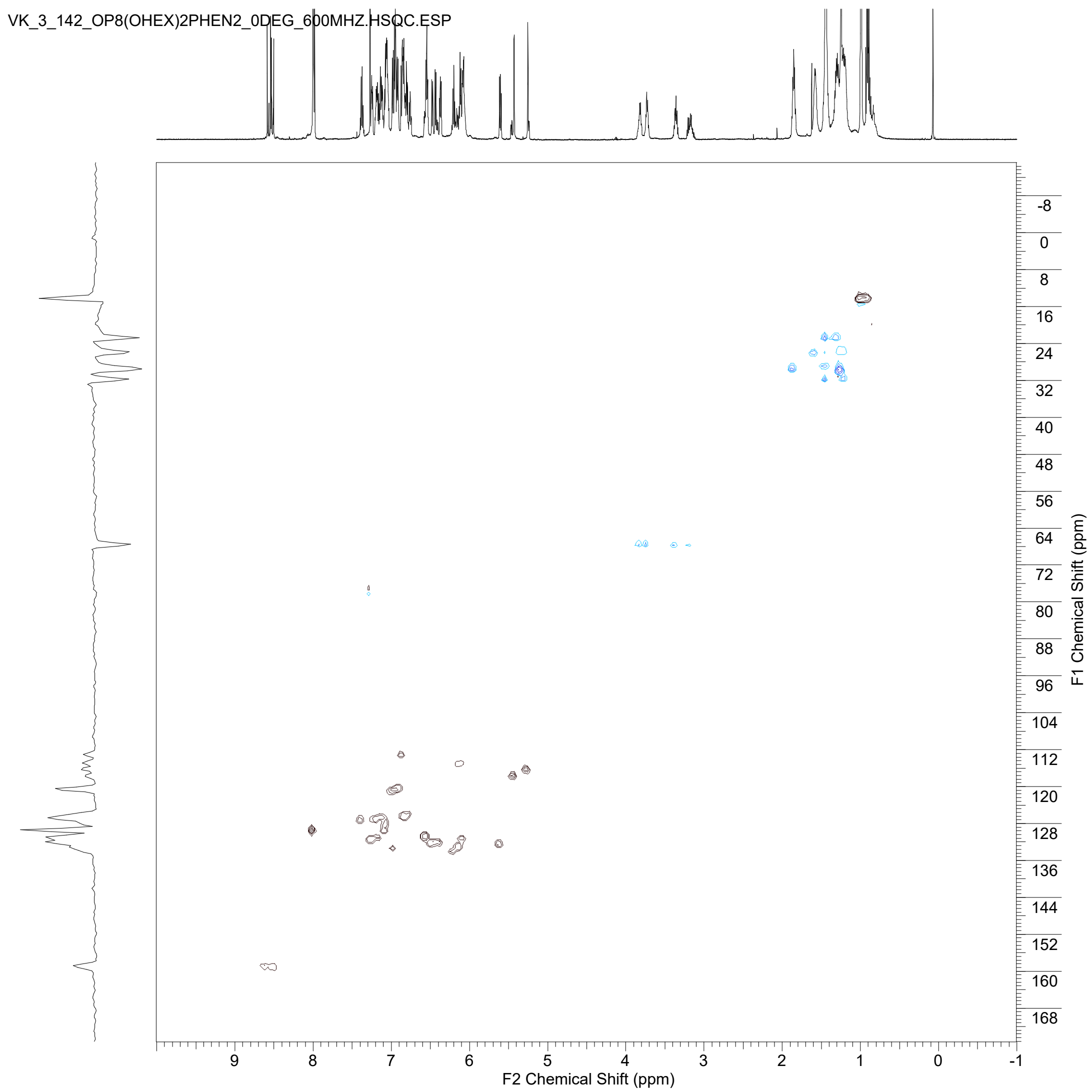

Figure S57. HSQC NMR spectrum (600 MHz, $CDCl_3$, 0 ℃) of $\mathbf{oP^8H(Phen)_{2+2}}$.

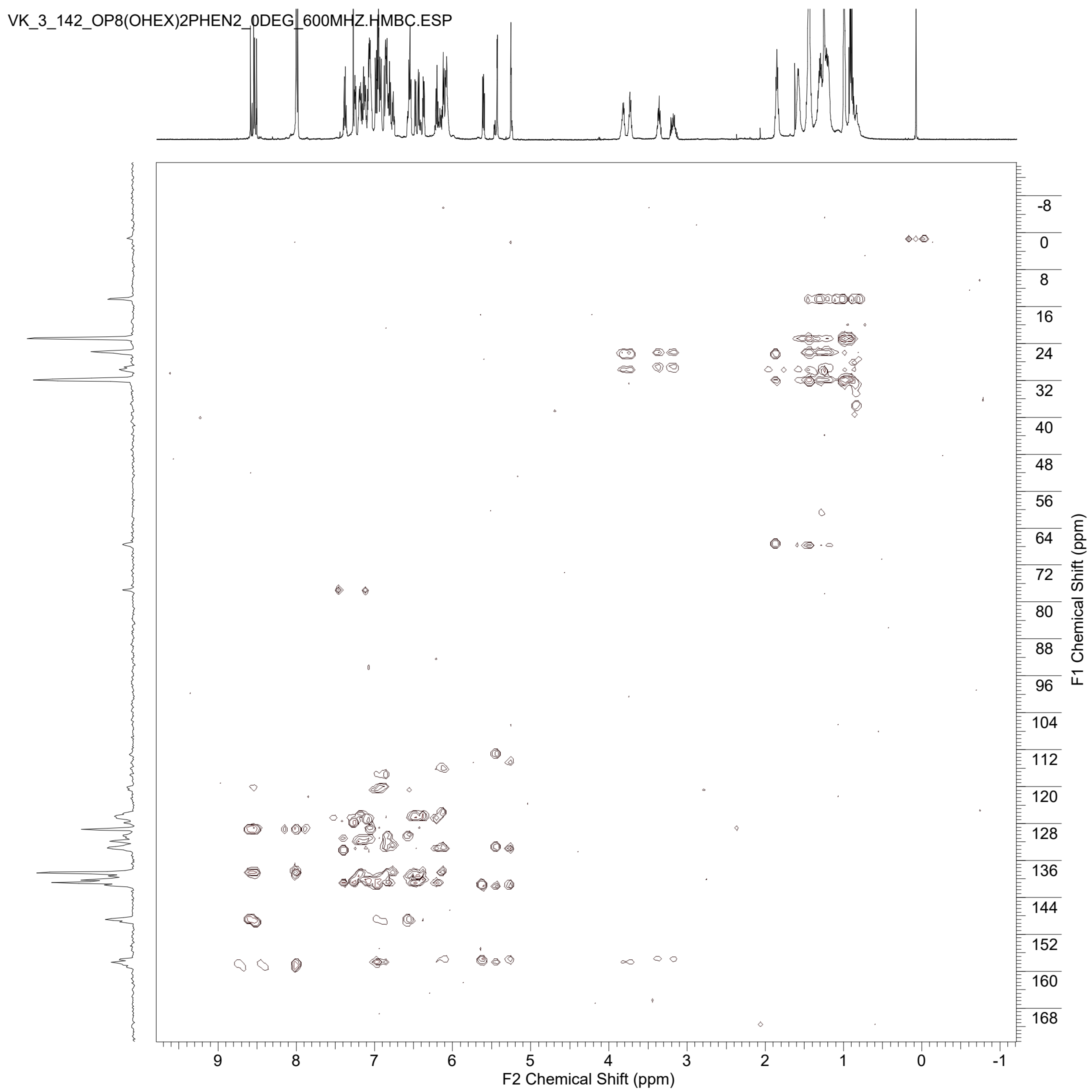

Figure S58. HMBC NMR spectrum (600 MHz, $CDCl_3$, 0 ℃) of $\mathbf{oP^8H(Phen)_{2+2}}$.

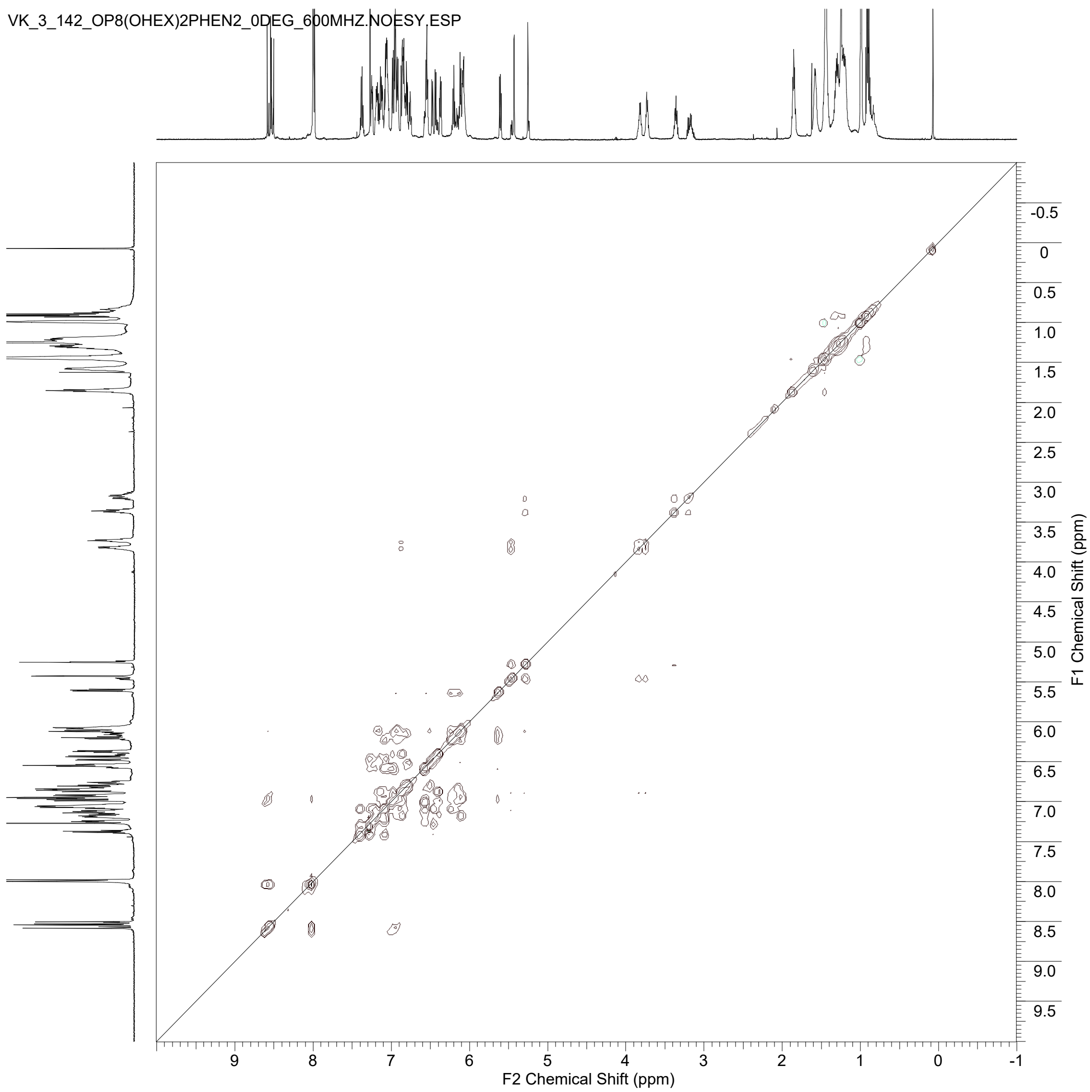

Figure S59. NOESY/EXSY NMR spectrum (600 MHz, $CDCl_3$, 0 ℃) of $\mathbf{oP^8H(Phen)_{2+2}}$.

oP^{8}F(DPB)$_{2+2}$

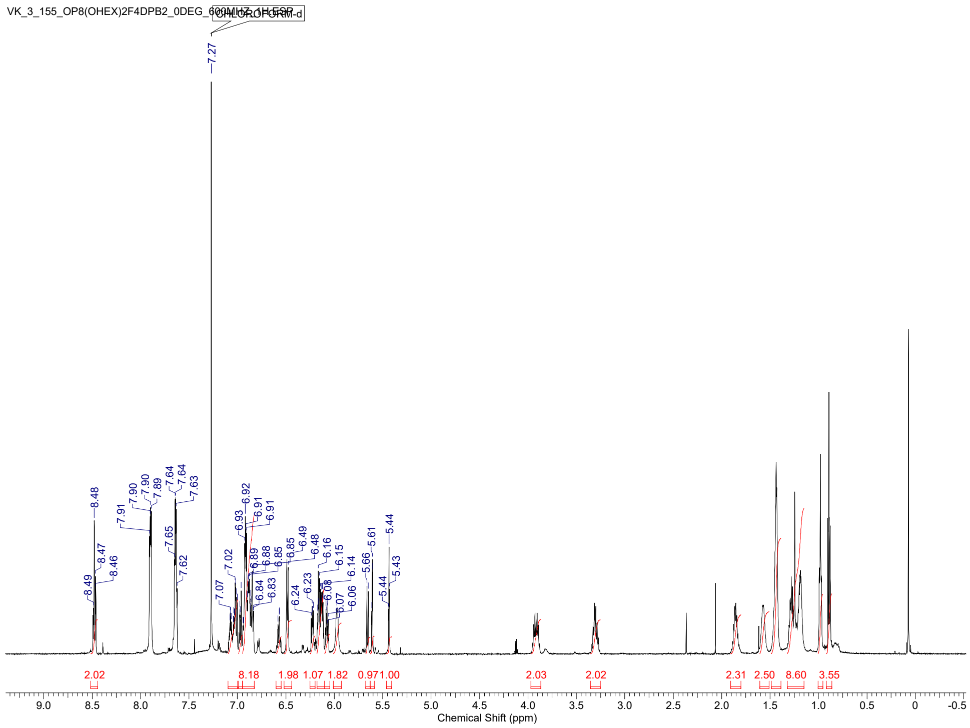

Figure S60. ^{1}H NMR spectrum (600 MHz, $CDCl_3$, 0 ℃) of **oP^{8}F(DPB)$_{2+2}$**.

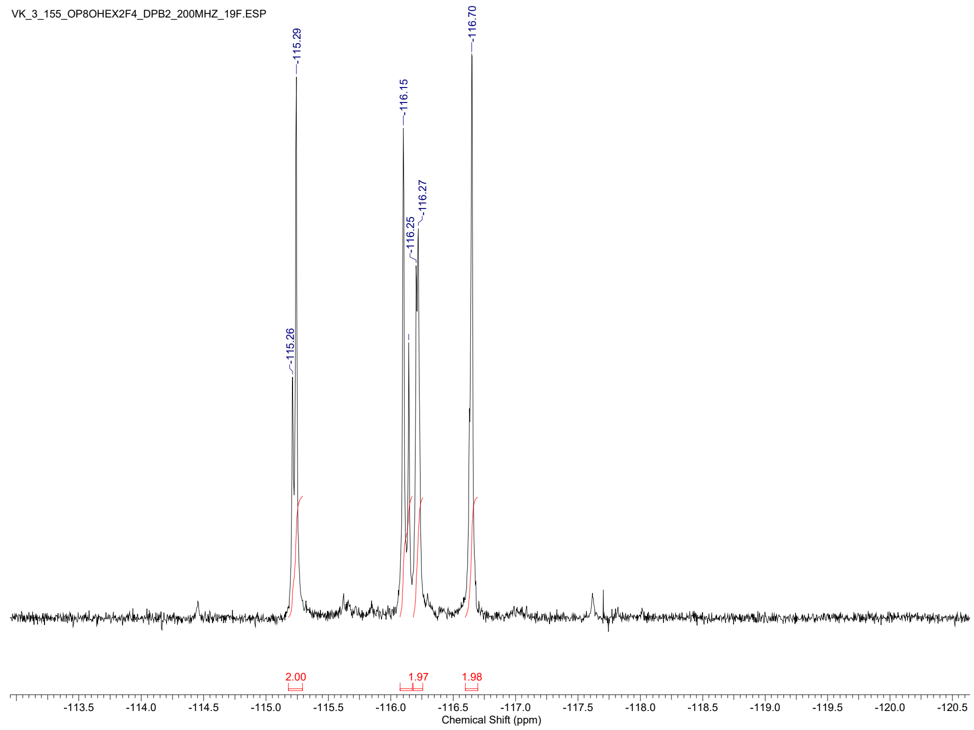

Figure S61. ^{19}F NMR spectrum (188 MHz, $CDCl_3$, 0 ℃) of **oP^{8}F(DPB)$_{2+2}$**.

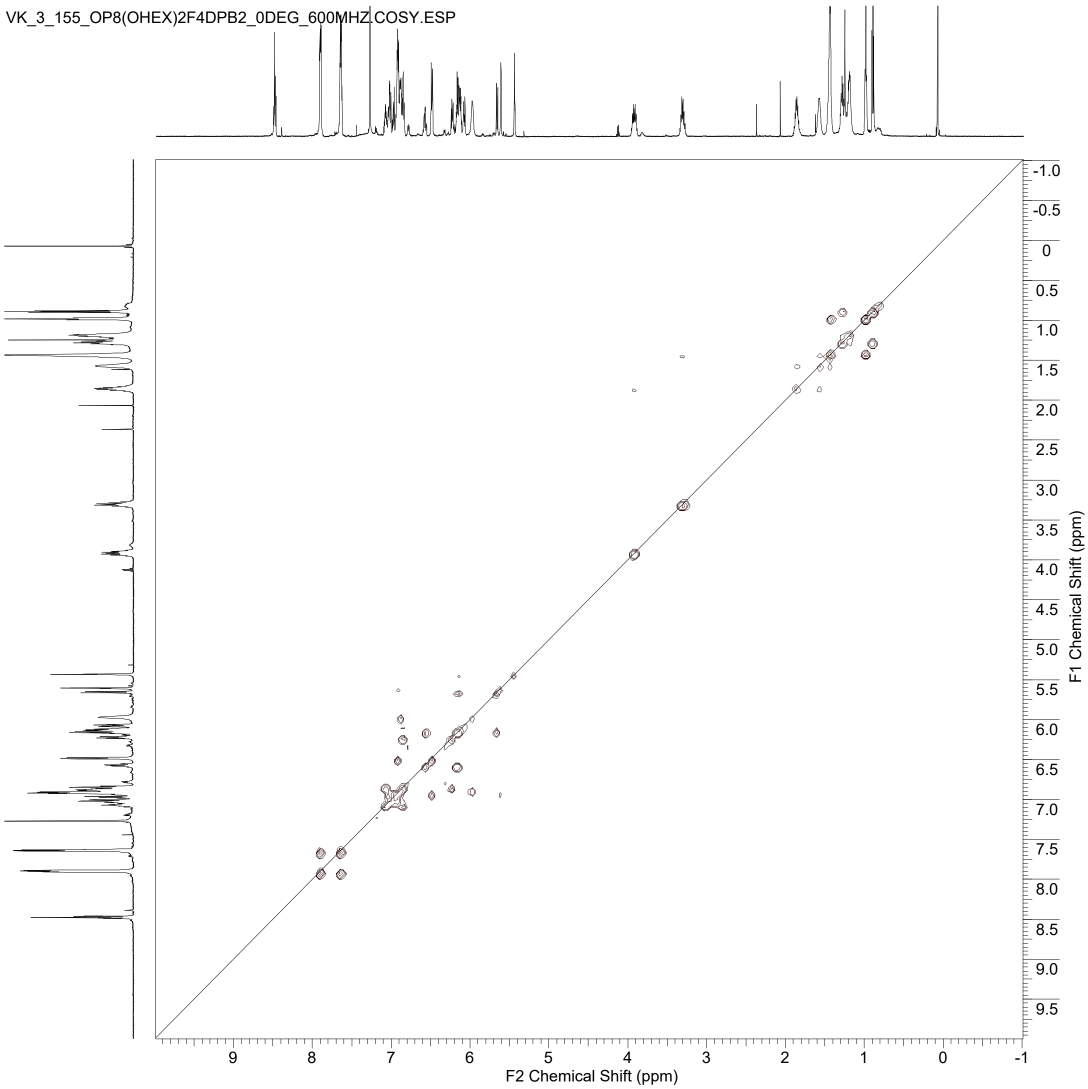

Figure S62. COSY NMR spectrum (600 MHz, $CDCl_3$, 0 ℃) of $\mathbf{oP^8F(DPB)_{2+2}}$.

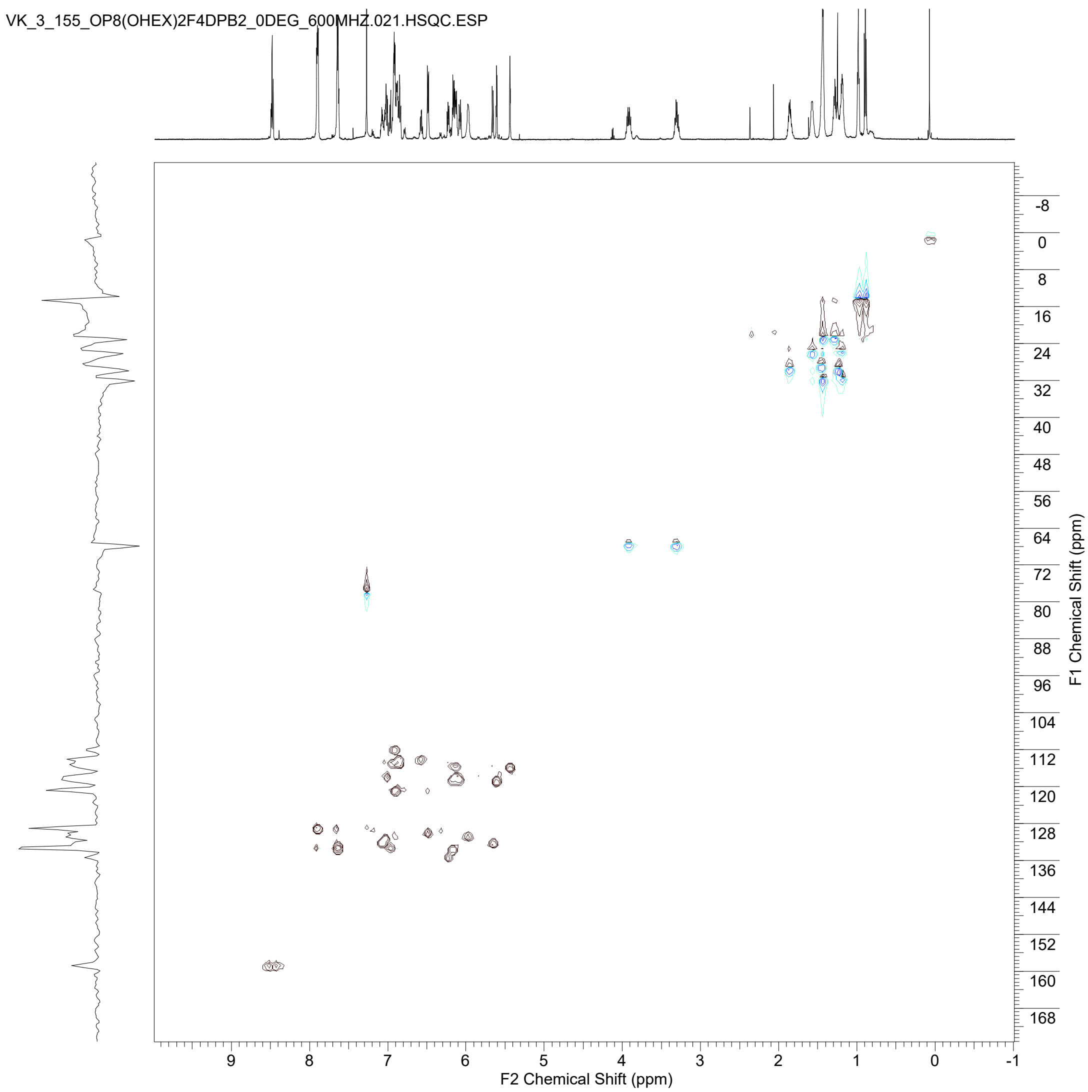

Figure S63. HSQC NMR spectrum (600 MHz, $CDCl_3$, 0 ℃) of **oP^{8}F(DPB)$_{2+2}$**.

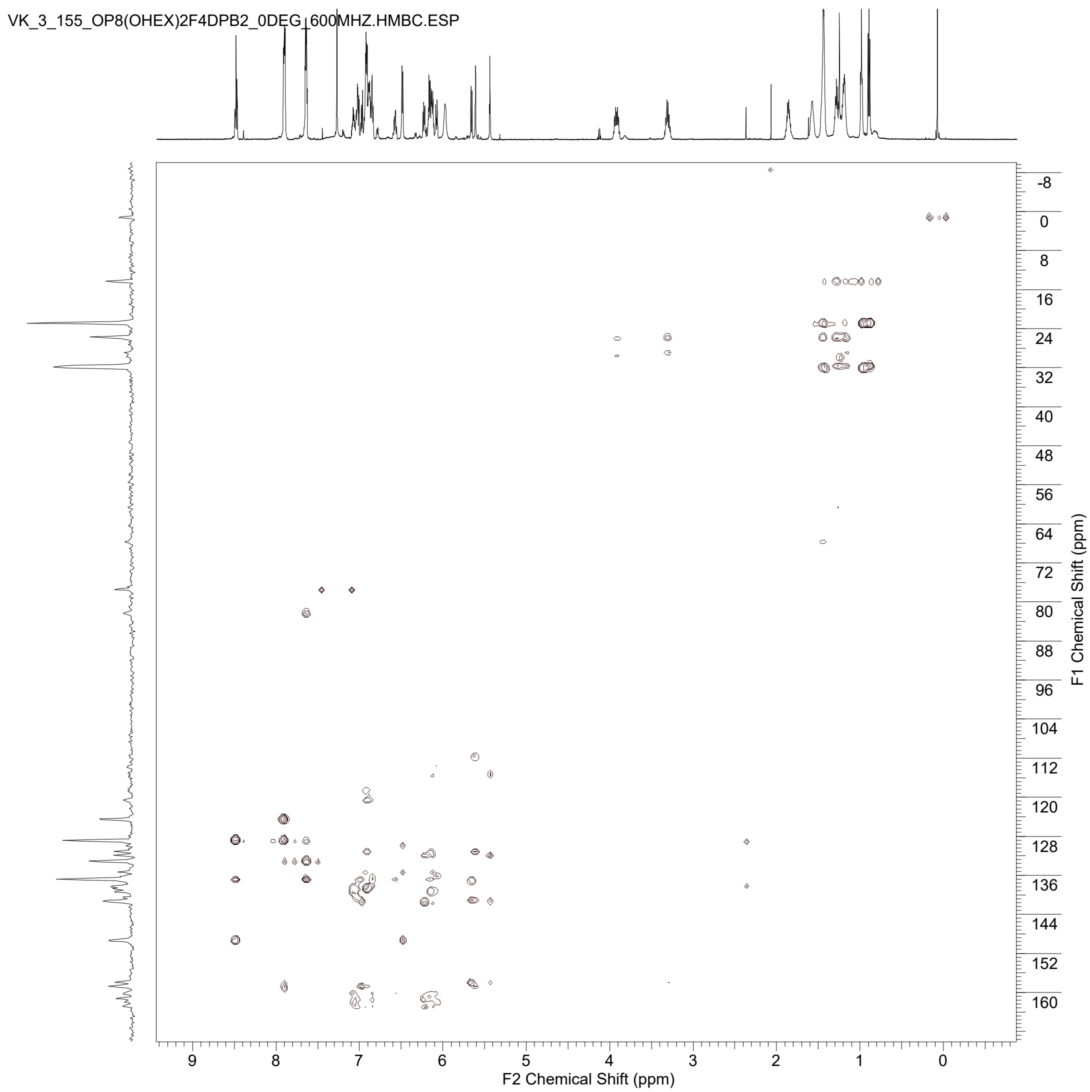

Figure S64. HMBC NMR spectrum (600 MHz, $CDCl_3$, 0 ℃) of **oP^{8}F(DPB)$_{2+2}$**.

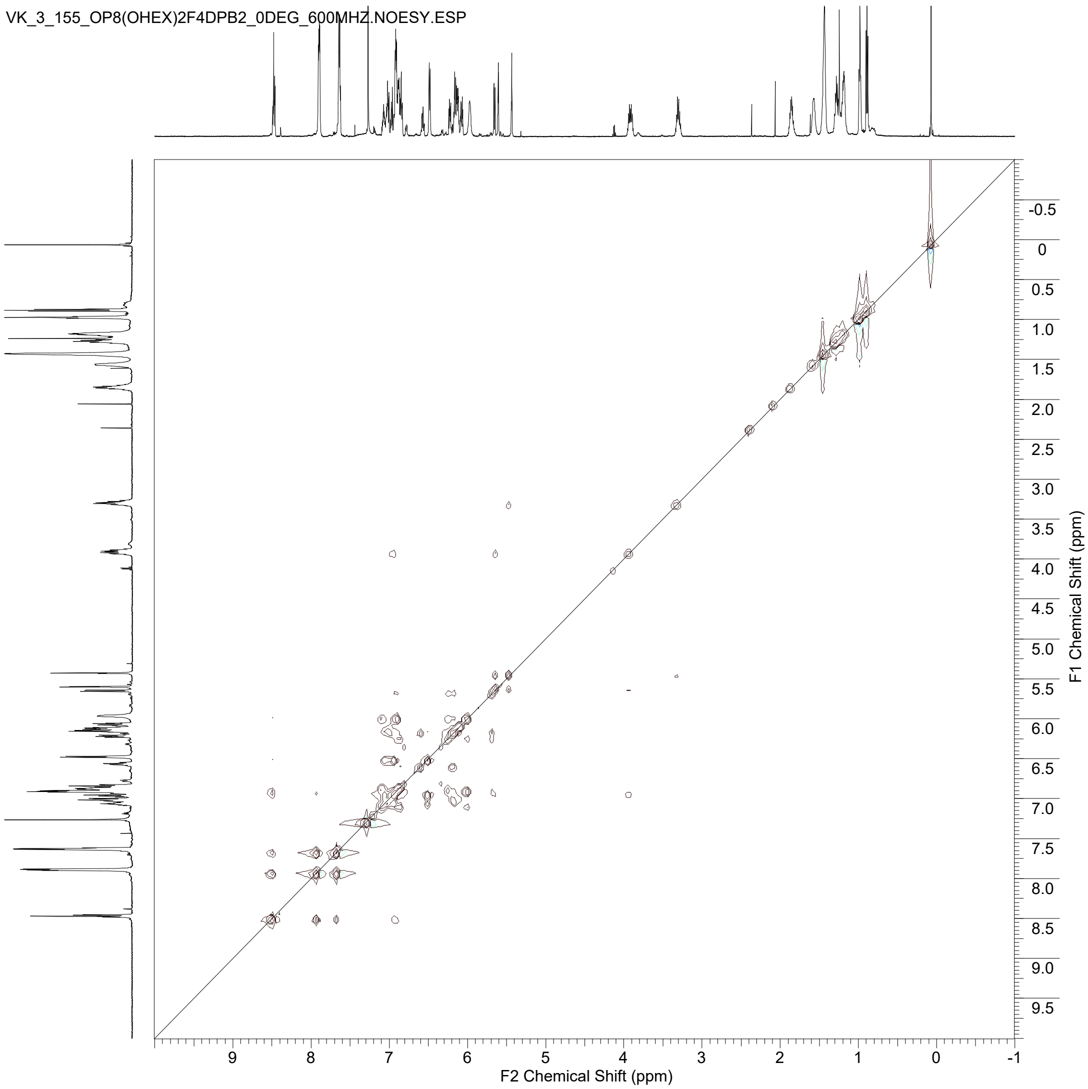

Figure S65. NOESY/EXSY NMR spectrum (600 MHz, $CDCl_3$, 0 ℃) of **oP^{8}F(DPB)$_{2+2}$**.

oP⁸F(Phen)$_{2+2}$

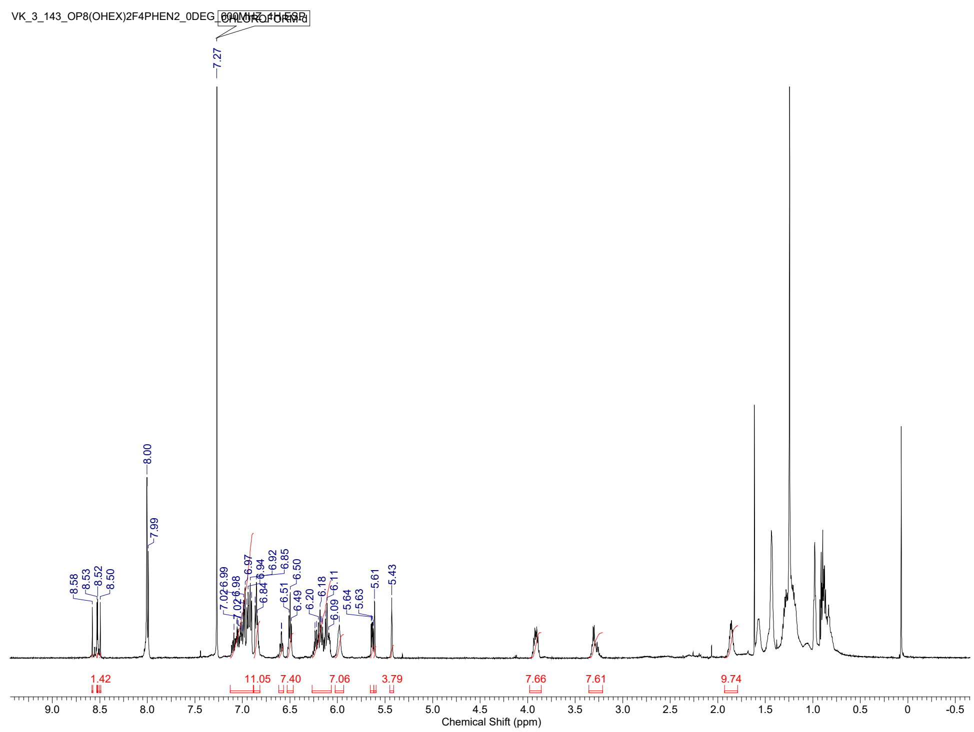

Figure S66. ^{1}H NMR spectrum (600 MHz, $CDCl_3$, 0 ℃) of **oP^{8}F(Phen)$_{2+2}$**.

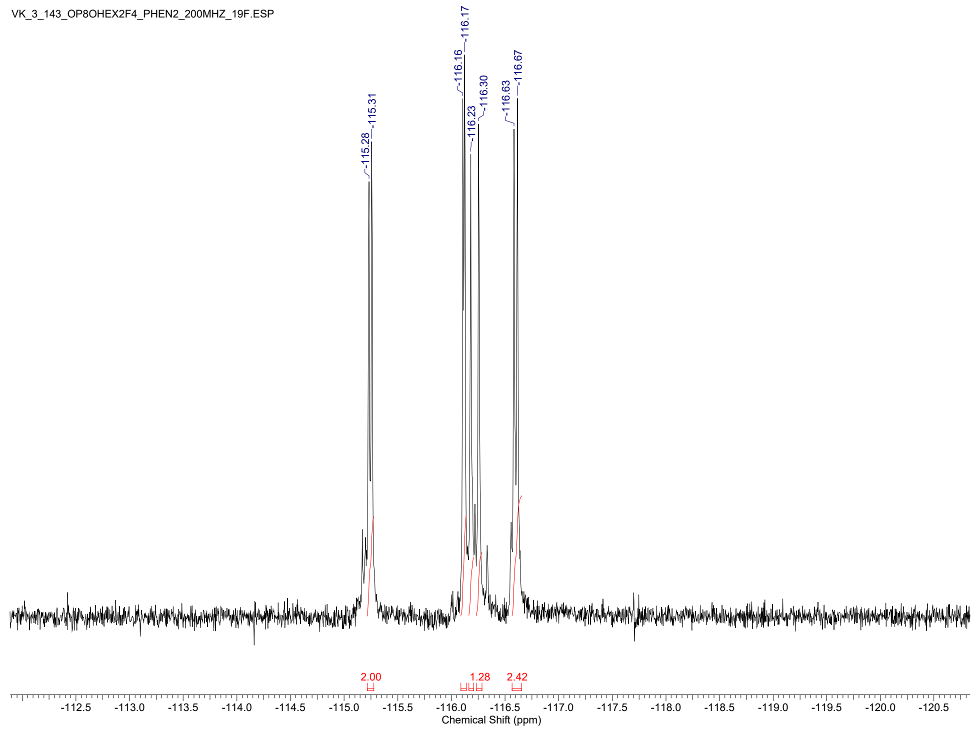

Figure S67. ^{19}F NMR spectrum (188 MHz, $CDCl_3$, 0 ℃) of **oP^{8}F(Phen)$_{2+2}$**.

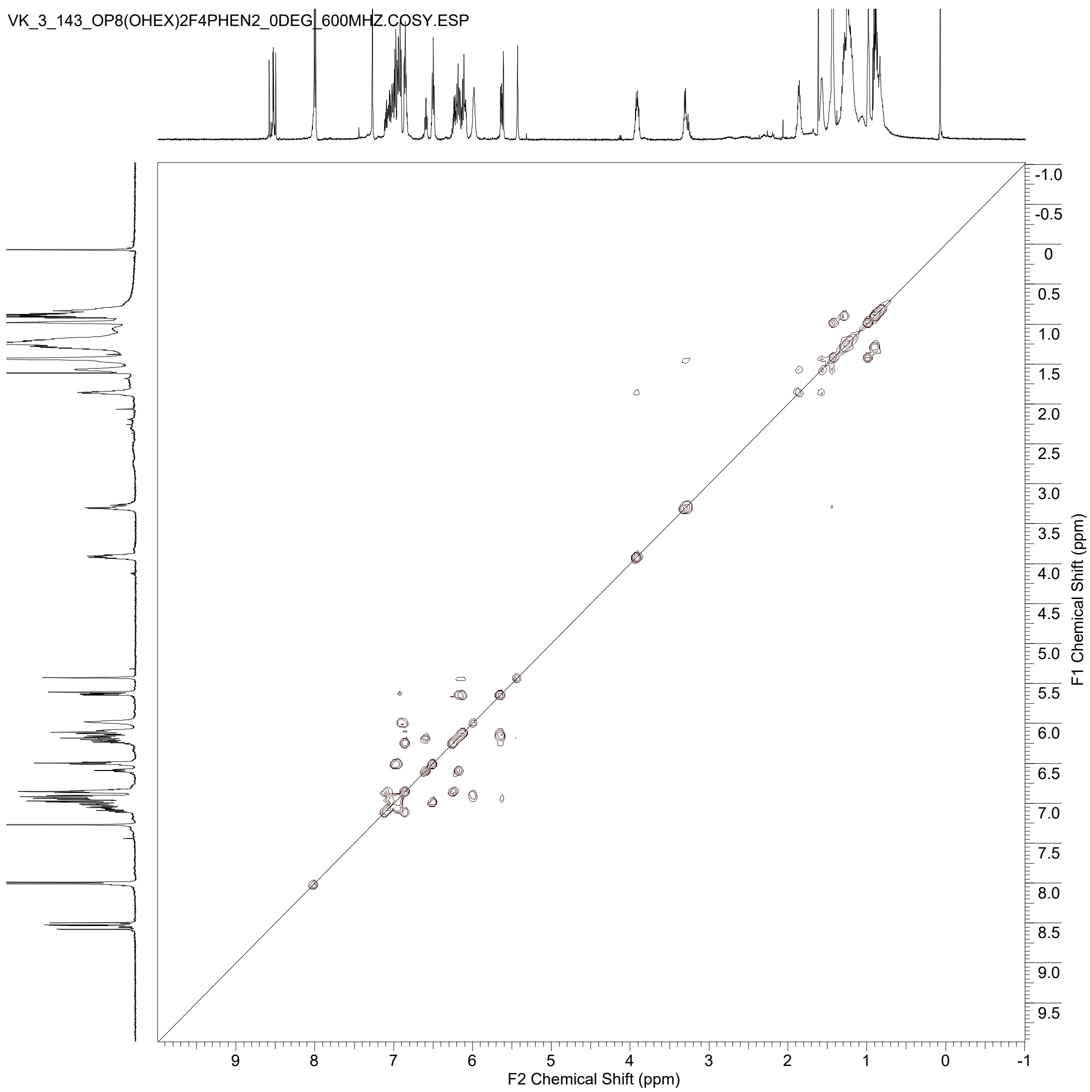

Figure S68. COSY NMR spectrum (600 MHz, $CDCl_3$, 0 ℃) of **oP^{8}F(Phen)$_{2+2}$**.

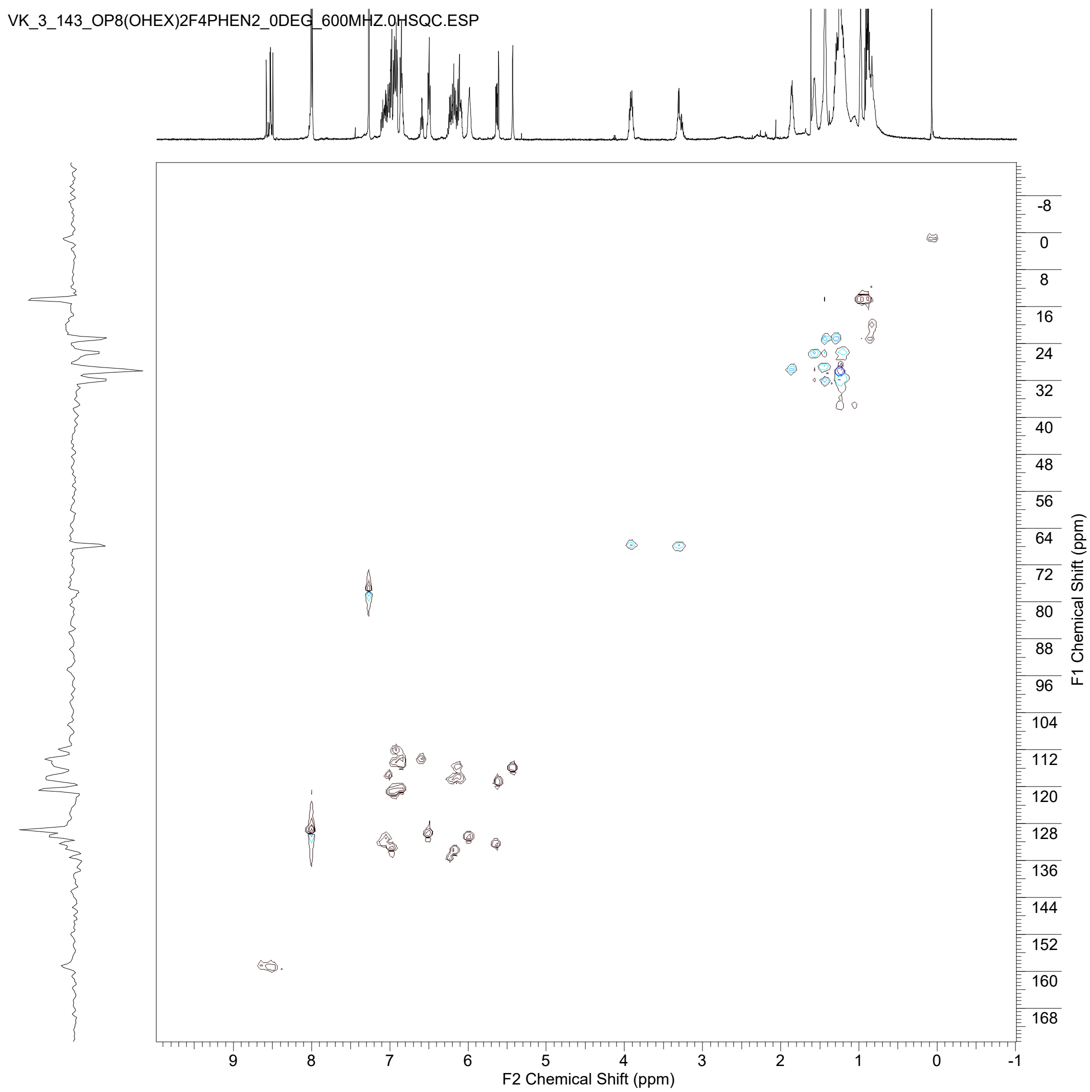

Figure S69. HSQC NMR spectrum (600 MHz, $CDCl_3$, 0 ℃) of $\mathbf{oP^8F(Phen)_{2+2}}$.

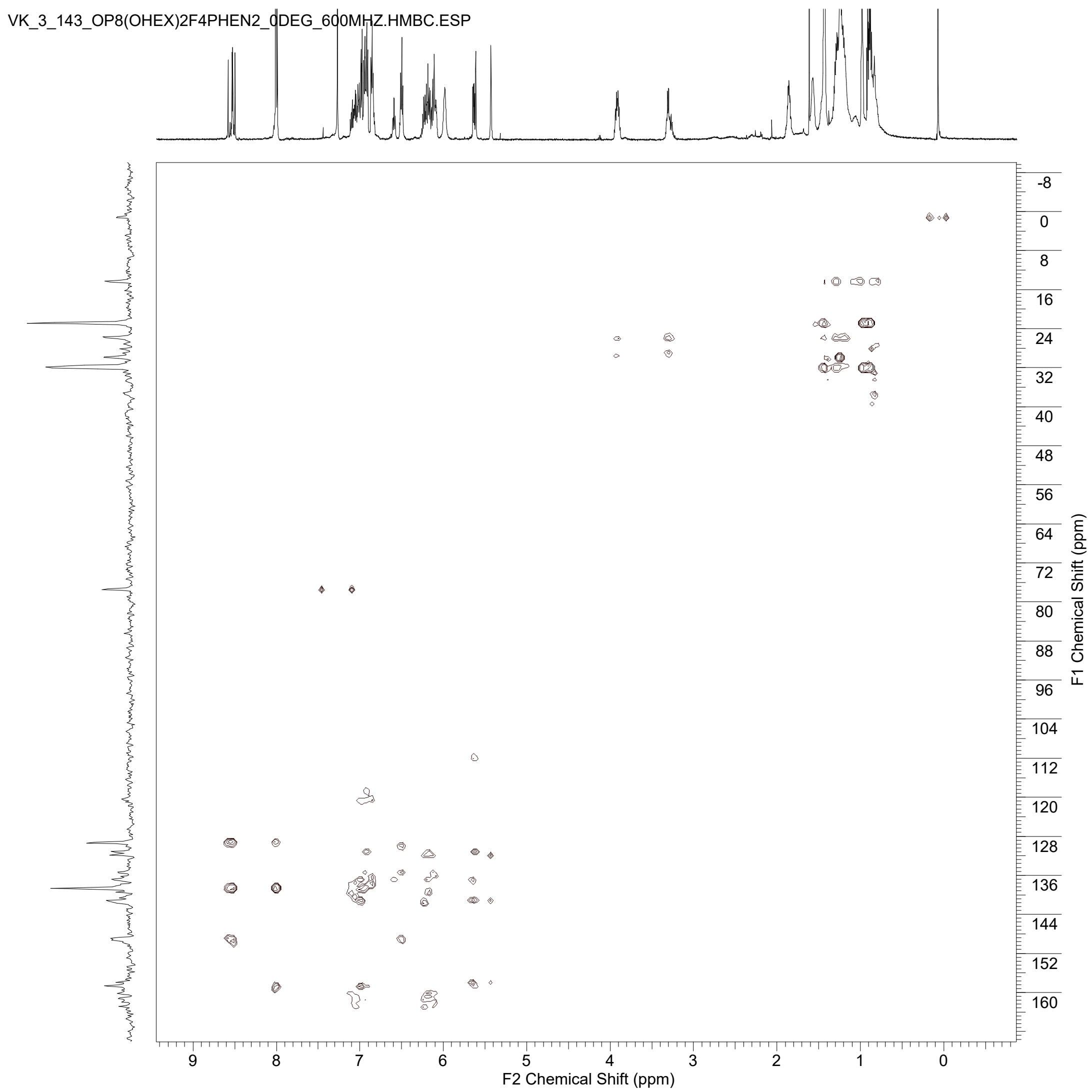

Figure S70. HMBC NMR spectrum (600 MHz, $CDCl_3$, 0 ℃) of **oP^{8}F(Phen)$_{2+2}$**.

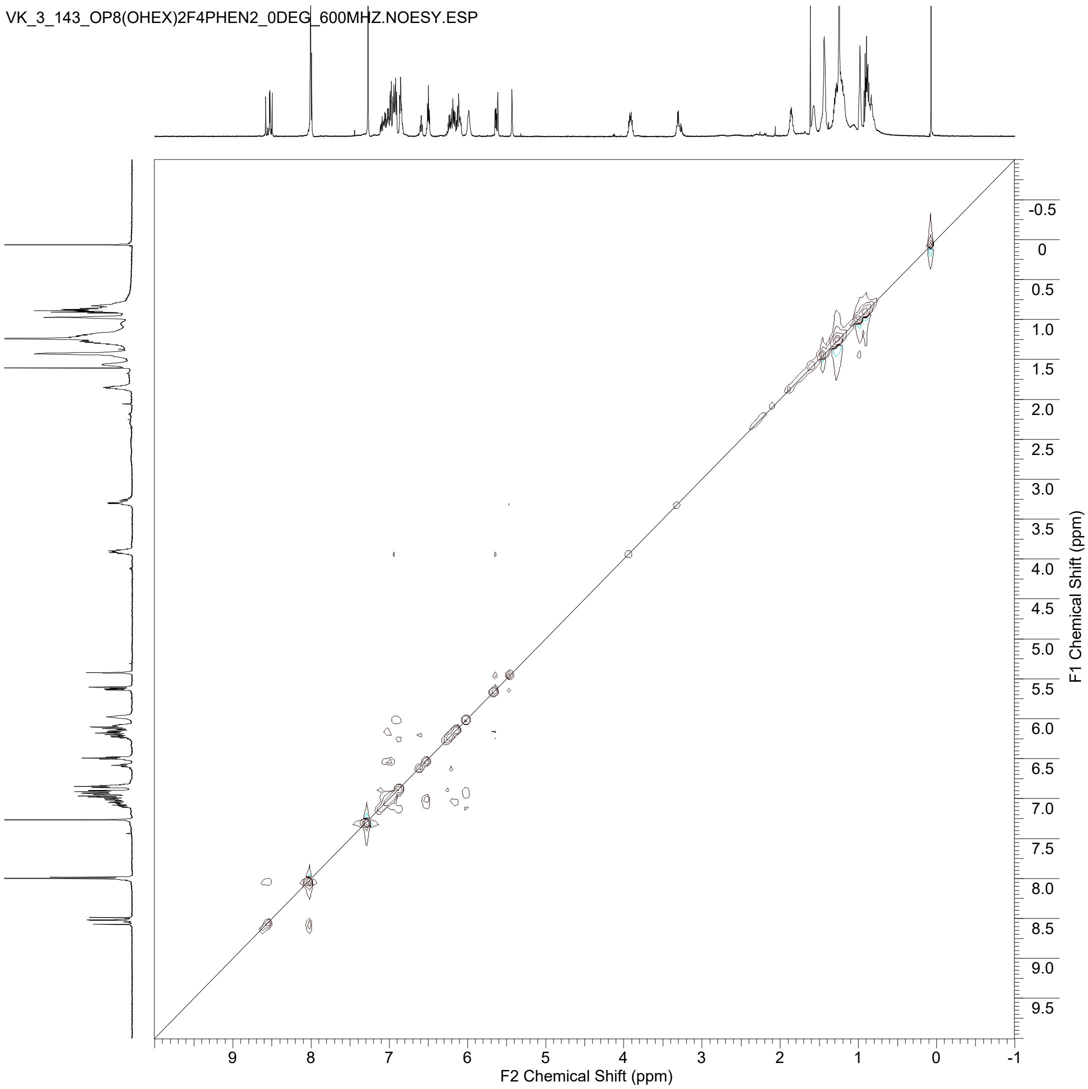

Figure S71. NOESY/EXSY NMR spectrum (600 MHz, $CDCl_3$, 0 ℃) of $\mathbf{oP^8F(Phen)_{2+2}}$.

Octamer 6

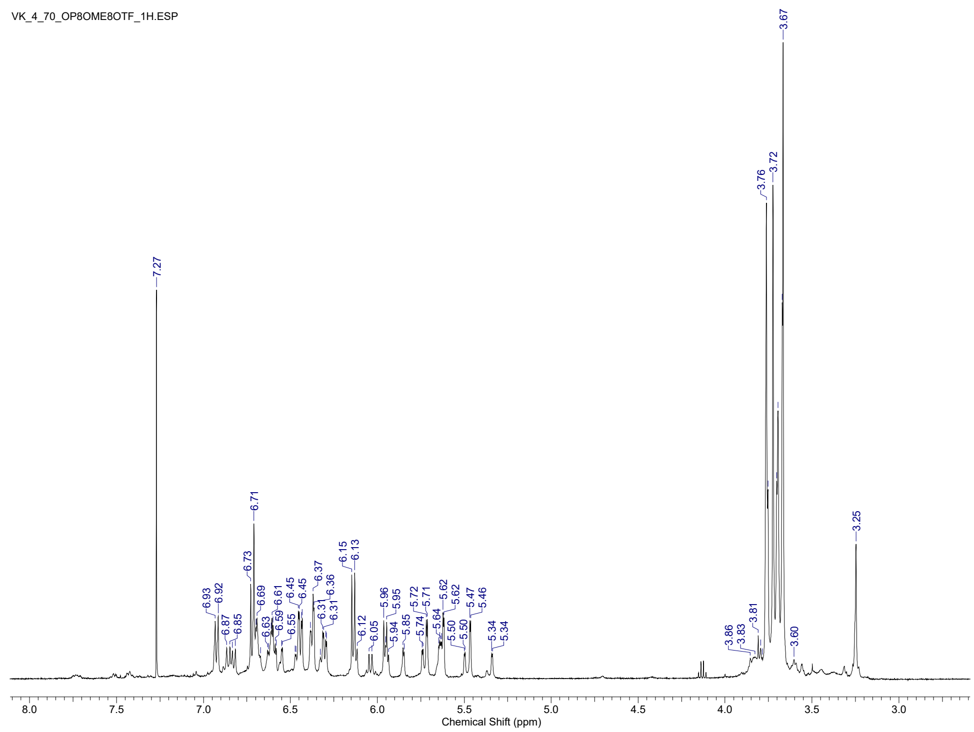

Figure S72. ^{1}H NMR spectrum (500 MHz, $CDCl_3$, 0 ℃) of **6**.

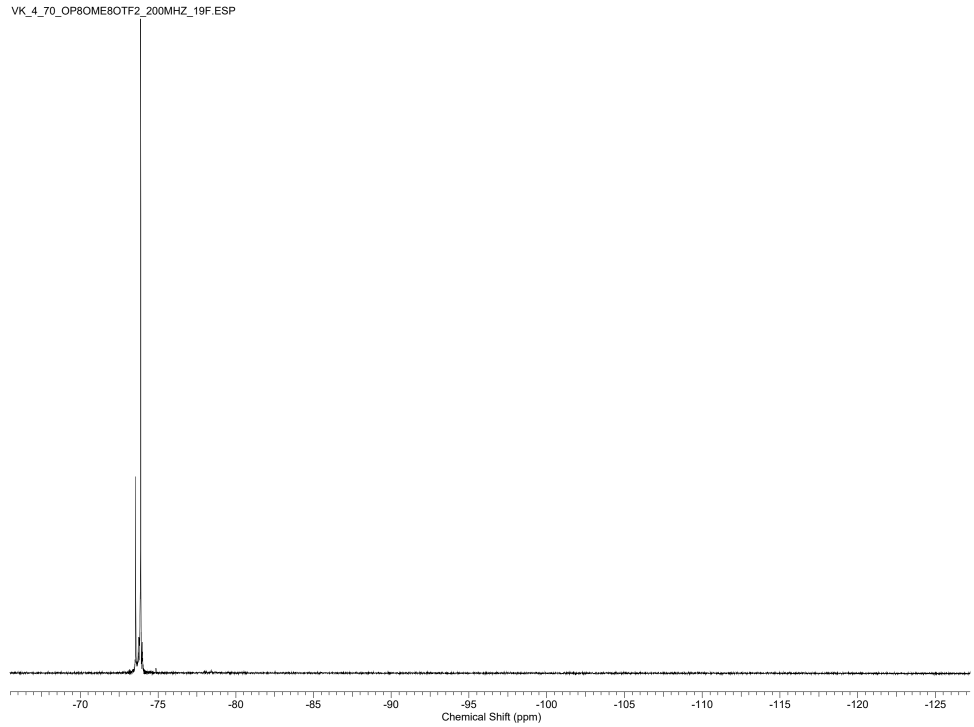

Figure S73. ^{19}F NMR spectrum (188 MHz, $CDCl_3$, 0 ℃) of **6**.

Octamer8a

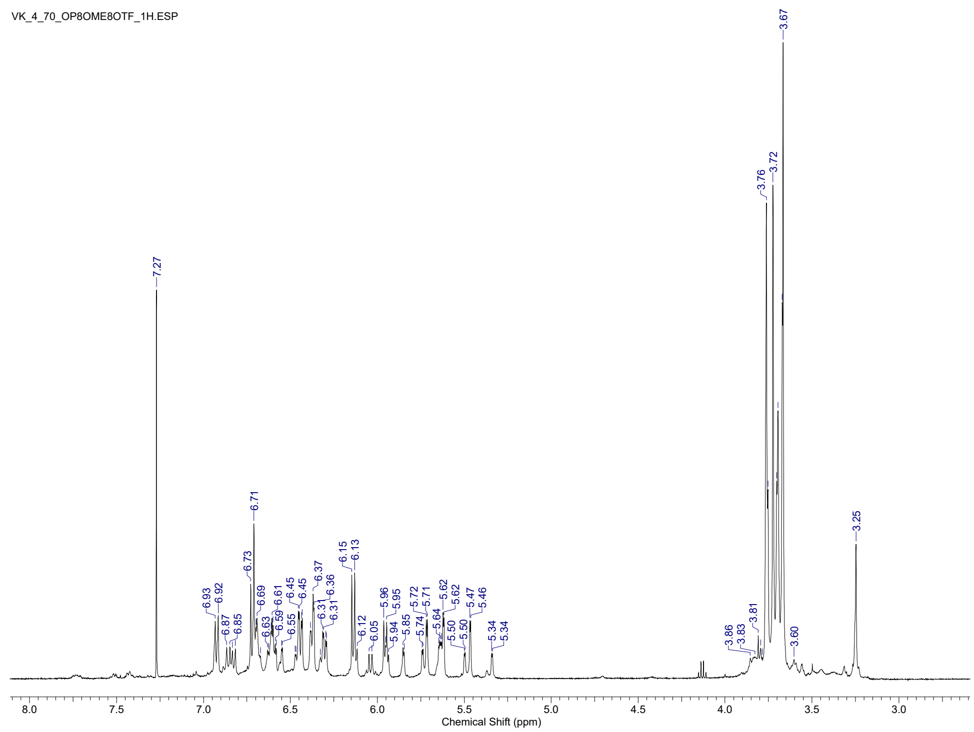

Figure S74. ^{1}H NMR spectrum (500 MHz, $CDCl_3$, 0 ℃) of **8a**.

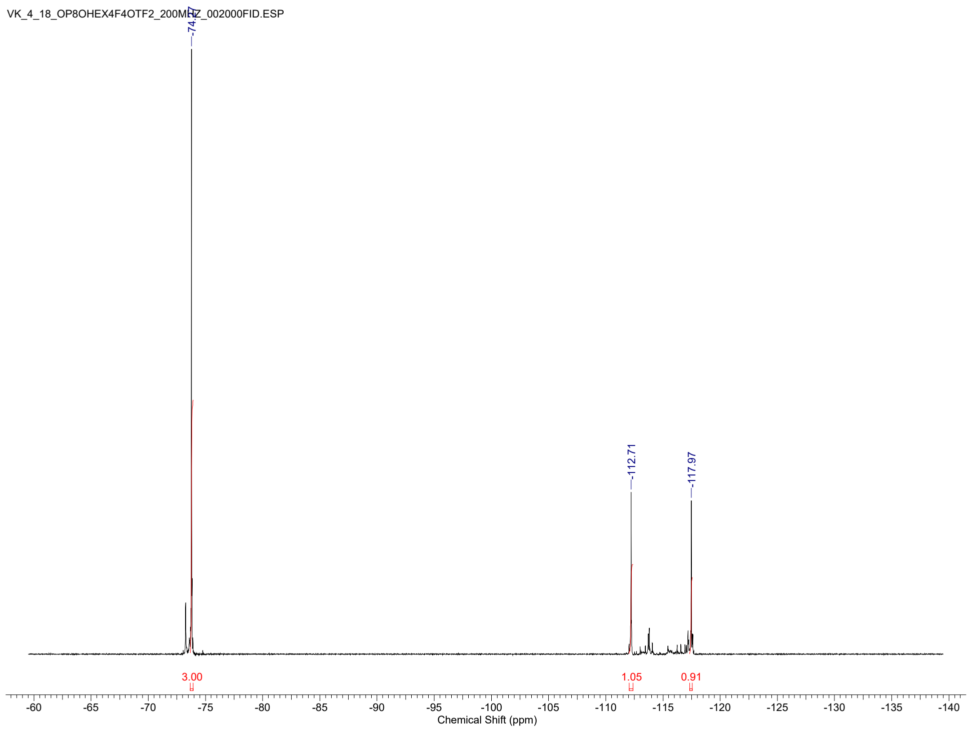

Figure S75. ^{19}F NMR spectrum (188 MHz, $CDCl_3$, 0 ℃) of **8a**.

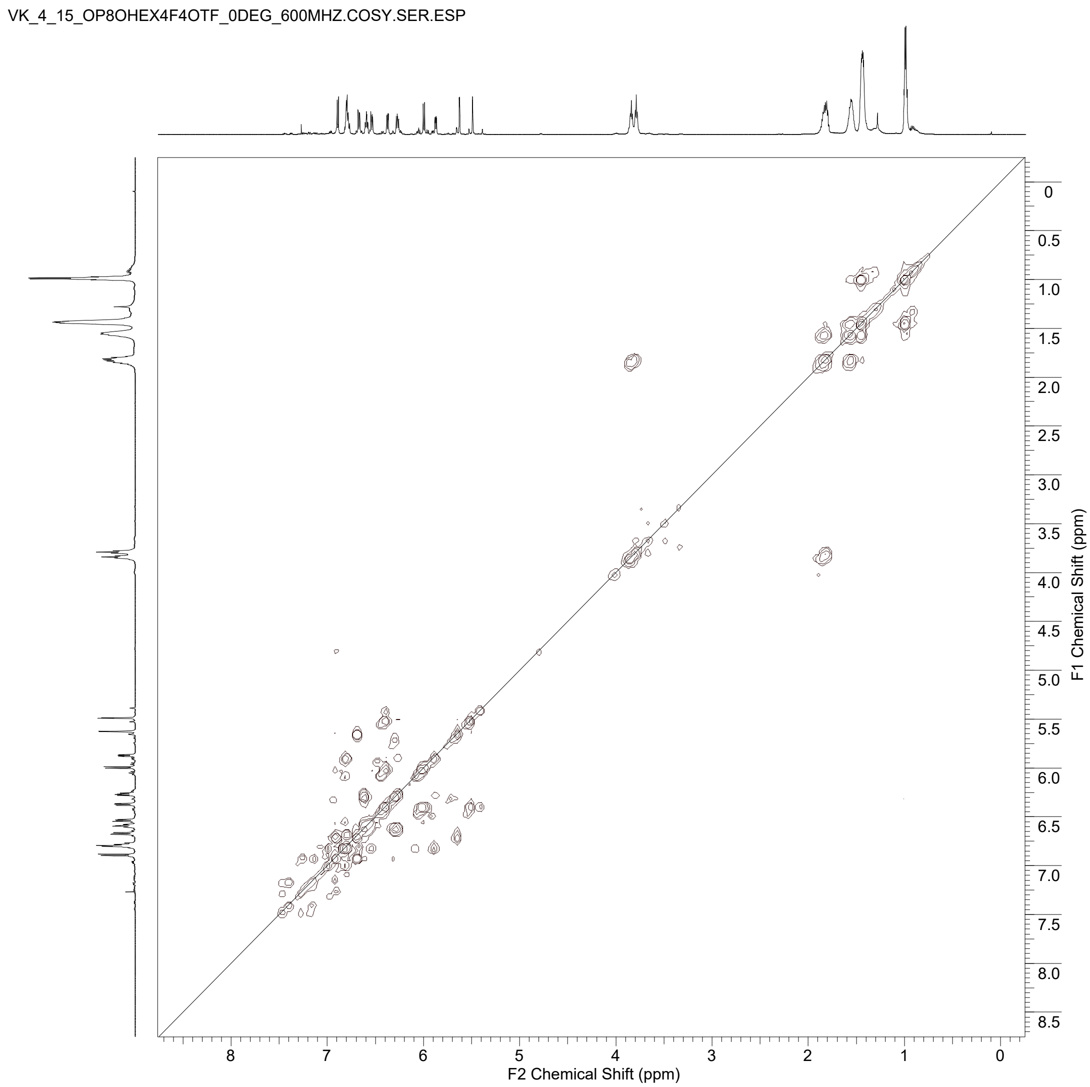

Figure S76. COSY NMR spectrum (500 MHz, $CDCl_3$, 0 ℃) of **8a**.

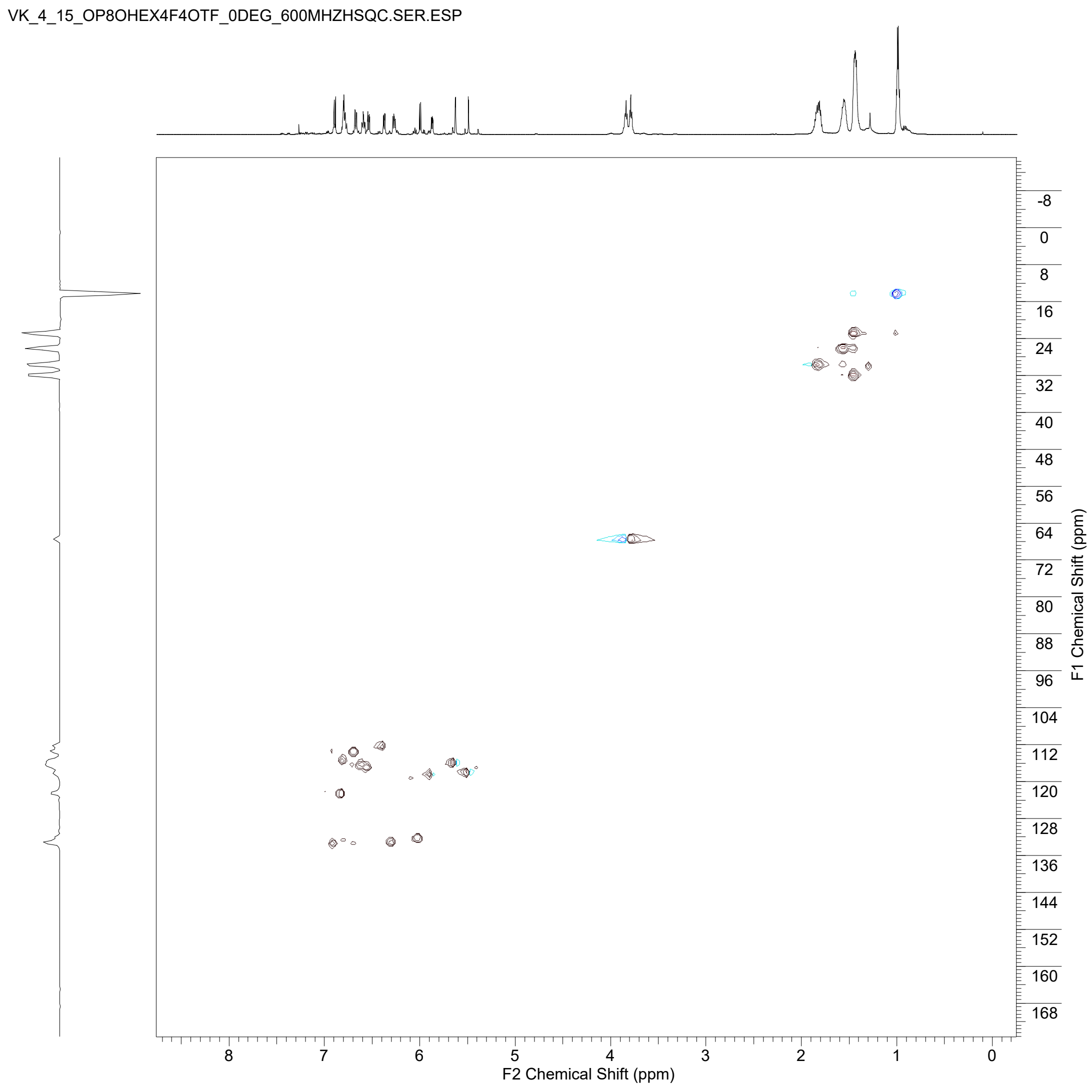

Figure S77. HSQC NMR spectrum (500 MHz, $CDCl_3$, 0 ℃) of **8a**.

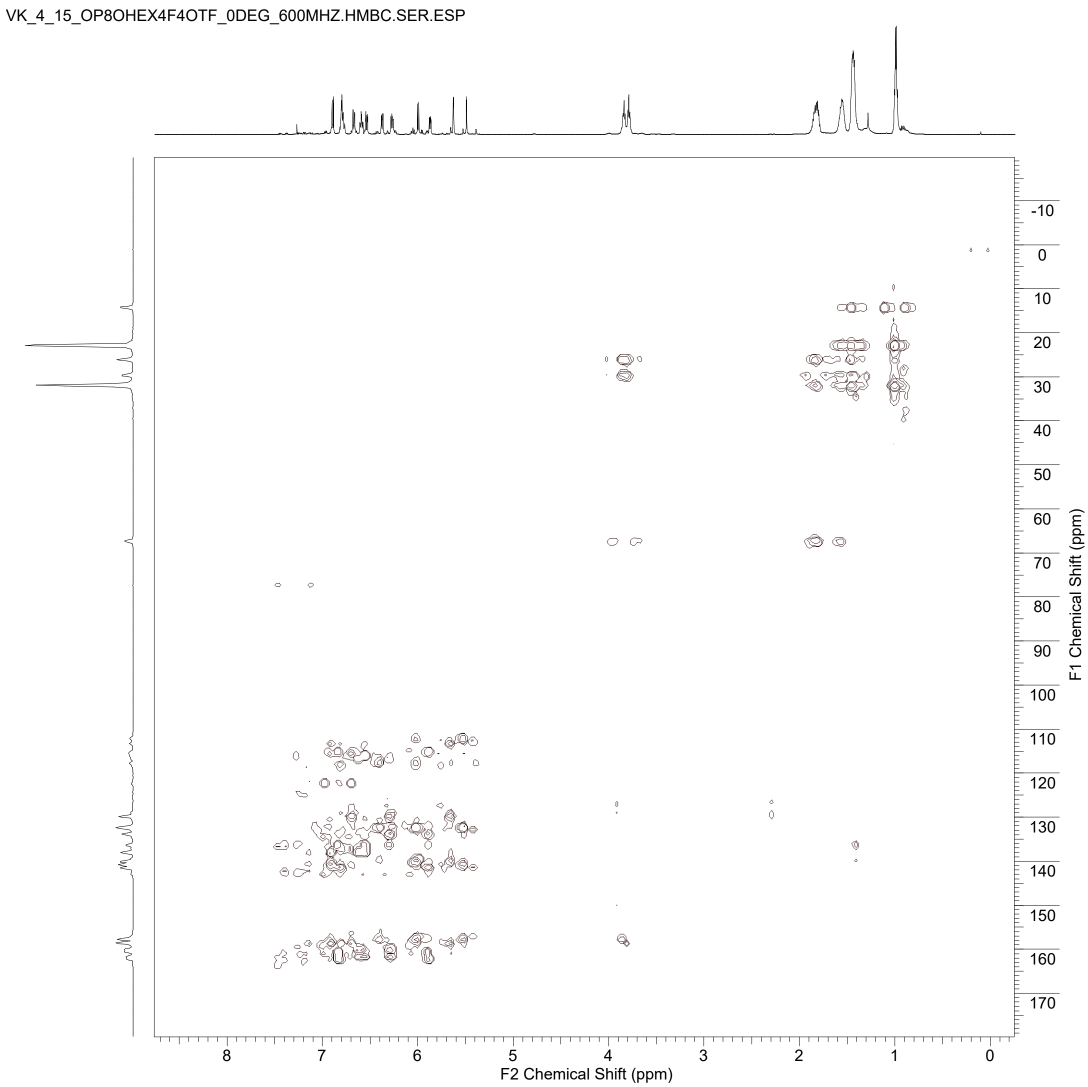

Figure S78. HMBC NMR spectrum (500 MHz, $CDCl_3$, 0 ℃) of **8a**.

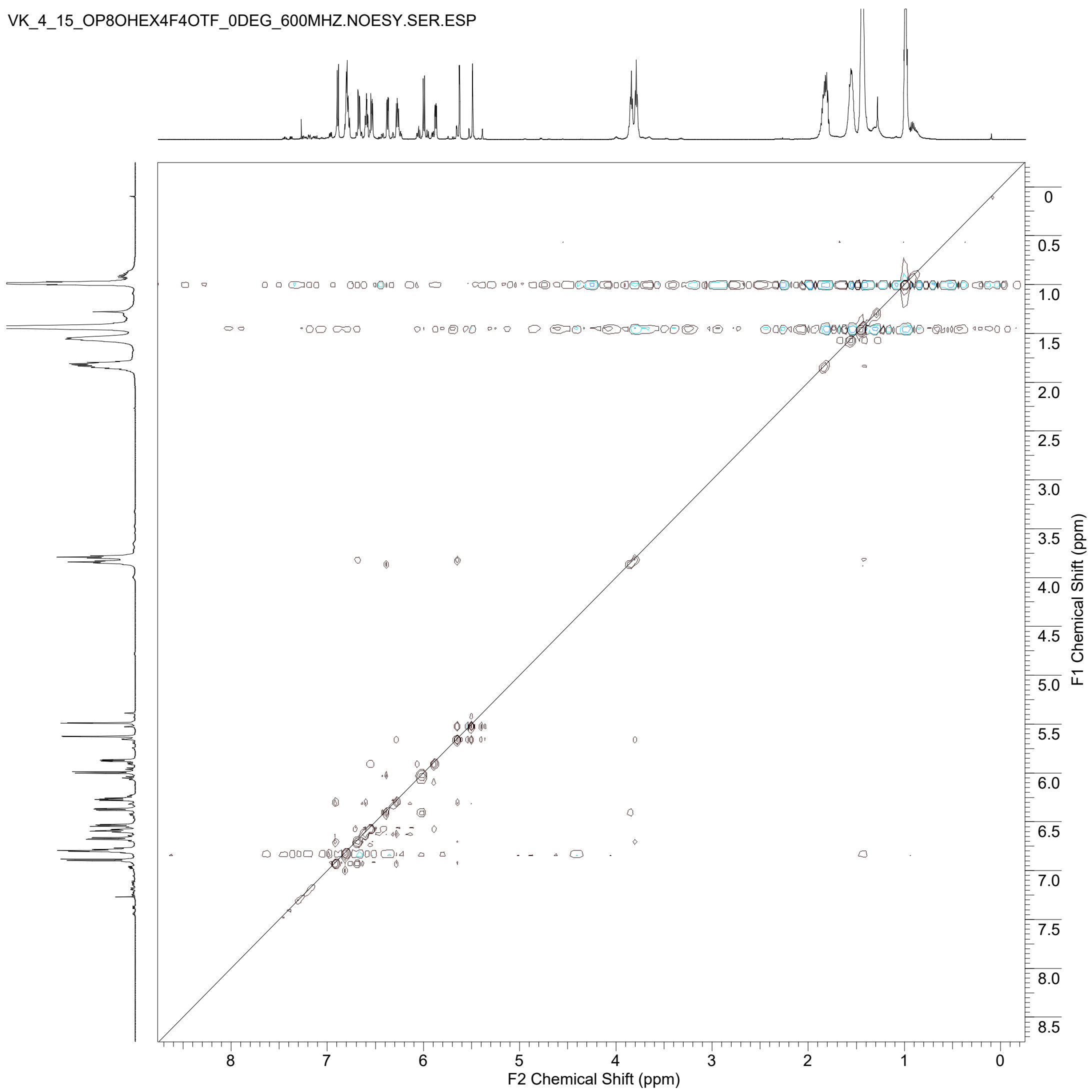

Figure S79. NOESY/EXSY NMR spectrum (500 MHz, $CDCl_3$, 0 ℃) of **8a**.

$oP^{10}OMe(NH_2)$

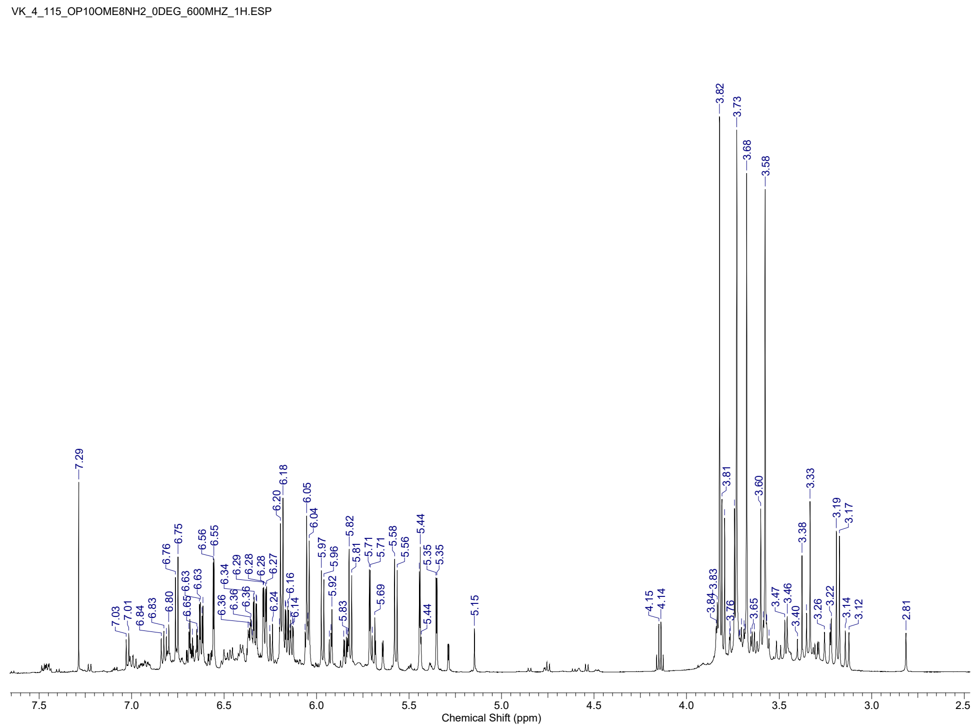

Figure S80. ^1H NMR spectrum (600 MHz, $CDCl_3$, 0 ℃) of **$oP^{10}OMe(NH_2)$**.

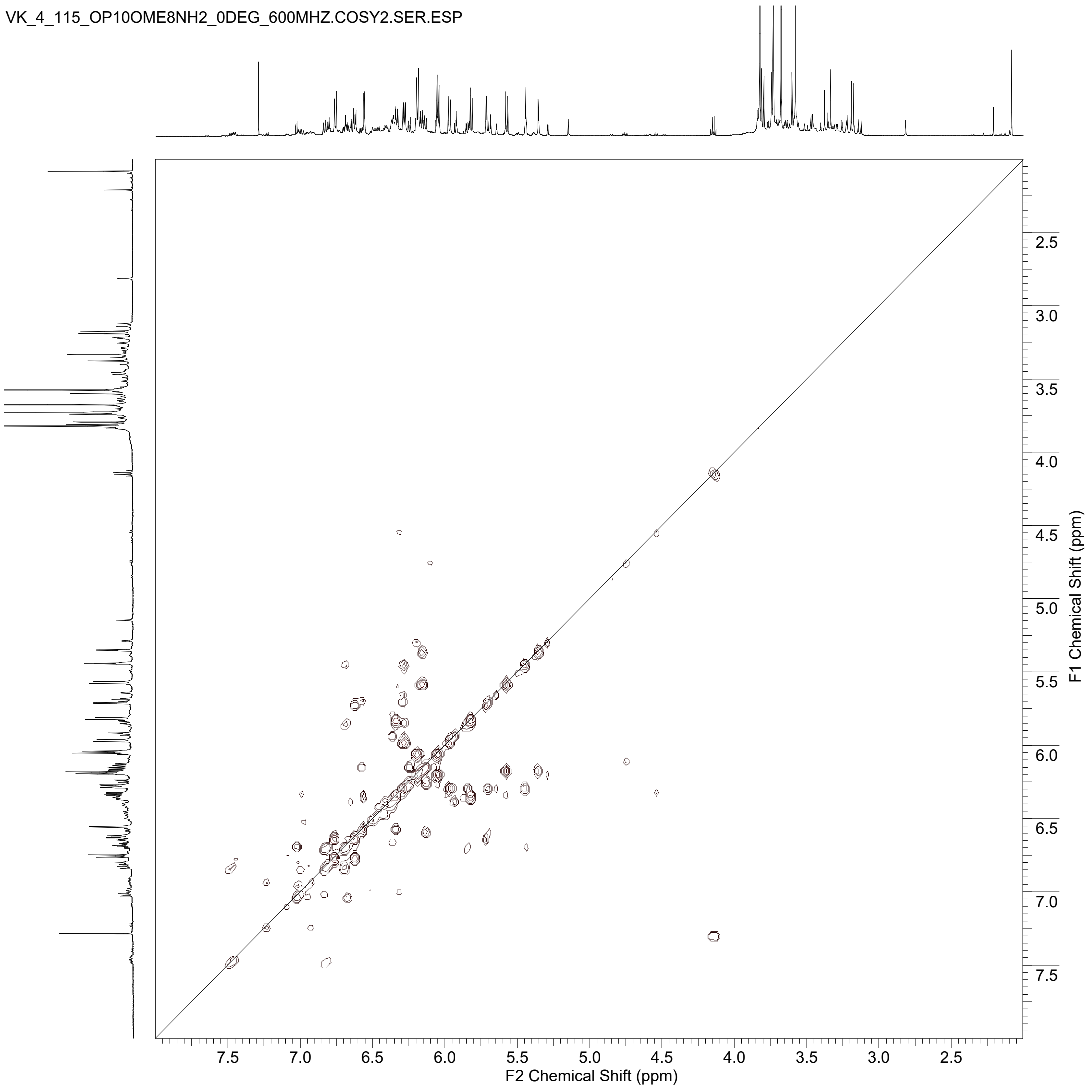

Figure S81. COSY NMR spectrum (600 MHz, $CDCl_3$, 0 ℃) of **$oP^{10}OMe(NH_2)$**.

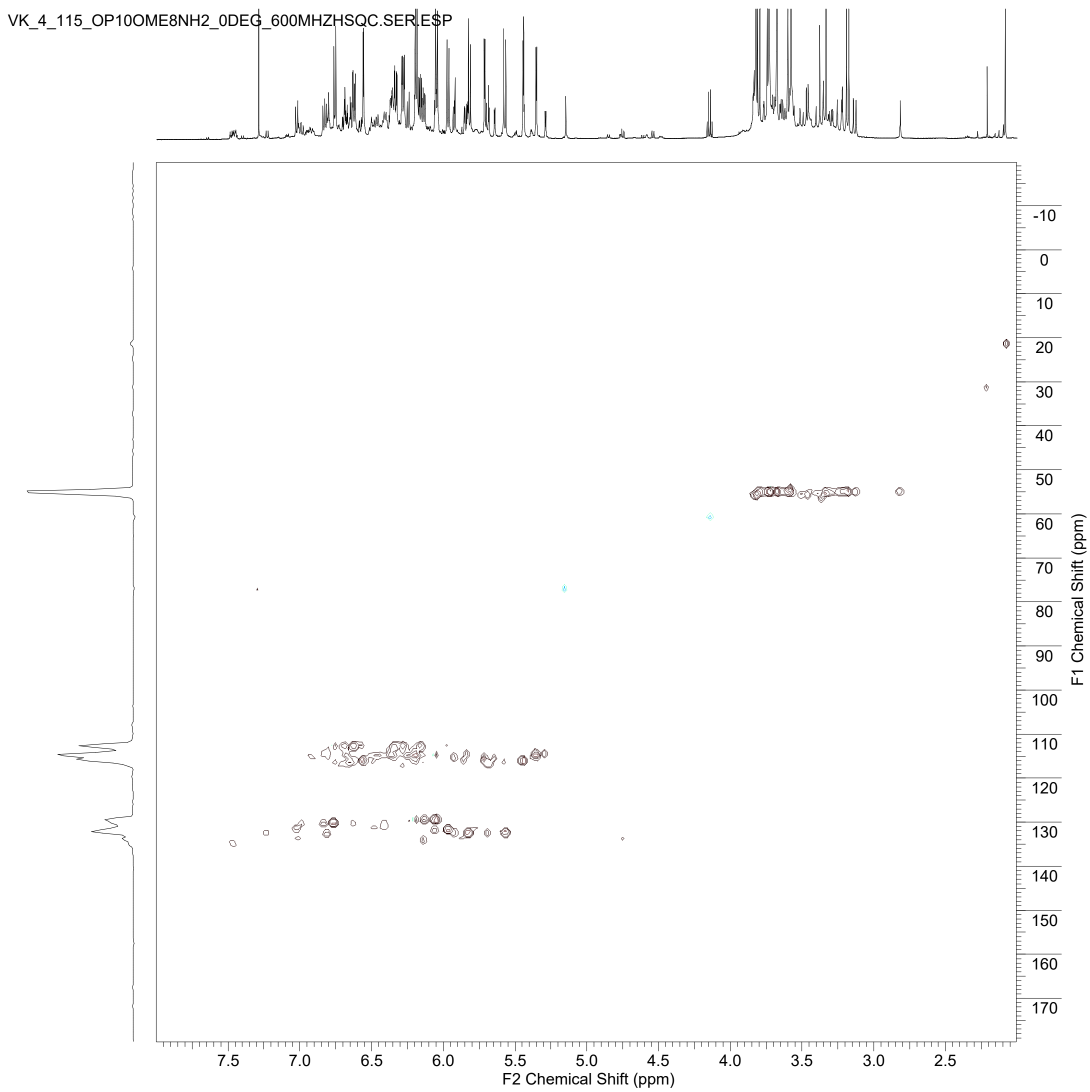

Figure S82. HSQC NMR spectrum (600 MHz, $CDCl_3$, 0 ℃) of **$oP^{10}OMe(NH_2)$**.

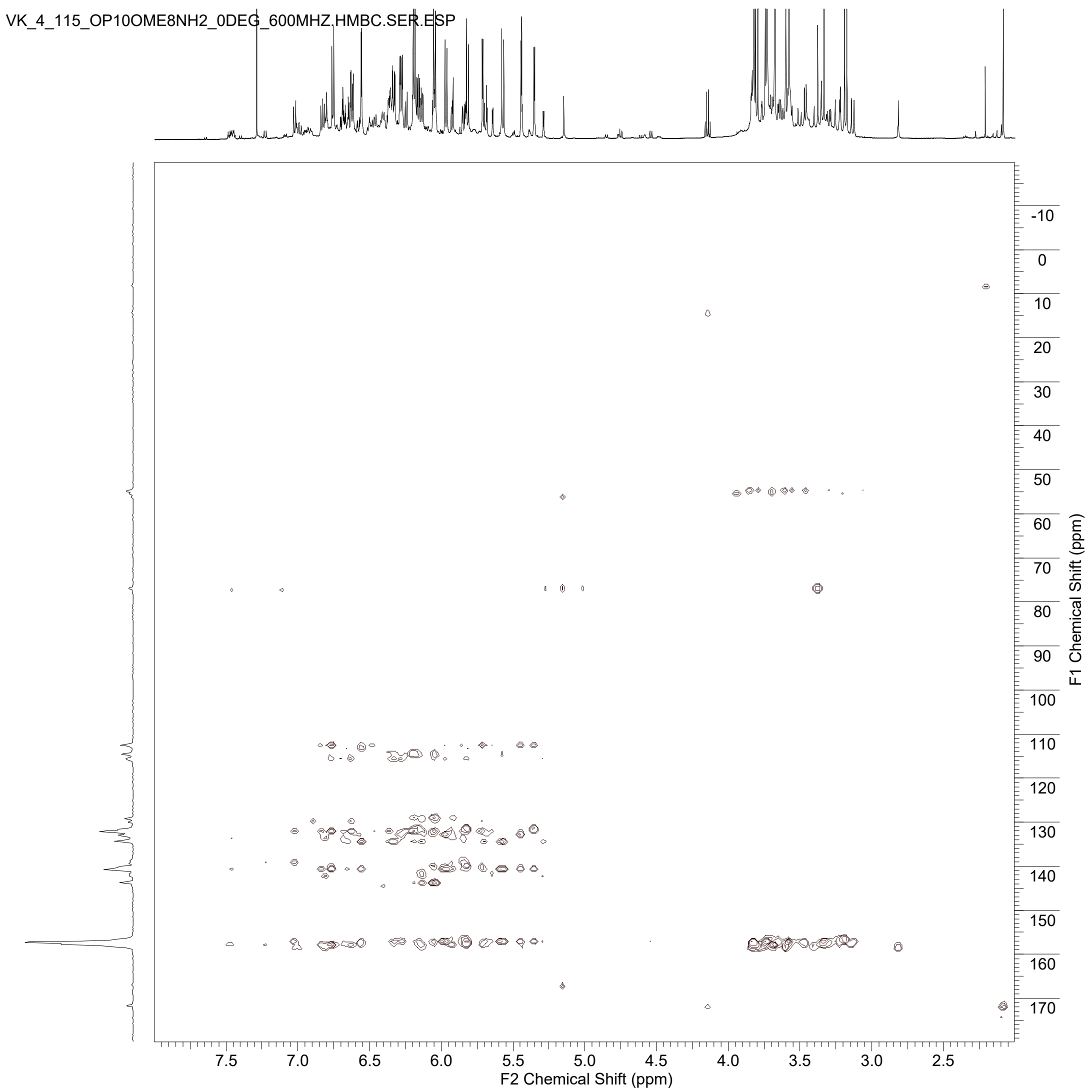

Figure S83. HMBC NMR spectrum (600 MHz, $CDCl_3$, 0 ℃) of **oP^{10}OMe(NH_2)**.

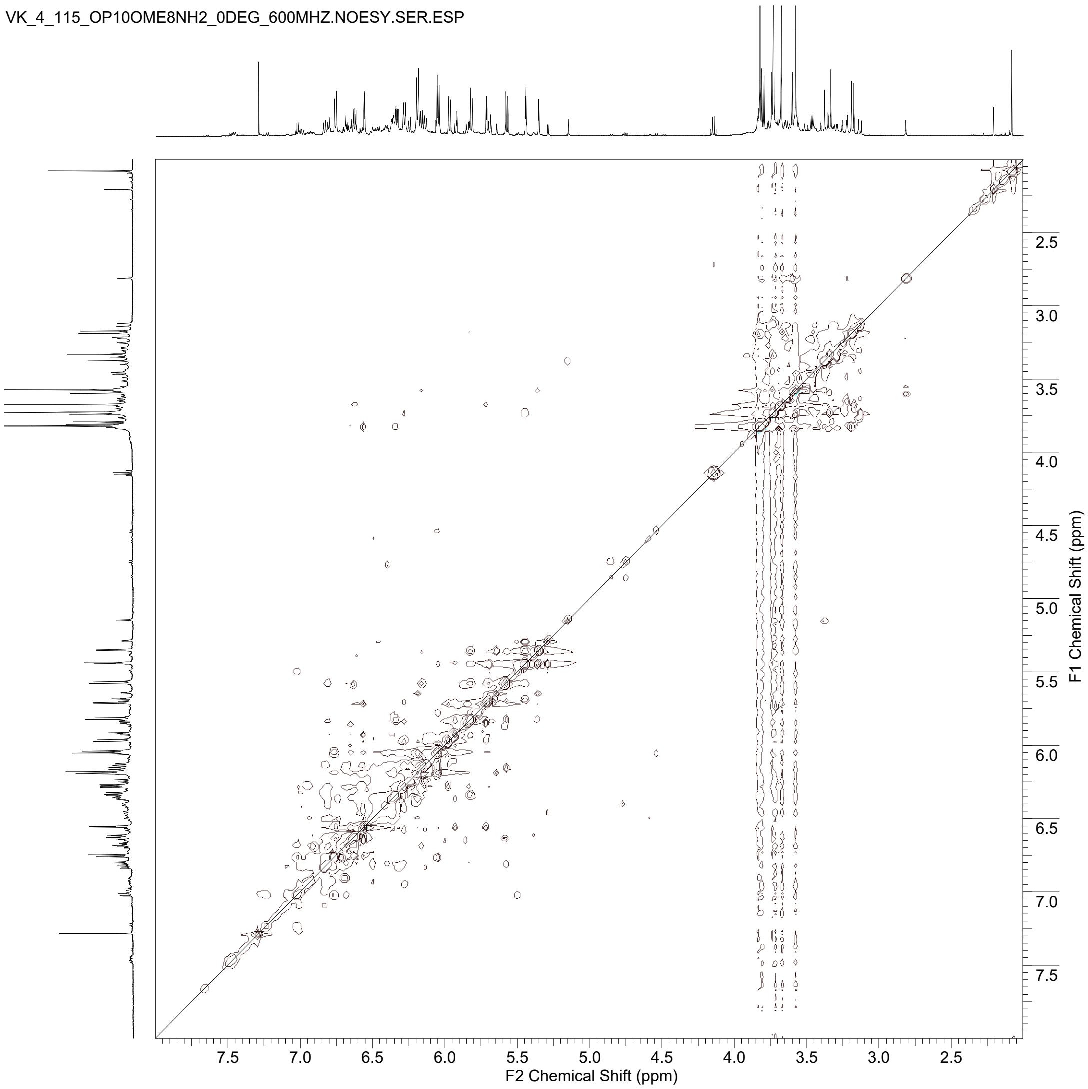

Figure S84. NOESY/EXSY NMR spectrum (600 MHz, $CDCl_3$, 0 ℃) of **oP^{10}OMe(NH_2)**.

oP¹⁰F(NH₂)

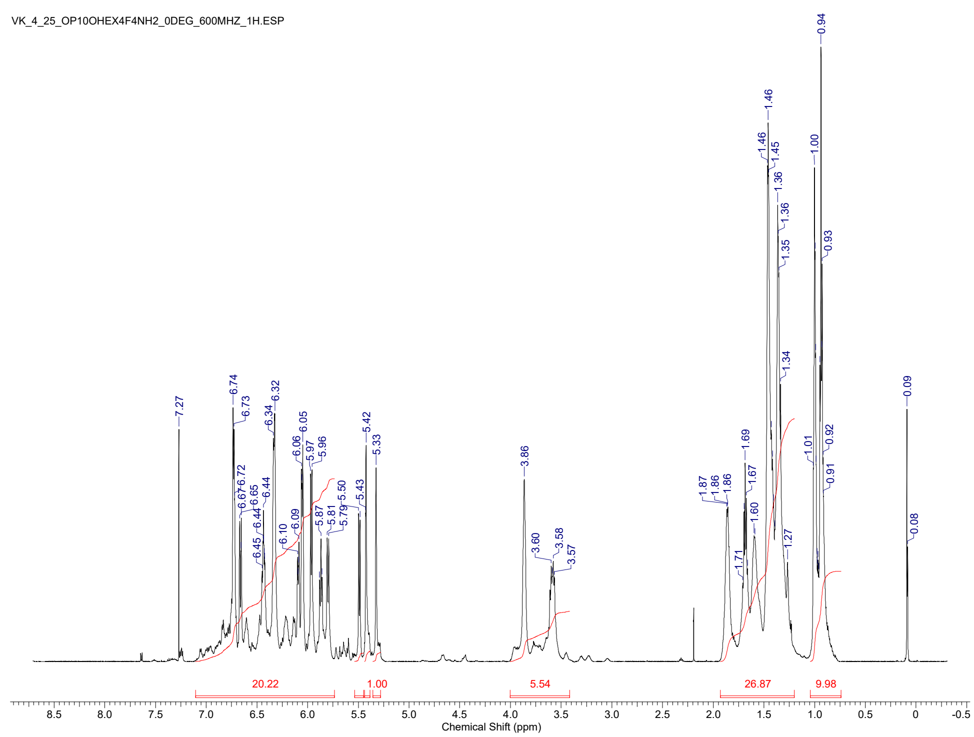

Figure S85. ^{1}H NMR spectrum (600 MHz, $CDCl_3$, 0 ℃) of **oP^{10}F(NH_2)**.

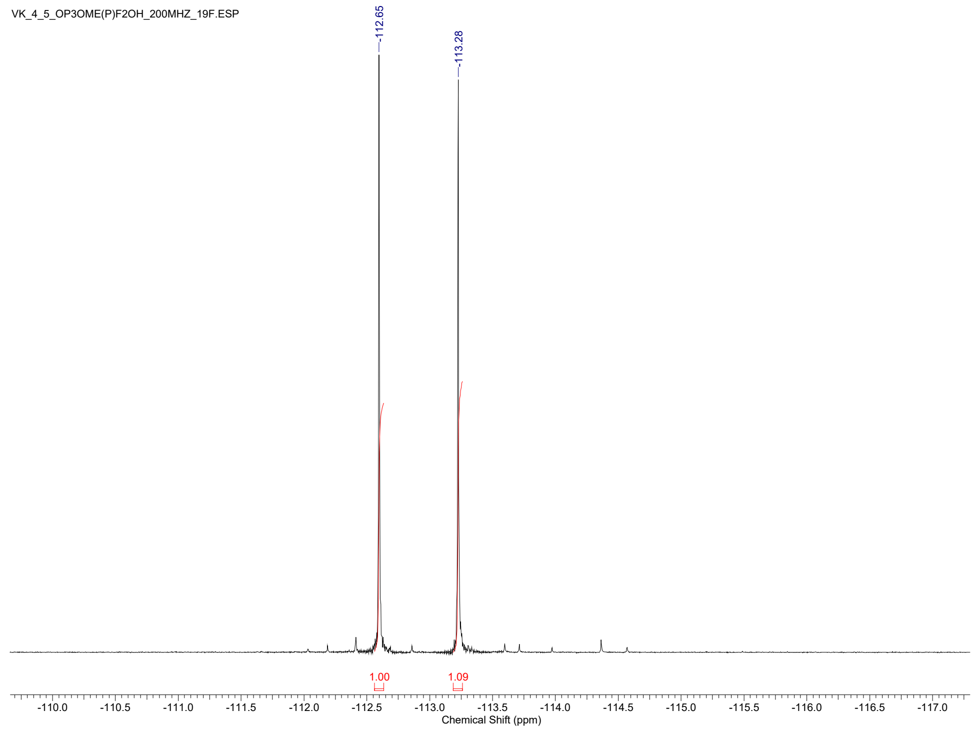

Figure S86. ^{19}F NMR spectrum (188 MHz, $CDCl_3$, 0 ℃) of **oP^{10}F(NH$_2$)**.

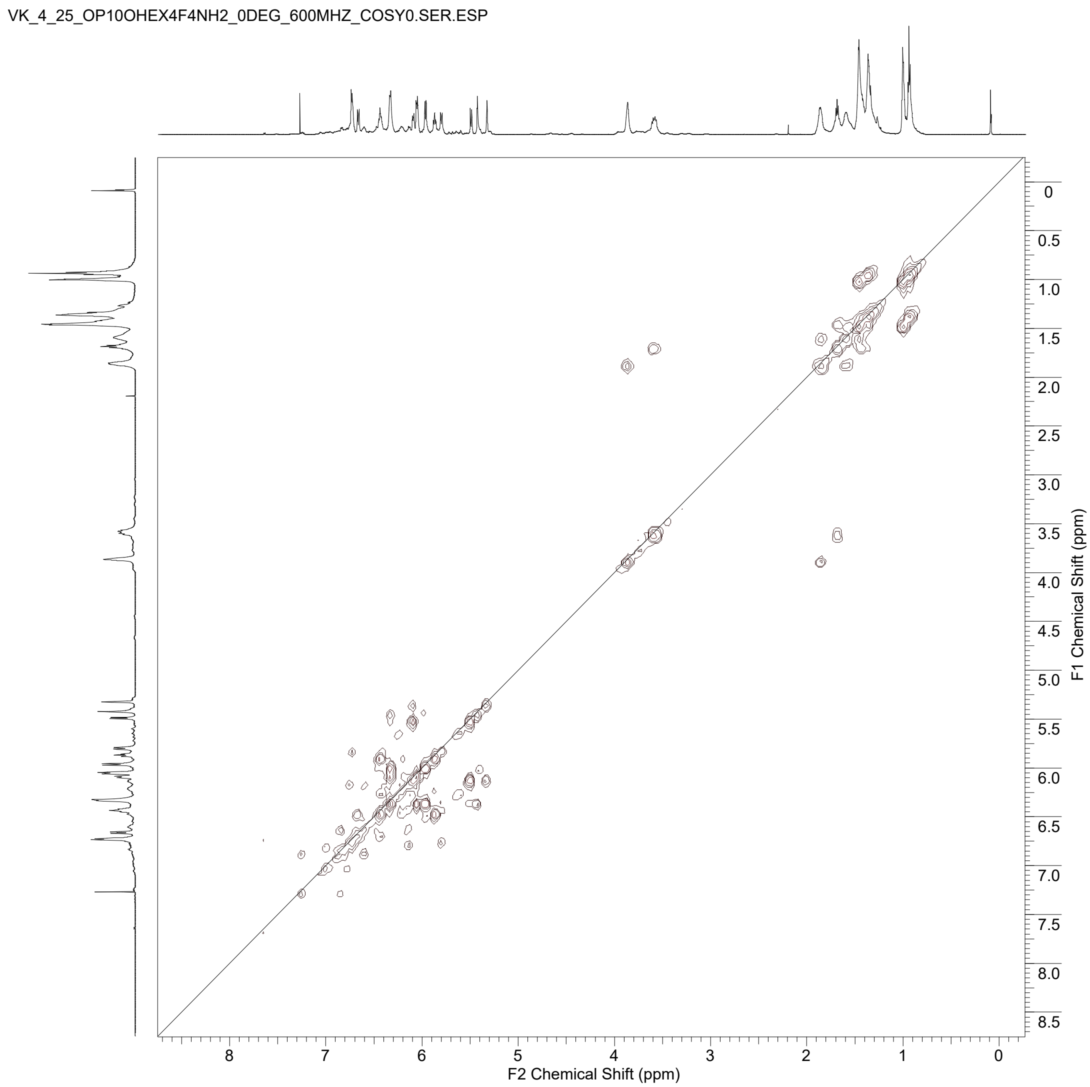

Figure S87. COSY NMR spectrum (600 MHz, $CDCl_3$, 0 ℃) of **oP^{10}F(NH_2)**.

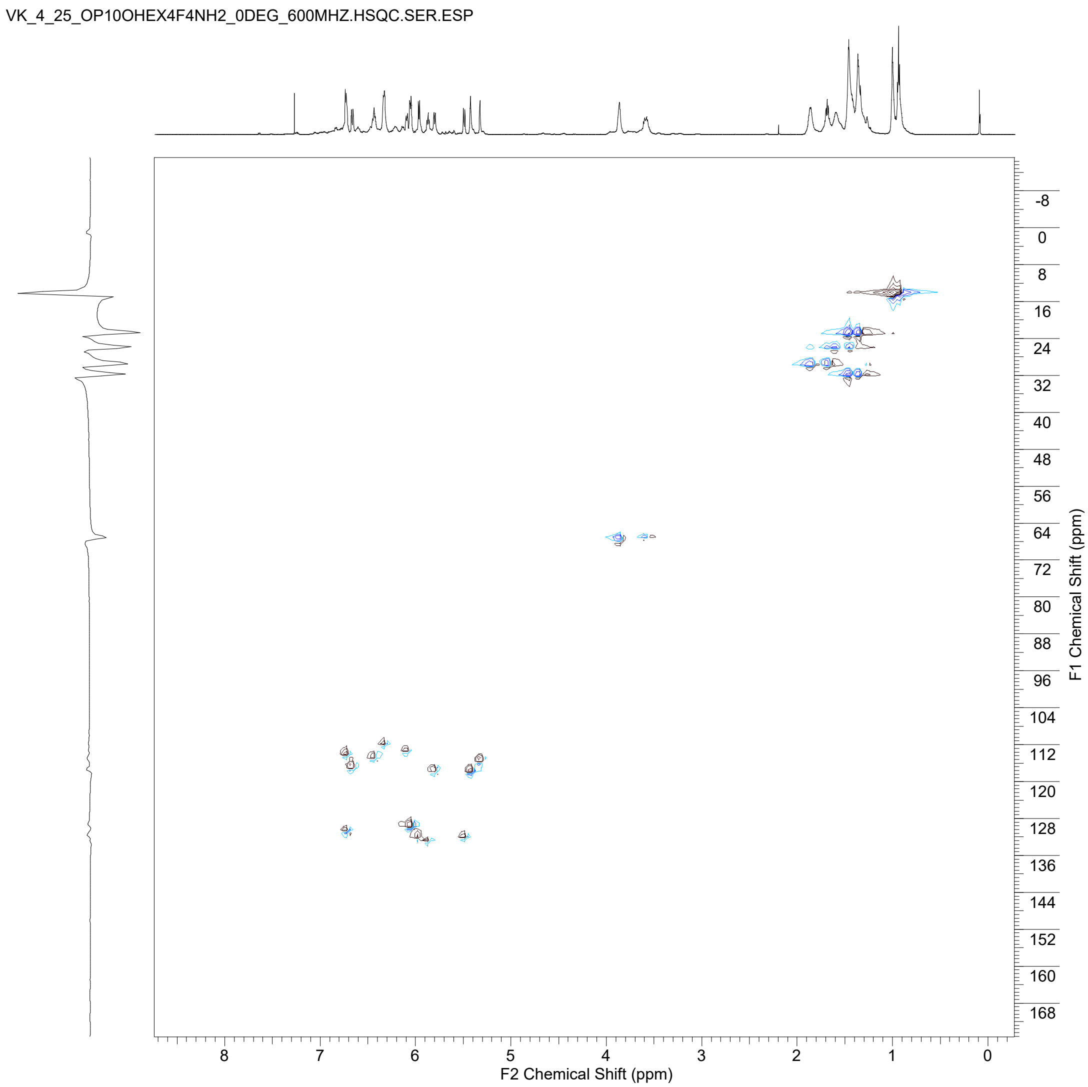

Figure S88. HSQC NMR spectrum (600 MHz, $CDCl_3$, 0 ℃) of **oP**

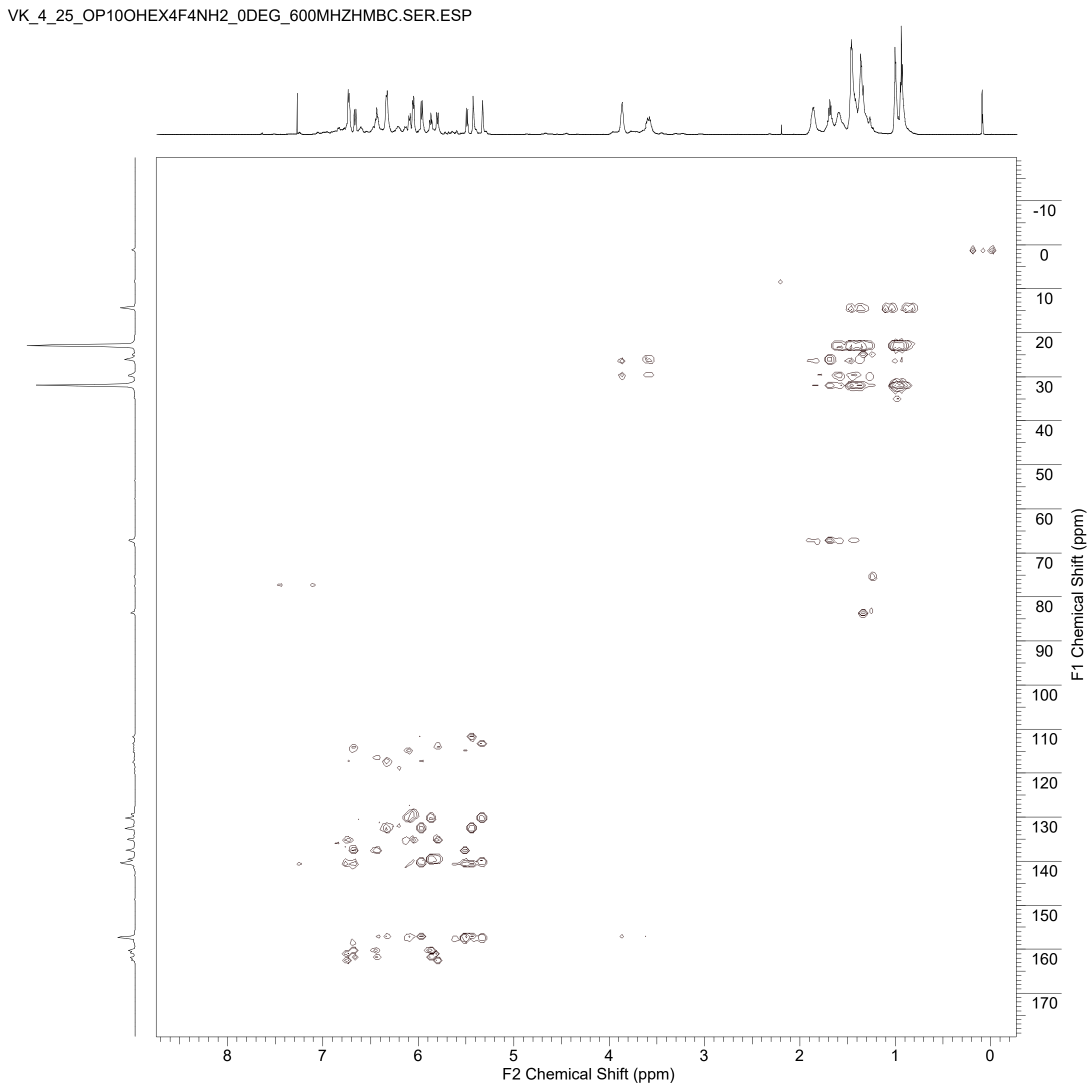

Figure S89. HMBC NMR spectrum (600 MHz, $CDCl_3$, 0 ℃) of **oP^{10}F(NH_2)**.

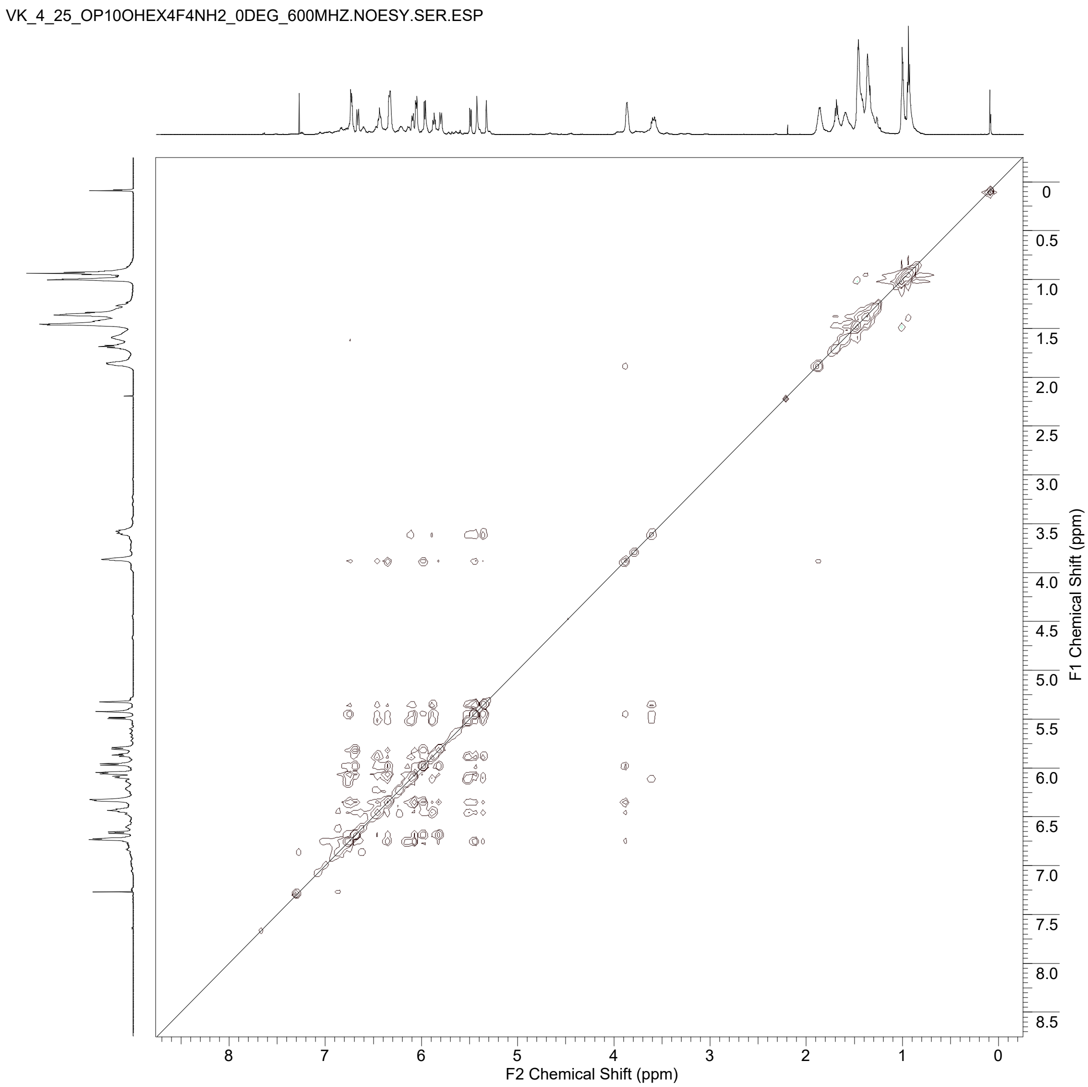

Figure S90. NOESY/EXSY NMR spectrum (600 MHz, $CDCl_3$, 0 ℃) of **oP^{10}F(NH$_2$)**.

oP¹⁰OMe(M)

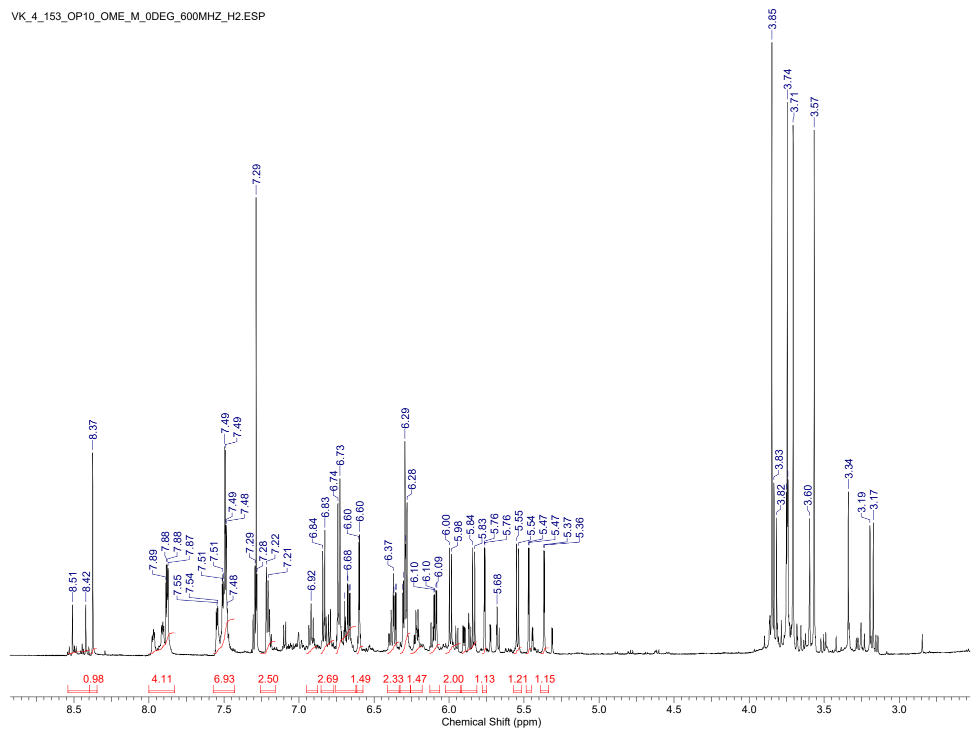

Figure S91. ^{1}H NMR spectrum (600 MHz, $CDCl_3$, 0 ℃) of **oP^{10}OMe(M)**.

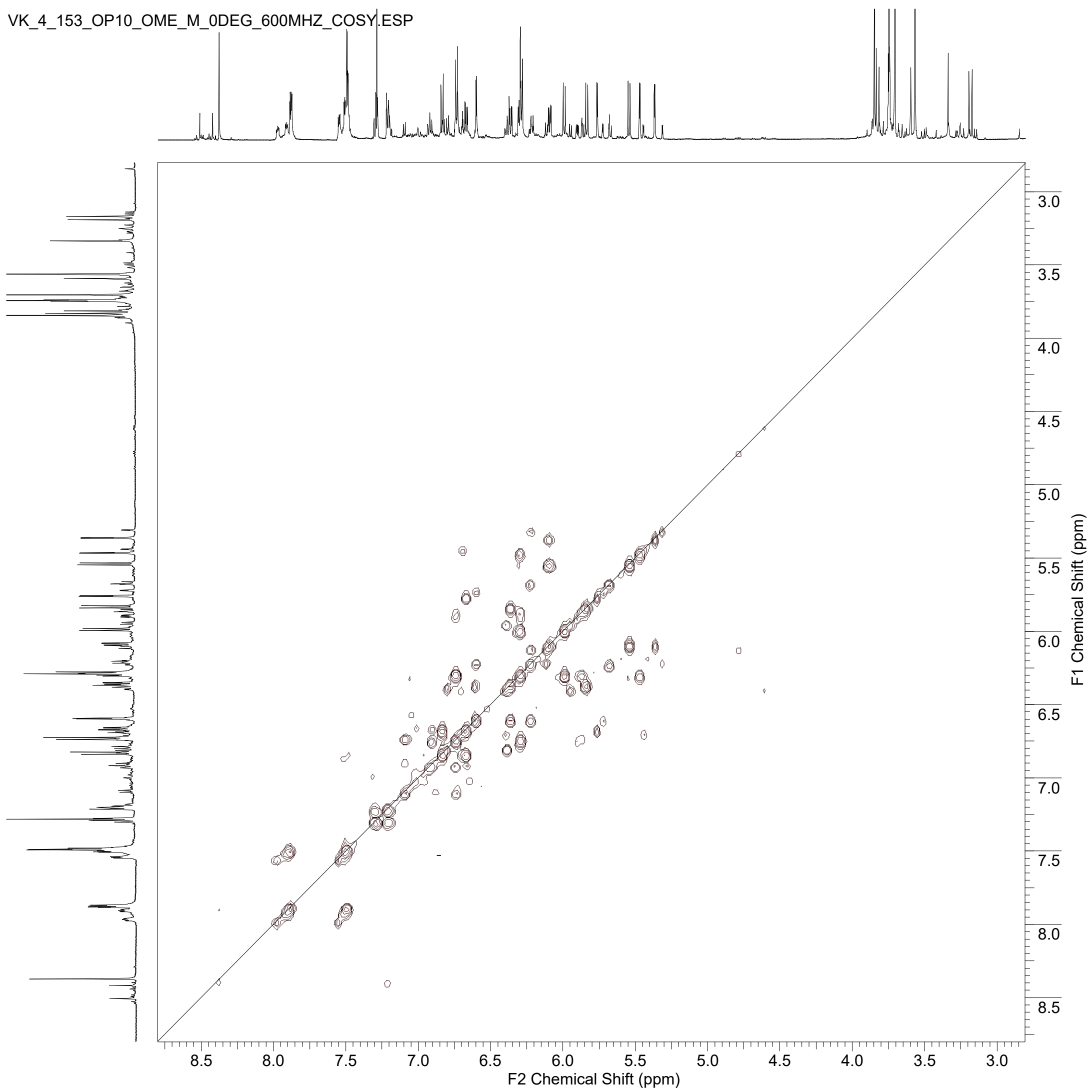

Figure S92. COSY NMR spectrum (600 MHz, $CDCl_3$, 0 ℃) of **oP^{10}OMe(M)**.

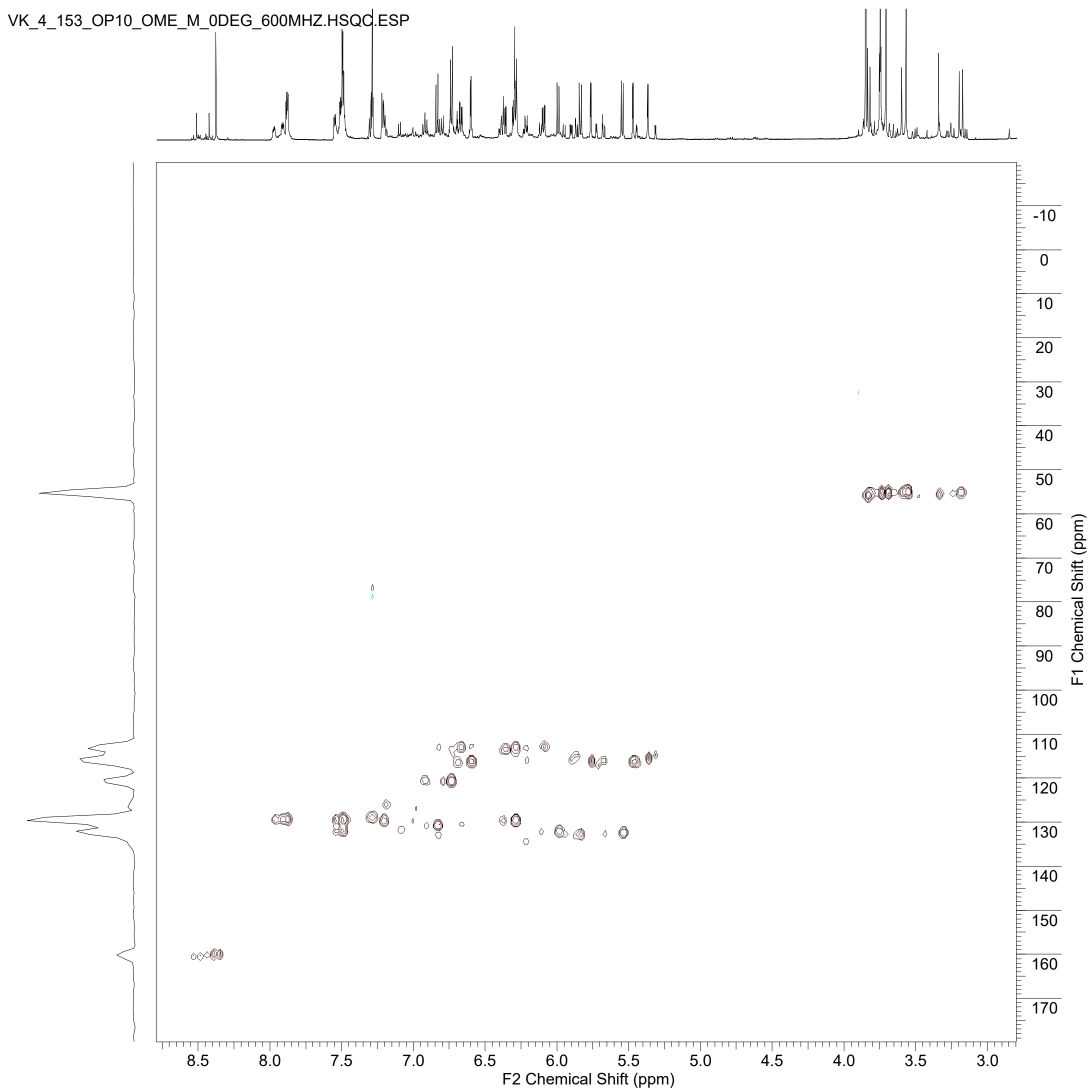

Figure S93. HSQC NMR spectrum (600 MHz, $CDCl_3$, 0 ℃) of **oP^{10}OMe(M)**.

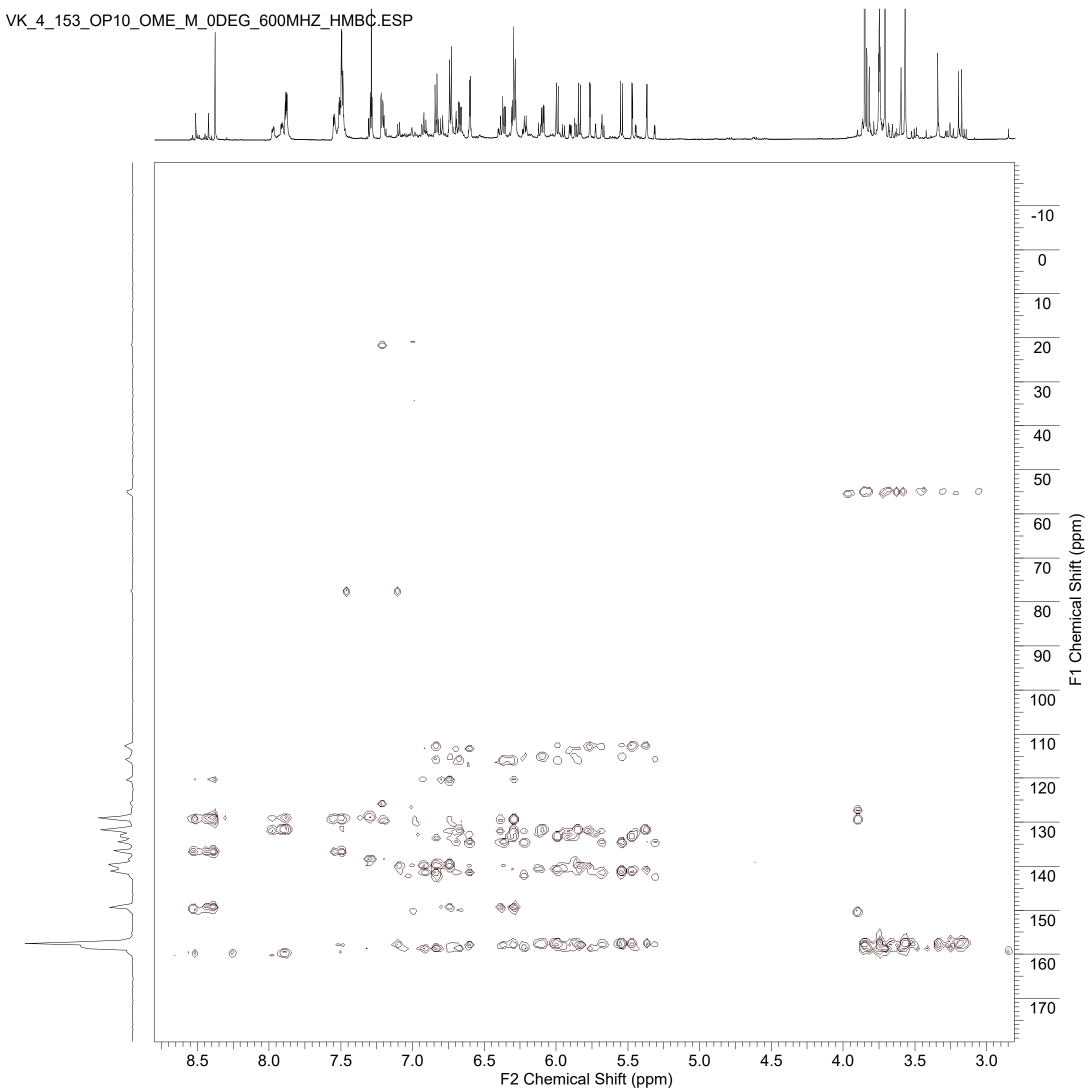

Figure S94. HMBC NMR spectrum (600 MHz, $CDCl_3$, 0 ℃) of **oP^{10}OMe(M)**.

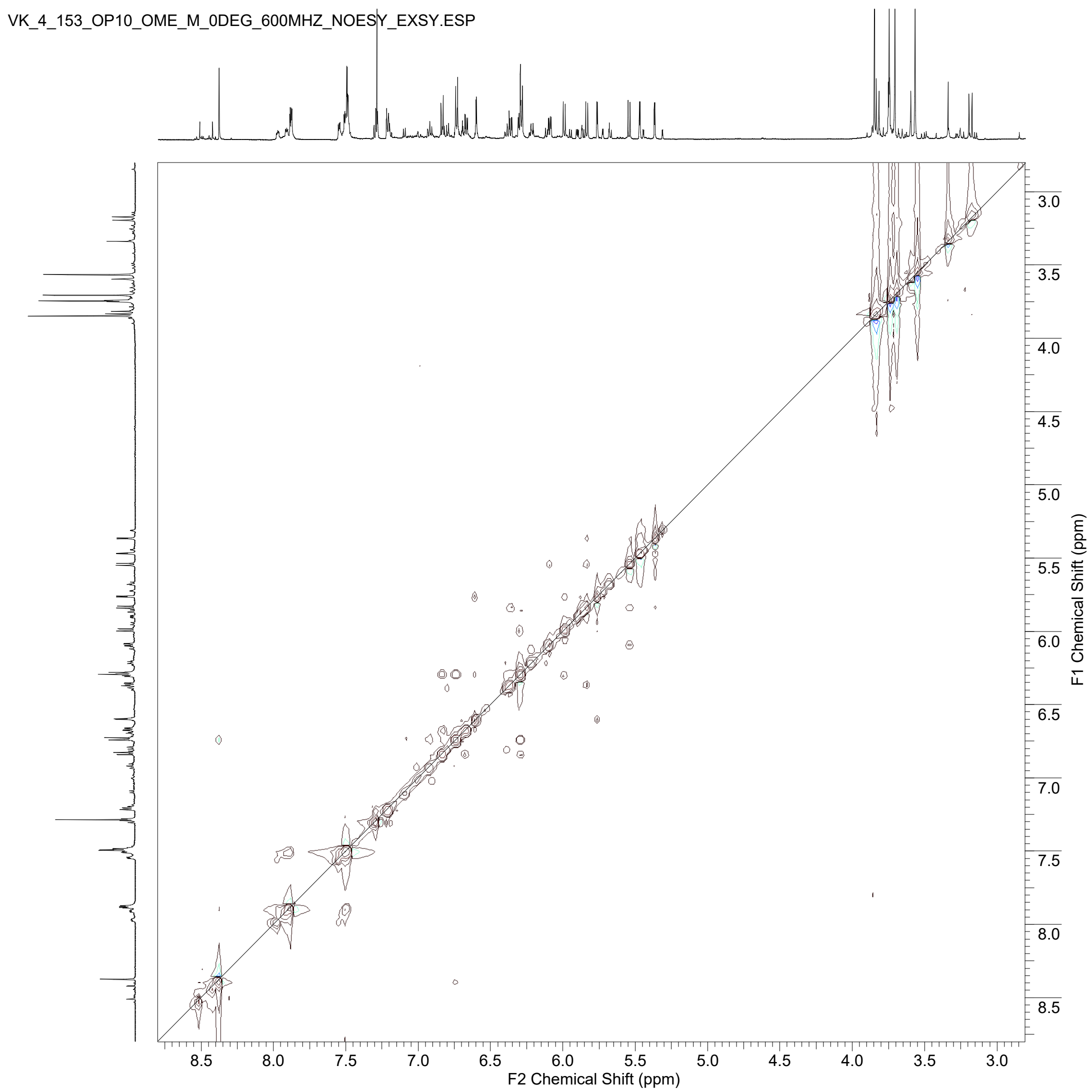

Figure S95. NOESY/EXSY NMR spectrum (600 MHz, $CDCl_3$, 0 ℃) of **oP[10]OMe(M)**.

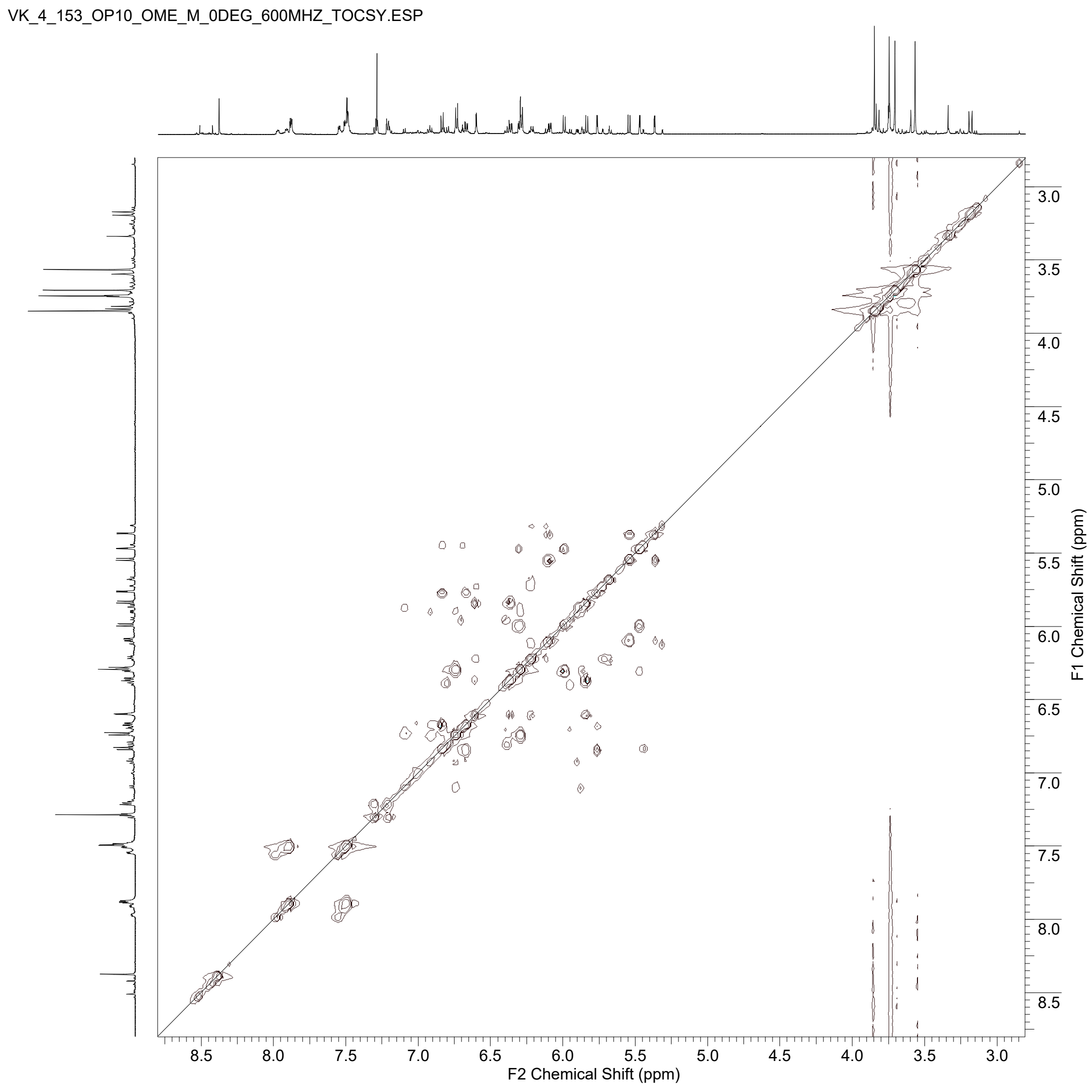

Figure S96. TOCSY NMR spectrum (600 MHz, $CDCl_3$, 0 ℃) of **oP^{10}OMe(M)**.

oP^10F(M)

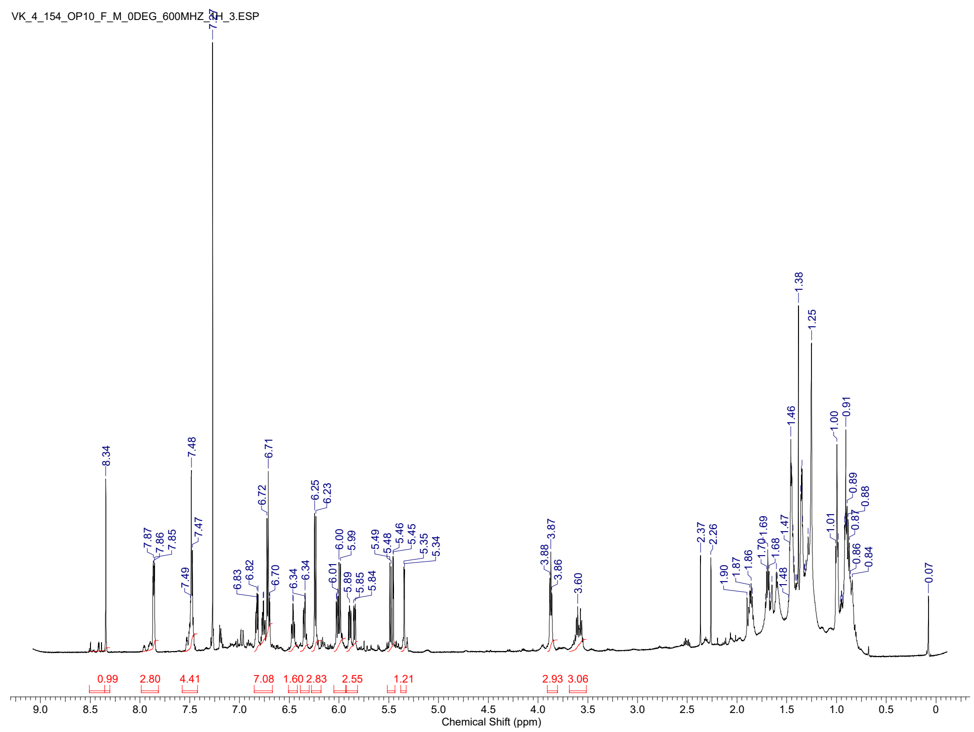

Figure S97. ^{1}H NMR spectrum (600 MHz, $CDCl_3$, 0 ℃) of **oP^10F(M)**.

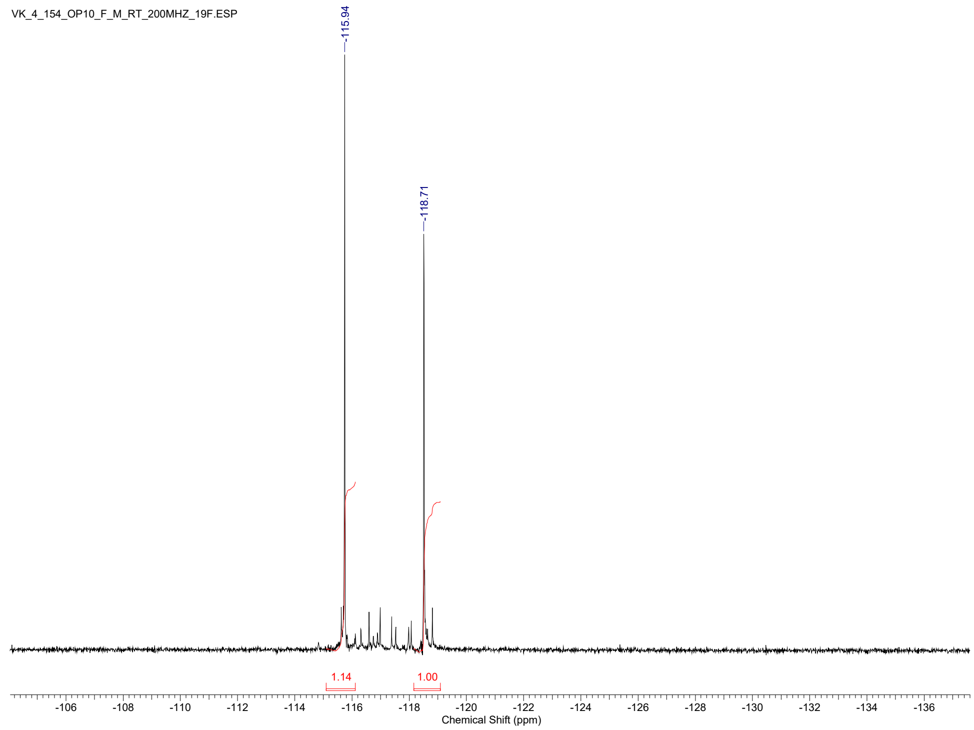

Figure S98. ^{19}F NMR spectrum (188 MHz, $CDCl_3$, 0 ℃) of **oP^{10}F(M)**.

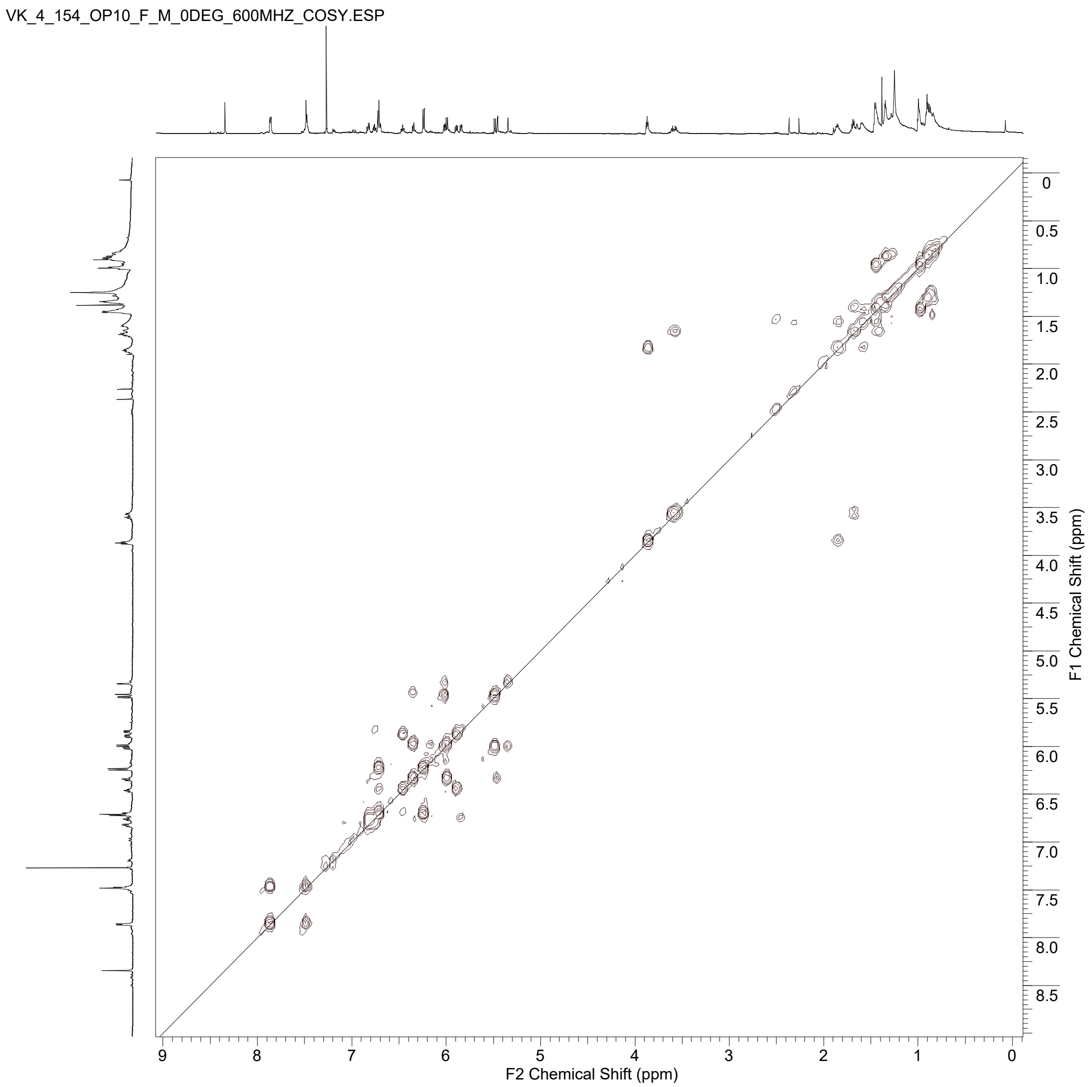

Figure S99. COSY NMR spectrum (600 MHz, $CDCl_3$, 0 ℃) of **oP^{10}F(M)**.

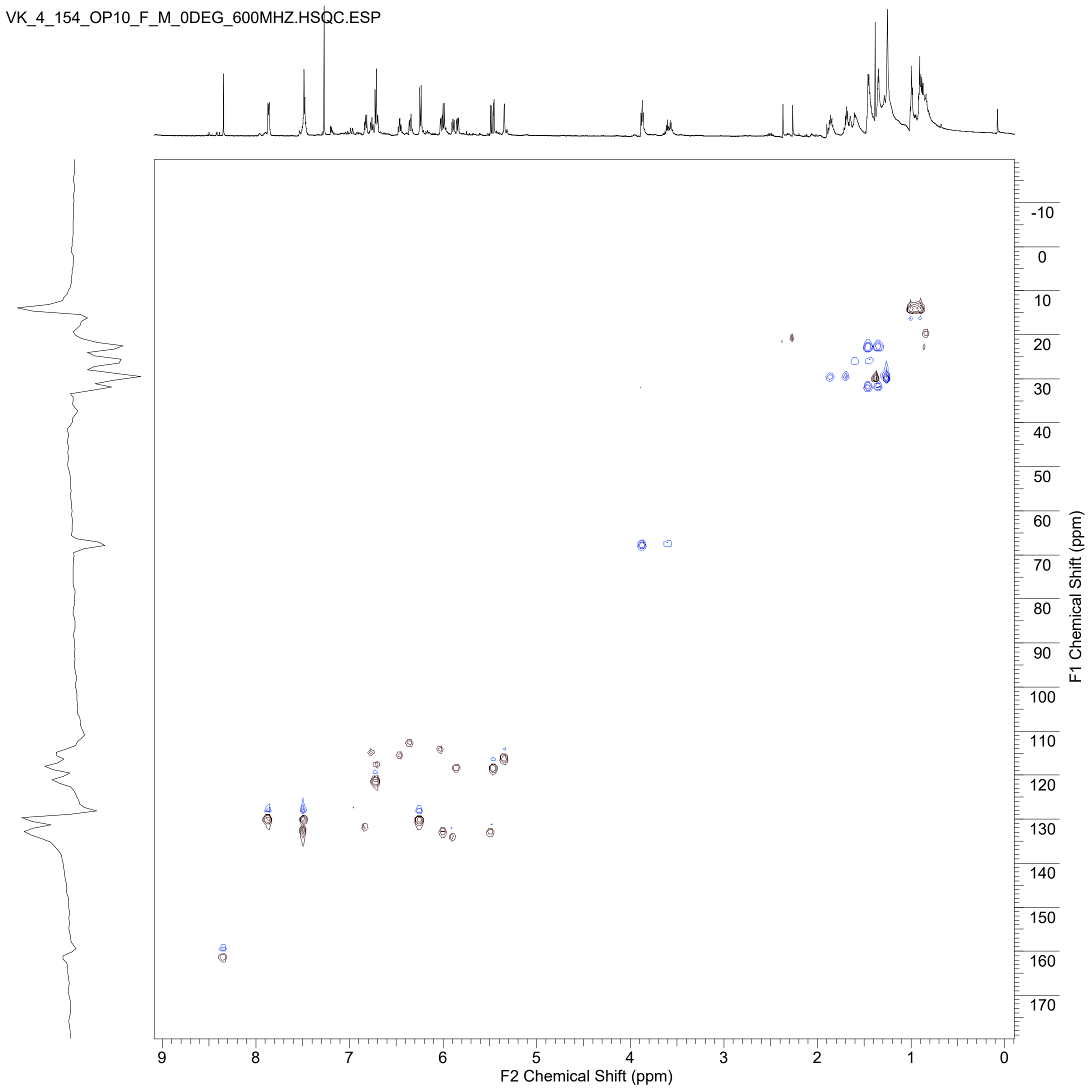

Figure S100. HSQC NMR spectrum (600 MHz, $CDCl_3$, 0 ℃) of **oP^{10}F(M)**.

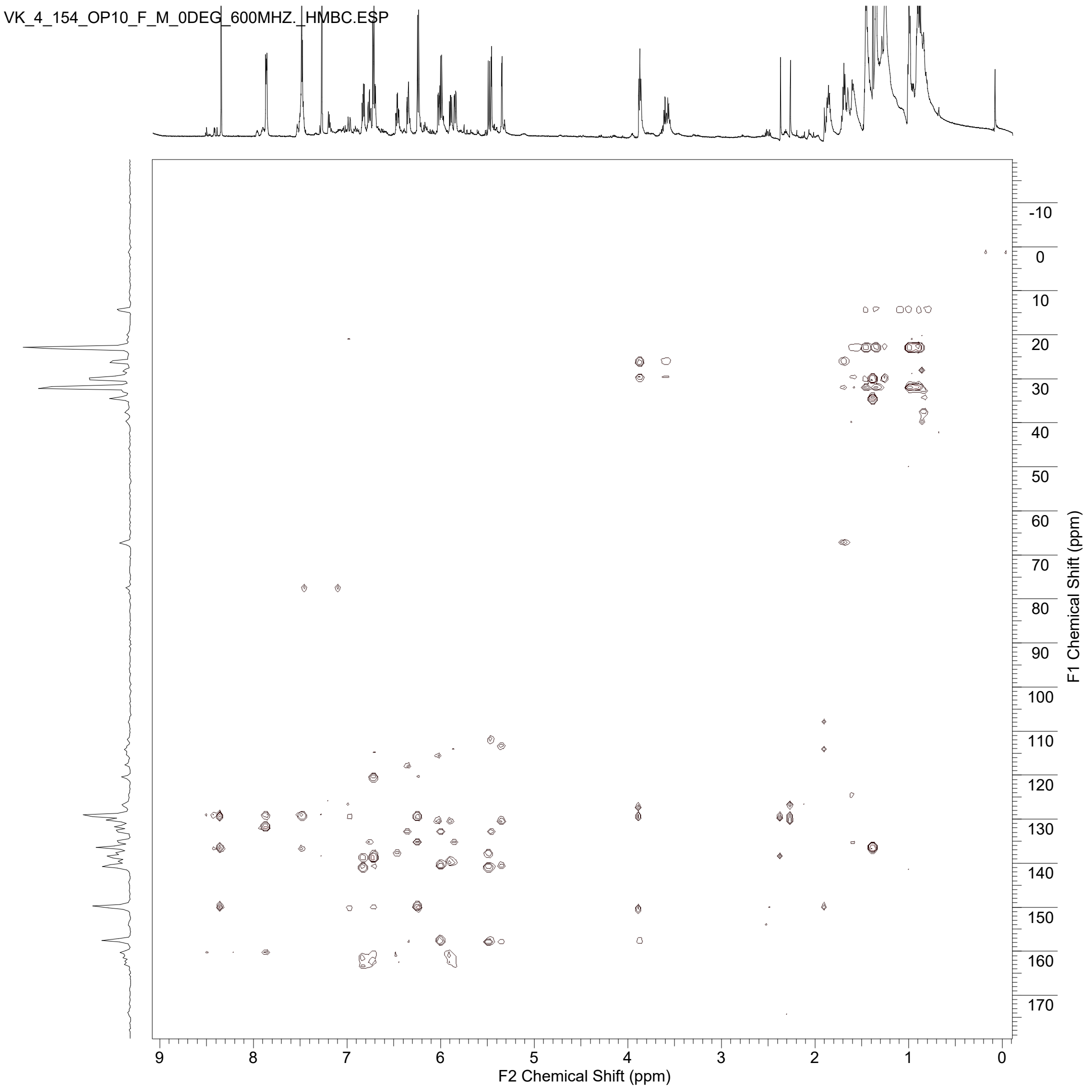

Figure S101. HMBC NMR spectrum (600 MHz, $CDCl_3$, 0 ℃) of **oP^{10}F(M)**.

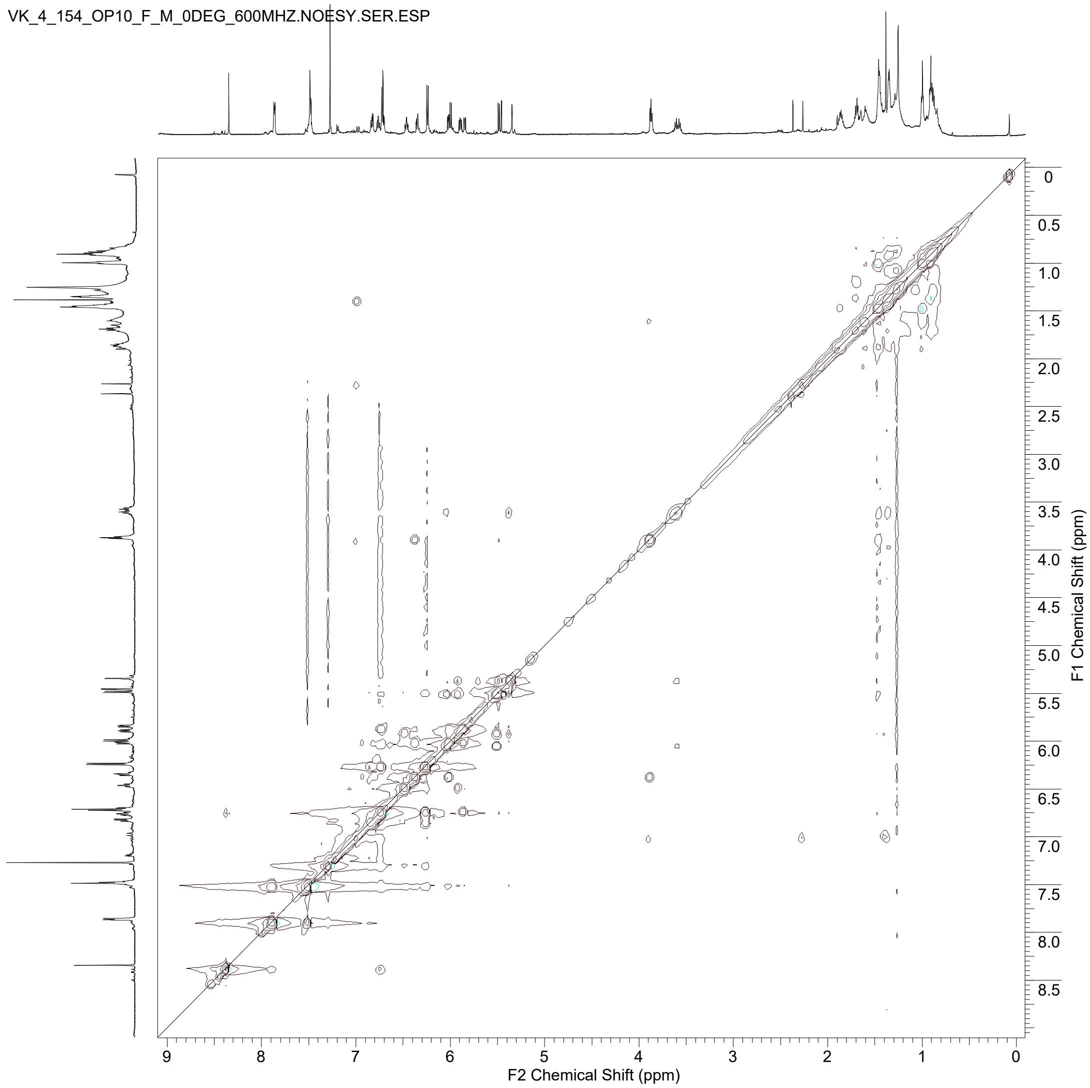

Figure S102. NOESY/EXSY NMR spectrum (600 MHz, $CDCl_3$, 0 ℃) of **oP^10^F(M)**.

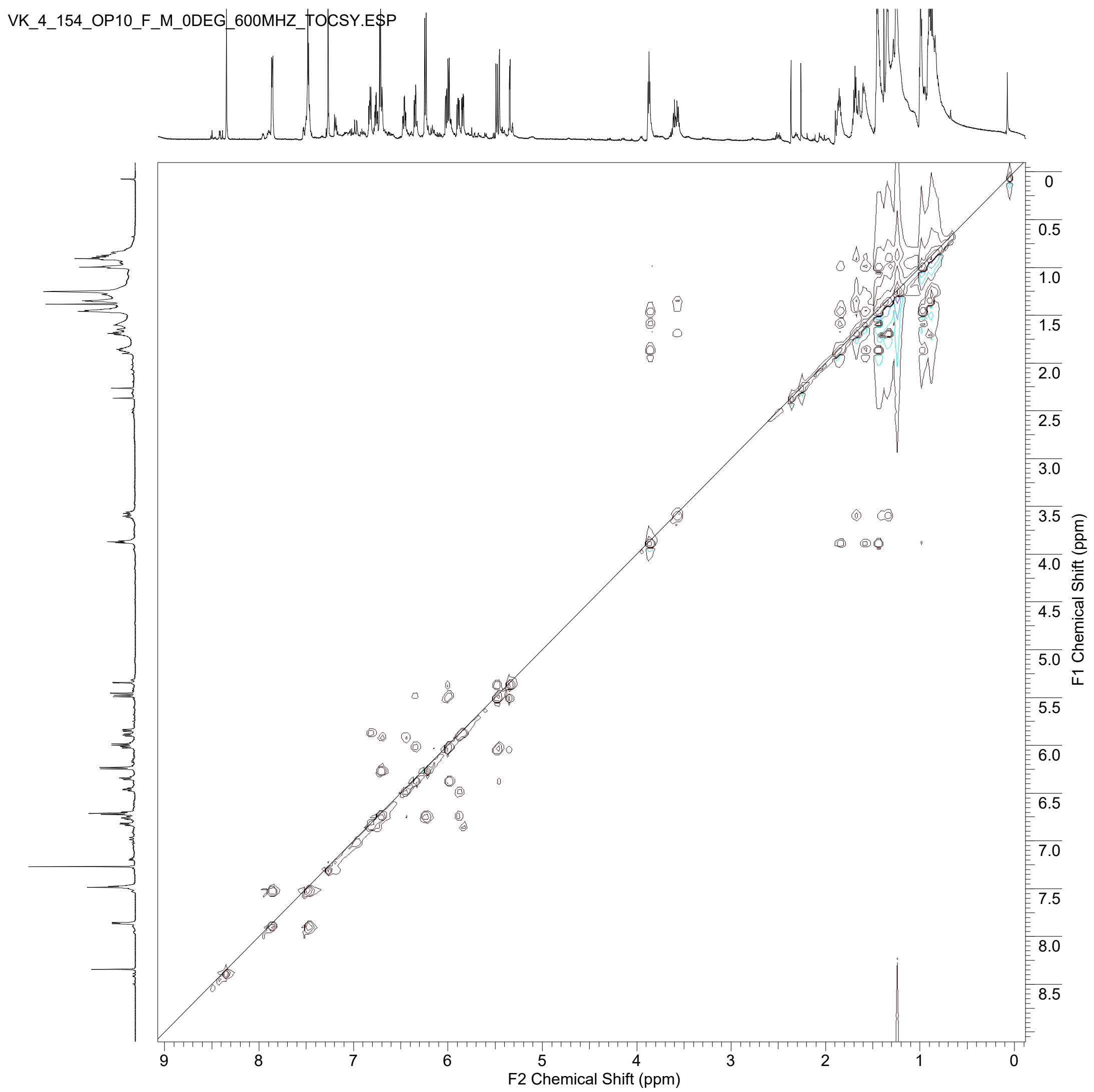

Figure S103. TOCSY NMR spectrum (600 MHz, $CDCl_3$, 0 ℃) of $\mathbf{oP^{10}F(M)}$.

oP^{10}F(DPB)$_{3+3}$

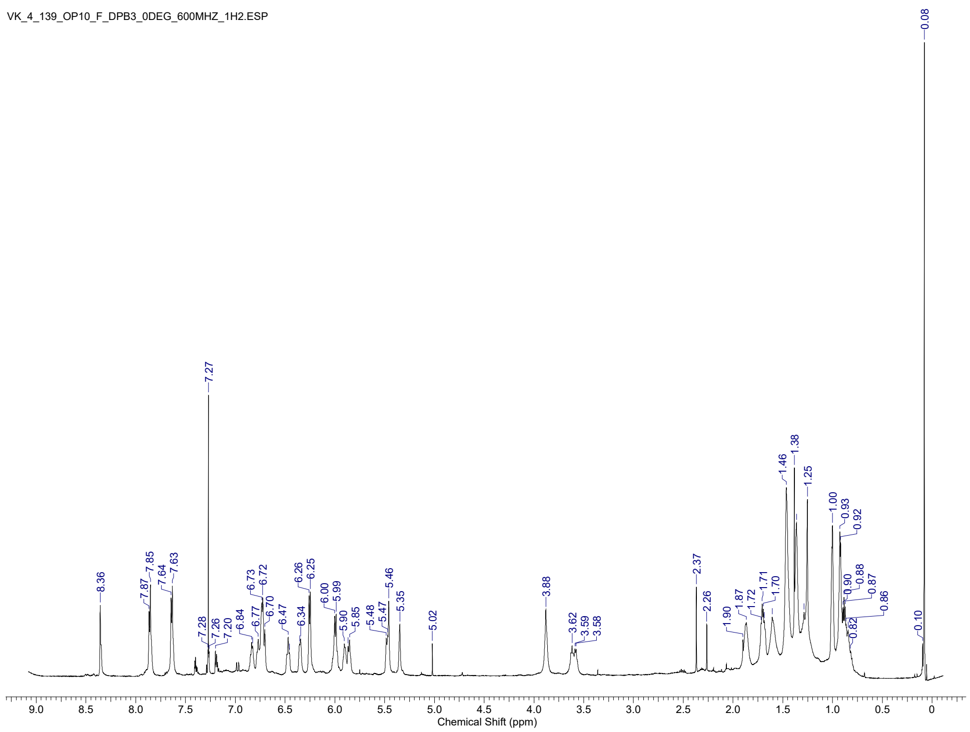

Figure S104. ^{1}H NMR spectrum (600 MHz, $CDCl_3$, 0 ℃) of **oP^{10}F(DPB)$_{3+3}$**.

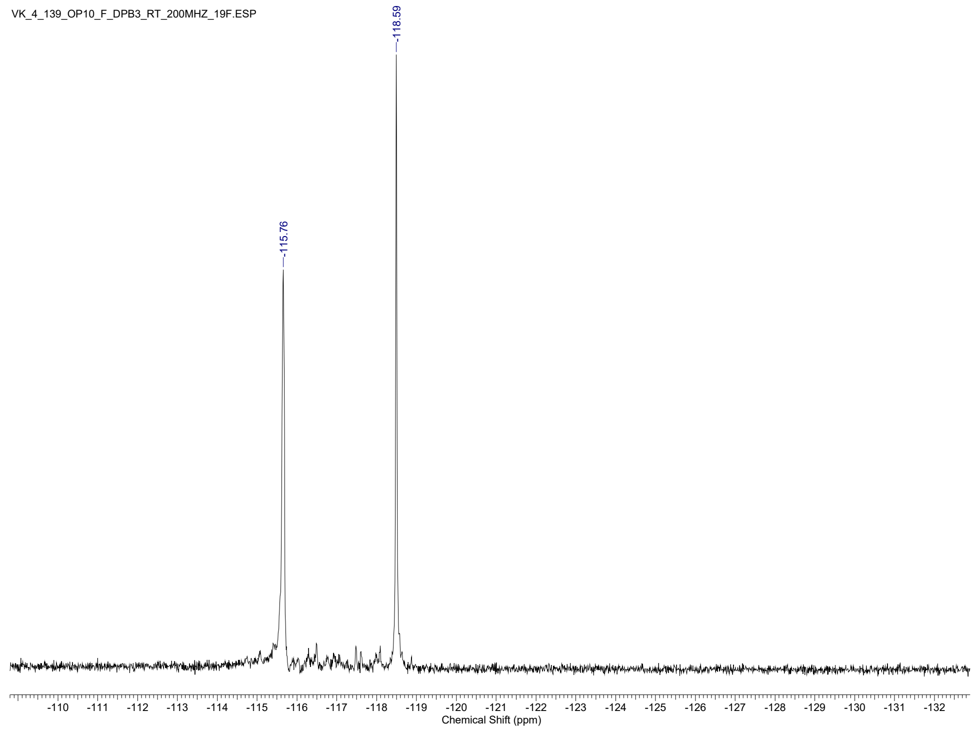

Figure S105. ^{19}F NMR spectrum (188 MHz, $CDCl_3$, 0 ℃) of **oP^{10}F(DPB)$_{3+3}$**.

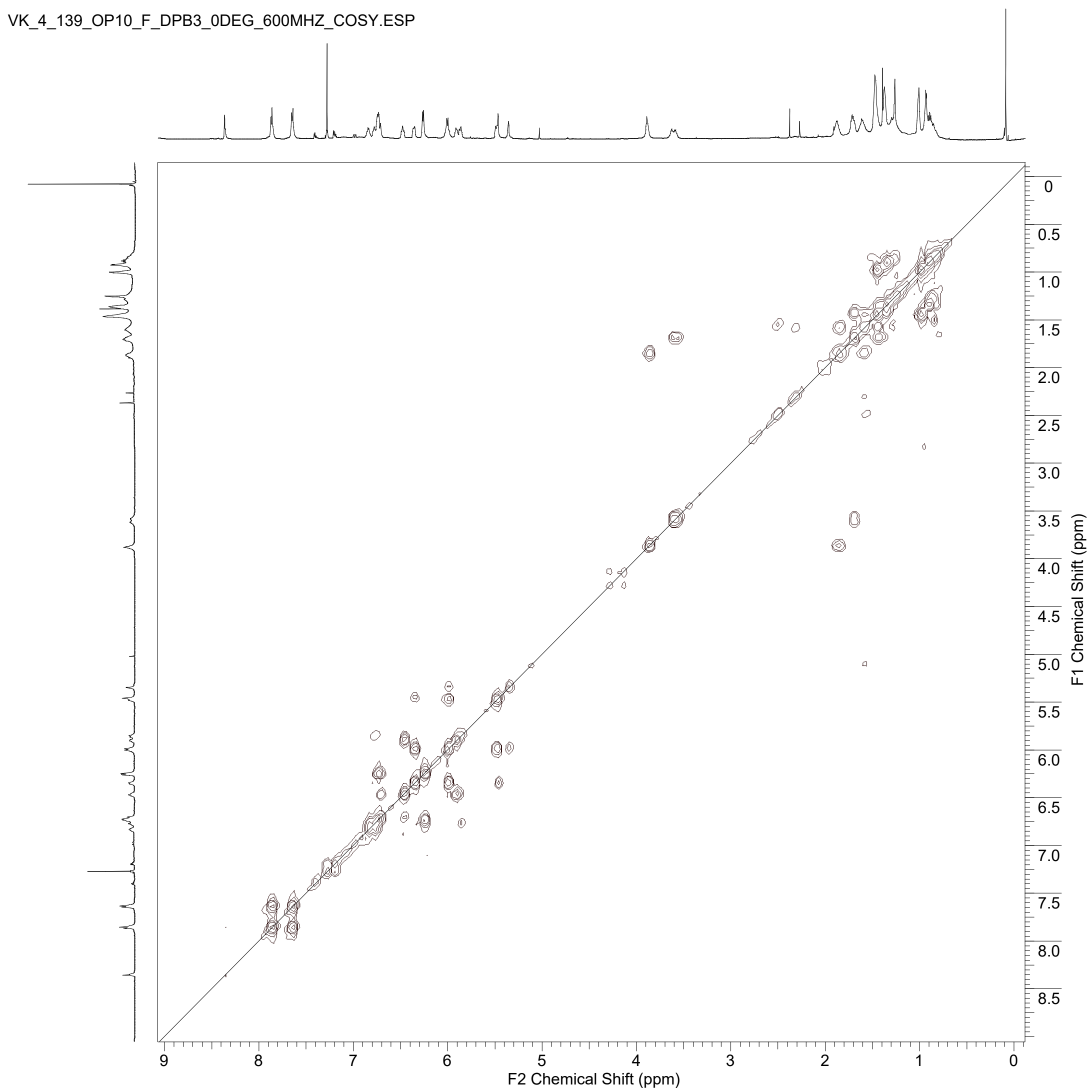

Figure S106. COSY NMR spectrum (600 MHz, $CDCl_3$, 0 ℃) of **oP^{10}F(DPB)$_{3+3}$**.

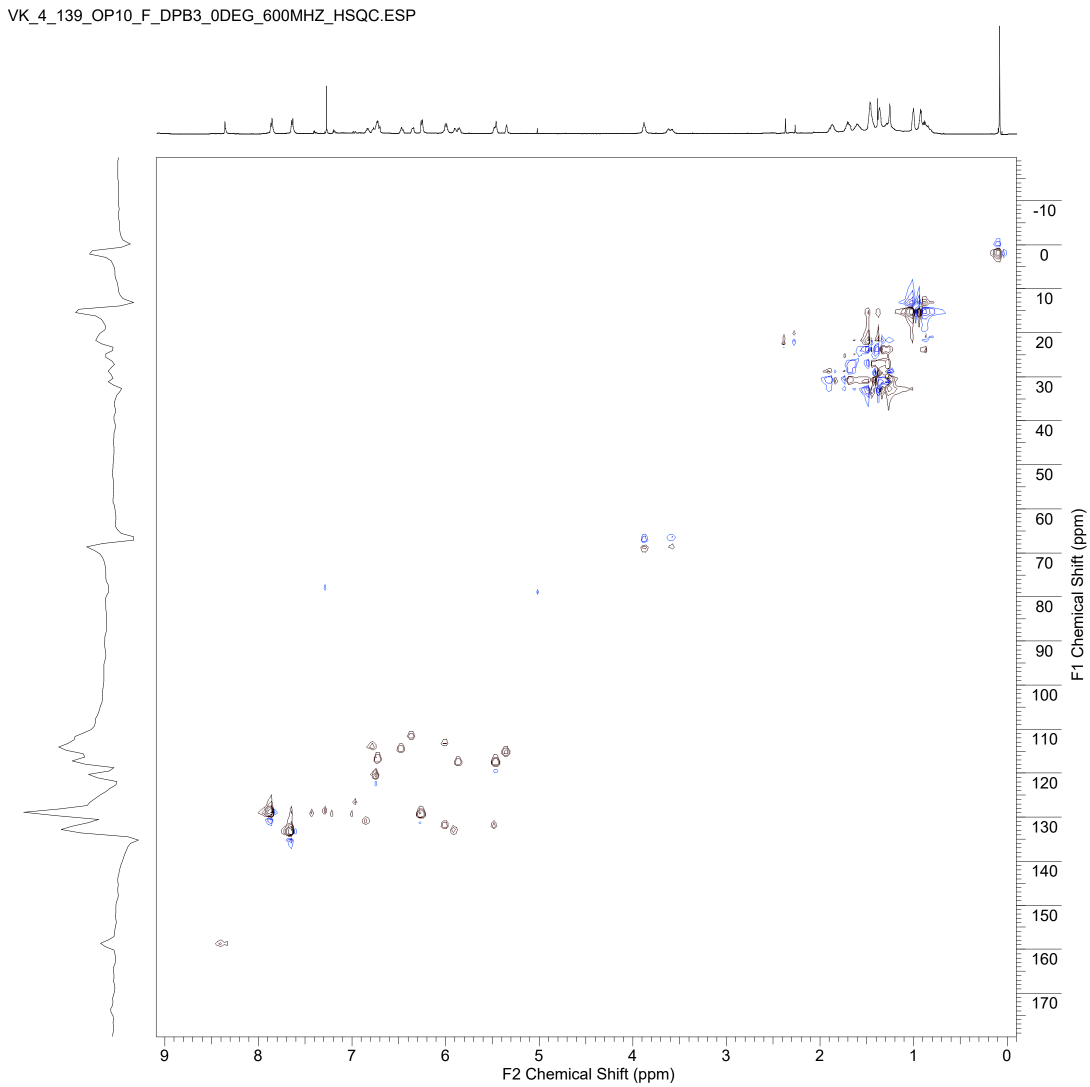

Figure S107. HSQC NMR spectrum (600 MHz, $CDCl_3$, 0 ℃) of $\mathbf{oP^{10}F(DPB)_{3+3}}$.

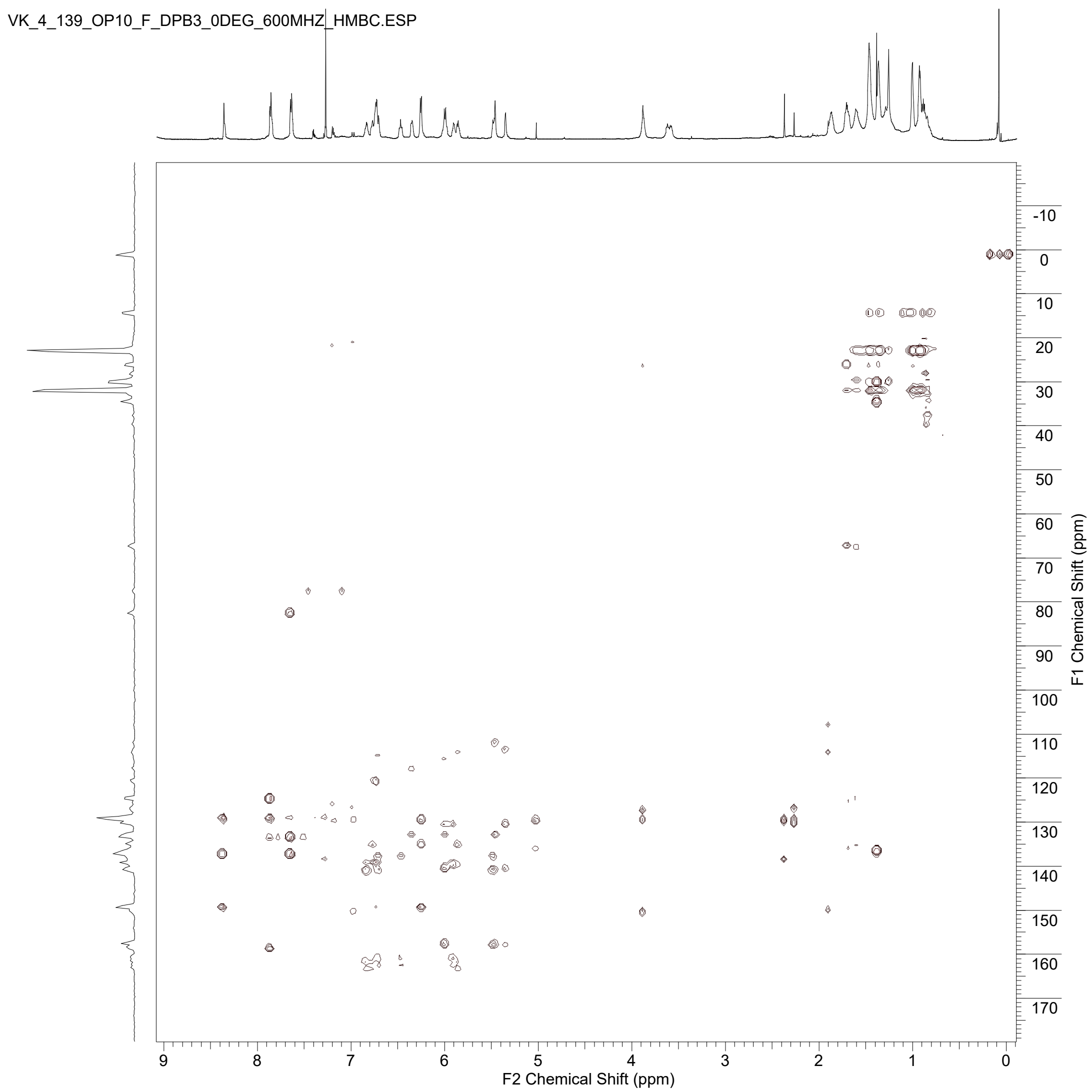

Figure S108. HMBC NMR spectrum (600 MHz, $CDCl_3$, 0 ℃) of $\mathbf{oP^{10}F(DPB)_{3+3}}$.

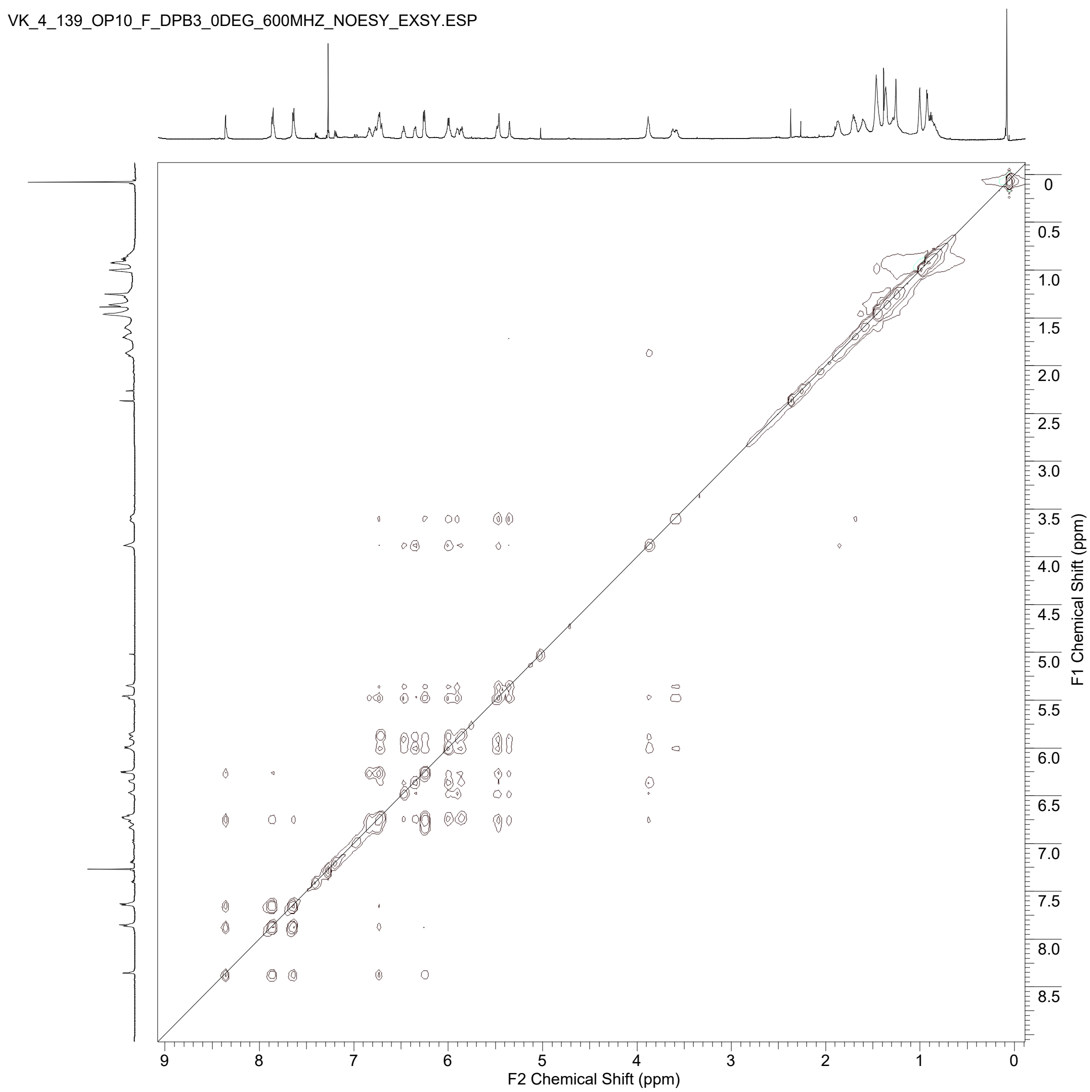

Figure S109. NOESY/EXSY NMR spectrum (600 MHz, $CDCl_3$, 0 ℃) of **oP^{10}F(DPB)$_{3+3}$**.

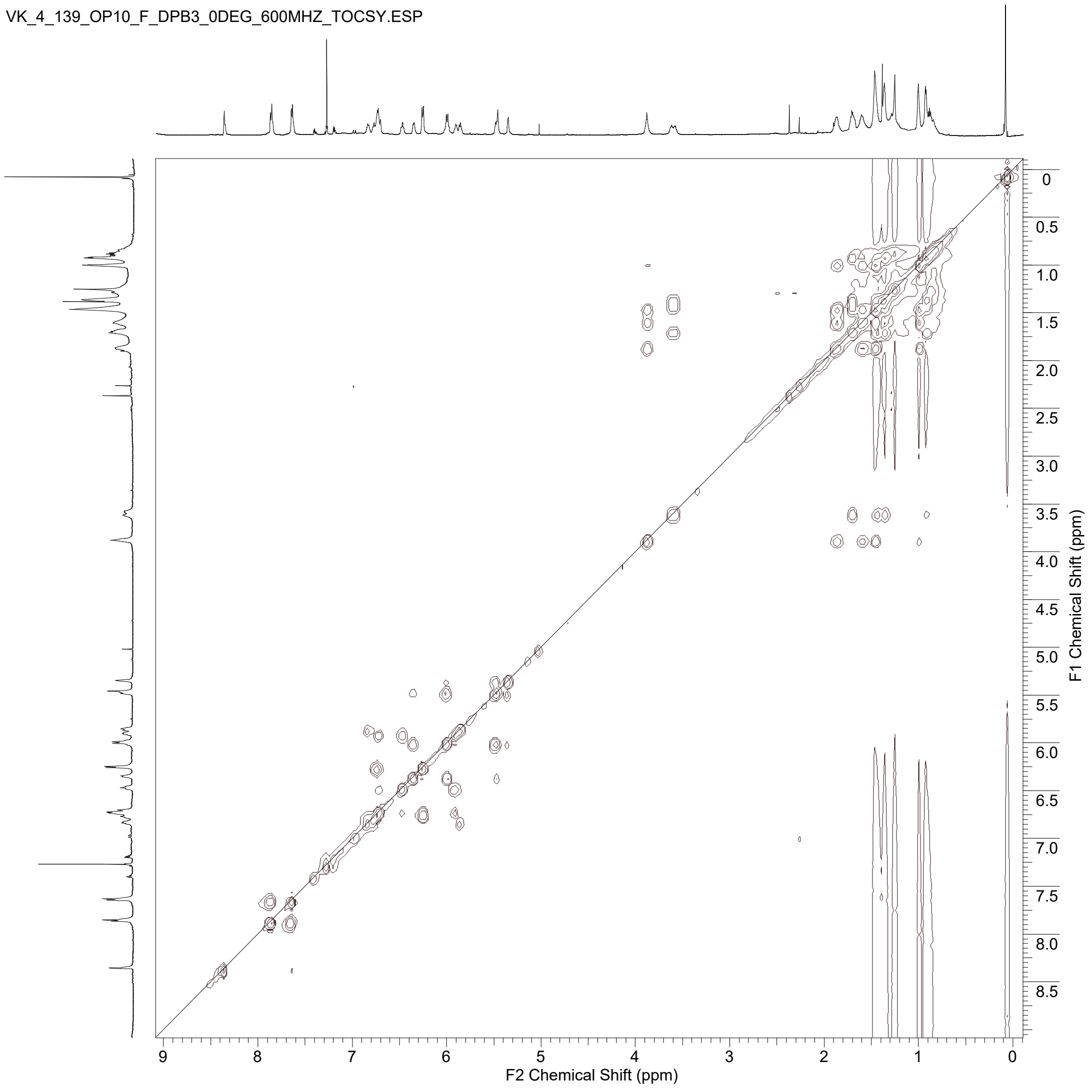

Figure S110. TOCSY NMR spectrum (600 MHz, $CDCl_3$, 0 ℃) of **oP^{10}F(DPB)$_{3+3}$**.

oP^{10}F(Phen)$_{3+3}$

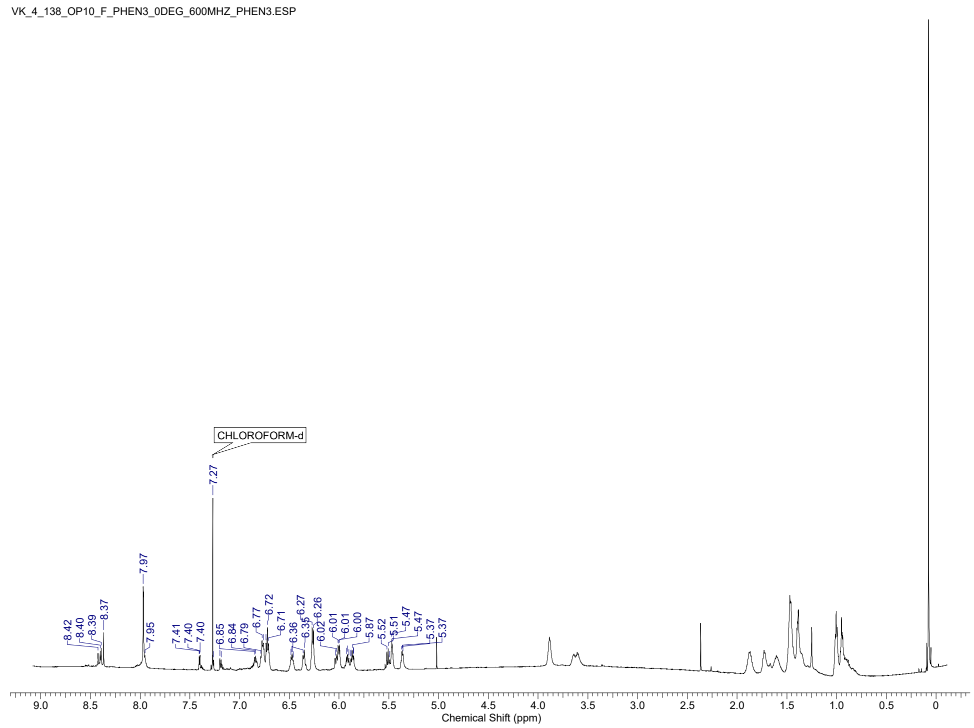

Figure S111. ^{1}H NMR spectrum (600 MHz, $CDCl_3$, 0 ℃) of **oP^{10}F(Phen)$_{3+3}$**.

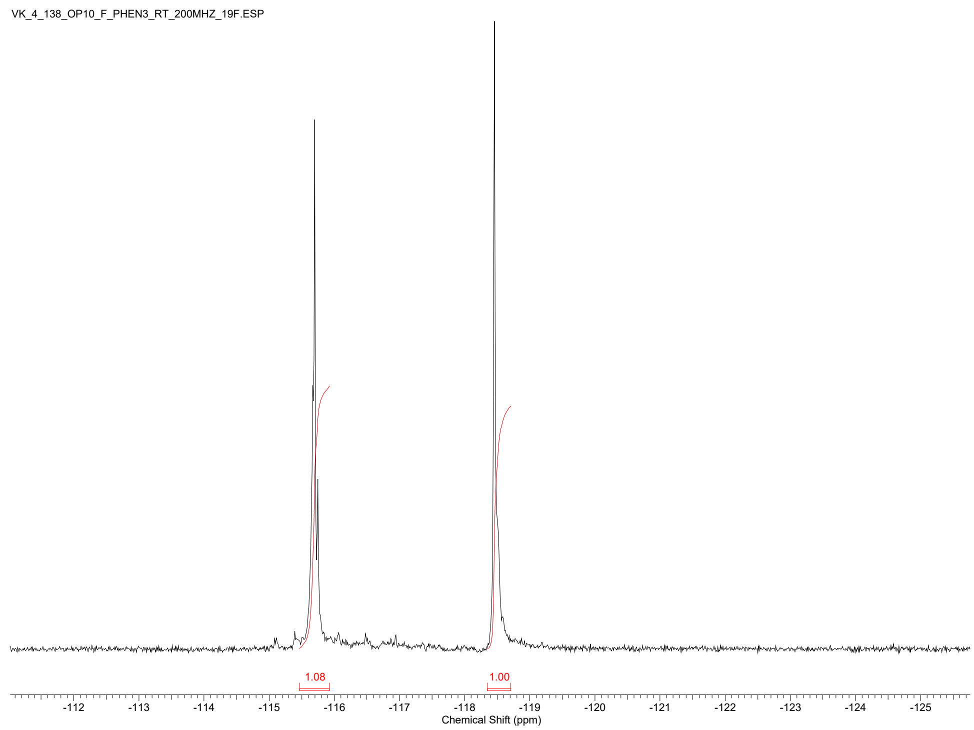

Figure S112. ^{19}F NMR spectrum (188 MHz, $CDCl_3$, 0 ℃) of **oP^{10}F(Phen)$_{3+3}$**.

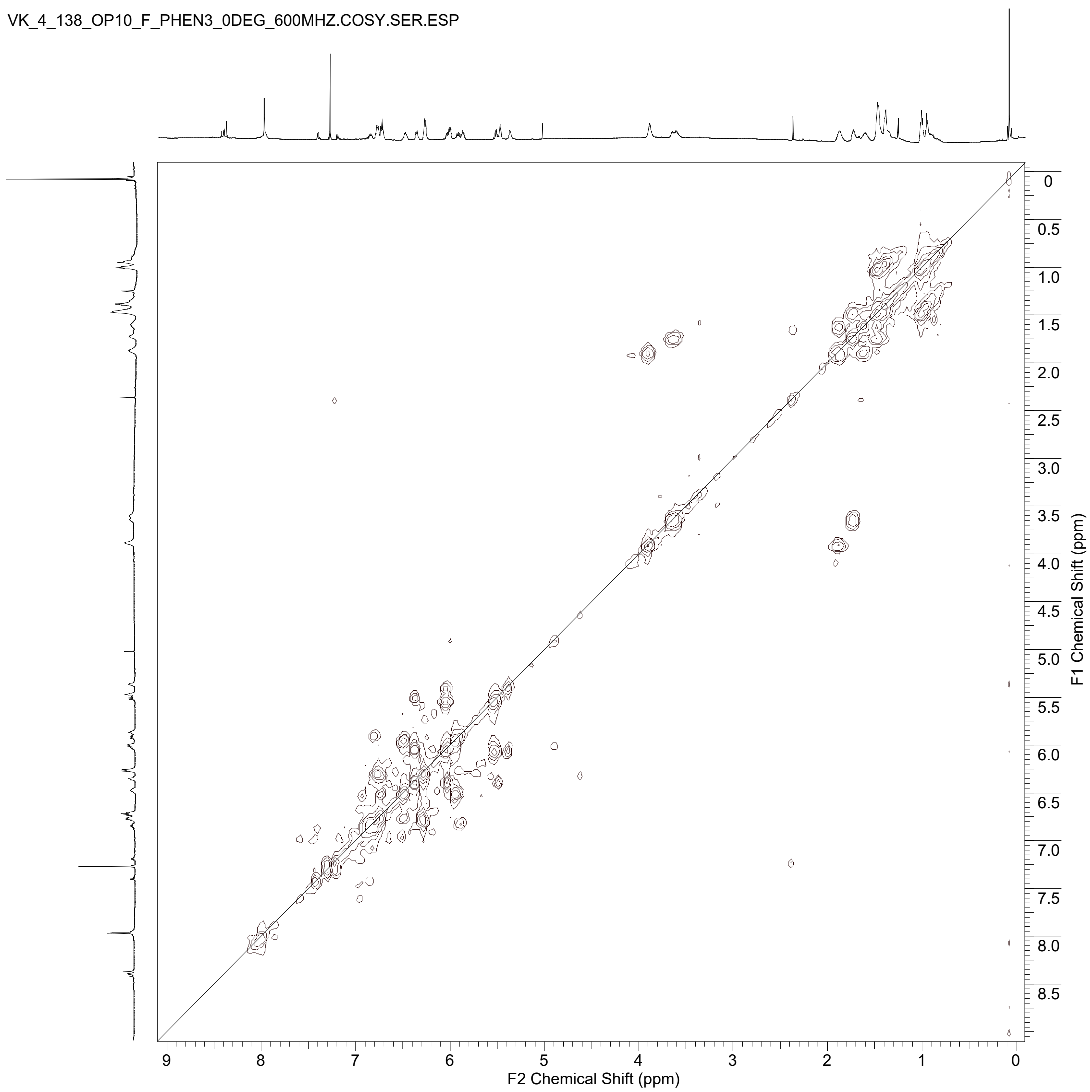

Figure S113. COSY NMR spectrum (600 MHz, $CDCl_3$, 0 ℃) of **oP^{10}F(Phen)$_{3+3}$**.

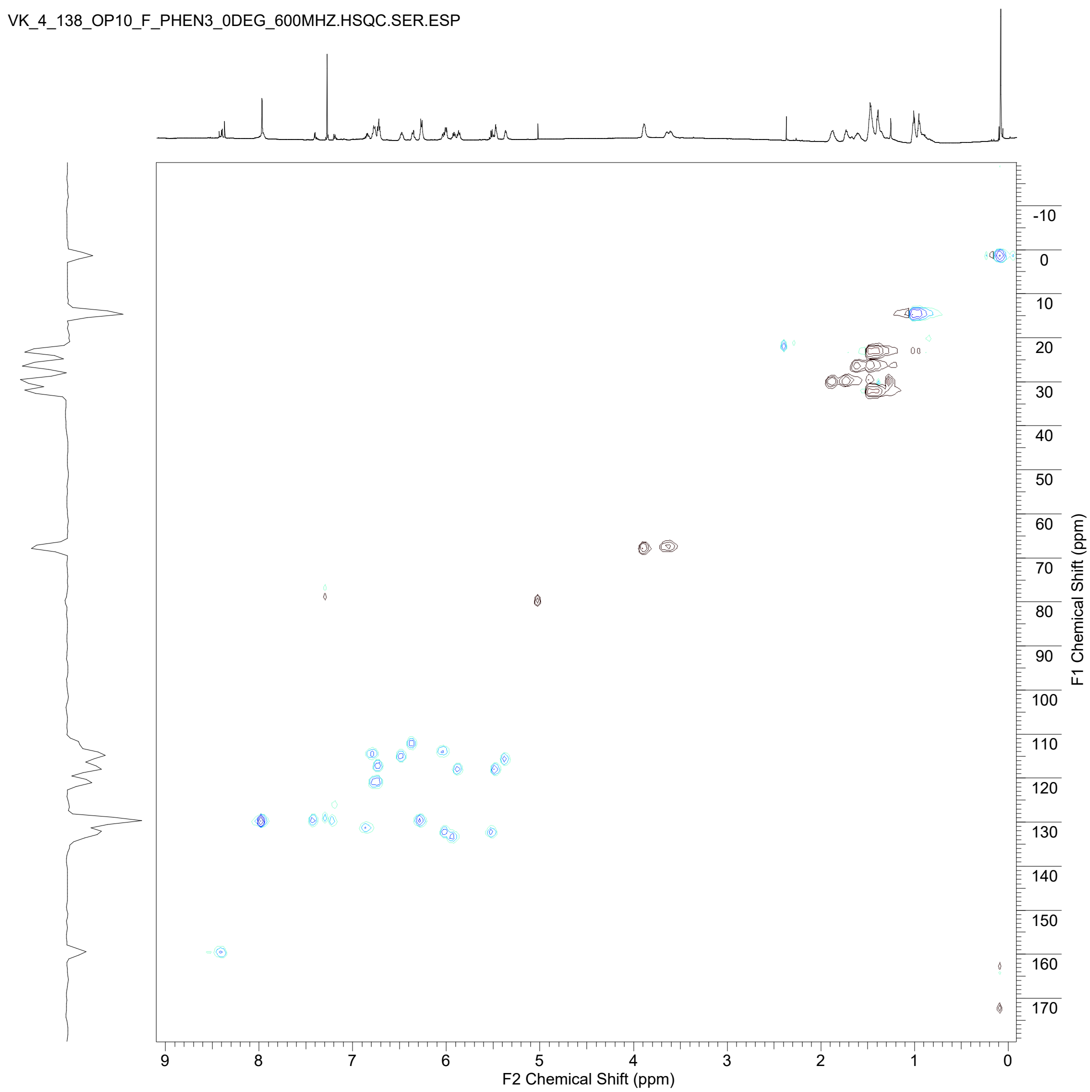

Figure S114. HSQC NMR spectrum (600 MHz, $CDCl_3$, 0 ℃) of **oP[10]F(Phen)$_{3+3}$**.

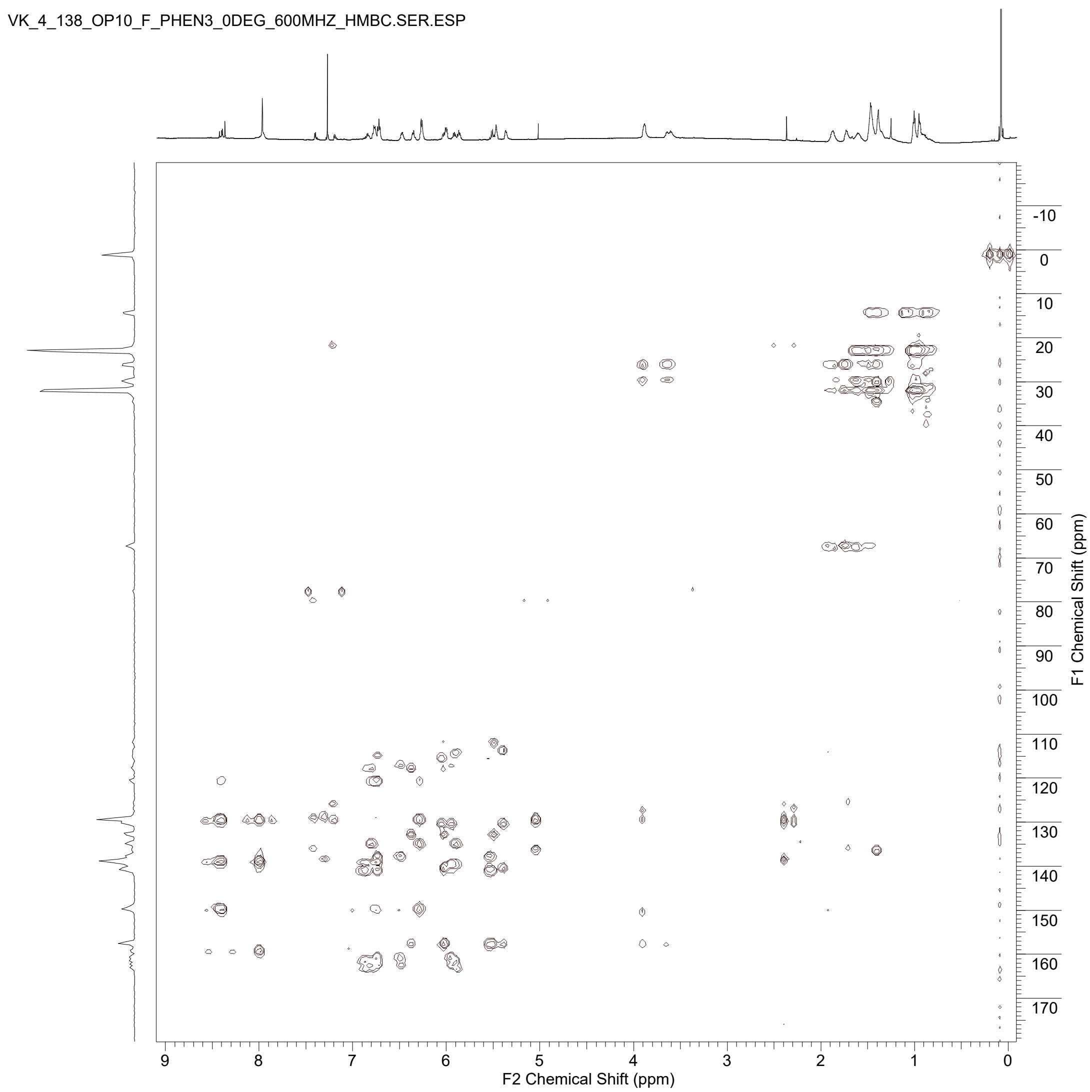

Figure S115. HMBC NMR spectrum (600 MHz, $CDCl_3$, 0 ℃) of **oP[10]F(Phen)$_{3+3}$**.

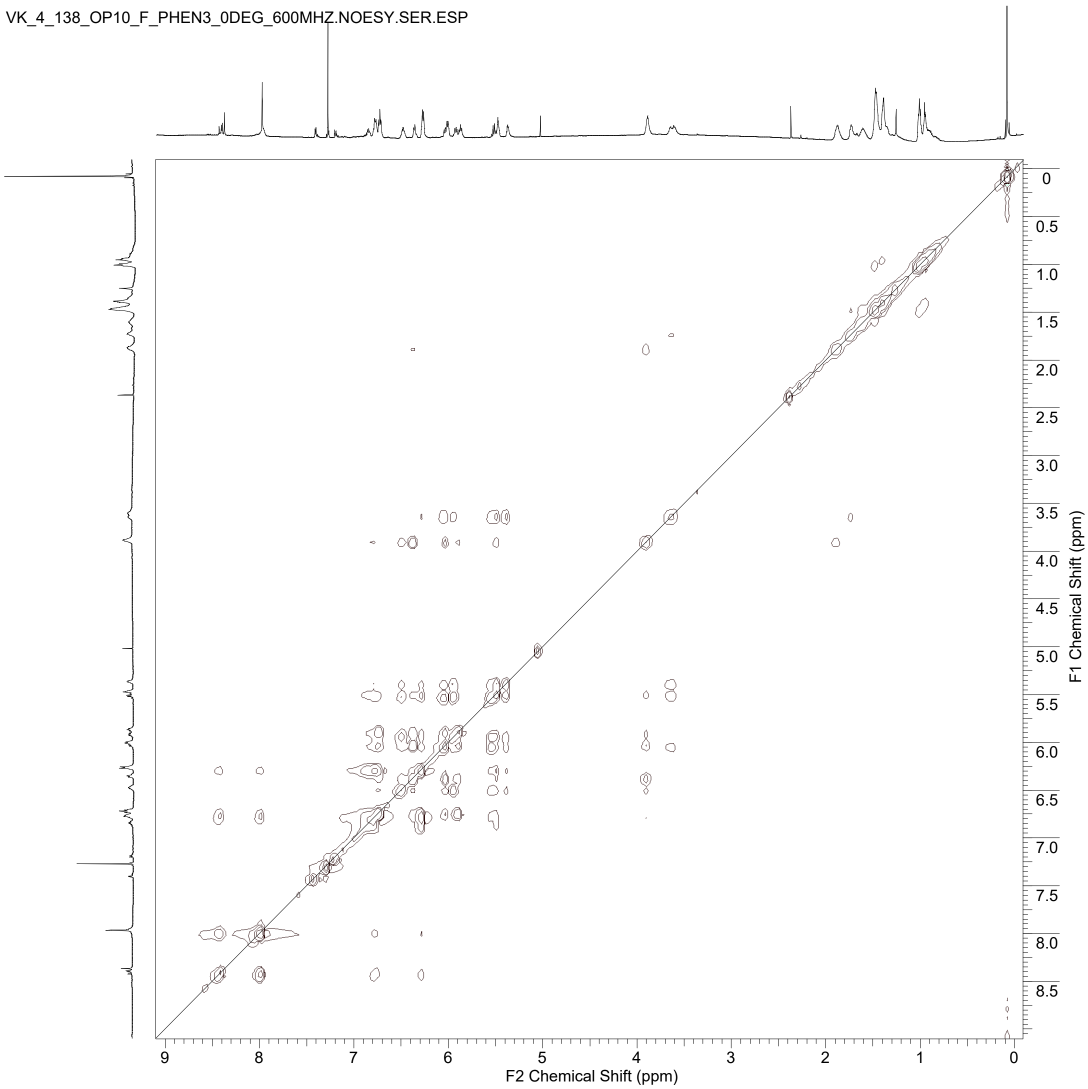

Figure S116. NOESY/EXSY NMR spectrum (600 MHz, $CDCl_3$, 0 ℃) of $\mathbf{oP^{10}F(Phen)_{3+3}}$.

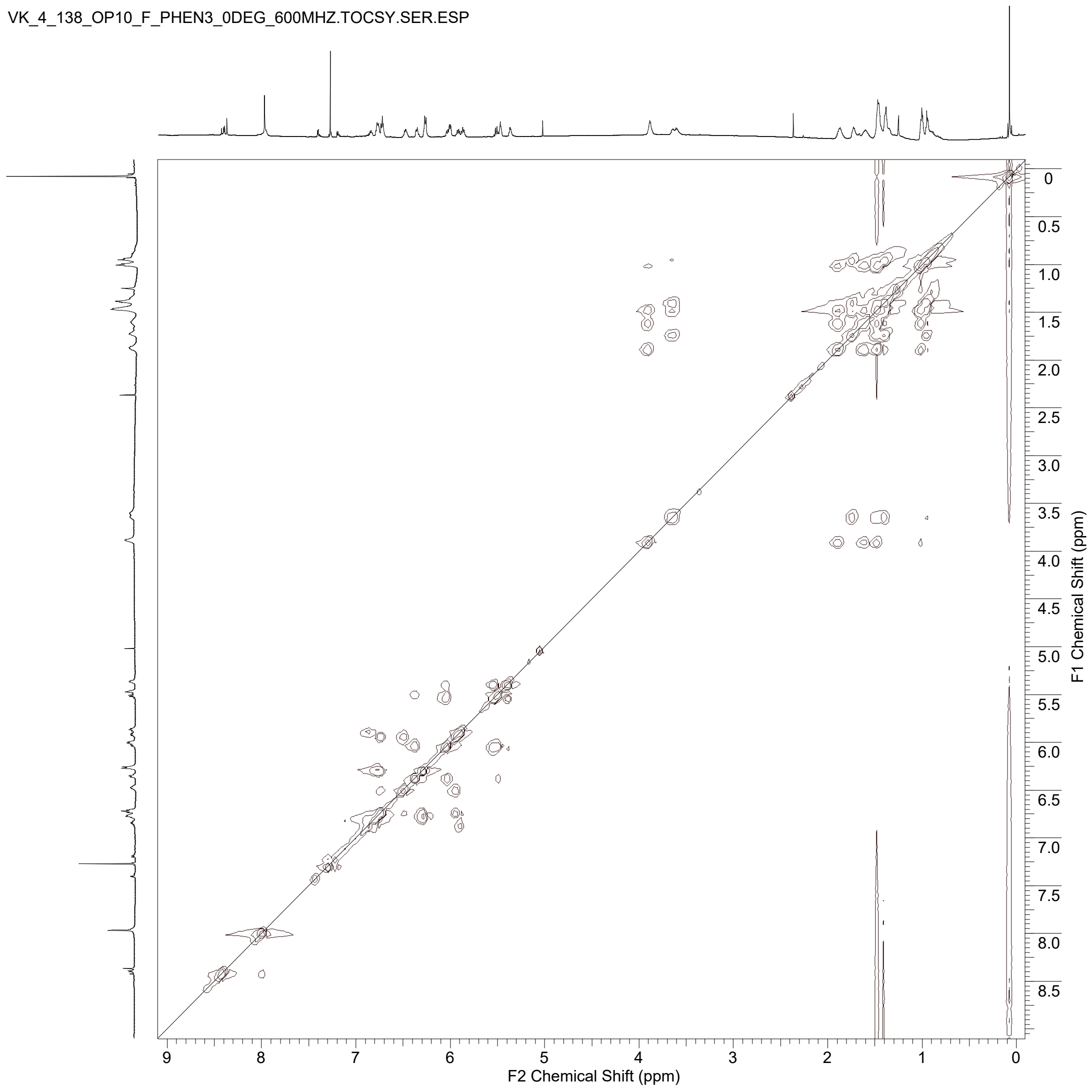

Figure S117. TOCSY NMR spectrum (600 MHz, $CDCl_3$, 0 ℃) of $\mathbf{oP^{10}F(Phen)_{3+3}}$.

oP^{10}OMe(DPB)$_{3+3}$

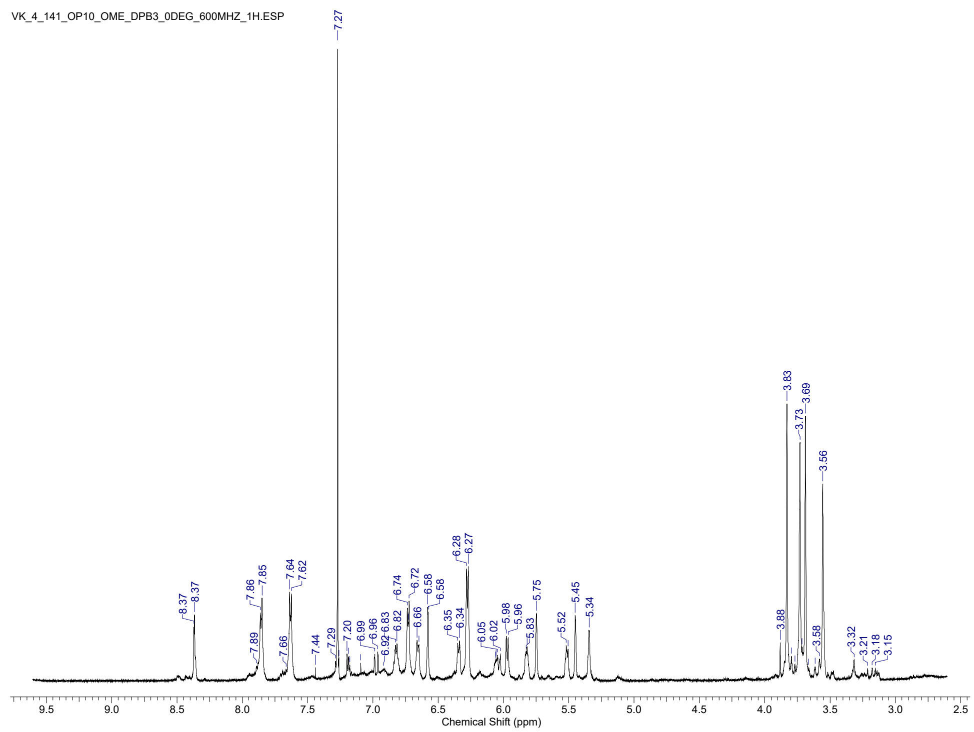

Figure S118. ^{1}H NMR spectrum (600 MHz, $CDCl_3$, 0 ℃) of **oP^{10}OMe(DPB)$_{3+3}$**.

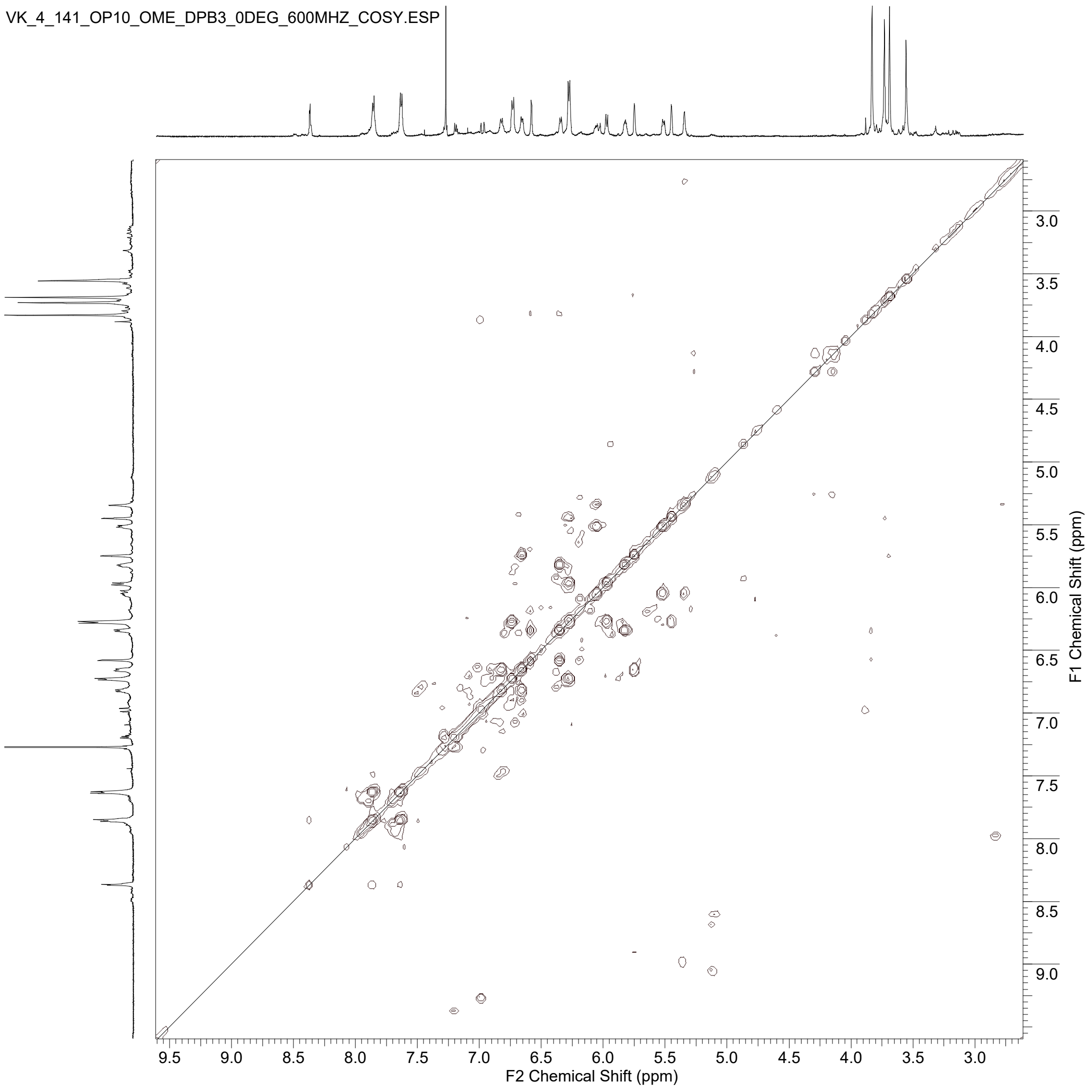

Figure S119. COSY NMR spectrum (600 MHz, $CDCl_3$, 0 ℃) of **oP^{10}OMe(DPB)$_{3+3}$**.

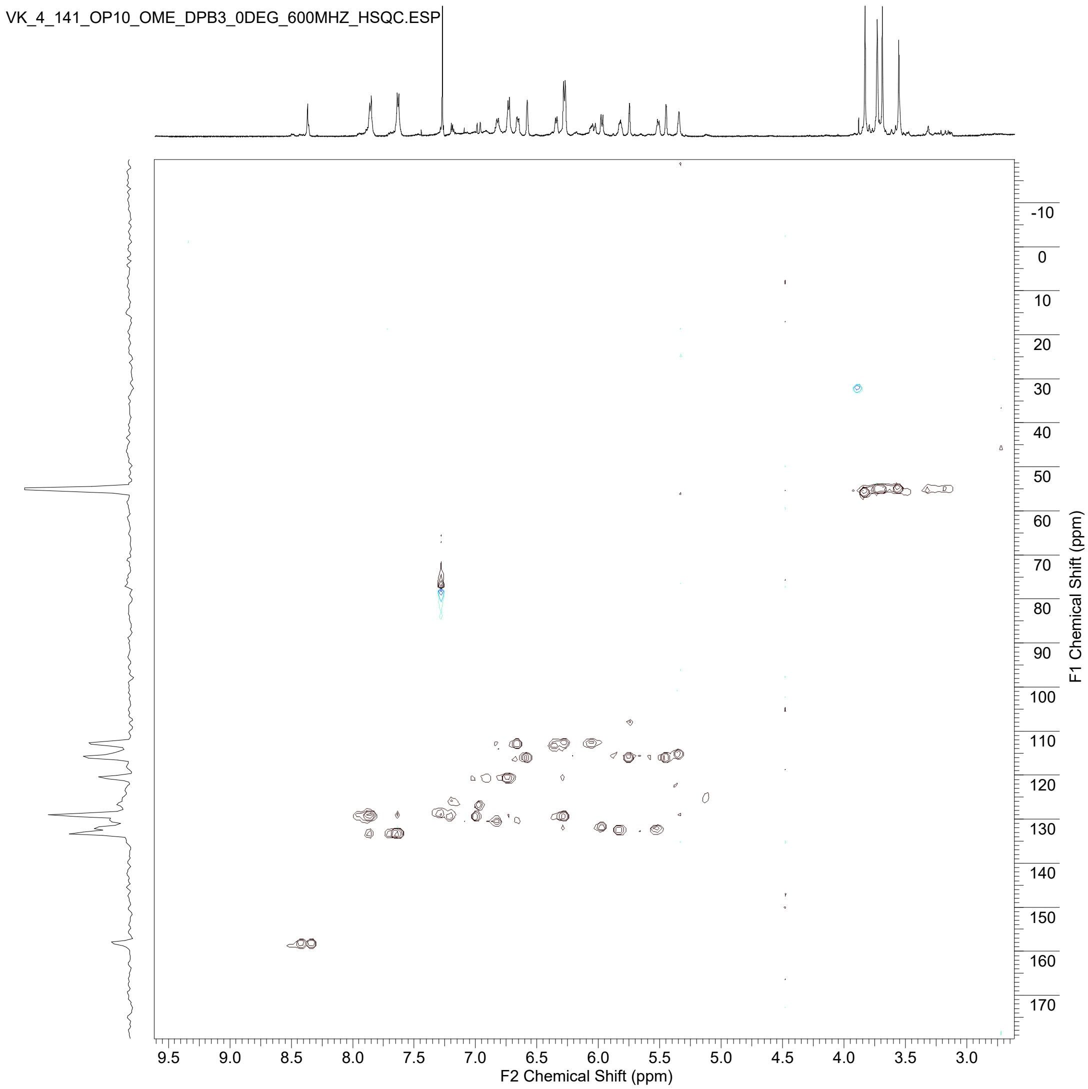

Figure S120. HSQC NMR spectrum (600 MHz, $CDCl_3$, 0 °C) of **$oP^{10}OMe(DPB)_{3+3}$**.

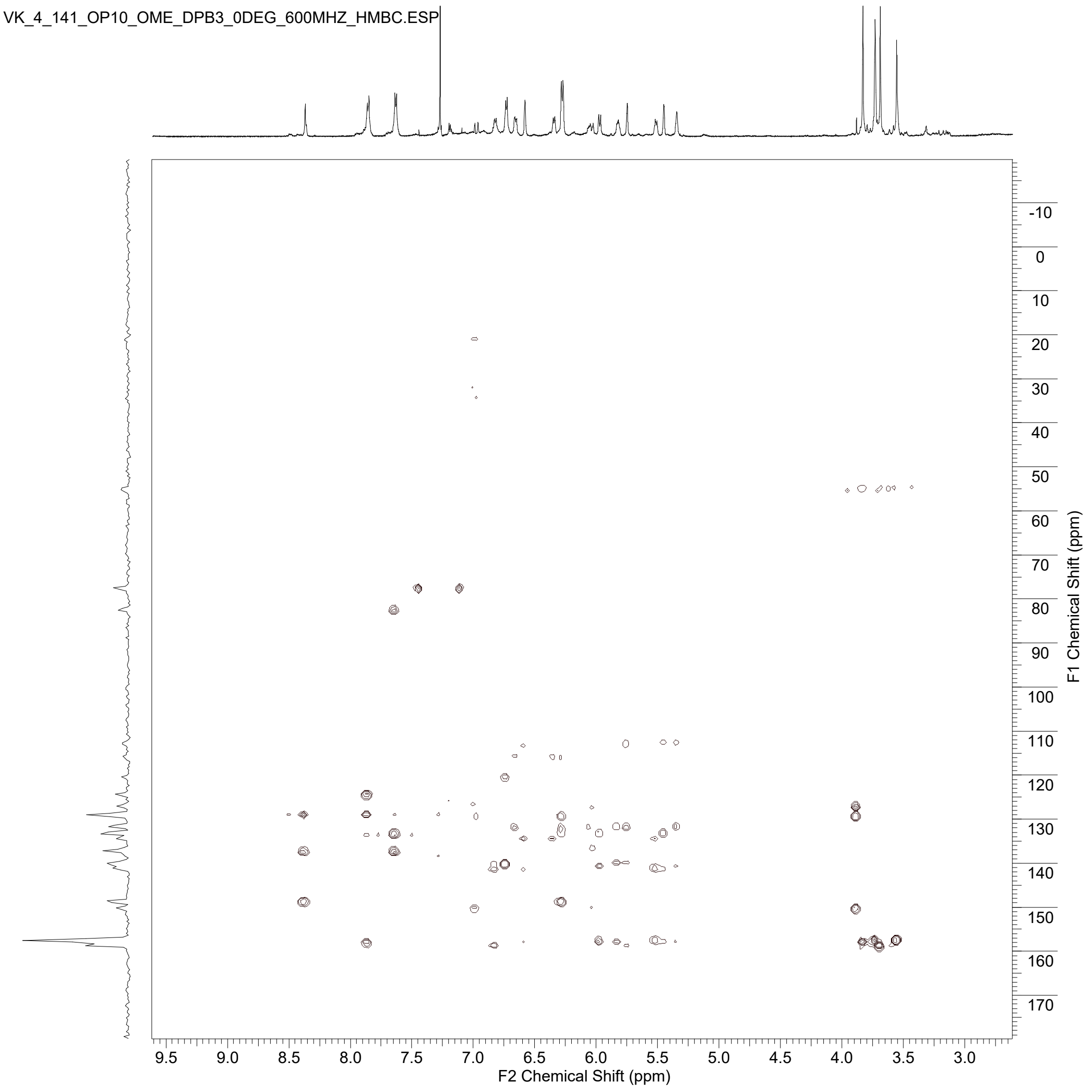

Figure S121. HMBC NMR spectrum (600 MHz, $CDCl_3$, 0 ℃) of **oP^{10}OMe(DPB)$_{3+3}$**.

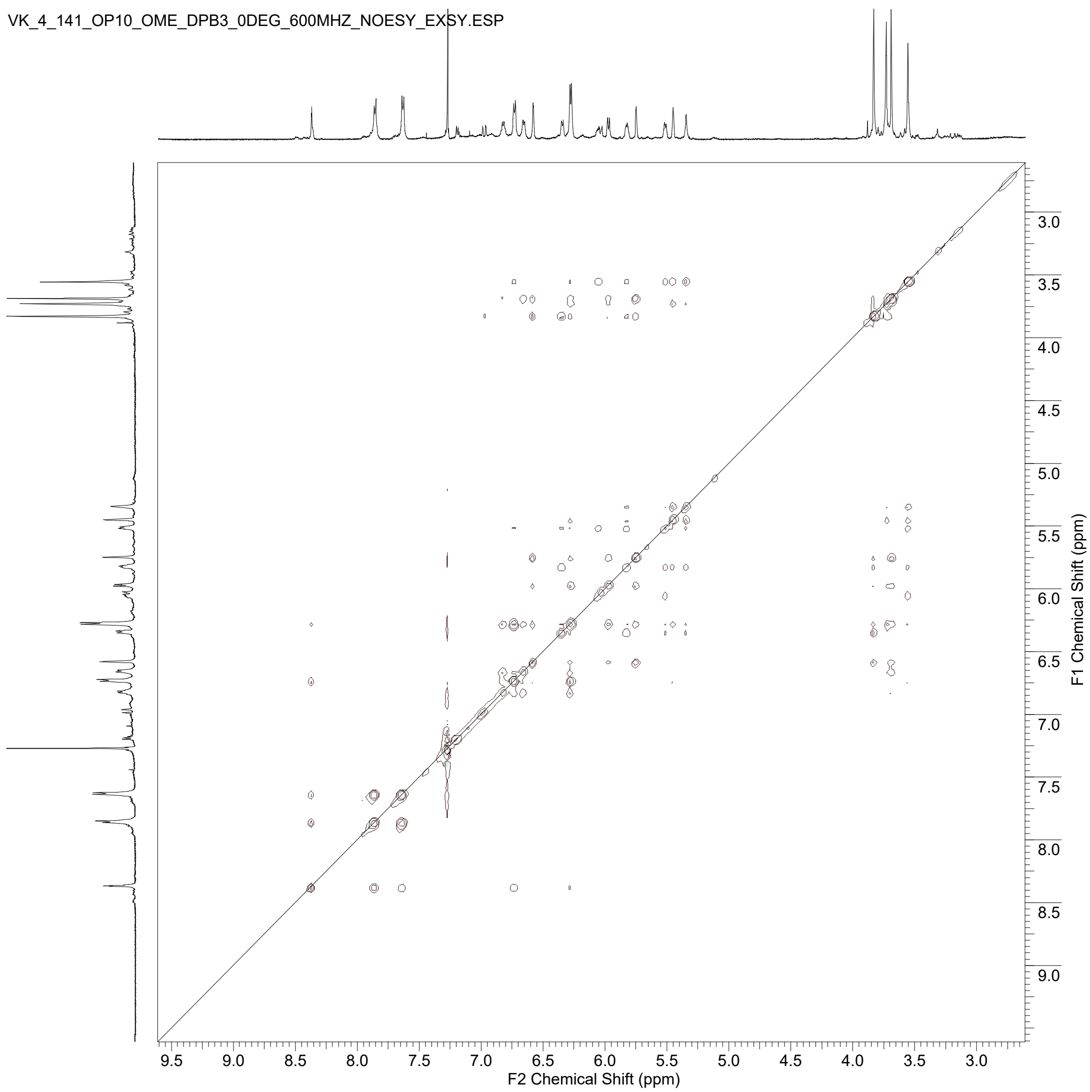

Figure S122. NOESY/EXSY NMR spectrum (600 MHz, $CDCl_3$, 0 ℃) of $\mathbf{oP^{10}OMe(DPB)_{3+3}}$.

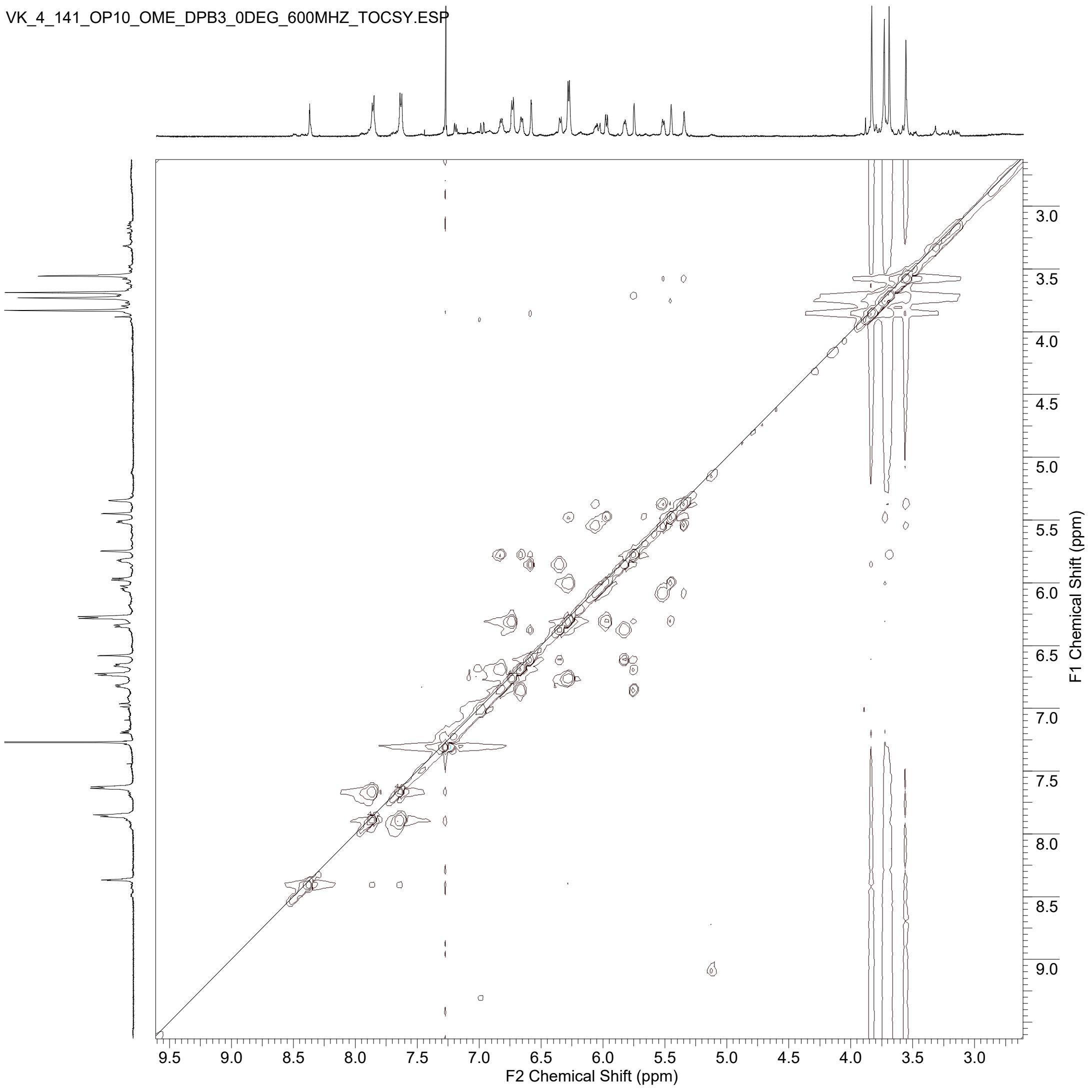

Figure S123. TOCSY NMR spectrum (600 MHz, $CDCl_3$, 0 ℃) of **oP[10]OMe(DPB)$_{3+3}$**.

oP^{10}OMe(DPB)$_{2+2}$

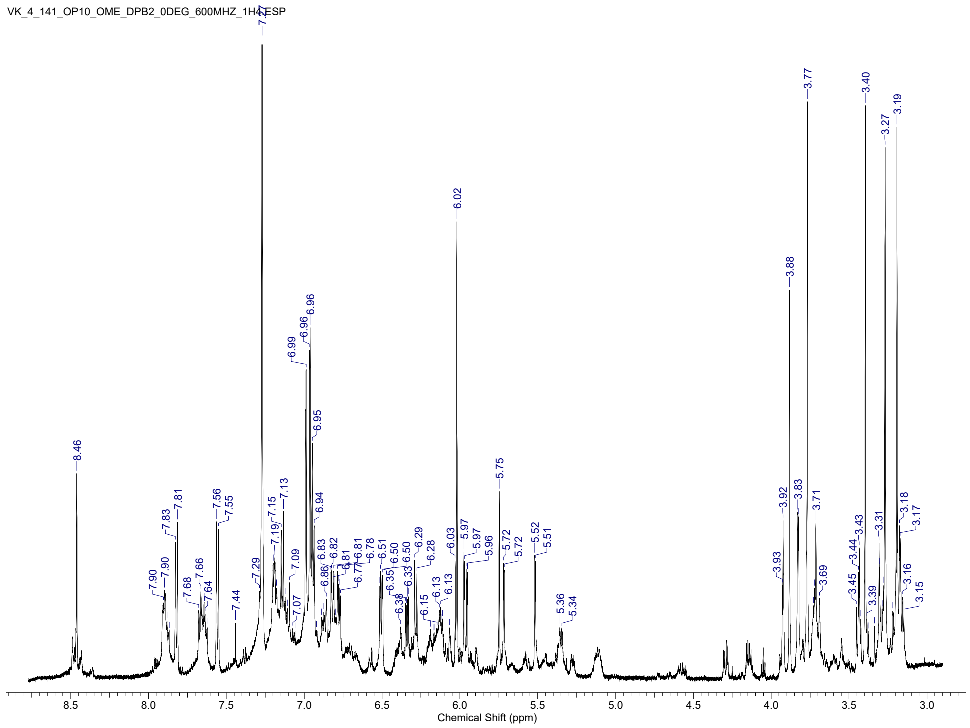

Figure S124. ^{1}H NMR spectrum (600 MHz, $CDCl_3$, 0 ℃) of **oP^{10}OMe(DPB)$_{2+2}$**.

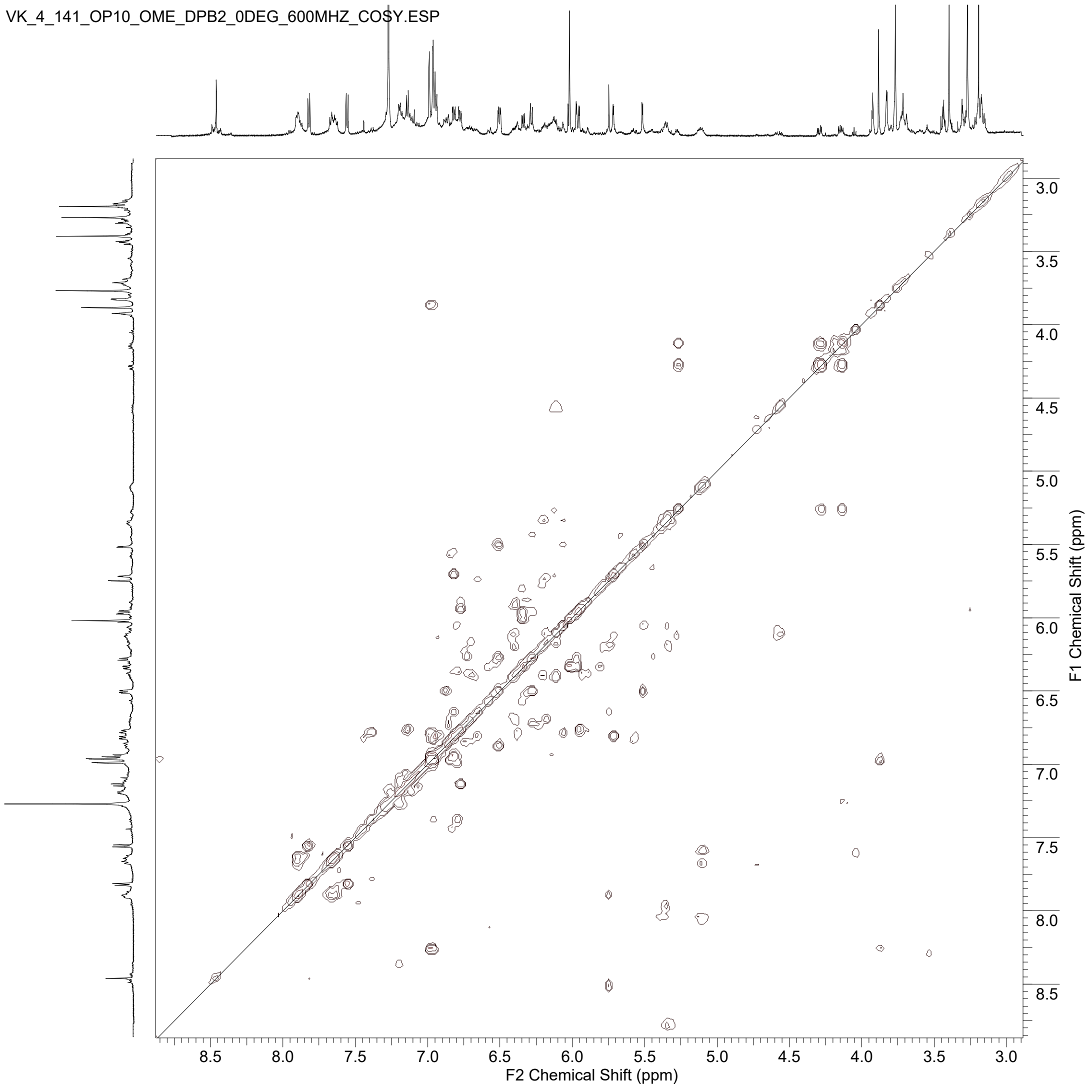

Figure S125. COSY NMR spectrum (600 MHz, $CDCl_3$, 0 ℃) of $\mathbf{oP^{10}OMe(DPB)_{2+2}}$.

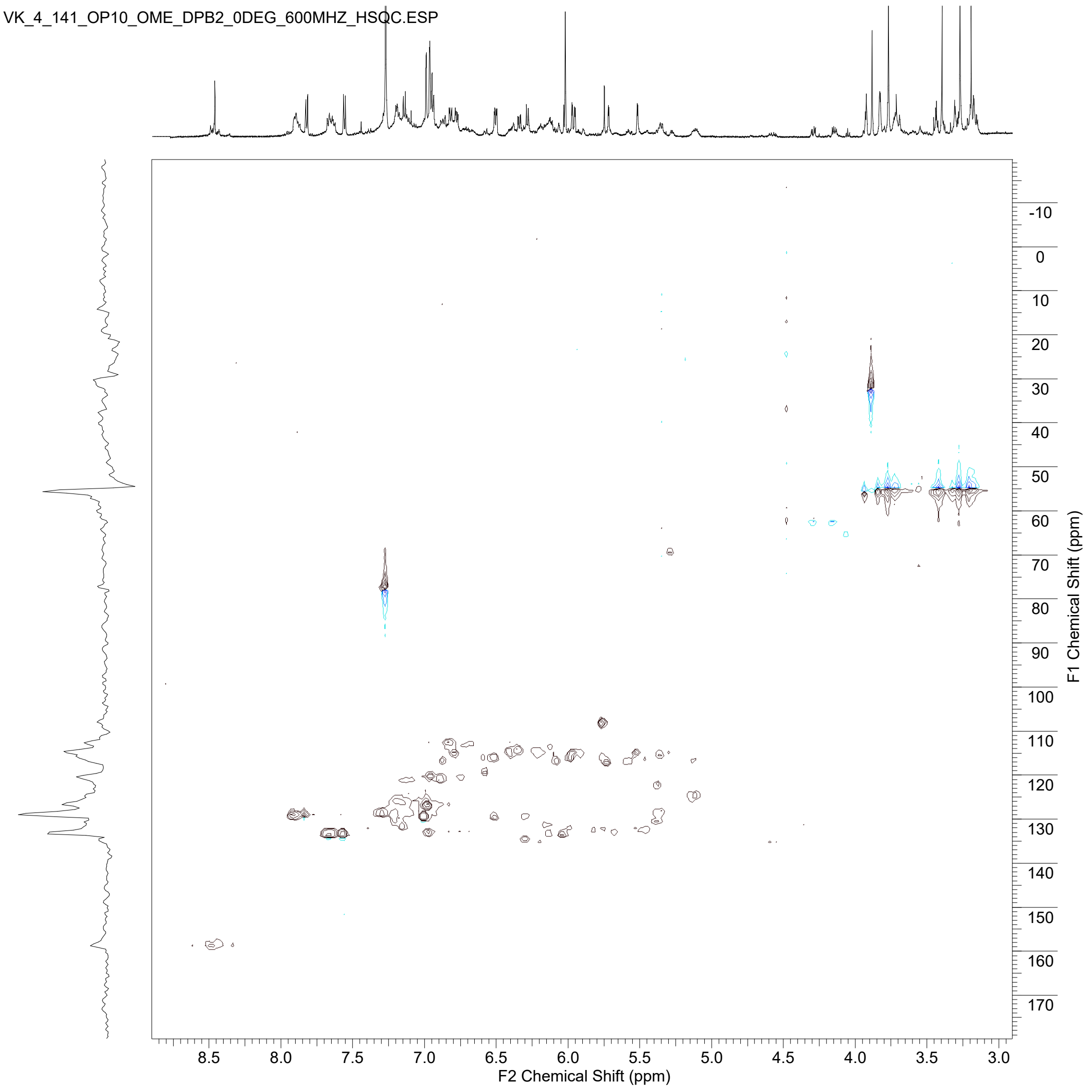

Figure S126. HSQC NMR spectrum (600 MHz, $CDCl_3$, 0 ℃) of **oP^{10}OMe(DPB)$_{2+2}$**.

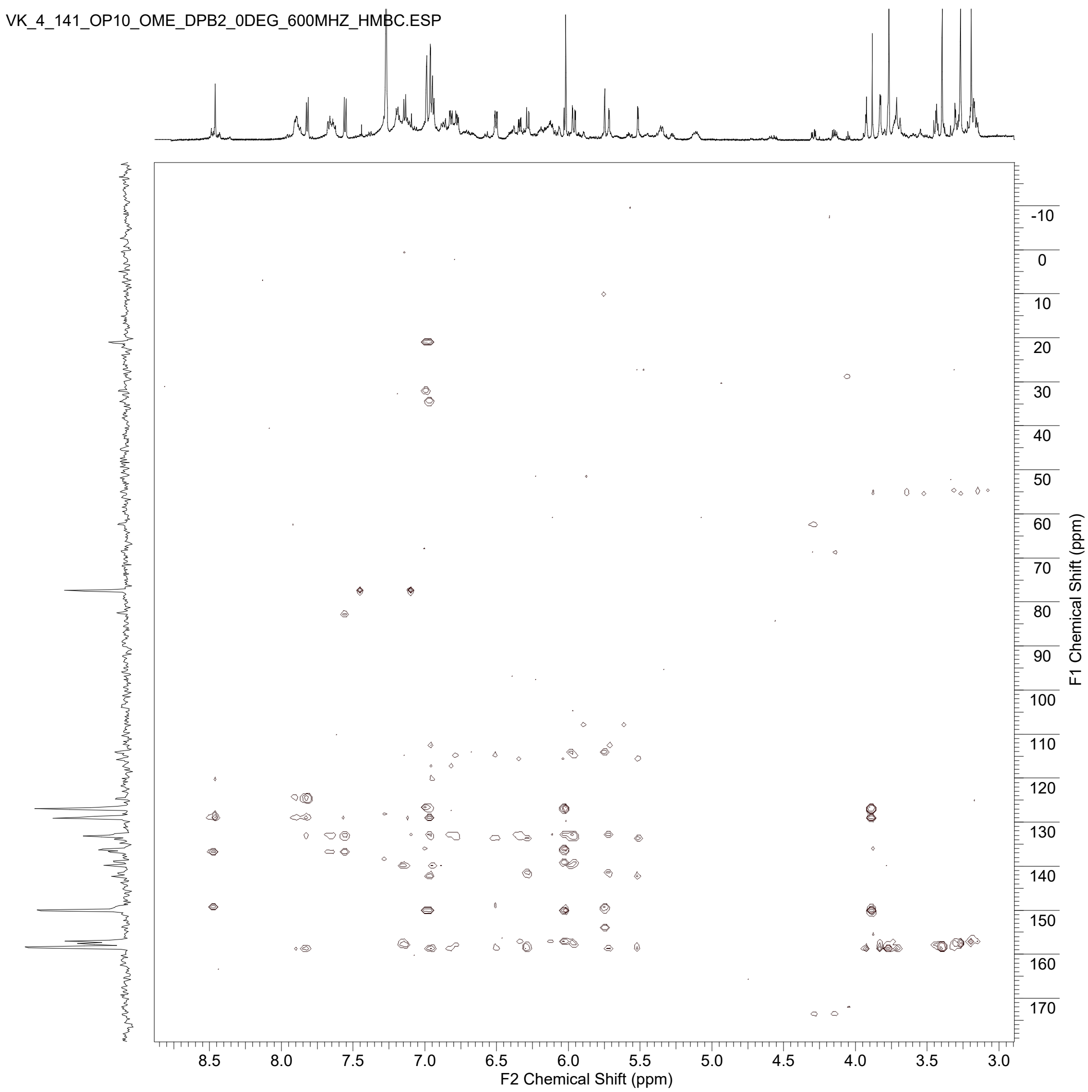

Figure S127. HMBC NMR spectrum (600 MHz, $CDCl_3$, 0 ℃) of **oP^{10}OMe(DPB)$_{2+2}$**.

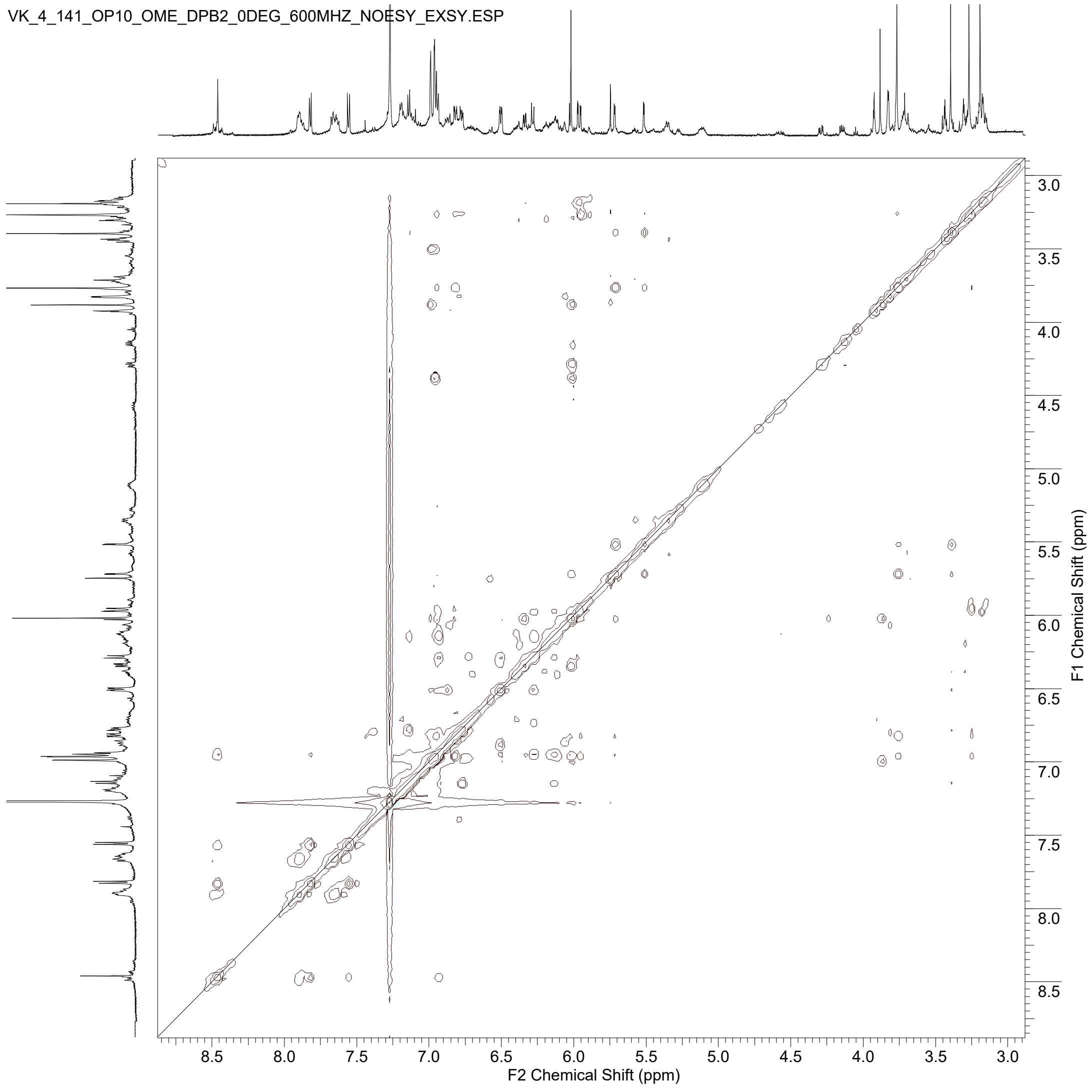

Figure S128. NOESY/EXSY NMR spectrum (600 MHz, $CDCl_3$, 0 ℃) of $\mathbf{oP^{10}OMe(DPB)_{2+2}}$.

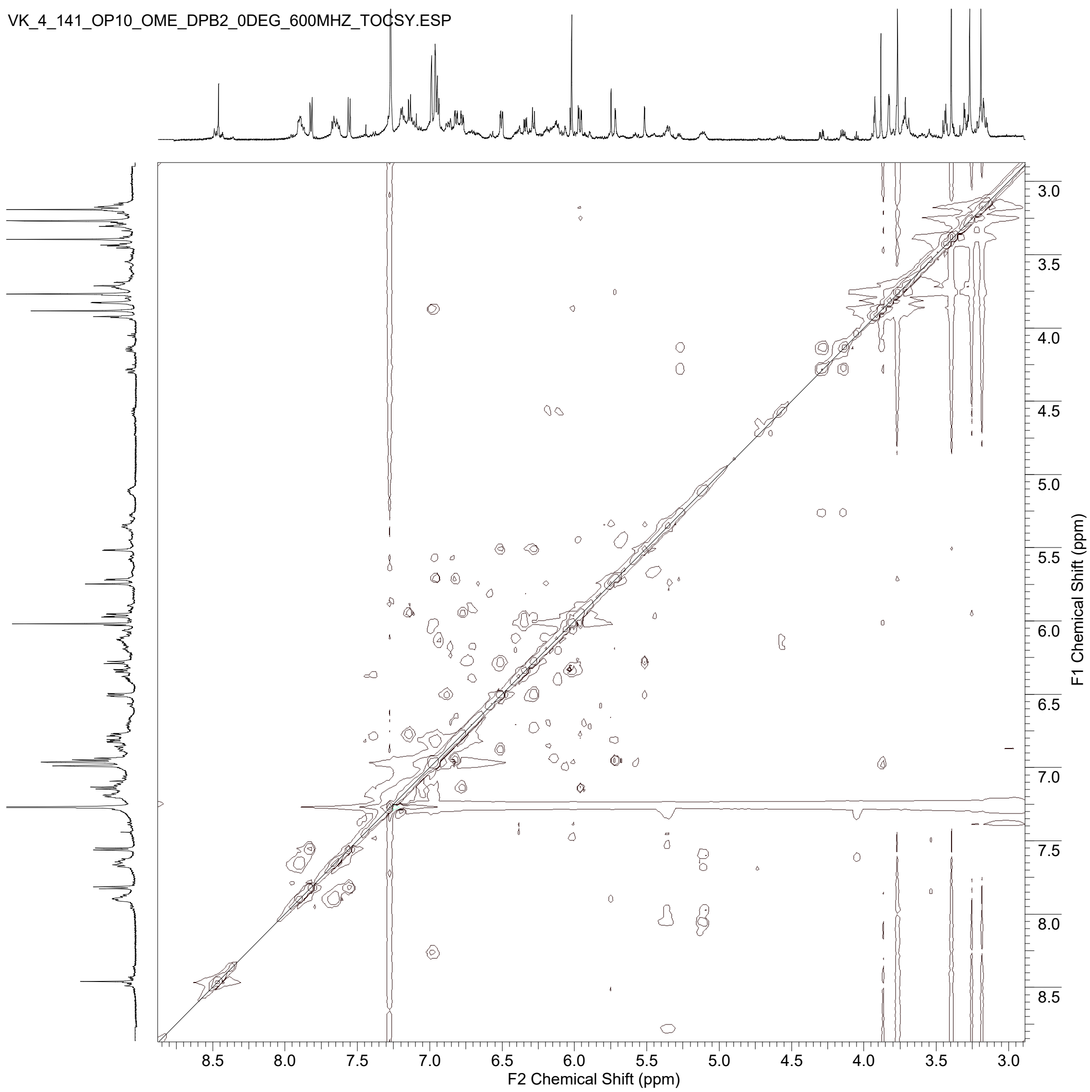

Figure S129. TOCSY NMR spectrum (600 MHz, $CDCl_3$, 0 ℃) of **$oP^{10}OMe(DPB)_{2+2}$**.

oP^{10}OMe(Phen)$_{3+3}$

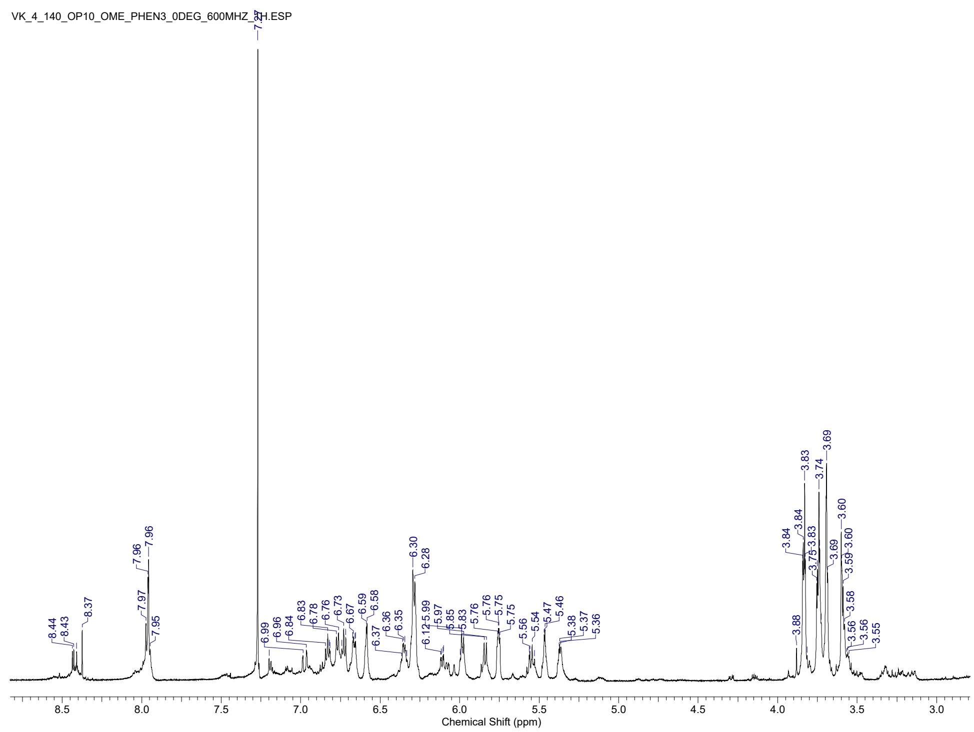

Figure S130. ^{1}H NMR spectrum (600 MHz, $CDCl_3$, 0 ℃) of **oP^{10}OMe(Phen)$_{3+3}$**.

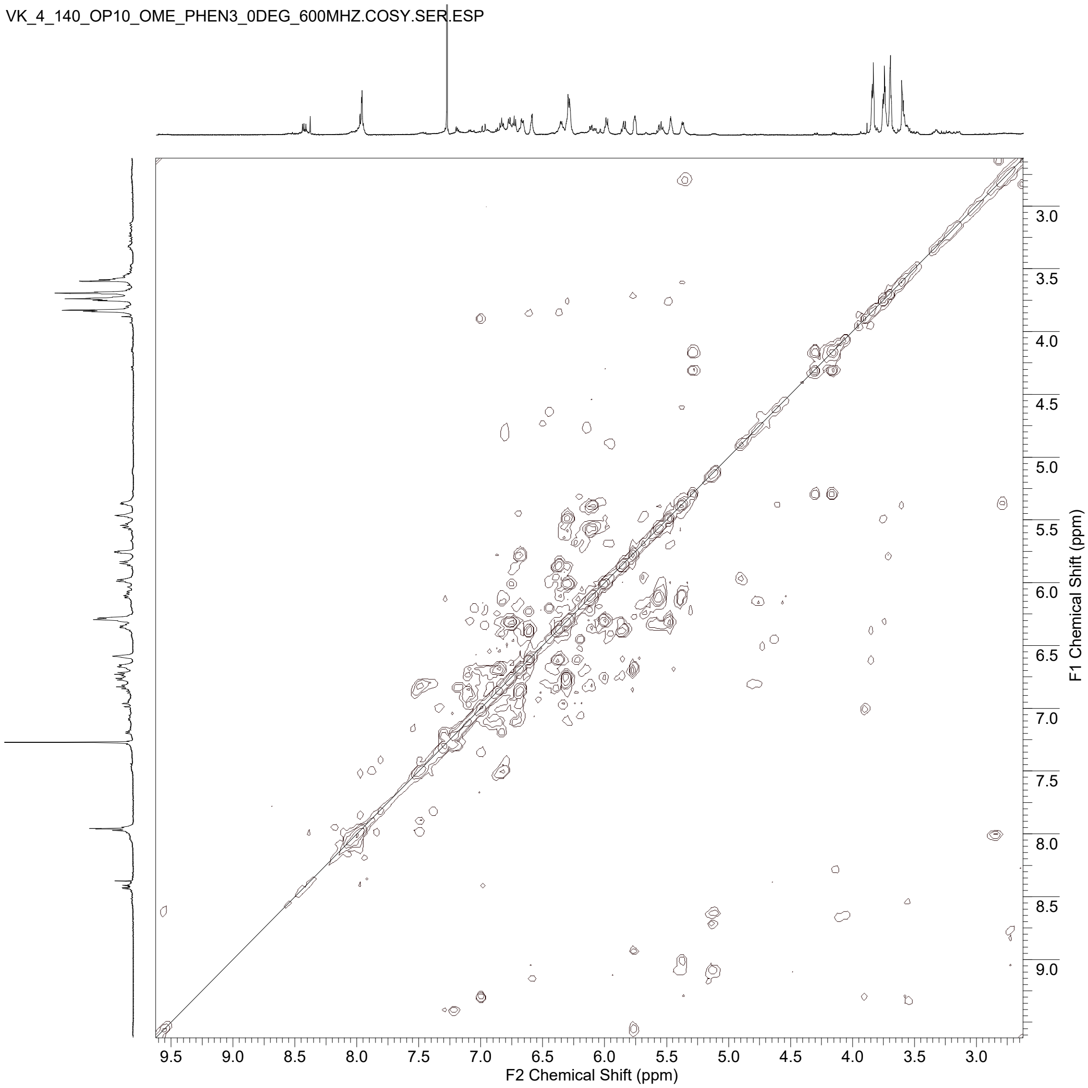

Figure S131. COSY NMR spectrum (600 MHz, $CDCl_3$, 0 ℃) of **oP^{10}OMe(Phen)$_{3+3}$**.

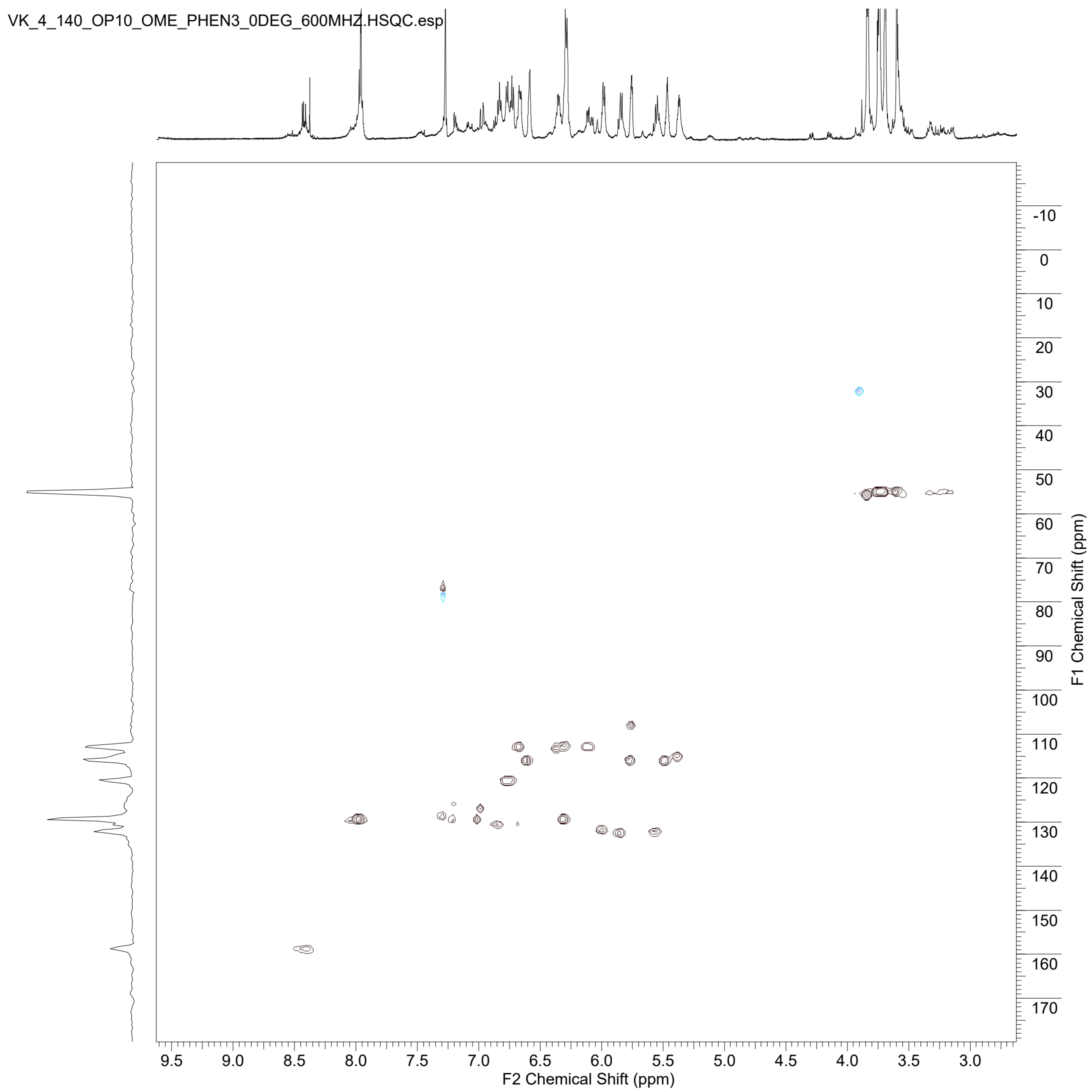

Figure S132. HSQC NMR spectrum (600 MHz, $CDCl_3$, 0 ℃) of $\mathbf{oP^{10}OMe(Phen)_{3+3}}$.

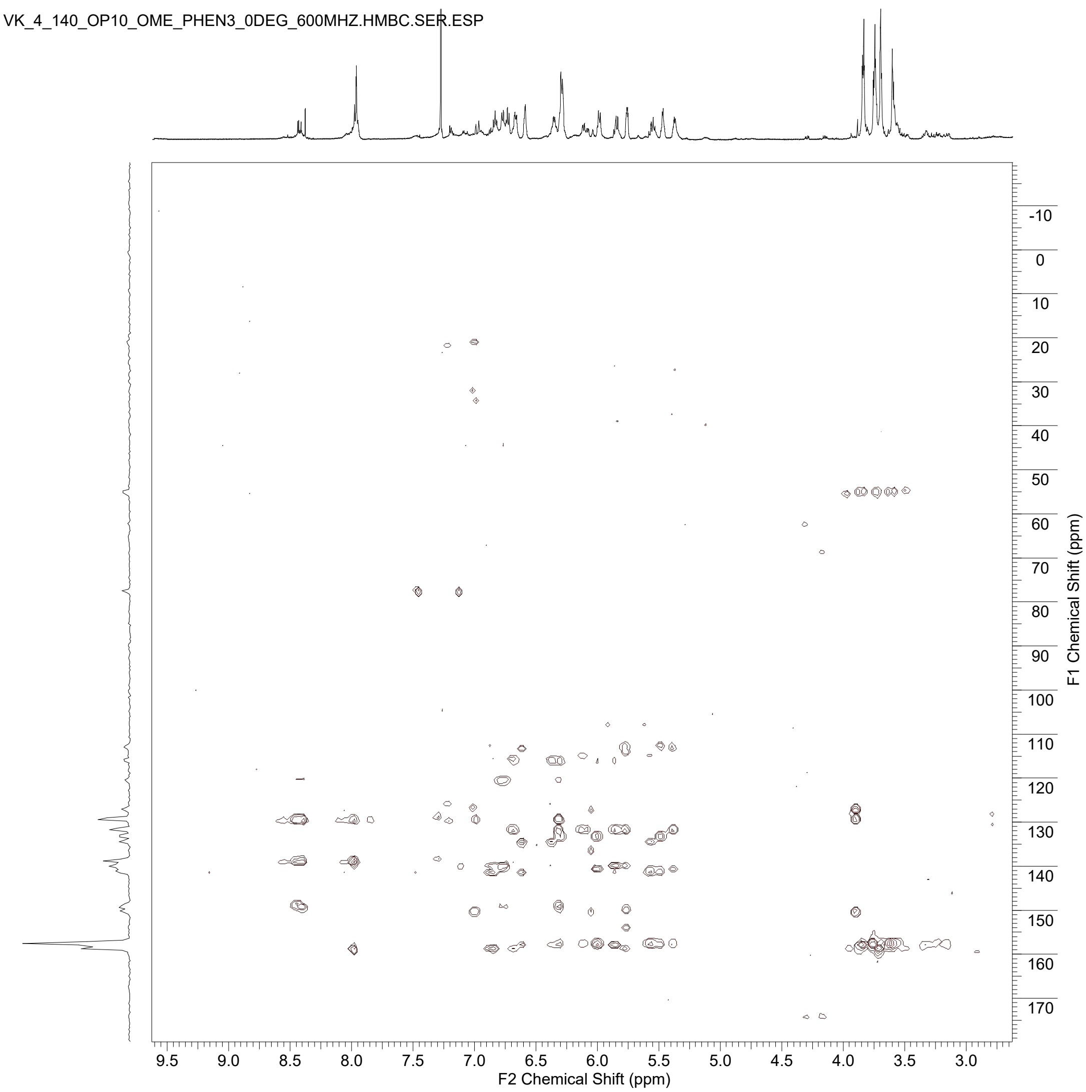

Figure S133. HMBC NMR spectrum (600 MHz, $CDCl_3$, 0 ℃) of **oP^{10}OMe(Phen)$_{3+3}$**.

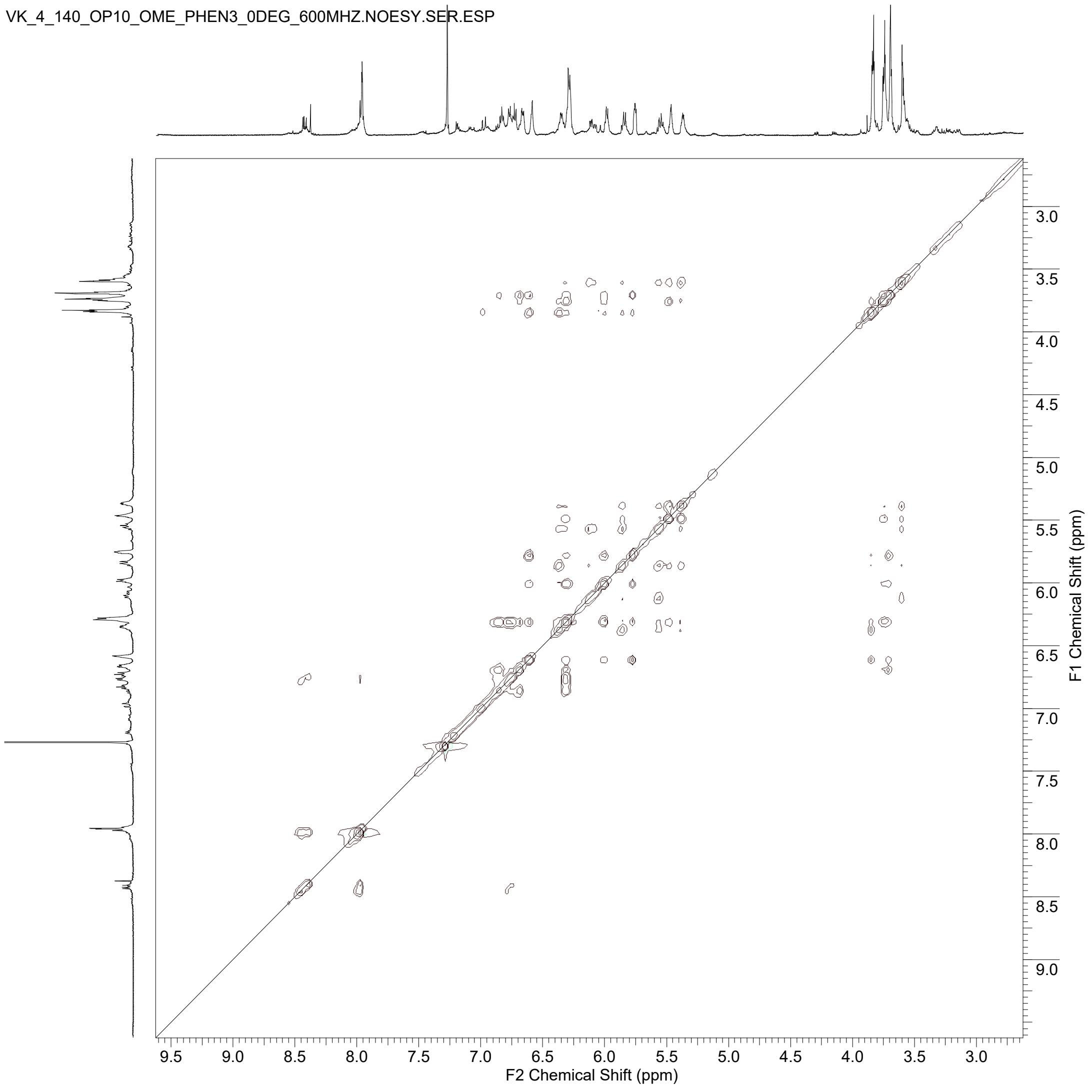

Figure S134. NOESY/EXSY NMR spectrum (600 MHz, $CDCl_3$, 0 ℃) of **$oP^{10}OMe(Phen)_{3+3}$**.

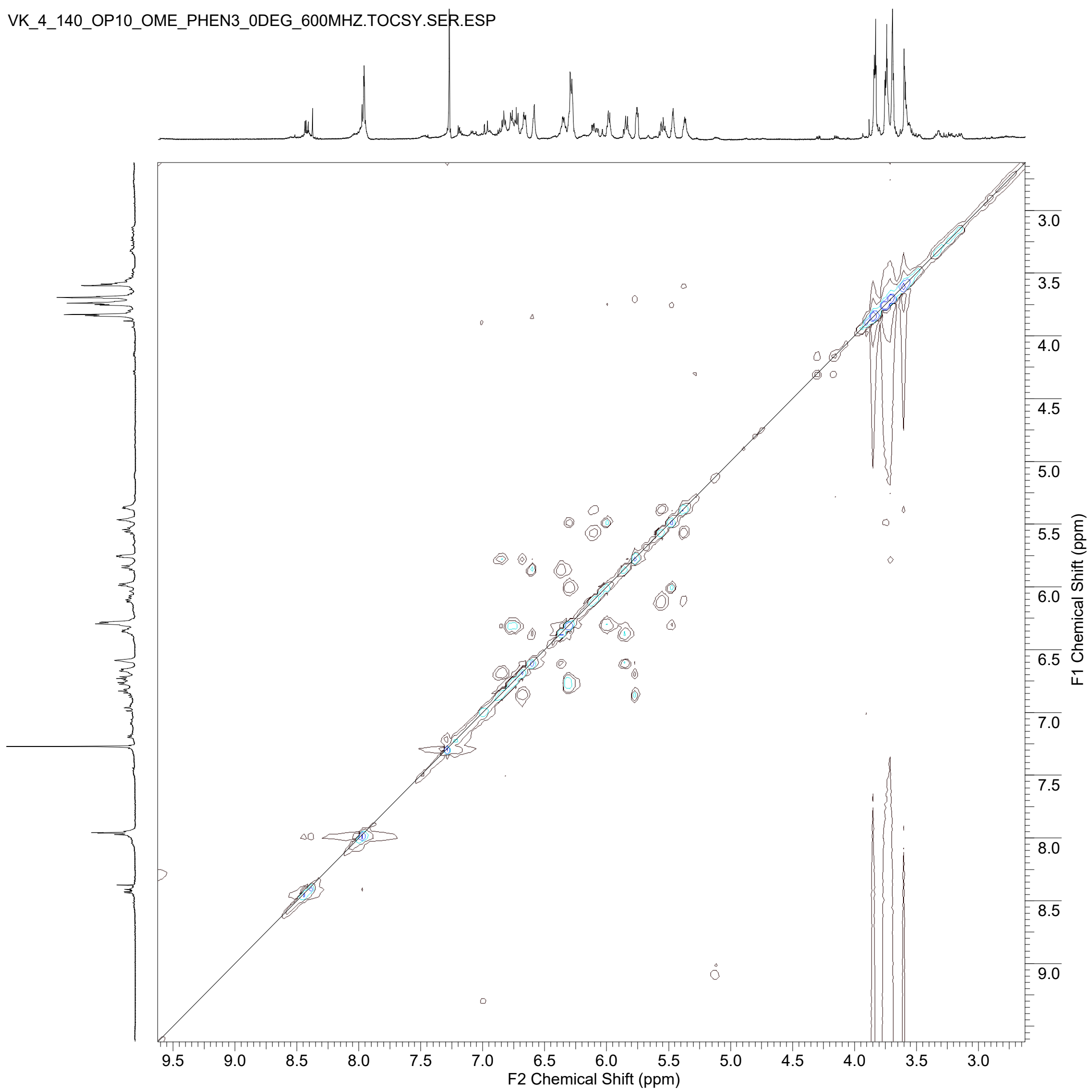

Figure S135. TOCSY NMR spectrum (600 MHz, $CDCl_3$, 0 ℃) of $\mathbf{oP^{10}OMe(Phen)_{3+3}}$.

oP¹⁰OMe(Phen)$_{2+2}$

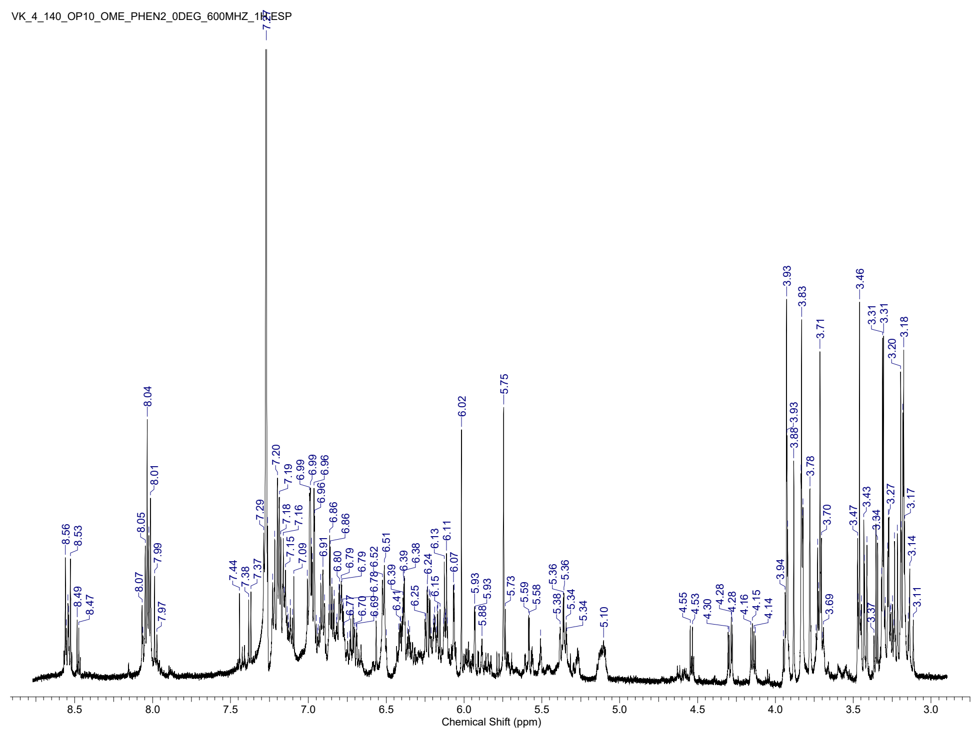

Figure S136. ^{1}H NMR spectrum (600 MHz, $CDCl_3$, 0 ℃) of **oP¹⁰OMe(Phen)$_{2+2}$**.

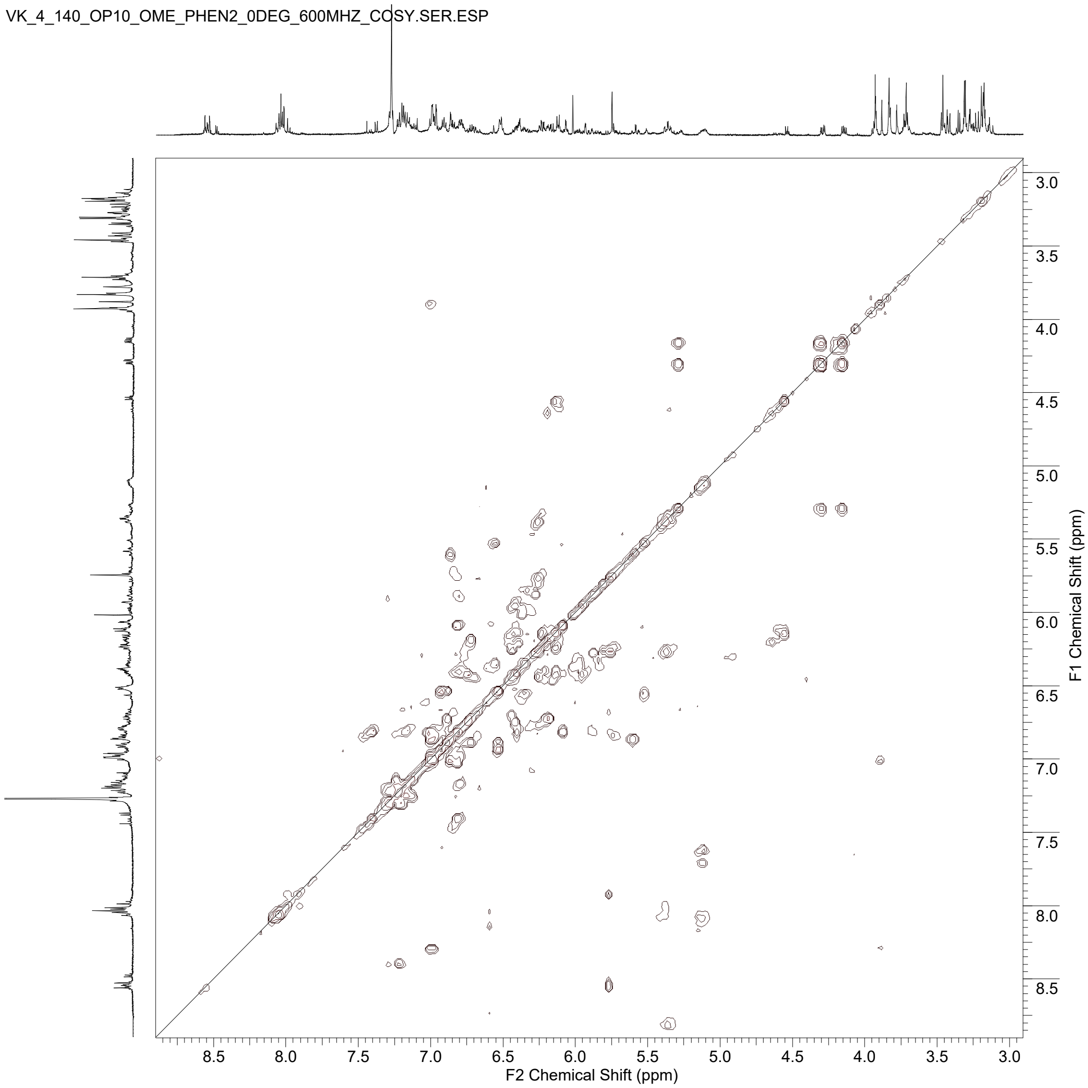

Figure S137. COSY NMR spectrum (600 MHz, $CDCl_3$, 0 ℃) of **oP^{10}OMe(Phen)$_{2+2}$**.

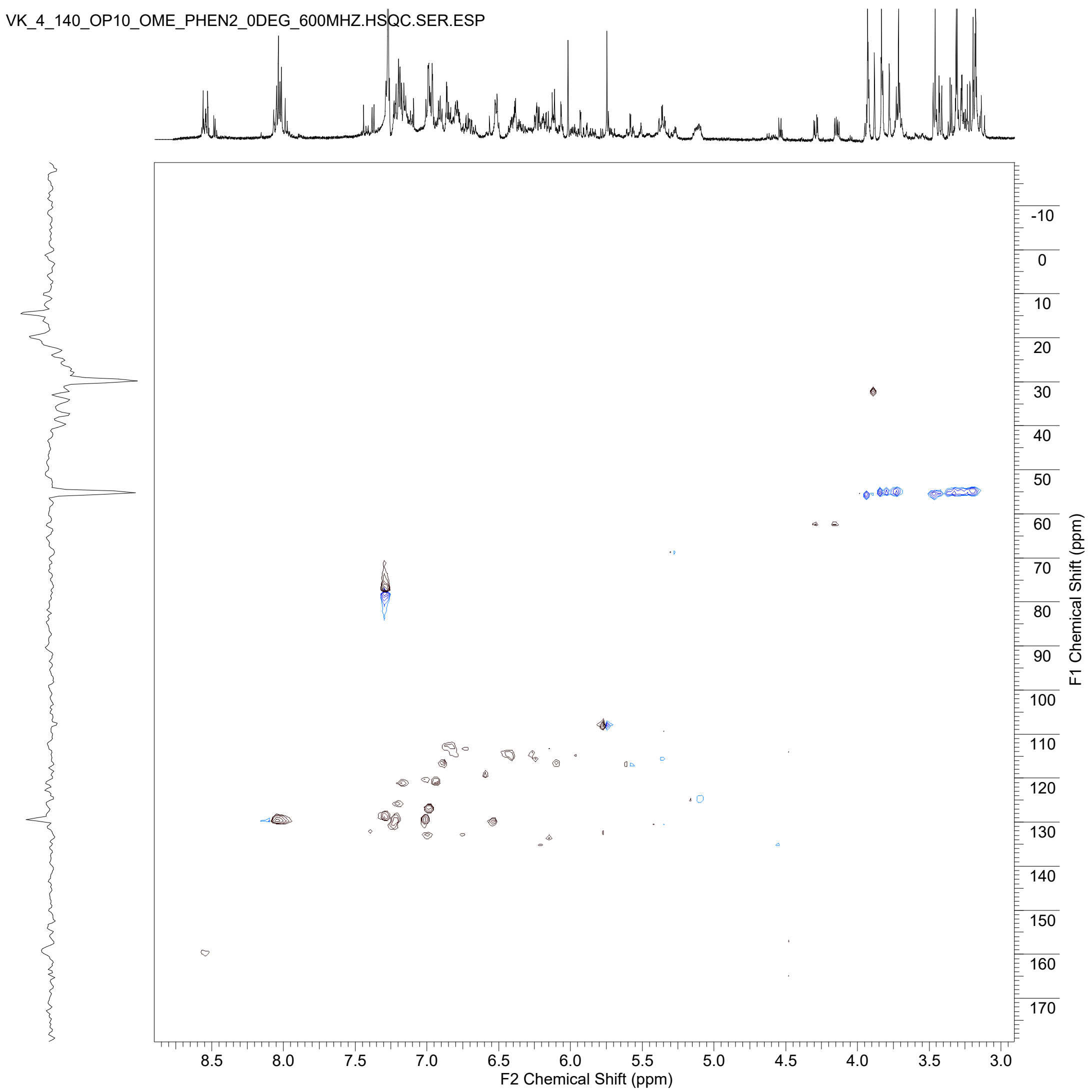

Figure S138. HSQC NMR spectrum (600 MHz, $CDCl_3$, 0 ℃) of **oP^{10}OMe(Phen)$_{2+2}$**.

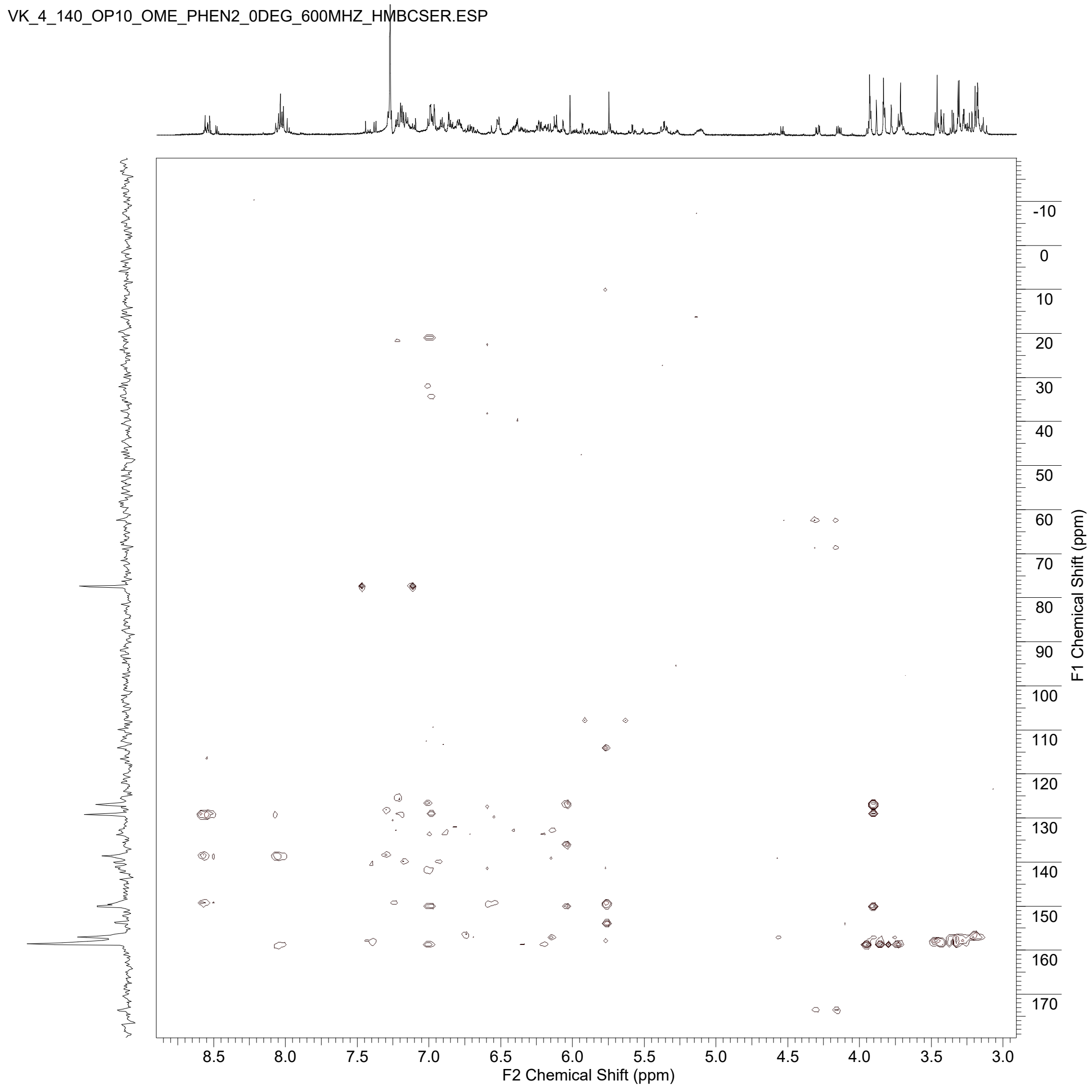

Figure S139. HMBC NMR spectrum (600 MHz, $CDCl_3$, 0 ℃) of $\mathbf{oP^{10}OMe(Phen)_{2+2}}$.

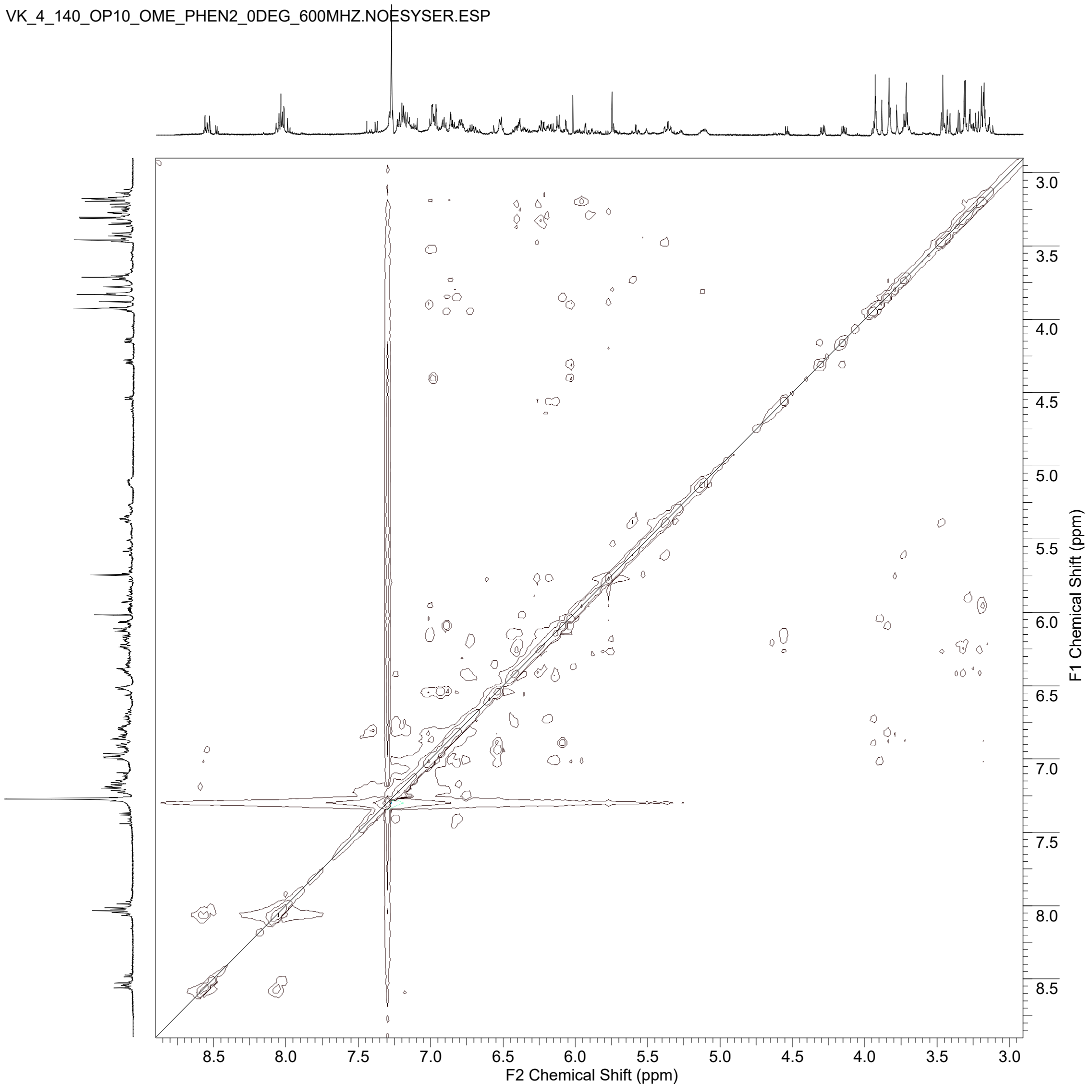

Figure S140. NOESY/EXSY NMR spectrum (600 MHz, $CDCl_3$, 0 ℃) of **oP^{10}OMe(Phen)$_{2+2}$**.

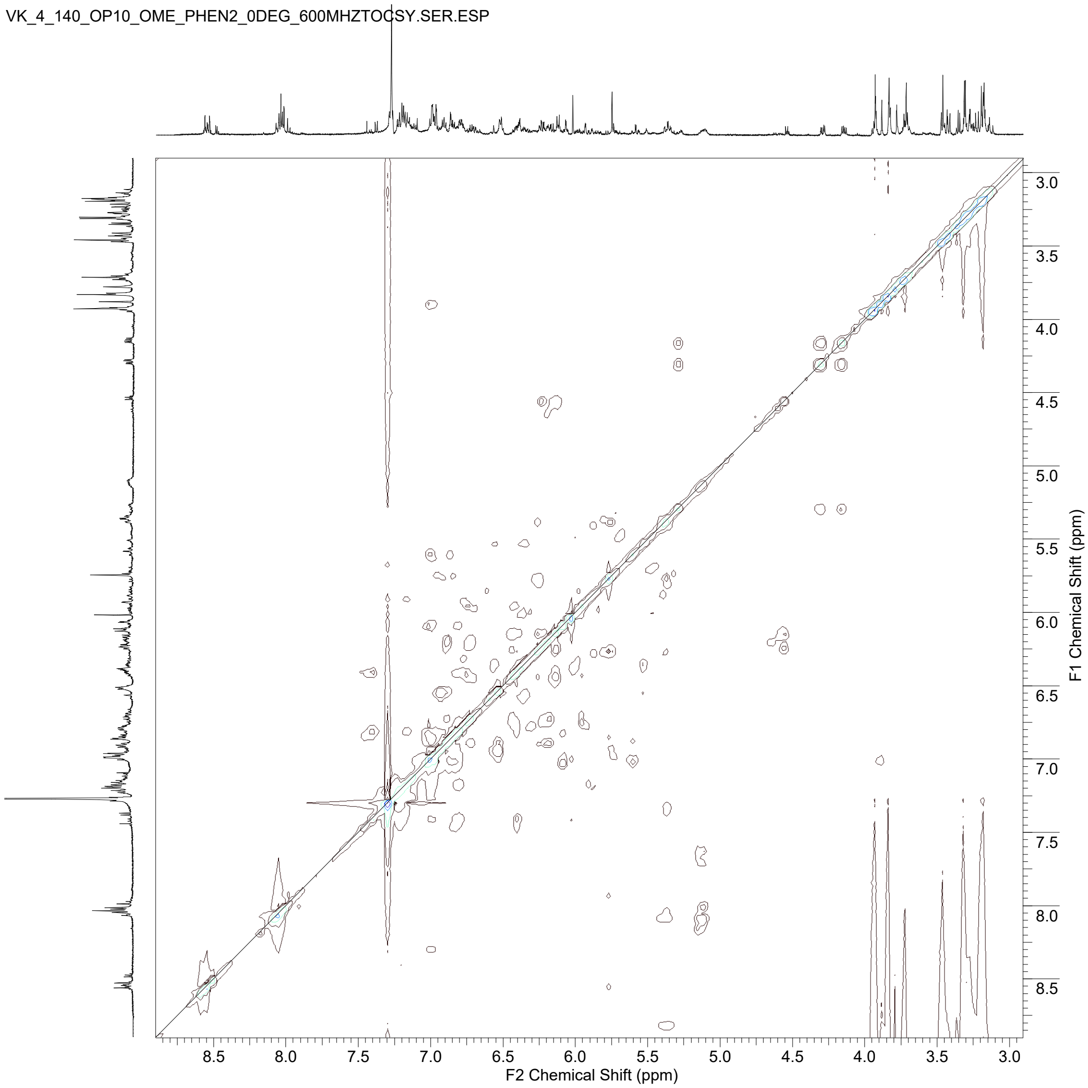

Figure S141. TOCSY NMR spectrum (600 MHz, $CDCl_3$, 0 °C) of **oP^{10}OMe(Phen)$_{2+2}$**.

References

(1) Hartley, C. S.; He, J. *J. Org. Chem.* **2010**, *75*, 8627−8636.

(2) Kinney, Z. J.; Kirinda, V. C.; Hartley, C. S. *Chem. Sci.* **2019**, *10*, 9057−9068.

(3) Wiitala, K. W.; Hoye, T. R.; Cramer, C. J. *J. Chem. Theory Comput.* **2006**, *2*, 1085−1092.

(4) Jain, R.; Bally, T.; Rablen, P. R. *J. Org. Chem.* **2009**, *74*, 4017−4023.

(5) Hartley, C. S. *Acc. Chem. Res.* **2016**, *49*, 646−654.

(6) Mathew, S.; Crandall, L. A.; Ziegler, C. J.; Hartley, C. S. *J. Am. Chem. Soc.* **2014**, *136*, 16666−16675.

(7) Borozdina, Y. B.; Mostovich, E.; Enkelmann, V.; Wolf, B.; Cong, P. T.; Tutsch, U.; Lang, M.; Baumgarten, M. *J. Mater. Chem. C* **2014**, *2*, 6618–6629.

(8) Mathew, S. M.; Hartley, C. S. *Macromolecules* **2011**, *44*, 8425–8432.

(9) Vemuri, G. N. External Control of ortho-Phenylene Folding, http://rave.ohiolink.edu/etdc/view?acc_num=miami1563204221995637, Ph.D. Thesis, Miami University, 2019.

(10) He, J.; Crase, J. L.; Wadumethrige, S. H.; Thakur, K.; Dai, L.; Zou, S.; Rathore, R.; Hartley, C. S. *J. Am. Chem. Soc.* **2010**, *132*, 13848–13857.

(11) Vemuri, G. N.; Pandian, R. R.; Spinello, B. J.; Stopler, E. B.; Kinney, Z. J.; Hartley, C. S. *Chem. Sci.* **2018**, *9*, 8260–8270.

(12) Nagao, I.; Shimizu, M.; Hiyama, T. *Angew. Chem.* **2009**, *121*, 7709–7712.